

MICROPLASTICS AND MARINE ENVIRONMENT

ARTICLES FOR FACULTY MEMBERS

<p>Title/Author</p>	<p>Coral annual growth band impregnated microplastics (Porites sp.): a first investigation report / Krishnakumar, S., Anbalagan, S., Hussain, S. M., Bharani, R., Godson, P. S., & Srinivasalu, S.</p>
<p>Source</p>	<p><i>Wetlands Ecology and Management</i> Volume 29 (2021) Pages 677–687 https://doi.org/10.1007/s11273-021-09786-9 (Database: ResearchGate)</p>
<p>Title/Author</p>	<p>Effect of aging of microplastics on gene expression levels of the marine mussel <i>Mytilus edulis</i>: Comparison in vitro/in vivo exposures / Jaouani, R., Roman, C., Decaix, J., Lagarde, F., & Châtel, A.</p>
<p>Source</p>	<p><i>Marine Pollution Bulletin</i> Volume 189 (2023) 114767 Pages 1-11 https://doi.org/10.1016/J.MARPOLBUL.2023.114767 (Database: ScienceDirect)</p>
<p>Title/Author</p>	<p>Effects of acute microplastic exposure on physiological parameters in <i>Tubastrea aurea</i> corals / Liao, B., Wang, J., Xiao, B., Yang, X., Xie, Z., Li, D., & Li, C.</p>
<p>Source</p>	<p><i>Marine Pollution Bulletin</i> Volume 165 (2021) 112173 Pages 1 –7 https://doi.org/10.1016/J.MARPOLBUL.2021.112173 (Database: ScienceDirect)</p>

MICROPLASTICS AND MARINE ENVIRONMENT

ARTICLES FOR FACULTY MEMBERS

<p>Title/Author</p>	<p>Exposure of <i>Mytilus galloprovincialis</i> to Microplastics: Accumulation, Depuration and Evaluation of the Expression Levels of a Selection of Molecular Biomarkers / Pizzurro, F., Nerone, E., Ancora, M., Domenico, M. Di, Mincarelli, L. F., Cammà, C., Salini, R., Renzo, L. Di, Giacinto, F. Di, Corbau, C., Bokan, I., Ferri, N., & Recchi, S.</p>
<p>Source</p>	<p><i>Animals</i> Volume 14 Issue 4 (2023) 103110 Pages 1-18 https://doi.org/10.3390/ANI14010004 (Database: MDPI)</p>
<p>Title/Author</p>	<p>Microplastic exposure represses the growth of endosymbiotic dinoflagellate <i>Cladocopium goreau</i> in culture through affecting its apoptosis and metabolism / Su, Y., Zhang, K., Zhou, Z., Wang, J., Yang, X., Tang, J., Li, H., & Lin, S.</p>
<p>Source</p>	<p><i>Chemosphere</i> Volume 244 (2020) 125485 Pages 1-8 https://doi.org/10.1016/J.CHEMOSPHERE.2019.125485 (Database: ScienceDirect)</p>
<p>Title/Author</p>	<p>Physiological stress response of the scleractinian coral <i>Stylophora pistillata</i> exposed to polyethylene microplastics / Lanctôt, C. M., Bednarz, V. N., Melvin, S., Jacob, H., Oberhaensli, F., Swarzenski, P. W., Ferrier-Pagès, C., Carroll, A. R., & Metian, M.</p>
<p>Source</p>	<p><i>Environmental Pollution</i> Volume 263 Part A (2020) 114559 Pages 1-9 https://doi.org/10.1016/J.ENVPOL.2020.114559 (Database: ScienceDirect)</p>

MICROPLASTICS AND MARINE ENVIRONMENT

ARTICLES FOR FACULTY MEMBERS

<p>Title/Author</p>	<p>Spatiotemporal characterisation of microplastics in the coastal regions of Singapore / Curren, E., & Yew Leong, S. C.</p>
<p>Source</p>	<p><i>Heliyon</i> Volume 9 Issue 1 (2023) e12961 Pages 1-14 https://doi.org/10.1016/J.HELIYON.2023.E12961 (Database: ScienceDirect)</p>
<p>Title/Author</p>	<p>Spatiotemporal microplastic occurrence study of Setiu Wetland, South China Sea / Ibrahim, Y. S., Hamzah, S. R., Khalik, W. M. A. W. M., Ku Yusof, K. M. K., & Anuar, S. T.</p>
<p>Source</p>	<p><i>Science of The Total Environment</i> Volume 788 (2021) 147809 Pages 1-12 https://doi.org/10.1016/J.SCITOTENV.2021.147809 (Database: ScienceDirect)</p>
<p>Title/Author</p>	<p>Spatial and temporal variations of microplastic concentrations in Portland's freshwater ecosystems / Talbot, R., Granek, E., Chang, H., Wood, R., & Brander, S.</p>
<p>Source</p>	<p><i>Science of The Total Environment</i> Volume 833 (2022) 155143 Pages 1-14 https://doi.org/10.1016/J.SCITOTENV.2022.155143 (Database: ScienceDirect)</p>

ARTICLES FOR FACULTY MEMBERS

MICROPLASTICS AND MARINE ENVIRONMENT

Title/Author	Coral annual growth band impregnated microplastics (Porites sp.): a first investigation report / Krishnakumar, S., Anbalagan, S., Hussain, S. M., Bharani, R., Godson, P. S., & Srinivasalu, S.
Source	<i>Wetlands Ecology and Management</i> Volume 29 (2021) Pages 677–687 https://doi.org/10.1007/s11273-021-09786-9 (Database: ResearchGate)

See discussions, stats, and author profiles for this publication at: <https://www.researchgate.net/publication/349492961>

Coral annual growth band impregnated microplastics (Porites sp.): a first investigation report

Article in *Wetlands Ecology and Management* · October 2021

DOI: 10.1007/s11273-021-09786-9

CITATIONS

12

READS

983

6 authors, including:



Krishna kumar Subbiah

Malankara Catholic College Mariyagiri

73 PUBLICATIONS 2,087 CITATIONS

[SEE PROFILE](#)



s. Anbalagan

Anna University, Chennai

16 PUBLICATIONS 95 CITATIONS

[SEE PROFILE](#)



Seshachalam Srinivasalu

Anna University, Chennai

124 PUBLICATIONS 3,350 CITATIONS

[SEE PROFILE](#)



Prince Samuel Godson

University of Kerala

44 PUBLICATIONS 1,025 CITATIONS

[SEE PROFILE](#)



Coral annual growth band impregnated microplastics (*Porites* sp.): a first investigation report

S. Krishnakumar · S. Anbalagan · S. M. Hussain · R. Bharani · Prince Samuel Godson · S. Srinivasalu

Received: 20 August 2019 / Revised: 13 November 2020 / Accepted: 27 January 2021
© The Author(s), under exclusive licence to Springer Nature B.V. part of Springer Nature 2021

Abstract Microplastic pollution in marine environments has increased rapidly during the last decades. These microplastic particles are transported into the coral reef environment from terrestrial origin. Recent investigations suggest that microplastic ingestion can adversely affect marine invertebrates, especially in the coral reef ecosystem. The present attempt has been carried out to identify the coral growth band impregnated microplastics from polished coral slabs and acid leached insoluble residues through microscopic examination. The impregnated microplastics have been present in the following descending order: Nylon > Polyester > Polypropylene > Polyethylene.

The irregular-shaped black and red microplastic particles have been dominantly observed. The annual growth band impregnated microplastics are most probably derived from tourist activities and chiefly controlled by oceanic currents and sediment re-suspension. The maximum distribution of microplastics has been observed in the coral annual growth bands of 1964 and 2005.

Clinical Trials Registration The present work is not a clinically related project. Hence clinical registration is not obtained/not required for publishing the results.

S. Krishnakumar (✉) · S. Anbalagan · S. Srinivasalu
Institute for Ocean Management, Anna University,
Chennai 600025, India
e-mail: coralkrishna@gmail.com

S. Anbalagan
e-mail: paleoanbu1986@gmail.com

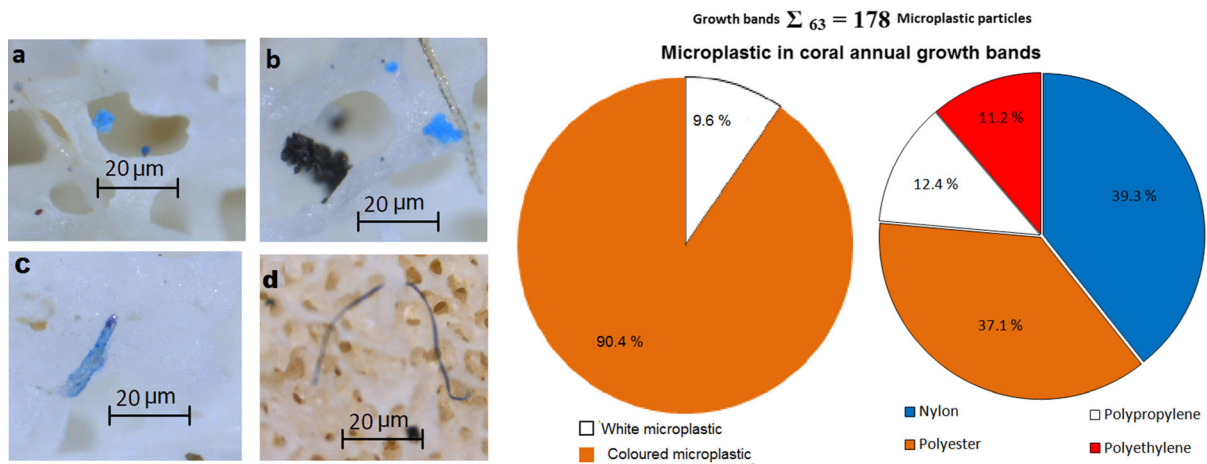
S. Srinivasalu
e-mail: ponmozhisrini2001@yahoo.com

S. M. Hussain
Department of Geology, University of Madras, Guindy
Campus, Chennai 600 025, India
e-mail: hussain.sm7@gmail.com

R. Bharani
Department of Electrical and Electronics Engineering,
Anna University, Guindy Campus, Chennai 600 025,
India
e-mail: bharanikrishnakumar@gmail.com

P. S. Godson
Department of Environmental Sciences, University of
Kerala, Thiruvananthapuram 695581, India
e-mail: princegodsons@keralauniversity.ac.in

Graphic Abstract



Keywords Growth bands · *Porites* sp. · Microplastic fibers · Insoluble residues · FTIR · EPSEM-EDAX

Introduction

Microplastics can originate from various sources, including industrial processes and household items (Thompson 2015; Boucher and Friot 2017). Microplastic particles are transported from the natural environment to the biota through the life cycle of organisms and natural habits, including ingestion and egestion (Allen et al. 2017; Hankins et al. 2018; Reichert et al. 2018). Since the last decade, numerous notable microplastic (< 5 mm) investigations have been taken up by national and international researchers at different environments such as gravitational dust (Cai et al. 2017), marine and freshwater sediments (Veerasingam et al. 2016; Arunkumar et al. 2016), living biota (Karthik et al. 2018; Phuong et al. 2018) and human consumer products (Seth and Shrivastav 2018; Iniguez et al. 2017).

Coral colonies fulfill their energy needs in two ways, via photosynthetic materials from zooxanthellae and nearly 15 to 35% from exogenous sources like planktons. During the ingestion of zooplankton, the small microplastic debris is captured and ingested by corals. The ingestion of microplastics by other marine invertebrates like marine worms, crabs, and oysters significantly affects their health and reproduction (Wright et al. 2013; Watts et al. 2015; Sussarellu

et al. 2016). However, the high-density microplastic polymers (HDMPs) can serve as a growing medium for microbes and bioavailable material for benthos and corals (Hankins et al. 2018). The coral ingested microplastics have significantly reduced the needs of exogenous food sources during the calcification process, especially under stress conditions. Very recently, systematic studies on the microplastic distribution (Krishnakumar et al. 2018), availability of microplastics in coral tissue (Hall et al. 2015), and their impact on ecologically sensitive marine organisms and ecosystem, including coral reef, have been carried out around the world (Nunes et al. 2018; Denuncio et al. 2017; Reichert et al. 2018; Shim et al. 2016). The coral genera's (*Acropora*, *Pocillopora*, and *Porites*) response to microplastic exposure and health-related impact have been documented by Reichert et al. (2018). This study shows that the coral genus responds differently to microplastic exposure like cleaning mechanism (direct interaction, mucus production), overgrowth, and negative effect on health like bleaching and tissue necrosis. Hankins et al. (2018), have reported that two coral species, namely *M. cavernosa* and *O. faveolata* respond differently, and recognize and reject indigestible material. Allen et al. (2017) have carried out a detailed study on the consumption and retention of microplastics by corals through direct measurement of the plastics from the egestion tank.

Rameswaram Island is part of the Gulf of Mannar Marine National Park (GOMMNP). The coral islands of the Gulf of Mannar and their 10 km buffer zone

have been declared as a marine national park by the Government of India in 1989. The coastal zones of the coral islands flourish with seaweeds, reef-building coral communities, and marine vegetation. Besides, Rameswaram is one of the important Hindu pilgrim centers of India. The total area of the Rameswaram island is about 96 km², among which town area covers approximately 52 km², and has a local population of about 82,682 as of 2011. The study area experiences a tropical climatic condition with low humidity. The total solid waste generation of Rameswaram municipality is approximately 11MT (Vasudeo et al. 2018). The majority of solid waste is generated from tourist and pilgrim activities. The preliminary studies on microplastic contamination in marine sediments/beach sediments of Rameswaram Island have been investigated by various Indian researchers (Karthik et al. 2018; Krishnakumar et al. 2018). The response of reef-building corals to microplastic exposure has been widely studied by international researchers (Reichert et al. 2018; Hankins et al. 2018; Hall et al. 2015). No comprehensive study has been carried out in the present study area in the response of coral reefs to microplastic exposures, especially the scleractinian corals. Under this circumstance, the current work aims to study the coral annual growth band (*Porites* sp.) impregnated microplastics at the Gulf of Mannar, Southeast coast of India.

Materials and methods

The coral core (*Porites* sp.) was retrieved from the reef flat at the northeastern part of the Rameswaram Island, Gulf of Mannar (Fig. 1), during 2015 using an assembled electric rotary core driller with a manual speed controller. The average water depth of the sampling point was about 2 m, and the length of the core sample was 51.52 cm. After the collection of core sample, the sampling pit was properly closed/sealed with a pre-prepared concrete cylinder (1.5 inches diameter) and a waterproof polymer paste to protect the corals from marine borers. The retrieved core sample was washed with double distilled water, and the growth direction is marked at the sampling station. Before transferring the core to the laboratory, the coral core was entirely covered with an aluminum foil sheet and kept in a wooden core box for further analysis. Before the coral growth band subsampling, the

laboratory environment was pre-cleaned using alcoholic wipes and was maintained free from plastic fibers. The entire sub-sampling procedures were carried out in a stainless steel laminar flow air hood bench to minimize the contamination level. The blank measurement procedure was performed to reduce the error percentage during the sampling process and microscopic examination. The blank laboratory procedure did not show any microplastic materials in the blanks. The core sample was cut along the growth axis (along the growth direction), and the core slab surface was polished using a petrological polishing machine (Model—METCO Bainpol PMV 023). The polished slabs were observed under Leica® optical stereo zoom microscope (Model—Leica DMC 4500) using the polarized light mode to study the impregnated microplastics. The X-ray image was taken from the polished coral slab at the local health care center, and the negative image was converted into a positive image for annual coral growth band counting. The detected microplastic pieces within the growth band were photographed and documented. The subsamples were collected from coral annual growth rings using a dentist driller (Model number—Marathon ES-8 and Marathon SDE-M33E with 0.3 mm diameter bur tip). The total number of retrieved annual growth band subsample was 63 (from 1952 to 2015). The growth band-associated microplastic and lithogenic fragments were separated from 0.2 g of coral growth band subsample treated with nitric acid and digested in a closed teflon beaker with a steel jacket. The insoluble residues were filtered through the nitrocellulose membrane filter (Whatman® filter paper—Pore size—0.45 µm). The composition of insoluble residues was examined through EPSEM combined EDAX facility (JEOL JSM 6360 and JEOL JED 2300 model). The microscopic examination was carried out on insoluble residues, and the microplastics were studied by Intertek Fourier-Transform Infrared spectrometer (µ-FTIR) coupled with Attenuated Total Reflectance (ATR) diamond crystal attachment to find out the impregnated polymer composition. The spectra of reef incorporated microplastics were compared with the Raman spectral library standards (Standards include: ASTM E168, E1252) for polymers (Lenz et al. 2015).

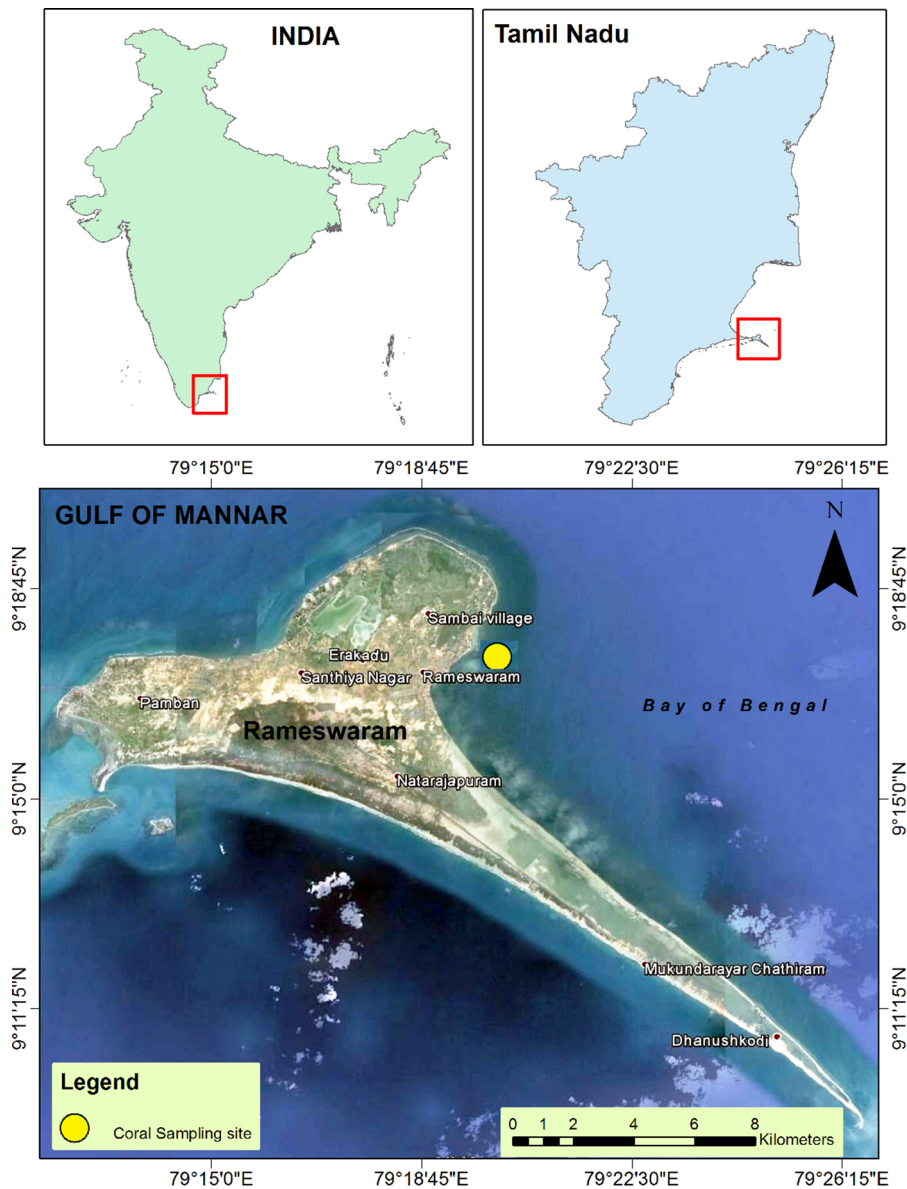


Fig. 1 Sampling location at Rameswaram Island, Tamil Nadu, India

Results and discussion

The coral core (*sp.Porites sp.*) shows growth bands from 1952 to 2015. The impregnate microplastic pieces of coral annual growth bands are shown in Fig. 2. A few pieces of microplastics have been noticed during the microscopic examination on the polished coral slabs (11 pieces: In detail—3 pieces in 1996 band; 4 pieces in 2010 band; 2 pieces from 2013 band and one each from 1965 and 1992). The acid

leaching method has been followed to study the microplastic distribution in annual growth rings of corals (*Porites sp.*). The coral annual growth band thickness depends on the environmental condition, especially water temperature, salinity, sedimentation and light intensity, etc. (Rodrigues and Grotoli 2006). However, with monsoonal effects, freshwater input into the coral reef system, and pollution-related impacts have harmed coral reef growth. The average annual growth rate over 63 years (1952–2015) ranges

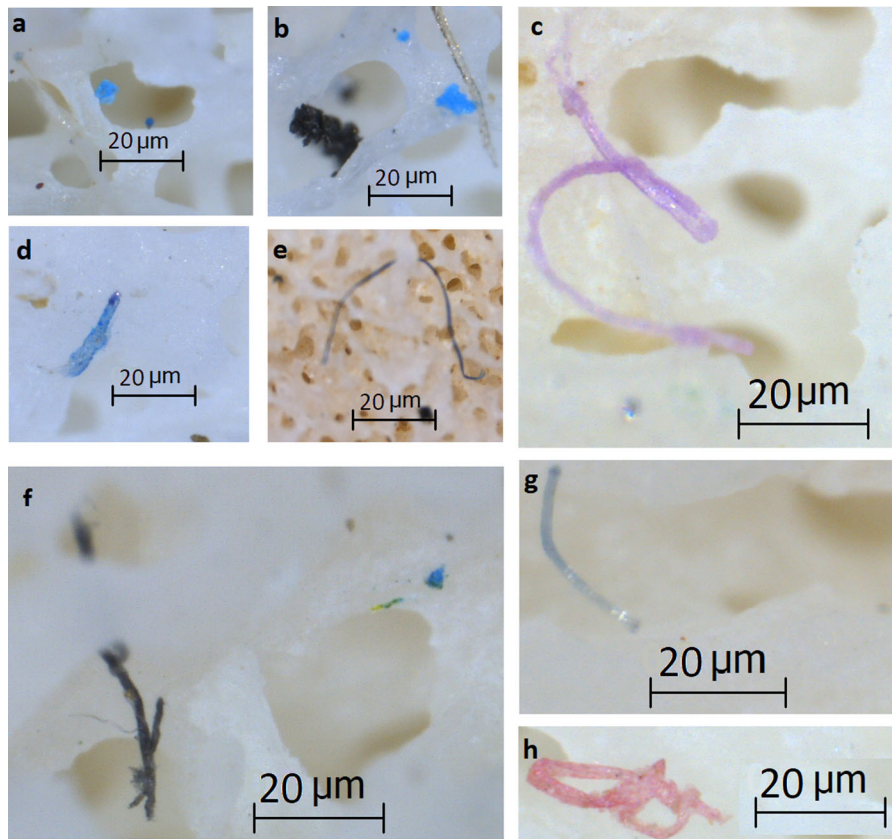


Fig. 2 a–h Coral growth band associated/impregnated microplastics under optical stereo zoom microscope

from 0.48 to 1.33 mm/year. The maximum and minimum thickness of the growth rings has been observed during 2000 and 1964, respectively. The observed microplastics are dominated by black and red color (Table 1). The coral growth band available microplastic shows the following descending order of colour classification: Black (38.2%) > Red (27.5%) > Blue (14.6%) > Green (10.1%) > White (9.6%). Irregular (~ 1.2%) and fibrous (~ 98.8%) shaped microplastics have been observed in the annual growth rings of corals. The abundance of fiber shaped microplastics in coral growth rings is most probably due to fragmentation (secondary microplastics), rather than the pre-production of resin pellets or scrubbers from cleaning products (primary microplastics) (Hall et al. 2015). The ingestion/feeding habit of the coral organism is also an important parameter for the maximum distribution of fiber-shaped microplastics. The size classification of growth-band incorporated microplastics ranged from 0.5 to 130 µm. The growth-band associated microplastics are chiefly made up of

nylon, polyester, polypropylene, and polyethylene, and these fibers show the following decreasing order: Nylon (39.3%) > Polyester (37.1%) > Polypropylene (12.4%) > Polyethylene (11.2%). The entrapped microplastic is associated with coral growth bands due to wave motion, currents, redistributed sediments. However, the microplastics are impregnated with coral growth bands during ingestion or due to the feeding habits of the coral colonies. The coral species may be exposed to microplastics, particularly at low tide, when floating plastics are likely to come into contact with corals on shallow reef crests and flats. According to Hall et al. (2015), before being ingested, the microplastic particles tend to aggregate and form a film like a thin layer covering the surface of the coral, appearing to cling to the mucus layer covering the coral tissue. However, the availability of microplastics in coral growth rings is dependent on buoyancy, density characteristics, and the source of microplastic to the marine environment. In addition to these, the incorporation of microplastics in coral annual growth

Table 1 Year wise growth ring thickness, percentage of insoluble residue, colour and composition classification of microplastics in annual growth rings of coral (*Porites sp.*), Gulf of Mannar, Southeast coast of India

S. no.	Year	Thickness of the band (in centimeters)	Insoluble residue (in %)	Colour						Composition				Total ^a
				Red	Black	Blue	Green	White	Nylon	Polyester	Polypropylene	Polyethylene		
1	2015	0.8	8	1	2	1	1	0	0	2	2	1	0	5
2	2014	0.63	11	0	1	0	0	0	0	0	1	0	0	1
3	2013	0.71	10	1	2	0	0	0	0	1	2	0	0	3
4	2012	0.73	9	1	0	1	1	0	0	2	0	1	0	3
5	2011	0.9	8.2	0	1	0	1	0	0	1	1	0	0	2
6	2010	0.58	9.6	2	2	1	0	0	0	1	2	0	2	5
7	2009	0.68	11.5	1	1	0	0	0	0	1	1	0	0	2
8	2008	0.63	9.5	3	2	1	0	0	0	2	2	1	1	6
9	2007	0.58	9	1	3	0	2	0	0	1	2	2	1	6
10	2006	0.96	11	2	1	1	0	0	0	1	1	1	1	4
11	2005	0.58	15	4	5	2	0	2	0	7	4	1	1	13
12	2004	0.61	12.4	0	0	0	0	0	0	0	0	0	0	0
13	2003	0.75	10.5	1	4	0	0	0	0	2	2	0	0	5
14	2002	0.77	8.8	0	1	0	2	0	0	0	1	1	1	3
15	2001	0.59	9.8	0	1	0	0	1	1	1	1	0	0	2
16	2000	0.48	7.6	1	2	1	0	0	0	2	1	1	0	4
17	1999	0.8	9.4	1	1	1	2	0	0	2	2	0	1	5
18	1998	0.97	10.2	1	1	0	0	1	1	0	1	1	1	3
19	1997	1	9.6	0	0	0	0	0	0	0	0	0	0	0
20	1996	0.89	16.2	3	2	1	0	4	3	3	3	3	1	10
21	1995	0.93	8.9	0	1	0	0	0	0	0	1	0	0	1
22	1994	1.25	8.4	0	0	0	0	0	0	0	0	0	0	0
23	1993	0.8	9.6	1	1	2	0	0	0	1	2	0	1	4
24	1992	0.61	8.6	2	0	1	0	0	0	1	1	1	0	3
25	1991	0.55	9.6	0	3	1	1	0	0	2	2	1	0	5
26	1990	0.5	9.2	1	1	0	0	0	0	1	1	0	0	2
27	1989	0.69	9.1	1	0	1	1	0	0	0	2	0	1	3
28	1988	0.88	10.5	0	0	0	0	0	0	0	0	0	0	0

Table 1 continued

S. no.	Year	Thickness of the band (in centimeters)	Insoluble residue (in %)	Colour				Composition				Total ^a	
				Red	Black	Blue	Green	White	Nylon	Polyester	Polypropylene		Polyethylene
29	1987	0.8	10.2	0	0	1	0	1	1	0	0	1	2
30	1986	0.65	6.7	1	2	0	0	0	1	1	1	0	3
31	1985	0.73	8.6	0	0	0	0	0	0	0	0	0	0
32	1984	0.74	9.3	1	0	0	0	0	0	1	0	0	1
33	1983	1	8.7	1	1	0	0	0	1	1	0	0	2
34	1982	0.95	9.9	0	1	0	1	0	1	1	0	0	2
35	1981	1.14	11.4	1	2	0	0	0	1	2	0	0	3
36	1980	1.05	10.9	0	0	0	0	0	0	0	0	0	0
37	1979	1.1	9.8	0	0	0	0	0	0	0	0	0	0
38	1978	0.78	9.6	1	0	1	0	0	1	1	0	0	2
39	1977	1.13	9.2	0	2	0	1	0	1	1	0	1	3
40	1976	0.87	8.9	3	3	1	0	2	3	4	1	1	9
41	1975	0.97	9.1	0	0	0	0	0	0	0	0	0	0
42	1974	0.86	10.2	0	0	0	0	0	0	0	0	0	0
43	1973	1.03	10.5	1	0	0	0	0	1	0	0	0	1
44	1972	0.77	10.2	0	0	0	0	0	0	0	0	0	0
45	1971	0.56	11.3	2	4	2	0	1	5	2	1	1	9
46	1970	0.78	9.9	0	0	0	1	0	1	0	0	0	1
47	1969	0.54	10.2	0	0	0	0	0	0	0	0	0	0
48	1968	0.58	9.8	0	1	0	0	0	1	0	0	0	1
49	1967	0.62	10.2	0	0	0	0	0	0	0	0	0	0
50	1966	0.64	11.1	0	1	0	0	0	1	0	0	0	1
51	1965	0.75	9.9	1	0	0	2	0	0	2	0	1	3
52	1964	1.33	13.9	4	6	2	0	3	8	3	3	1	15
53	1963	1.1	9.8	0	1	1	0	0	1	1	0	0	2
54	1962	0.97	10.3	0	1	2	0	0	0	2	0	1	3
55	1961	0.82	10.5	0	1	0	0	0	0	1	0	0	1
56	1960	0.91	11.2	1	1	0	0	0	0	2	0	0	2
57	1959	0.91	9.9	0	0	0	0	0	0	0	0	0	0

Table 1 continued

S. no.	Year	Thickness of the band (in centimeters)	Insoluble residue (in %)	Colour					Composition				Total ^a
				Red	Black	Blue	Green	White	Nylon	Polyester	Polypropylene	Polyethylene	
58	1958	0.69	10.5	1	1	0	0	0	1	1	0	0	2
59	1957	0.84	11.6	1	0	1	1	2	3	1	1	0	5
60	1956	0.98	10.9	1	1	0	0	0	1	1	0	0	2
61	1955	0.8	11.2	0	0	0	0	0	0	0	0	0	0
62	1954	0.71	10.8	1	0	0	0	0	1	0	0	0	1
63	1953	0.76	9.8	0	0	0	0	0	0	0	0	0	0
64	1952	0.81	9.5	0	1	0	1	0	1	1	0	0	2

^aTotal = the impregnated microplastic particles with polished slabs and acid leached insoluble residues of coral growth rings

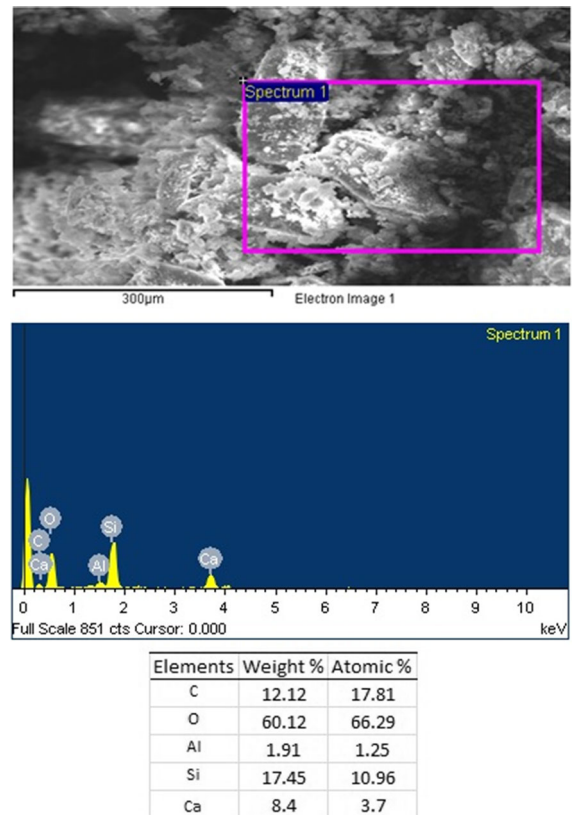


Fig. 3 EPSEM-EDAX image of the reef growth band associated insoluble residues

rings changes in concern with the intensity of cleaning mechanisms like mucus formation and direct interaction. The above-said process has been reported in detail in *Acropora sp.* and *Porites sp.* by Reichert et al. (2018). The coral growth ring incorporated nylon and polyester are mostly derived from loose fishing ropes and polyester cloths from pilgrim centres. The maximum number of microplastics has been associated with the annual growth bands of 1964, 1971, 1976, 1996, and 2005 (1964—15 particles; 1971—9 particles; 1976—9 particles; 1996—10 particles; 2005—13 particles). The elevated count of microplastic fibers with coral growth bands is most likely due to terrestrial, freshwater input during the rainy season, re-suspended sediments during high energy events, regional climate fluctuations, and alterations in the oceanic current pattern.

The microplastic distribution level in a freshwater environment (large rivers and lake) is similar to the

marine environmental condition (Duis and Coors 2016). According to Lee et al. (2013), microplastic levels are significantly affected by the freshwater input from the riverine sources of the densely populated areas along the coast. Free et al. (2014) have reported that the most populated areas and tourist areas are the chief sources of elevated microplastic levels. A detailed investigation related to the source of insoluble residues has been carried out on corals by various researchers (Krishnakumar et al. 2015; Pingitore et al. 2002). The quantity and geochemical variation of growth-band associated insoluble residues provide information about the source of sediments, environmental changes in the study area, including anthropogenic impact on the coral ecosystem (Naqvi 1994; Wyndham et al. 2004; Mertz-Kraus et al. 2009). The composition of this insoluble residue is dominated by quartz and feldspar minerals, and a few grains of opaques are also observed. The composition of the residues were reconfirmed by the EPSEM-EDAX facility (Fig. 3). The composition of the residue suggests that they may be derived from charnockitegneisses, and meta-sedimentary sequences. The meta-sedimentary sequences were mainly made up of quartzite, carbonate, and metapelite with a minor metabolic component (Jonathan et al. 2004).

The insoluble residues was observed under a microscope for growth-band available microplastic

fibers. The presence of insoluble residue with opaque grains and microplastic fibers is shown in Fig. 4. The composition of microplastics have been studied using Fourier-Transform Infrared Spectroscopy (FTIR). The FTIR spectra of the microplastics are shown in Fig. 5. The insoluble residue percentage ranges from 8.9 to 16.2%. The maximum percentage of insoluble residue has been noticed in the 1996 annual growth ring (Table 1). According to Reichert et al. (2018), the overgrowth and mucus production incorporated the

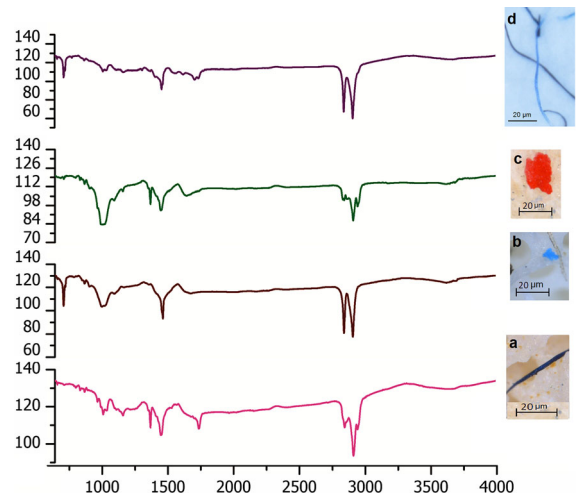


Fig. 5 μ -FTIR peaks of the microplastics (a polyester, b Nylon, c polypropylene, d polyethylene)

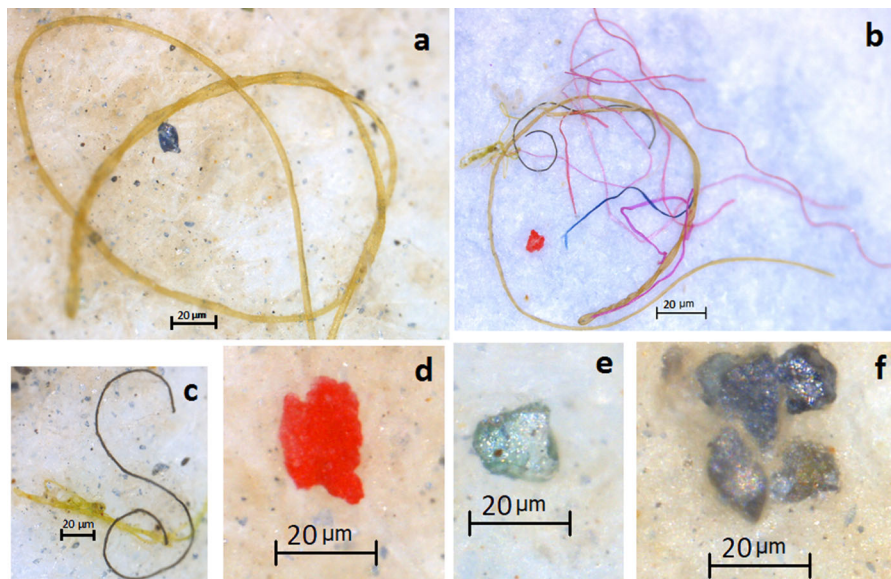


Fig. 4 a–d Extracted microplastics from insoluble residues of coral growth band. e–f coral growth band impregnated opaques and mineral grains

microplastics within the *Porites sp.* growth rings. The annual growth ring size and amount of insoluble residue did not show significant relationships with the microplastics. The above observation has been concluded from the total number of microplastics and insoluble residue percentage in every growth ring.

Conclusion

The present pilot investigation on microplastic distribution in annual growth bands of *Porites sp.* reveals that impregnated microplastics are seen in the following descending order: Nylon > Polyester > Polypropylene > Polyethylene. Irregular-shaped, black and red microplastics are found to be dominant. The annual growth band impregnated microplastics are most probably derived from tourist activities and primarily controlled by oceanic currents and sediment re-suspension. The maximum distribution of microplastics were noticed in the coral annual growth bands of 1964 and 2005. The detailed study in the response of reef-building corals to microplastic exposure in the Gulf of Mannar will be helpful in understanding the impact of microplastics on the coral reef ecosystem.

Author contributions SK and SS: Conceptualization, Investigation, Writing—original draft. SA and PSG: Conceptualization, Investigation, Methodology, Sample analysis. SMH and RB: Methodology, Software, Validation, Data curation, review and editing.

Funding The principal author (Dr.S.Krishnakumar) is thankful to the National Post Doctoral Fellowship Scheme (File No PDF/2017/000030 dated 14th November 2017) of the Department of Science and Technology (DST), New Delhi, for its financial assistance in carrying out this work.

Data availability The authors confirm that the data supporting the findings of this study are available within the article.

Compliance with ethical standards

Conflict of interest The authors declare no conflict of interest connected with this manuscript entitled “Coral annual growth band impregnated microplastics (*Porite Sp.*): A first investigation report”.

Ethical approval Opinions and statements included in the paper are solely those of the individual author and are not

necessarily adopted, endorsed, or verified as accurate by the Committee on Reproducibility and Replicability in Science.

References

- Al-Rousan S, Al-Shloul R, Al-Horani F, Abu-Hilal A (2007) Heavy metal contents in growth bands of *Porites* corals: record of anthropogenic and human developments from the Jordanian Gulf of Aqaba. *Mar Pollut Bull* 54 (12): 1912–1922
- Allen AS, Seymour AC, Rittschof D (2017) Chemoreception drives plastic consumption in a hard coral. *Mar Pollut Bull* 124(1): 198–205.
- Arunkumar A, Sivakumar R, Sai Rutwik Reddy Y, Bhagya Raja MV, Nishanth T, Revanth V (2016) Preliminary study on marine debris pollution along Marina beach, Chennai, India. *Region Stud Marine Sci* 5:35–40
- Boucher J, Friot D (2017) Primary microplastics in the oceans: a global evaluation of sources. IUCN, Gland, Switzerland
- Cai L, Wang J, Peng J, Tan Z, Zhan Z, Tan X, Chen Q (2017) Characteristic of microplastics in the atmospheric fallout from Dongguan city, China: preliminary research and first evidence. *Environ Sci Pollut Res* 24(32):24928–24935
- Denuncio P, Mandiola MA, Pérez-Salles SF, Machado R, Ott PH, De Oliveira LR, Rodriguez D (2017) Marine debris ingestion by the south American fur seal from the southwest Atlantic ocean. *Mar Pollut Bull* 122(1–2):420–425
- Duis K, Coors A (2016) Microplastics in the aquatic and terrestrial environment: sources (with a specific focus on personal care products), fate and effects. *Environ Sci Eur* 28(1):2
- Free CM, Jensen OP, Mason SA, Eriksen M, Williamson NJ, Boldgiv B (2014) High-levels of microplastic pollution in a large, remote, mountain lake. *Mar Pollut Bull* 85:156–163
- Hall NM, Berry KLE, Rintoul L, Hoogenboom MO (2015) Microplastic ingestion by scleractinian corals. *Mar Biol* 162:725–732
- Hankins C, Duffy A, Drisco K (2018) Scleractinian coral microplastic ingestion: potential calcification effects, size limits, and retention. *Mar Pollut Bull* 135:587–593
- Íñiguez ME, Conesa JA, Fullana A (2017) Microplastics in Spanish table salt. *Sci Rep* 7(1):8620
- Jiang W, Yu K, Song Y, Zhao JX, Feng YX, Wang Y, Xu S (2018) Coral geochemical record of submarine groundwater discharge back to 1870 in the northern South China Sea. *Palaeogeogr Palaeoclimatol Palaeoecol* 507:30–38
- Jonathan MP, Ram-Mohan V, Srinivasalu S (2004) Geochemical variations of major and trace elements in recent sediments, off the Gulf of Mannar, the southeast coast of India. *Environ Geol* 45(4):466–480
- Karthik R, Robin RS, Purvaja R, Ganguly D, Anandavelu I, Raghuraman R, Hariharan G, Ramakrishna A, Ramesh R (2018) Microplastics along the beaches of southeast coast of India. *Sci Total Environ* 645:1388–1399
- Krishnakumar S, Ramasamy S, Magesh NS, Chandrasekar N, Peter TS (2015) Metal concentrations in the growth bands of *Porites sp.*: a baseline record on the history of marine pollution in the Gulf of Mannar. India. *Mar Pollut Bull* 101(1):409–416

- Krishnakumar S, Srinivasalu S, Saravanan P, Vidyasakar A, Magesh NS (2018) A preliminary study on coastal debris in Nallathanni Island, Gulf of Mannar Biosphere Reserve, Southeast coast of India. *Mar Pollut Bull* 131:547–551
- Kumar A, Sivakumar R, Reddy YSR, Raja B, Nishanth T, Revanth V (2016) Preliminary study on marine debris pollution along Marina beach, Chennai. *India Reg Stud Mar Sci* 5:35–40
- Lee J, Hong S, Song YK, Hong SH, Jang YC, Jang M, Heo NW, Han GM, Lee MJ, Kang D, Shim WJ (2013) Relationships among the abundances of plastic debris in different size classes on beaches in South Korea. *Mar Pollut Bull* 77:349–354
- Lenz R, Enders K, Stedmon CA, Mackenzie DMA, Nielsen TG (2015) A critical assessment of visual identification of marine microplastic using Raman spectroscopy for analysis improvement. *Mar Poll Bull* 100(1):82–91
- Mertz-Kraus R, Brachert TC, Jochum KP, Reuter M, Stoll B (2009) LA-ICP-MS analyses on coral growth increments reveal heavy winter rain in the Eastern Mediterranean at 9 Ma. *Palaeogeogr Palaeoclimatol Palaeoecol* 273:25–40
- Naqvi SAS (1994) Seasonal variation in an annually-banded coral *Porites*: a scanning electron microscopy investigation. *Mar Geol* 118(3–4):187–194
- Nunes JAC, Sampaio CL, Barros F, Leduc AO (2018) Plastic debris collars: an underreported stressor in tropical reef fishes. *Mar Pollut Bull* 129(2):802–805
- Phuong NN, Poirier L, Pham QT, Lagarde F, Zalouk-Vergnoux A (2018) Factors influencing the microplastic contamination of bivalves from the French Atlantic coast: location, season and/or mode of life? *Mar Pollut Bull* 129(2):664–674
- Pingitore NE Jr, Iglesias A, Bruce A, Lytle F, Wellington GM (2002) Valences of iron and copper in coral skeleton: X-ray absorption spectroscopy analysis. *Microchem J* 71(2–3):205–210
- Reichert J, Schellenberg J, Schubert P, Wilke T (2018) Responses of reef building corals to microplastic exposure. *Environ Pollut* 237:955–960
- Rodrigues LJ, Grottoli AG (2006) Calcification rate and the stable carbon, oxygen, and nitrogen isotopes in the skeleton, host tissue and zooxanthellae of bleached and recovering Hawaiian corals. *Geochim Cosmochim Acta* 70:2781–2789
- Saha N, Rodriguez-Ramirez A, Nguyen AD, Clark TR, Zhao JX, Webb GE (2018) Seasonal to decadal scale influence of environmental drivers on Ba/Ca and Y/Ca in coral aragonite from the southern Great Barrier Reef. *Sci Total Environ* 639:1099–1109
- Seth CK, Shrivastav A (2018) Contamination of Indian sea salts with microplastics and a potential prevention strategy. *Environ Sci Pollut Res* 25(30):30122–30131
- Shim WJ, Song YK, Hong SH, Jang M (2016) Identification and quantification of microplastics using Nile Red staining. *Mar Pollut Bull* 113(1–2):469–476
- Thompson RC (2015) Microplastics in the marine environment: sources, consequences and solutions. In *Marine anthropogenic litter*. Springer, Cham, pp 185–200
- Vasudeo G, Saraswathi V, Sridhar K, Saravanan R, Edward L, Thirumalaiselvan S (2018) Solid waste management in Rameswaram Island—“Green Ramesawaram project”. In: *National conference on Marine debris (CoMaD)*, pp 178–181
- Veerasingam S, Mugilarasan M, Venkatachalapathy R, Vethamony P (2016) Influence of 2015 flood on the distribution and occurrence of microplastic pellets along the Chennai coast. *India Mar Pollut Bull* 109(1):196–204
- Wyndham T, McCulloch M, Fallon S, Alibert C (2004) High-resolution coral records of rare earth elements in coastal seawater: biogeochemical cycling and a new environmental proxy. *Geochim Cosmochim Acta* 68(9):2067–2080

Publisher's Note Springer Nature remains neutral with regard to jurisdictional claims in published maps and institutional affiliations.

ARTICLES FOR FACULTY MEMBERS

MICROPLASTICS AND MARINE ENVIRONMENT

Title/Author	Effect of aging of microplastics on gene expression levels of the marine mussel <i>Mytilus edulis</i>: Comparison in vitro/in vivo exposures / Jaouani, R., Roman, C., Decaix, J., Lagarde, F., & Châtel, A.
Source	<i>Marine Pollution Bulletin</i> Volume 189 (2023) 114767 Pages 1-11 https://doi.org/10.1016/j.MARPOLBUL.2023.114767 (Database: ScienceDirect)



Effect of aging of microplastics on gene expression levels of the marine mussel *Mytilus edulis*: Comparison *in vitro*/*in vivo* exposures

Rihab Jaouani^{a,b}, Coraline Roman^a, Justine Decaix^a, Fabienne Lagarde^b, Amélie Châtel^{a,*}

^a Biology of Organisms Stress Health Environment (BIOSSE), Université Catholique de l'Ouest, Angers, France

^b Institut des Molécules et des Matériaux du Mans, UMR CNRS 6283, Le Mans Université, Avenue Olivier Messiaen, 72085 Le Mans Cedex, France

ARTICLE INFO

Keywords:
Microplastic
Aging
Transcriptomic
Bivalve
Mytilus edulis

ABSTRACT

In the present study, effects of aging MPs of polyethylene (PE) were investigated in the marine mussel *Mytilus edulis*, commonly used as bioindicator of aquatic ecosystem, using both *in vitro* and *in vivo* exposures, using concentrations found in marine waters (0.008, 10 and 100 $\mu\text{g}\cdot\text{L}^{-1}$). Changes in gene expression levels implicated in detoxification, immune system, cytoskeleton and cell cycle control were evaluated by quantitative RT-qPCR. Results demonstrated differential expression levels depending upon the state of plastic degradation (aged vs non-aged) and way of exposure (*in vitro* vs *in vivo*). This study highlighted the interest of using molecular biomarkers based on analysis of gene expression pattern in an ecotoxicological context that gives indication of relative slight changes between tested conditions as compared to other biochemical approaches (e.g. enzymatic activities). In addition, *in vitro* analysis could be used to generate large amount of data as regards to the toxicological effects of MPs.

1. Introduction

The tremendous increase in plastic production has resulted in several plastic waste pollution in natural environments, which adversely affects wildlife, wildlife habitat, and humans (Botterell et al., 2019; Hale et al., 2020; Horton and Barnes, 2020). Plastic debris have been detected in marine ecosystems worldwide and are considered as a global threat for diverse marine organisms (Li et al., 2019). Plastics are widely used in daily life (e.g.; aerospace, industry, pharmaceuticals and agriculture) due to their advantages such as light weight, wear resistance, chemical stability, high plasticity, and low cost. (Andrady, 2011; Barnes et al., 2009). Since the 1970s, the existence of floating plastic in the water has been documented (Colton et al., 1974; Moore, 2008). Microplastics (MPs) are debris which size <5 mm (NOOA, 2008), it is the result of the degradation of larger plastics pieces (Wright et al., 2013). According to recent reports, MPs represent 90 % of plastic waste discovered in pelagic environments, with an estimated 5 trillion pieces of plastic in marine waters (Browne et al., 2010; Eriksen et al., 2013). They can be classified into two types: primary MPs of particles manufactured and used as MPs (microbeads), mostly found in cosmetic products, and secondary MPs that result from the fragmentation of macroplastics through different abiotic factors such as, mechanical abrasion, UV radiation, and

biological degradation via micro-organisms (Cole et al., 2011). Ingestion and negative impact of MPs have been evaluated in various marine species such as zooplankton (Cole et al., 2013), lugworms (Wright et al., 2013), bivalves (Choi et al., 2021; Dowarah et al., 2020; Klasios et al., 2021; Phuong et al., 2018), fish (Digka et al., 2018; Giani et al., 2019) and marine mammals (Donohue et al., 2019; Hernandez-Gonzalez et al., 2018).

Plastics have many characteristics such as surface charge, roughness, porosity, polarity and hydrophobicity. In the natural environment, these characteristics could be changed with time, ultraviolet radiation, turbulence and salinity (J. Liu et al., 2019b; Suhrhoff and Scholz-Böttcher, 2016) that could influence adsorption of environmental pollutants (heavy metals, chemicals additives and others) on the MPs and their entrance within the organisms (G. Liu et al., 2019a; Zhang et al., 2018). However, only few studies have investigated the effects of aged-microplastics on aquatic organisms. Vroom et al. (2017) have demonstrated that *Calanus finmarchicus* and females of *Acartia longiremis* prefer aged plastic beads rather than pristine plastic beads. In addition, it has been shown that aged-microplastics inhibit strongly the growth of *Chlorella vulgaris* compared to pristine microplastics (Fu et al., 2019; Luo et al., 2019).

Bioaccumulation of MPs in marine organisms, can reduce growth,

* Corresponding author.

E-mail address: amelie.chatel@uco.fr (A. Châtel).

maturation and reproduction (Murphy and Quinn, 2018; Sussarellu et al., 2016; Trestrail et al., 2020; Ziajahromi et al., 2018). For decades, bivalves have been extensively used as bioindicators to monitor environmental pollution due to their particular characteristics, such as filtration capacity, a large geographic distribution, easy accessibility, as sentinel organisms, and high tolerance to a wide range of ambient conditions (Li et al., 2019). The interest of this invertebrate group for studying the ecotoxicological impact of microplastics has grown since recent years (Tang et al., 2020; Trestrail et al., 2021; Zhou et al., 2021). For example, according to Van Cauwenberghe et al. (2015) and Bour et al. (2018), MPs can change the energy reserves in marine bivalves. Moreover, MPs ingestion reduces energy intake in the clam *Atactodea striata* (Xu et al., 2017), it can also decrease the activity of digestive enzymes and the filtration capacity in the mussel *Mytilus coruscus* (F. Wang et al., 2021; J. Wang et al., 2020).

Effects of MPs have been assessed in the past years using different techniques both at cellular and individual levels. Among them, the transcriptomic analysis represents a sensitive tool to establish molecular toxicity profiles of MPs, linking gene expression to cellular metabolism. In addition, transcriptomic tools could be considered as a suitable approach to evaluate the toxicity of MPs as it allows to screen many endpoints in a relatively short amount of time (Barrick et al., 2019). Transcriptomic could be considered as an HTS “high throughput screening” techniques and will enable researchers to understand MP's mode of action and may help to predict responses of these MPs across the aquatic ecosystem. Revel et al., (2017) showed that transcriptomic could be used to evaluate effects of environmental contaminants on defense mechanisms, immune system, cell membrane transporter, metabolic pathway, DNA repair, nervous system and also development, growth and reproduction. This technique allows a rapid identification of potential effects through modification on specific genes. In the context of microplastics, generating large quantities of data would help getting reliable database as regards to the toxicity of microplastics useful for regulatory agencies (European Environment Agency).

Studies have already evaluate the impacts of microplastics with a transcriptomic technique on aquatic organisms. Xiao et al. (2020) showed that genes involved in cellular processes, genetic information processing, organismal systems and metabolisms were dysregulated in the freshwater microalgae *Euglena gracilis* after exposure to polystyrene microplastics (5 µm). Environmental MP alone (50 µg.L⁻¹) or combined with B[a]P (1 µg.L⁻¹) induced a shift towards a cell apoptotic event in exposed mussels *Mytilus galloprovincialis*. *P53* and *DNA-ligase* increased at 1-day exposure, whereas after 3 days increase of *bax*, *Cas-3* and *P53* and decrease of *Bcl-2* and *DNA-ligase* were revealed (Romdhani et al., 2022). Embryonic and larval zebrafish *Danio rerio* also showed gene expression impairments after exposure to fluorescently labelled polyethylene microspheres (5 and 20 mg.L⁻¹) (LeMoine et al., 2018). Transcriptomics revealed a transient and extensive change in larval gene expression within 48 h exposure, which largely disappeared by 14 days (Romdhani et al., 2022).

In the context, this work aims to evaluate the ecotoxicological effect of virgin and aged MPs (PE) on the marine bivalve *Mytilus edulis*, under realistic concentrations of exposure, both *in vitro* and *in vivo*. For this propose, transcriptomic approach was applied in order to measure expression of genes implicated in detoxification, immune system, cytoskeleton and cell cycle control.

2. Materiel and methods

2.1. Preparation and characterization of microplastics

To obtain aged MPs, 10 g of virgin LDPE pellet (×3 replicates) were weighed in Petri dishes and were artificially irradiated for 30 days by UV light in a custom-made chamber (chamber with a UV light inside), at a temperature of 70 °C (Juliene et al., 2019). Three grams of LDPE were put into a sample container containing a magnetic bar or impactor and

both sides of the container were closed with two stainless steel caps. The container was inserted into a cryogenic mechanical miller (SPEX, 6770 Freezer-mill) filled with liquid nitrogen. During the milling process, an oscillating magnetic field was generated, which drove the magnetic bar forward and backward inside the container and make the impacts with the caps. Milling consisted in 2 min of pre-cooling followed by 2 cycles of milling. Each cycle lasted 4 min with a 1-min pause between the 2 cycles. The so-obtained powders of PE particles were then sieved during 60 min, respectively on a stain sieve of 400 µm.

All the fraction under 400 µm was kept and a granulometry analysis. To characterize the virgin and aged particles of PE, 2 mg of each sample was weighed in glass tubes then 2 mL of 95 % ethanol were added, the whole was mixed for 2 min. Using a micropipette, 5 µL of each solution was placed on glass slides and allowed to dry. The two software Projective and Particle scout from the WiTec Apyron 300R Raman spectrometer was used for the characterization of the powder according to the size and number of particles, a mapping of the slide and images were carried out. A granulometry analysis were done using a particle laser diffractometer Beckman Coulter LS 130 to measure the size distribution of the particles. SEM characterization was performed to complete our data.

2.2. Animal collection

M. edulis individuals were collected from a relatively clean sight, Saint-Cast-le-Guildo (48°37'48"N 2°15'24"W), previously identified as suitable for experimental research (Chevé et al., 2014). Mussels were placed in artificial sea water (30 psu, at 15 °C with a 12-h light/day cycle) for a 2 days acclimatization period prior to testing. The two approaches chosen in this study (*in vitro* and *in vivo*) have been conducted using different model organisms.

2.3. Primary cell culture of hemocytes and *in vitro* exposure

Mussels were previously placed in 3 L aquariums and maintained in the same conditions as the acclimatization period. A primary cell culture on *M. edulis* hemocytes was established as described in Barrick et al. (2018). Algae and epibionts were removed from their shell and mussels were immersed in a 0.054 % bleach bath for 10 min to eliminate microorganisms before a seawater (30 psu) bath for 10 min. Mussels were then dried with 70 % ethanol before the extraction of haemolymph with a syringe introduced between the two valves. Haemolymph was filtered through a 70 µm filter into a falcon tube maintained at 4 °C until a final volume around 50 mL. Cell concentration was then recorded through trypan blue exclusion. Approximately 500,000 cells per well were added in a 96 well plate in a L-15 (20.2 g.L⁻¹ NaCl, 0.54 g.L⁻¹ KCl, 0.6 g.L⁻¹ CaCl₂, 1 g.L⁻¹ MgSO₄, 3.9 g.L⁻¹ MgCl₂, 100 units.mL⁻¹ penicillin G, 100 µg.mL⁻¹ streptomycin, 1 % gentamycin, 10 % glucose and 10 % Fetal Bovine Serum (FBS), pH 7.0) media for 24 h.

Cell culture media was removed and replaced with a cell culture media containing aged and non-aged MPs in suspension (0.008, 10 and 100 µg.L⁻¹) with 12 replicates per test concentration. Wells were then pooled by 3 and these 4 replicates were used for future analysis (see supplementary informations). These concentrations were the same used for the *in vivo* exposure, corresponding to environmental concentrations. Cells were then incubated for 24 h at 37 °C (Barrick et al., 2018). 50 µL of trypsin was added in each well to detach the cells. After 5 min, 200 µL of cell culture media containing 10 % FBS was added to stop trypsin activity. The cells were collected in an Eppendorf tube and centrifuged at 600g for 5 min at 4 °C to pellet the cells. Cell culture media was removed, and the cells were washed with PBS (1100 mOsm). This step was repeated three time, after which the cell pellet was stored at -80 °C prior to analysis.

2.4. *In vivo* mussel exposure

Mussels were placed in 3 L aquariums and maintained in the same conditions as the acclimatization period. MPs were spiked once into each aquarium at the three test concentrations (0.08, 10 and 100 $\mu\text{g}\cdot\text{L}^{-1}$). Organisms were exposed for 4 days, unfed and oxygenated using a glass Pasteur pipette, after which gills from 9 mussels per condition were dissected and stored at $-80\text{ }^{\circ}\text{C}$ prior to analysis.

2.5. Analysis of MP content in mussel tissues

Analysis of MPs content was conducted on gills of mussels exposed *in vivo* were performed according to the protocol of described in (Revel et al., 2020). Each sample was placed in a 600-mL glass beaker, and approximately 150 mL of 10 % (KOH) solution was added to digest organic matter. The removed digestive system was weighed and placed in a 250 mL conical flask. After addition of 150 mL of 10 % potassium hydroxide KOH solution, the flask was covered by aluminum foil following, using a magnetic stirrer, the sample solution was stirred at 100 rpm overnight at $60\text{ }^{\circ}\text{C}$ to remove the organic matter. The digested solution was filtered over a metallic grid (50 μm) using a vacuum system. The filters were placed into clean petri dishes until been dried. Blank experiments were carried out using the same setup without any tissue. Fiber clothing and plastic equipment's were avoided throughout the experiment. In addition, all the containers and conical flasks were rinsed three times with ultrapure water. The samples and solutions were always covered to avoid contamination.

MPs isolated on the metallic grids were then characterized by Fourier transform micro-infrared spectroscopy (micro-FT-IR, PerkinElmer Spotlight 400, USA) in transmittance mode. The system was operating by SPECTRUM IMAGE. Each filter was scanned 1 time for one hour in the wave number range of $4000\text{--}750\text{ cm}^{-1}$. The infrared image data were analyzed with SIMPLEX1.0.0, and the target infrared spectrum was compared with the standard spectral library (PerkinElmer Library).

2.6. Transcriptomic analysis

2.6.1. RNA extraction

RNA extraction was conducted using a previously defined protocol (Châtel et al., 2018). Briefly, the tissues from 3 mussels per conditions were pooled and ground in TRIzol Reagent® (Ref: 15596026, Invitrogen™). A centrifugation (12,000g for 10 min at $4\text{ }^{\circ}\text{C}$) was then used to suppress cellular debris. 0.2 mL Chloroform per 1 mL of TRIzol was added to the supernatant and shaken vigorously prior to centrifugation (12,000g for 15 min at $4\text{ }^{\circ}\text{C}$) to ensure a phase separation with the clear upper aqueous phase, containing RNA, being collected. 0.5 mL of isopropanol per mL of TRIzol Reagent® was then added and the solution was incubated for 10 min at room temperature, to precipitate the RNA. A centrifugation (12,000g for 10 min at $4\text{ }^{\circ}\text{C}$) was then used to the pellet RNA. The pellet was washed with 200 μL of absolute ethanol and the RNA was then pellet again through centrifugation (12,000g for 5 min at $4\text{ }^{\circ}\text{C}$). The ethanol was then removed, and the pellet was allowed to dry before adding 10 μL of Diethyl pyrocarbonate (DEPC) water.

2.7. Determination of Total RNA and preparation of cDNA

Determination of total RNA of each extraction was carried out using a Nanodrop (Thermo Scientific™ NanoDrop 2000). 1 μL of the suspension of RNA were deposited for each sample on to measure concentration and purity by spectrophotometric absorption at 260 and 280 nm. First strand cDNA synthesis was conducted, using 5 or 1 μg of RNA extract for *in vivo* and *in vitro* exposure, respectively, and then was mixed with oligo-dT primers following the SuperScript™ III First-Strand Synthesis SuperMix™ protocol supplied by Invitrogen™.

2.8. qRT-PCR analysis

cDNA amplification was performed using a LightCycler 480 Real Time PCR system (Biorad) using SYBR Green Power Master Mix (Invitrogen) with specific primer pairs (Table 1). Thermocycling was conducted using polymerase activation at $94\text{ }^{\circ}\text{C}$ for 10 min with an amplification and quantification cycle repeated for 50 cycles ($94\text{ }^{\circ}\text{C}$ for 30 s, $58\text{ }^{\circ}\text{C}$ for 30 s, $72\text{ }^{\circ}\text{C}$ 30 s). The *cq* (Threshold cycle) values were recorded for analysis. The expression levels of eight genes involved in oxidative stress, detoxication, immunity, cytoskeleton and apoptosis were analyzed by quantitative RT-PCR analysis using a set of forward and reverse primers.

Elongation factor (*EF*) was the most stable gene and hence was used as a reference gene (Andersen et al., 2004). Target genes were normalized using the Δc_q (target gene- reference gene) to determine relative abundances.

2.9. Statistical analysis

The statistical analyzed were performed using the software XLSTAT 2019 (version 21.4.63762). After the verification of the normality of the data (Shapiro-Wilk test) and due to the non-normality of the results, statistical analyzes were carried out using the non-parametric Kruskal-Wallis test followed by the Dunn test, to compare all of the conditions with the control. The significance level was set at 0.05.

3. Results

3.1. MP characterization

Results of SEM characterization of virgin and aged LDPE particles showed that all sizes varied between 50 and 400 μm (Figs. 1-3). The carbonyl index is often used as an indicator of the presence of carbonyl groups, which may result from polymer degradation (Rodrigues et al., 2018). The (CI) of aged LDPE particles was 1,85. Fig. 4, represents the spectrums showing the evolution of LDPE aging compared to the virgin LDPE with the appearance of the characteristic pic in 1750 cm^{-1} .

3.2. *In vivo* mussel exposure

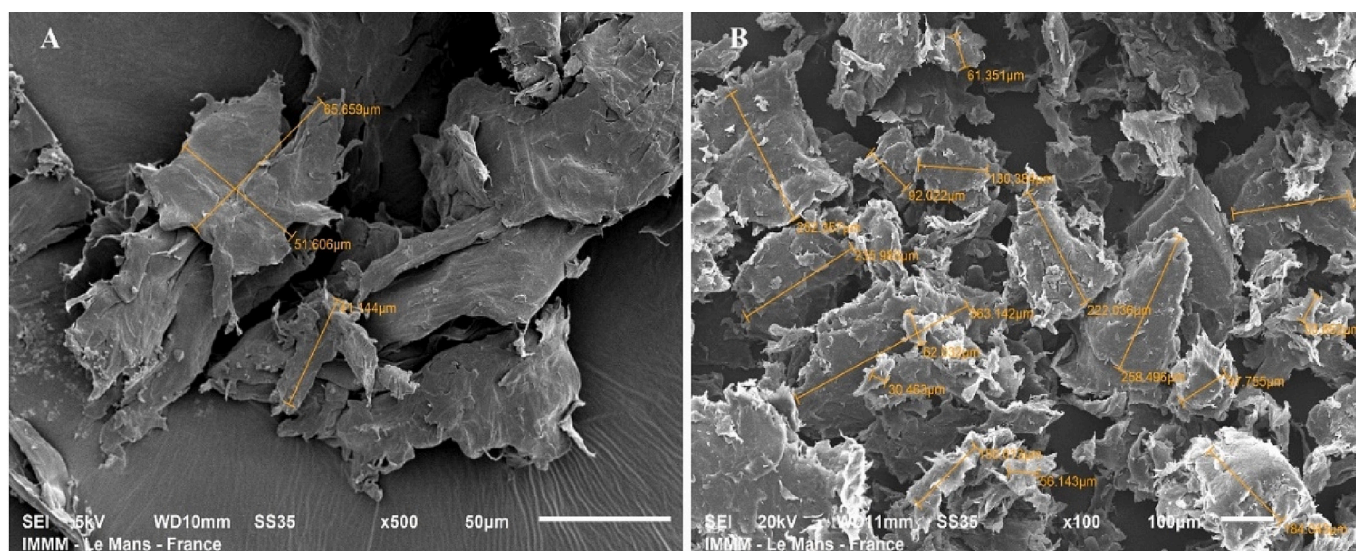
Filter FTIR analysis following gill digestion of mussels exposed *in vivo* no revealed any presence of MP (data not shown). As shown in Table 2, mussels showed a significant strong down-regulation of genes involved in response to the oxidative stress after exposure to 10 and 100 $\mu\text{g}\cdot\text{L}^{-1}$ of non-aged MPs and 100 $\mu\text{g}\cdot\text{L}^{-1}$ of aged MPs (catalase (*cat*): -4.34 ; -5.44 and -4.29). *P53* gene expression was significantly slightly induced when clams were exposed to 10 and 100 $\mu\text{g}\cdot\text{L}^{-1}$ of non-aged microplastics. Moreover, glutathione-S-transferase(*gst*) expression level was significantly up-regulated after exposure to 10 $\mu\text{g}\cdot\text{L}^{-1}$ for both microplastics (*gst*: 2.01 and 2.07) whereas the trend was reversed when mussels were exposed to 100 $\mu\text{g}\cdot\text{L}^{-1}$ of aged microplastics (*gst*: -1.99). Only a significant down-regulation of this gene expression was observed after mussel exposure to 0.008 $\mu\text{g}\cdot\text{L}^{-1}$ of aged microplastics (metallothionein (*mts*): -1.43).

Statistical comparison between aged and non-aged MPs after *in vivo* exposure (Table 3) showed significant differences for the genes involved in detoxication between the different types of plastics. Indeed, results showed significant differences of *gst* and *mt* expression levels between aged and non-aged MPs after mussel exposure to 100 $\mu\text{g}\cdot\text{L}^{-1}$ and 10 $\mu\text{g}\cdot\text{L}^{-1}$, respectively. *Act* expression was also significantly changed between aged and non-aged MPs when mussels were exposed to 0.008 $\mu\text{g}\cdot\text{L}^{-1}$. The comparison between aged and non-aged MPs showed significant differences concerning genes involved in oxidative stress, detoxication process, cytoskeleton and apoptosis regulation (Table 4 and Supplementary information). Gene involved in response to the oxidative stress showed a strong significant down-regulation after exposure to 100 $\mu\text{g}\cdot\text{L}^{-1}$.

Table 1

List of Genes used in the study with the role they serve. The GenBank Accession number with the forward and reverse primers are provided.

Gene	Function	Short Name	GenBank Accession No.	Forward Primer	Reverse Primer
Superoxide dismutase	Transformation of oxygen radicals to H ₂ O ₂	<i>sod</i>	AJ581746	TTTCTCGCAGTT TACGGTCA	AACTCGTGAACG TGGAAACC
Catalase	Transformation of H ₂ O ₂ to H ₂ O and O ₂	<i>cat</i>	AY580271	TGGGATCTGGTG GGAAATAA	ATCAGGAGTTCC ACGGTCAG
Glutathione S-transferase	Xenobiotic transformation	<i>gst</i>	AY557404	GATGACGGTTTC CAGCTTGT	ATGGCTCTTTTC CTGCTTCA
Metallothionein	Metal transport and detoxification	<i>mt</i>	AJ005453	TAAACATGCCT GCACCTTG	TTGCCACAGTCA CAGCTACC
Cytochrome P450 family 1-like 1 protein	Hydroxylation of endogenous and exogenous compounds	<i>cyp</i>	JX885878	ATGGGTGCTGGA TTTGAGAC	GTCGGTTGTCGT TGAATGTG
Lysozyme	Hydrolysis of bacteria	<i>lys</i>	DQ268868	GTTTACTGGGAT GGCTGTGG	TGAATATGGCTC CCGTAACC
P53 tumor suppressor-like protein	DNA repair, cell cycle regulation, apoptosis	<i>P53</i>	AY579472	TCAACATCGACC AGGAATCA	TCAGGAGCA GGGAGTCATCT
Actin	Cytoskeleton, cell division, cell adhesion	<i>act</i>	AF172606	AGCCATCCAAGC TGTCTGT	CAGCGGTAGTTG TGAACGAA

**Fig. 1.** Scanning electron microscopic (SEM) images of the surface of Polyethylene (PE) particles; (A) virgin PE, (B) aged PE.

L⁻¹ of non-aged MPs compared to 10 µg.L⁻¹ of aged MPs. Concerning detoxication process, *gst* was strongly up-regulated with 100 µg.L⁻¹ of non-aged MPs compared to 100 µg.L⁻¹ of aged MPs whereas *mt* was significantly up-regulated with 10 µg.L⁻¹ of non-aged MPs in comparison to all the aged MPs but for 0.008 µg.L⁻¹ of aged MPs a strong down-regulation in gene expression is observed compared to 100 µg.L⁻¹ of non-aged MPs. *act* expression level was significantly up-regulated with an exposure to 0.008 µg.L⁻¹ of aged MPs compared to non-aged MPs. Apoptosis gene expression was significantly up-regulated after exposure to 10 µg.L⁻¹ of non-aged MPs compared to 0.008 and 100 µg.L⁻¹ of aged MPs but a significant down-regulation is observed for 0.008 µg.L⁻¹ of non-aged MPs in comparison to 10 µg.L⁻¹ of aged MPs.

3.3. *In vitro* mussel exposure

As shown in Table 3, actin gene expression level was slightly up-regulated after exposure to non-aged microplastics at 0.008 µg.L⁻¹ and to 100 µg.L⁻¹ of aged microplastics with a Differential gene expression (DGE) at 1.23 and 0.90, respectively. The anti-oxidative system in mussels was impacted by the exposure to 0.008 µg.L⁻¹ of non-aged MPs with an up-regulation (*cat*: 2.17). Regarding immunity, a significant down-regulation of lysozyme (*lys*) gene expression after exposure to 10 and 100 µg.L⁻¹ of non-aged MPs (-1.03 and -1.40,

respectively). In addition, mussels showed a significant down-regulation of *p53* gene level after exposure to 0.008 µg.L⁻¹ of aged MPs (*p53*: -1.03).

Statistical comparison between aged and non-aged MPs after *in vitro* exposure showed significant differences observed mainly for the exposure to the lowest concentrations (0.008 µg.L⁻¹) for the genes involved in detoxication, immunity, cytoskeleton and cell cycle regulation. The comparison between aged and non-aged MPs showed significant differences concerning genes involved in oxidative stress, immunity, cytoskeleton and apoptosis regulation (Table 5 and Supplementary information). *cat* expression level was strongly up-regulated after exposure to all the non-aged MPs compared to 0.008 µg.L⁻¹ of aged MPs and also for 0.008 µg.L⁻¹ of non-aged MPs in comparison to 10 µg.L⁻¹ of aged MPs. Gene involved in the immunity system was significantly up-regulated when clams were exposed to 0.008 µg.L⁻¹ of non-aged MPs compared to all the aged MPs. Concerning *act*, its expression level was significantly up-regulated with the exposure to 0.008 µg.L⁻¹ of non-aged MPs in comparison to the aged one but a significant down-regulation is also observed after exposure to 10 and 100 µg.L⁻¹ of non-aged MPs compared to 0.008 µg.L⁻¹ of aged MPs. *p53* gene was strongly up-regulated for 0.008 µg.L⁻¹ of non-aged MPs in comparison to the aged one.

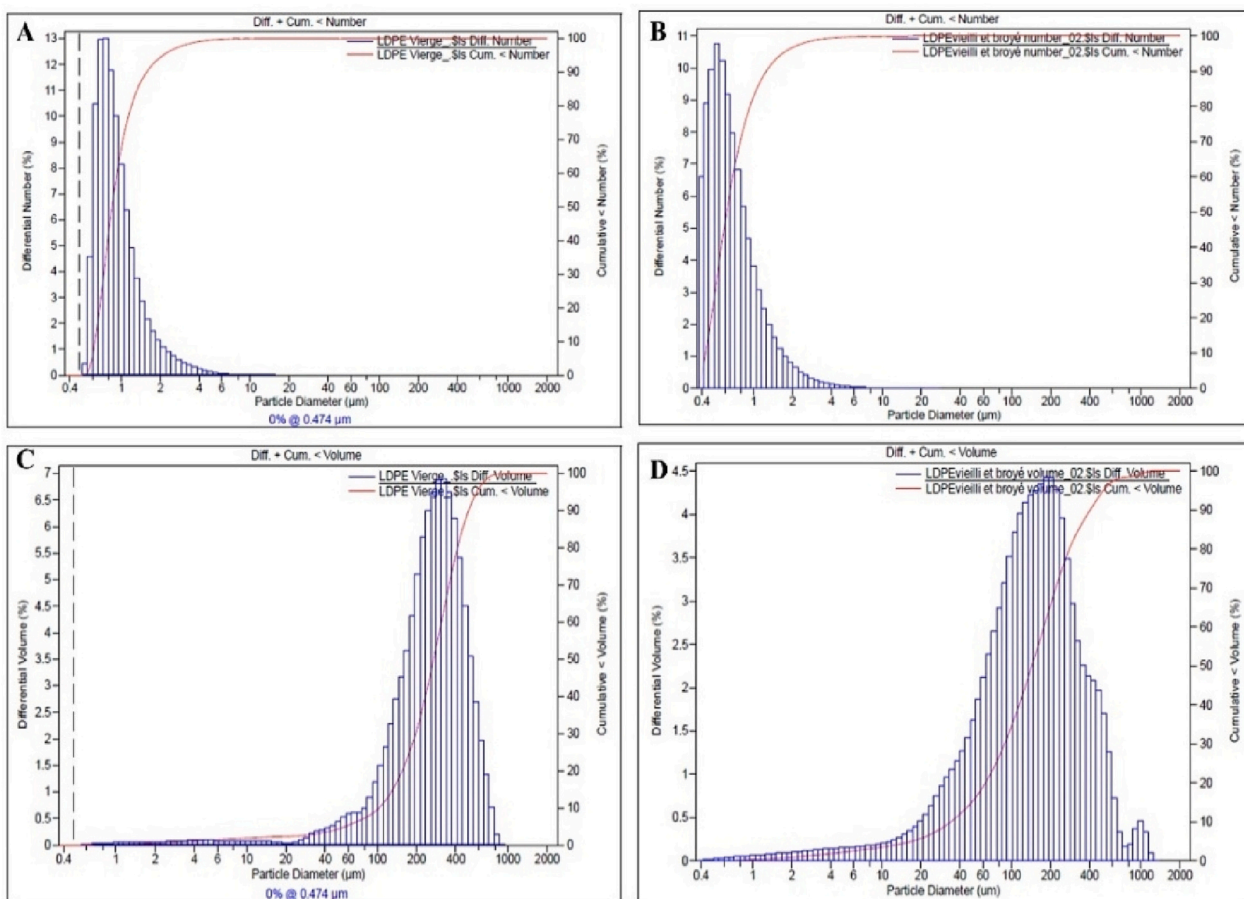


Fig. 2. Granulometry analysis of LDPE particles. Number: A: Raw LDPE, B: aged LDPE. Volume: C: Raw LDPE and D: aged LDPE.

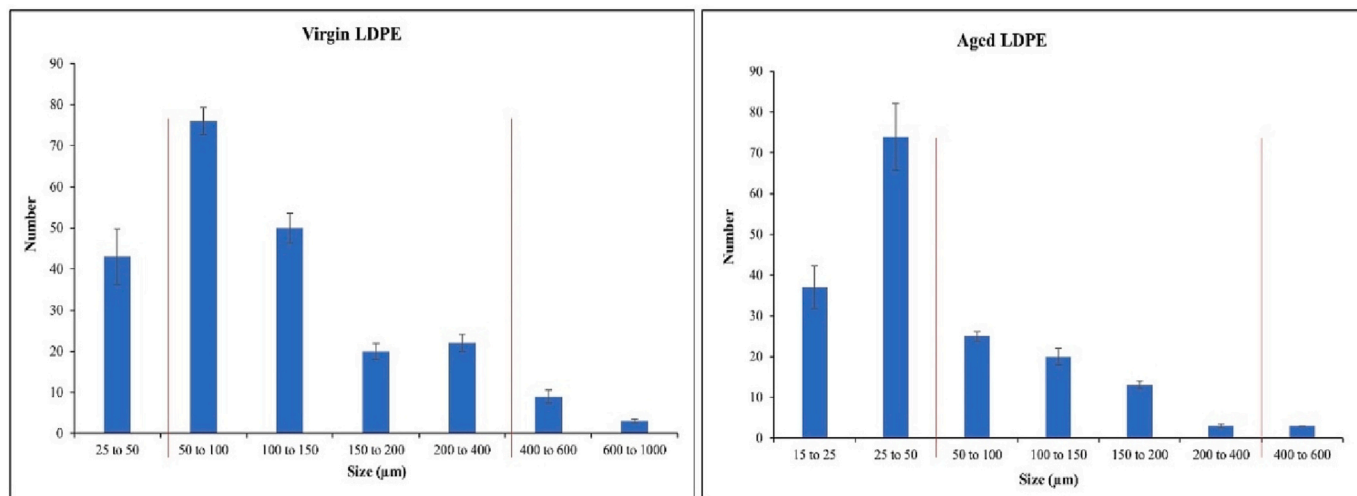


Fig. 3. Characterization of LDPE particles with Raman.

4. Discussion

Weathering of plastics can occur through physical or chemical degradation with photolytic, thermolytic, oxidative, ozone-induced, hydrolytic and biological as main processes (Singh and Sharma, 2008; Webb et al., 2013). However, different plastic polymers exhibit different degradation patterns in the environment. In this context, plastic aging makes ecotoxicity assessment challenging due to the potential release of chemical additive and polymer degradation products that could act as a

veritable cocktail of stressors (Fred-Ahmadu et al., 2020; Gaur et al., 2020; Webb et al., 2013). Ecotoxicological assessment hence requires discriminating between the physical effects of MPs from those associated with the additives (Barrick et al., 2021).

The objectives of this present study were to assess the impact of aging of MPs on the marine mussel *M. edulis* using two exposure scenarios: *in vivo* and *in vitro* approaches. Even though majority of studies focused on the effects of commercial MPs, not representative of those found in natural environments, one originality of the present study was to

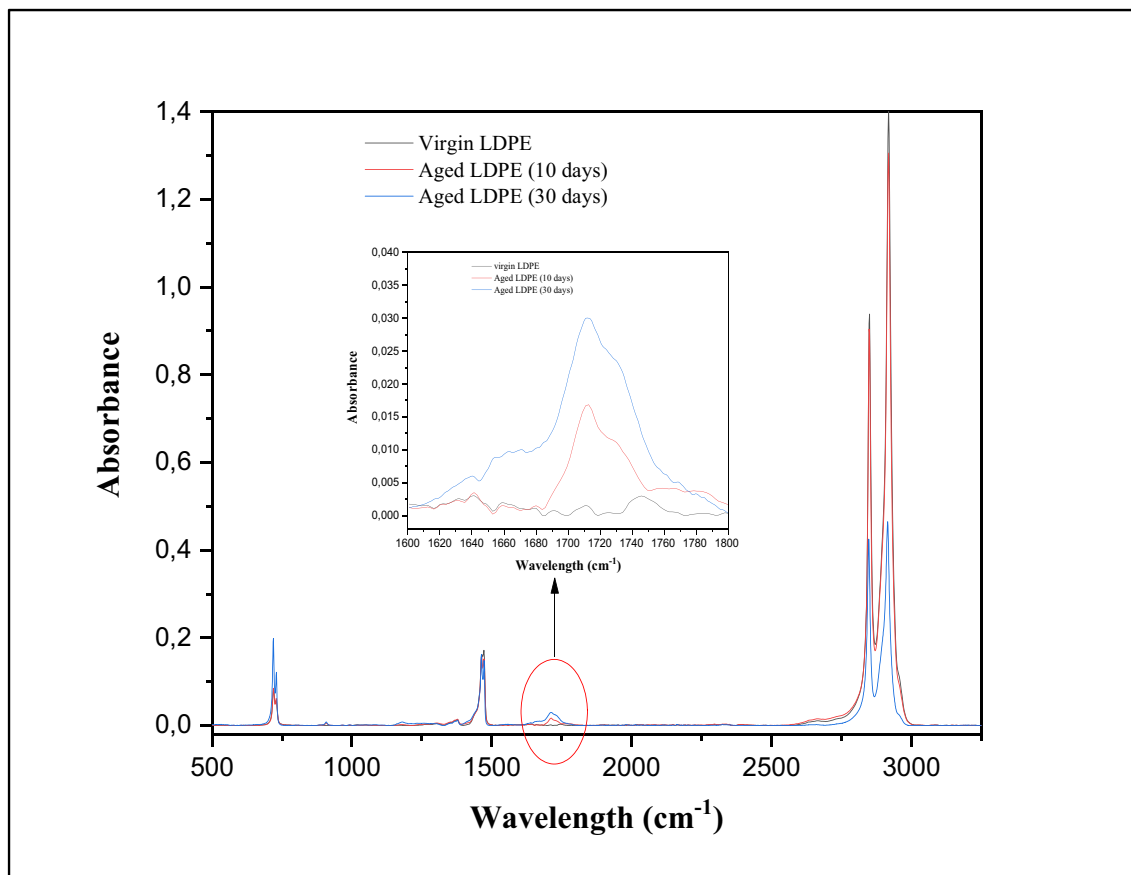


Fig. 4. Aging of LDPE particles.

Table 2

Differential gene expression (DGE) in *M. edulis* after 4 days *in vivo* exposure to aged and non-aged microplastics at 0.008, 10 and 100 $\mu\text{g}\cdot\text{L}^{-1}$. Only DGE significantly different from the control are presented. Green indicating an Up-regulation and Red indicating a down-regulation.

		Gills - 4 days - <i>In vivo</i> exposure					
		Non-aged MPs 0.008	Non-aged MPs 10	Non-aged MPs 100	Aged MPs 0.008	Aged MPs 10	Aged MPs 100
Oxidative stress	sod						
	cat		-4,349981413	-5,445175618			-4,298481193
Detoxication	gst		2,013710148			2,072086276	-1,993975299
	mt				-1,431292254		
	cyp						
Immunity	lys						
Apoptosis	p53		0,864251706	0,651890872			
Cytoskeleton	act			1,853321937	4,368244976	1,658129417	

investigate the effect of aging on the toxicity induced by PE on the marine mussel. PE microbeads have been aged in laboratory to reproduce its natural fate in marine environments and concentrations close to the ones recorded in marine waters were selected (0.008; 10 and 100 $\mu\text{g}\cdot\text{L}^{-1}$) which are representative of coastal regions or gyres (Goldstein et al., 2013; Ivar Do Sul et al., 2014).

In the present study, two ways of exposure were investigated and two tissues were analyzed: gills (for *in vivo* analysis) and hemocytes (available in the laboratory for cell culture). Gills represent a first site of MPs uptake from the water, and are also sensitive to MPs toxic effects (Magara et al., 2018). Hemocytes then allow translocation of MPs towards different organs (Kolandhasamy et al., 2018; Browne et al., 2008; Magni et al., 2018; Paul-Pont et al., 2016; Von Moos et al., 2012). Even if those tissues are different, it allowed to compare their response under

different time of exposure (acute exposure 24 h *in vitro* on hemocytes and 4 days exposure *in vivo* on whole mussels). Vroom et al. (2017) showed that aged MPs are ingested by more copepods and at higher rates as compared to pristine plastics. In the present study, no MPs were found in tissues of mussels exposed *in vivo* to PE MPs nor to aged-PE MPs. In a previous study in the laboratory, mussels exposed to PE and polypropylene (PP) MPs depicted the presence of MPs only in the digestive gland from mussels exposed to the highest tested concentration (100 $\mu\text{g}\cdot\text{L}^{-1}$) and a very small number of particles was observed. The size of particles identified in digestive glands were lower than in biodeposits, suggesting that MPs were rapidly eliminated with faeces or pseudofaeces (Revel et al., 2019) like it was previously observed in oysters *Crassostrea gigas* exposed to Polystyrene (PS) (Sussarellu et al., 2016).

Only few studies investigated the effects of aging on marine

Table 3

Differential gene expression (DGE) in *M. edulis* after 24 h *in vitro* exposure to aged and non-aged microplastics at 0.008, 10 and 100 µg.L⁻¹. Only DGE significantly different from the control are presented. Green indicating an Up-regulation and Red indicating a d²own-regulation.

		Hemocytes - 24 hours - <i>In vitro</i> exposure					
		Non-aged MPs 0.008	Non-aged MPs 10	Non-aged MPs 100	Aged MPs 0.008	Aged MPs 10	Aged MPs 100
Oxidative stress	sod						
	cat	2,177890536					
Detoxication	gst						
	mt						
	cyp						
Immunity	lys		-1,033043074	-1,401079669			
Apoptosis	p53				-1,038327014		
Cytoskeleton	act	1,230325611					0,909788555

Table 4

P-values, measured through Kruskal-Wallis and Dunn, of *M. edulis* hemocytes exposed *in vivo* between exposure to non-aged and aged microplastics at 0.008, 10 and 100 µg.L⁻¹. Only p-values <0.05 are indicated.

		Gills - 4 days - <i>In vivo</i> exposure		
		Non-aged MPs 0.008	Non-aged MPs 10	Non-aged MPs 100
sod	Aged MPs 0.008			
	Aged MPs 10			
	Aged MPs 100			
cat	Aged MPs 0.008			
	Aged MPs 10			0,025236552
	Aged MPs 100			
gst	Aged MPs 0.008			
	Aged MPs 10			0,026229017
	Aged MPs 100			
mt	Aged MPs 0.008		0,001	0,035
	Aged MPs 10		0,021	
	Aged MPs 100		0,021	
cyp	Aged MPs 0.008			
	Aged MPs 10			
	Aged MPs 100			
lys	Aged MPs 0.008			
	Aged MPs 10			
	Aged MPs 100			
act	Aged MPs 0.008	0,041		
	Aged MPs 10			
	Aged MPs 100			
p53	Aged MPs 0.008		0,017817189	
	Aged MPs 10	0,017817189		
	Aged MPs 100		0,048325342	

organisms. Bringer et al. (2022) have demonstrated in the marine oyster *C. gigas*, effects on survival, responses to defense biomarkers, and fertilization success as well as alterations in swimming behavior, development and growth of larvae after 2 months exposure to environmental-aged MPs. It has also been demonstrated in fish that the joint treatment of aged microplastics and an antibiotic (SMX) increased the disorders of metabolism-related CYP enzymes (Huang et al., 2021).

Table 5

P-values, measured through Kruskal-Wallis and Dunn, of *M. edulis* hemocytes exposed *in vitro* between exposure to non-aged and aged microplastics at 0.008, 10 and 100 µg.L⁻¹. Only p-values <0.05 are indicated.

		Hemocytes - 24 h - <i>In vitro</i> exposure		
		Non-aged MPs 0.008	Non-aged MPs 10	Non-aged MPs 100
sod	Aged MPs 0.008			
	Aged MPs 10			
	Aged MPs 100			
cat	Aged MPs 0.008	0,000	0,035	0,012
	Aged MPs 10	0,048		
	Aged MPs 100			
gst	Aged MPs 0.008			
	Aged MPs 10			
	Aged MPs 100			
mt	Aged MPs 0.008			
	Aged MPs 10			
	Aged MPs 100			
cyp	Aged MPs 0.008			
	Aged MPs 10			
	Aged MPs 100			
lys	Aged MPs 0.008	0,012		
	Aged MPs 10	0,041		
	Aged MPs 100	0,048		
act	Aged MPs 0.008	0,002	0,030	0,015
	Aged MPs 10			
	Aged MPs 100			
p53	Aged MPs 0.008	0,005		
	Aged MPs 10			
	Aged MPs 100			

4.1. Detoxification process

Results of the present study showed induction of detoxification processes after mussel exposure to aged and non-aged MPs.

sod represents the first defensive system against reactive oxygen species (ROS) production since it catalyzes the dismutation of O₂⁻ to H₂O₂. Catalase is an enzyme involved in the first stage of the detoxification process, that help protect cell from oxidative damage. This enzyme catalyzes the conversion of H₂O₂ into H₂O. Results showed no modification of sod gene expression for any of the tested conditions. However, cat gene expression was modified in mussels exposed *in vivo* for the high concentrations (10 and 100 µg/L for non-aged MP and 100 µg/L for aged MP). Ribeiro et al. (2017) also demonstrated an increase in

cat activity in gills of the estuarine bivalve *S.plana* after 21 days (14 days of exposure and 7 days of depuration) to PS MPs (20 μm , 1 mg.L^{-1}). The same result has also been observed in digestive glands of the mussel *Mytilus* spp. after 10 day exposure to 0.008 and 10 $\mu\text{g.L}^{-1}$ of PE and PP (400 μm) (Revel et al., 2019) but not in the oyster *C.gigas* after exposure to the same conditions (Revel et al., 2020). In the present study, the only *cat* expression modification observed *in vitro* at 0.008 $\mu\text{g/L}$ could be due to a more direct toxic effect of MP on cell culture as compared *in vivo* where only high concentrations of plastic have an effect. Whereas both types of plastics (non-aged and aged MP) induced *cat* gene expression modification *in vivo*, only non-aged MP depict mRNA *cat* expression induction *in vitro*. This suggest that cells could be more sensitive to differences in MP aging state compared to whole organisms.

gst is the main phase II enzyme involved in the oxidative stress response which catalyzes the conjugation of xenobiotics and endogenous compounds to the GSH (reduced glutathione). Results did not depict any difference between MP exposed mussels and control ones as regards to *gst* gene expression. However, a significant difference of this gene expression was observed between aged and non-aged-MP at a concentration of 100 $\mu\text{g.L}^{-1}$. A meta-analysis conducted by Li et al. (2021) specifically on bivalves and their responses to oxidative stress induced by MPs showed a strong response of the antioxidant system during MPs short-term exposure to counteract the imbalance of ROS production and suggested that *cat* activity could be a better reliable biomarker as compared to *gst* for long-term studies of exposure to MPs. Whereas *gst* mRNA expression was not different in all tested plastic conditions *in vitro* as compared to control group, it showed an increase in mussels exposed *in vivo* to 10 $\mu\text{g/L}$ of aged and non-aged MP and a decrease after exposure to 100 $\mu\text{g/L}$ of aged MP. This indicated that detoxification process occurred only *in vivo* after exposure of gills to MP.

In addition, (MTs) gene expression, also involved in both antioxidant defense and metal detoxification showed a decrease in mussels exposed *in vivo* to aged-MP (0.008 $\mu\text{g.L}^{-1}$) as compared to control mussels. In addition, its expression was significantly different when mussels were exposed to aged-MPs compared to non-aged MPs, suggesting that the fate of MPs has an influence on their detoxification out of the organisms and that different retention times could explain differences in MPs toxicity within organisms. Boyle et al. (2020) have also demonstrated that exposure of zebrafish larvae to PVC for 24 h induced a dose-dependent increase in gene expression of metallothionein 2 (mt2).

4.2. Immune system

Mussels also presented a decrease in gene expression of lysozyme when they were exposed *in vitro* to non-aged MPs (10 and 100 $\mu\text{g.L}^{-1}$). Short HDPE MPs exposures have been demonstrated to induce inflammatory cellular response as well as production of reactive oxygen species in the marine mussel (Canesi et al., 2015; Von Moos et al., 2012), also observed in the digestive gland of mussels exposed to PS and PE using microarray (Avio et al., 2015). Franzellitti et al. (2019) also exposed *M. galloprovincialis* embryos to 3 μm PS MPs and observed up-regulation of transcripts related to immune responses, and down-regulation of those involved in lysosome. This suggest MPs uptake by mussels and hence stimulation of the digestive and immune system, that are closely interconnected (Balseiro et al., 2013; Dyachuk, 2016). Tang et al. (2020) also demonstrated that PS MPs exert immunotoxic impacts on blood clam through interrupting immune, Ca^{2+} levels, and apoptosis related molecular pathways. The only effect on lysosome gene expression *in vitro* could be explained by the fact that hemocytes, as immune cells in mussels, respond directly to MP, as gills may not be ideal cells to measure this parameter.

4.3. Cytoskeleton

In addition to this induction of immune system and ROS production, actin filaments, responsible of particle transport throughout the

cytoplasm are known to be sensitive to ROS production (Pollard and Cooper, 2009; Tomanek et al., 2011).

The induction of ROS theoretically allows elimination of the exogenous substance (Dupré-Crochet et al., 2013). However, excessive intracellular ROS may also inhibit the phagocytic activity not only *via* induction of oxidative stress (Pollard and Cooper, 2009; Tomanek et al., 2011), but also triggering apoptosis and subsequently constraining the number of hemocytes available for phagocytic reaction (Circu and Aw, 2010; Faggio et al., 2016; Savorelli et al., 2017; Sehonova et al., 2018). Whatever the approach tested (*in vitro* and *in vivo*) and the type of tissues analyzed (hemocytes and gills), results showed that this type of PE MP induced p53 gene expression modification that might be due to potential DNA damage inductions. The results obtained in this study suggest that PE MPs may exert immunotoxic impacts on mussels through disruption of the cell cycle regulator p53 and potentially inducing apoptosis. Tang et al., (2020) also showed in the clam exposure to PS MPs, an impairment of immune system, Ca^{2+} levels, and apoptosis related molecular pathways. The inhibition of p53 gene expression levels after *in vitro* hemocyte exposure to aged MPs could be a consequence of an over induction of apoptosis induced by elevated intracellular ROS and indicate an interruption of apoptosis process, which may hamper the normal function of hemocytes and result in reduced immune ability (Tang et al., 2020).

4.4. Importance of experimental approach for MP risk assessment evaluation

Results of this present study demonstrated that slight differences between toxicity mechanisms could be addressed *via* a transcriptomic approach that is a sensitive tool to detect small changes between conditions. Molecular analysis contributes to a better understanding of the complex responses of organisms facing different stressors (Détrée and Gallardo-Escárate, 2017). In addition, the interest of using transcriptomic analyses based on analysis of gene expression patterns has been highly demonstrated in an ecotoxicological context (Baillon et al., 2015a, 2015b; Campos et al., 2012; Denslow et al., 2007; Moisset et al., 2015; Pierron et al., 2011; Qian et al., 2014).

In vivo MPs exposures demonstrated statistical differences between aged and non-aged MPs as regards to detoxification processes and cytoskeleton whereas *in vitro* exposure showed more significant differences between types of MPs on detoxification, immune system, cytoskeleton and cell cycle regulation processes. This demonstrates the sensitivity of *in vitro* exposures, coupled with transcriptomic analysis, to rapidly screen toxicity of such emerging contaminants before investigated more time consuming (and also more environmental representative) exposures such as *in vivo* exposures (Barrick et al., 2017). As a global concern, there is an urgent need to generate data on the toxicity mechanisms implicated by MPs and in this context, the use of *in vitro* approaches appear relevant to rapidly screen a large range of chemicals (Revel et al., 2020).

This study gave first insights about the study of the effects of aged-MPs versus non aged-MPs in the marine mussel *M. edulis* using two exposure scenarios. Further studies need to be investigated to test the effects of those types of MPs for longer period of exposure, than would allow also to measure additional individual markers such as energetic reserves or behavioural markers so as to link molecular effects to individual ones in the context of an Adverse Outcome Pathway (AOP) approach.

Funding

This work was supported by the project TROPHIPLAST, funded by the French national agency ANSES (grant agreement 2018/1/017). Authors also acknowledge the University of Carthage and Le Mans University, which provided financial support for this work. Thanks are also due for Le Mans Technology Transfer Center, where microplastics IR analysis were realized.

CRediT authorship contribution statement

Rihab Jaouani and Coraline Roman have both contributed to experiments (production of microplastics, exposures, transcriptomic analysis).

Justine Decaix conducted qPCR analysis.

Fabienne Lagarde and Amélie Châtel have supervised the work.

Declaration of competing interest

The authors declare that they have no known competing financial interests or personal relationships that could have appeared to influence the work reported in this paper.

Data availability

Data will be made available on request.

Appendix A. Supplementary data

Supplementary data to this article can be found online at <https://doi.org/10.1016/j.marpolbul.2023.114767>.

References

- Andersen, C.F., Anand, M., Boesen, T., Van, L.B., Kinzy, T.G., Andersen, G.R., 2004. Purification and crystallization of the yeast translation elongation factor eEF3. *Acta Crystallogr. D60*, 1304–1307. <https://doi.org/10.1107/S0907444904010716>.
- Andrady, A.L., 2011. Microplastics in the marine environment. *Mar. Pollut. Bull.* 62 (8), 1596–1605. <https://doi.org/10.1016/j.marpolbul.2011.05.030>.
- Avio, C.G., Gorbi, S., Milan, M., Benedetti, M., Fattorini, D., D'Errico, G., Pauletto, M., Bargelloni, L., Regoli, F., 2015. Pollutants bioavailability and toxicological risk from microplastics to marine mussels. *Environ. Pollut.* 198, 211–222. <https://doi.org/10.1016/j.envpol.2014.12.021>.
- Baillon, L., Oses, J., Pierron, F., Bureau du Colombier, S., Caron, A., Normandeau, E., Lambert, P., Couture, P., Labadie, P., Budzinski, H., Dufour, S., Bernatchez, L., Baudrimont, M., 2015. Gonadal transcriptome analysis of wild contaminated female european eels during artificial gonad maturation. *Chemosphere* 139, 303–309. <https://doi.org/10.1016/j.chemosphere.2015.06.007>.
- Baillon, L., Pierron, F., Coudret, R., Normandeau, E., Caron, A., Peluhet, L., Labadie, P., Budzinski, H., Durrieu, G., Sarraco, J., Elie, P., Couture, P., Baudrimont, M., Bernatchez, L., 2015. Transcriptome profile analysis reveals specific signatures of pollutants in Atlantic eels. *Ecotoxicology* 24 (1), 71–84. <https://doi.org/10.1007/s10646-014-1356-x>.
- Balseiro, P., Moreira, R., Chamorro, R., Figueras, A., Novoa, B., 2013. Immune responses during the larval stages of *Mytilus galloprovincialis*: metamorphosis alters immunocompetence, body shape and behavior. *Fish Shellfish Immunol.* 35 (2), 438–447. <https://doi.org/10.1016/j.fsi.2013.04.044>.
- Barnes, D.K.A., Galgani, F., Thompson, R.C., Barlaz, M., 2009. Accumulation and fragmentation of plastic debris in global environments. *Philos. Trans. R. Soc., B* 364 (1526), 1985–1998. <https://doi.org/10.1098/rstb.2008.0205>.
- Barrick, A., Châtel, A., Bruneau, M., Mouneyrac, C., 2017. The role of high-throughput screening in ecotoxicology and engineered nanomaterials. *Environ. Toxicol. Chem.* 36 (7), 1704–1714. <https://doi.org/10.1002/etc.3811>.
- Barrick, A., Guillet, C., Mouneyrac, C., Châtel, A., 2018. Investigating the establishment of primary cultures of hemocytes from *Mytilus edulis*. *Cytotechnology* 70 (4), 1205–1220. <https://doi.org/10.1007/s10616-018-0212-x>.
- Barrick, A., Manier, N., Lonchambon, P., Flahaut, E., Jrad, N., Mouneyrac, C., Châtel, A., 2019. Investigating a transcriptomic approach on marine mussel hemocytes exposed to carbon nanofibers: an in vitro/in vivo comparison. *Aquat. Toxicol.* 207 (November 2018), 19–28. <https://doi.org/10.1016/j.aquatox.2018.11.020>.
- Barrick, A., Champeau, O., Châtel, A., Manier, N., Northcott, G., Tremblay, L.A., 2021. Plastic additives: challenges in ecotox hazard assessment. *PeerJ* 9, e11300. <https://doi.org/10.7717/peerj.11300>.
- Botterell, Z.L.R., Beaumont, N., Dorrington, T., Steinke, M., Thompson, R.C., Lindeque, P. K., 2019. Bioavailability and effects of microplastics on marine zooplankton: a review. *Environ. Pollut.* 245, 98–110. <https://doi.org/10.1016/j.envpol.2018.10.065>.
- Bour, A., Haarr, A., Keiter, S., Hylland, K., 2018. Environmentally relevant microplastic exposure affects sediment-dwelling bivalves. *Environ. Pollut.* 236, 652–660. <https://doi.org/10.1016/j.envpol.2018.02.006>.
- Boyle, D., Catarino, A.L., Clark, N.J., Henry, T.B., 2020. Polyvinyl chloride (PVC) plastic fragments release pb additives that are bioavailable in zebrafish. *Environ. Pollut.* 263, 114422. <https://doi.org/10.1016/j.envpol.2020.114422>.
- Bringer, A., Cachot, J., Prunier, G., Huet, V., Clérandeau, C., Evin, L., Thomas, H., 2022. Intergenerational effects of environmentally-aged microplastics on the *Crasostrea gigas*. *Environmental Pollution*, 294 pp.118600.
- Browne, M.A., Galloway, T.S., Thompson, R.C., 2010. Spatial patterns of plastic debris along estuarine shorelines. *Environ. Sci. Technol.* 44 (9), 3404–3409. <https://doi.org/10.1021/es903784e>.
- Campos, A., Tedesco, S., Vasconcelos, V., Cristobal, S., 2012. Proteomic research in bivalves. Towards the identification of molecular markers of aquatic pollution. *J. Proteome* 75 (14), 4346–4359. <https://doi.org/10.1016/j.jprot.2012.04.027>.
- Canesi, L., Ciacci, C., Bergami, E., Monopoli, M.P., Dawson, K.A., Papa, S., Canonico, B., Corsi, I., 2015. Evidence for immunomodulation and apoptotic processes induced by cationic polystyrene nanoparticles in the hemocytes of the marine bivalve *Mytilus*. *Mar. Environ. Res.* 111, 34–40. <https://doi.org/10.1016/j.marenvres.2015.06.008>.
- Châtel, A., Lièvre, C., Barrick, A., Bruneau, M., Mouneyrac, C., 2018. Transcriptomic approach: a promising tool for rapid screening nanomaterial-mediated toxicity in the marine bivalve *Mytilus edulis*—application to copper oxide nanoparticles. *Comp. Biochem. Physiol. C: Toxicol. Pharmacol.* 205 (January), 26–33. <https://doi.org/10.1016/j.cbpc.2018.01.003>.
- Chevê, J., Bernard, G., Passelergue, S., Prigent, J.-L., 2014. *Suivi bactériologique des gisements naturels de coquillages de l'Île-et-Vilaine et des Côtes-d'Armor fréquentés en pêche à pied*, pp. 1–99.
- Choi, J.S., Kim, K., Hong, S.H., Park, K.I., Park, J.W., 2021. Impact of polyethylene terephthalate microfiber length on cellular responses in the Mediterranean mussel *Mytilus galloprovincialis*. *Mar. Environ. Res.* 168 (September 2020), 105320. <https://doi.org/10.1016/j.marenvres.2021.105320>.
- Circu, M.L., Aw, T.Y., 2010. Reactive oxygen species, cellular redox systems, and apoptosis. *Free Radic. Biol. Med.* 48 (6), 749–762. <https://doi.org/10.1016/j.freeradbiomed.2009.12.022>.
- Cole, M., Lindeque, P., Halsband, C., Galloway, T.S., 2011. Microplastics as contaminants in the marine environment: a review. *Mar. Pollut. Bull.* 62 (12), 2588–2597. <https://doi.org/10.1016/j.marpolbul.2011.09.025>.
- Cole, M., Lindeque, P., Fileman, E., Halsband, C., Goodhead, R., Moger, J., Galloway, T. S., 2013. Microplastic ingestion by zooplankton. *Environ. Sci. Technol.* 47 (12), 6646–6655. <https://doi.org/10.1021/es400663f>.
- Colton, J.B., Knapp, F.D., Bums, B.R., 1974. Plastic particles in surface. *Science* 185 (4150), 491–497. <https://science.sciencemag.org/content/185/4150/491>.
- Denslow, N.D., Garcia-Reyero, N., Barber, D.S., 2007. Fish “n” chips: the use of microarrays for aquatic toxicology. *Mol. Biosyst.* 3 (3), 172–177. <https://doi.org/10.1039/b612802p>.
- Détré, C., Gallardo-Escárate, C., 2017. Polyethylene microbeads induce transcriptional responses with tissue-dependent patterns in the mussel *Mytilus galloprovincialis*. *J. Molluscan Stud.* 83 (2), 220–225. <https://doi.org/10.1093/mollus/eyy005>.
- Digka, N., Tsangaris, C., Torre, M., Anastasopoulou, A., Zeri, C., 2018. Microplastics in mussels and fish from the northern Ionian Sea. *Mar. Pollut. Bull.* 135 (June), 30–40. <https://doi.org/10.1016/j.marpolbul.2018.06.063>.
- Donohue, M.J., Masura, J., Gelatt, T., Ream, R., Baker, J.D., Faulhaber, K., Lerner, D.T., 2019. Evaluating exposure of northern fur seals, *Callorhinus ursinus*, to microplastic pollution through fecal analysis. *Mar. Pollut. Bull.* 138 (October 2018), 213–221. <https://doi.org/10.1016/j.marpolbul.2018.11.036>.
- Dowarah, K., Patchaiyappan, A., Thirunavukkarasu, C., Jayakumar, S., Devipriya, S.P., 2020. Quantification of microplastics using Nile red in two bivalve species *Perna viridis* and *Meretrix meretrix* from three estuaries in Pondicherry, India and microplastic uptake by local communities through bivalve diet. *Mar. Pollut. Bull.* 153 (January), 110982. <https://doi.org/10.1016/j.marpolbul.2020.110982>.
- Dupré-Crochet, S., Erard, M., Nüße, O., 2013. ROS production in phagocytes: why, when, and where? *J. Leukoc. Biol.* 94 (4), 657–670. <https://doi.org/10.1189/jlb.1012544>.
- Dyachuk, V.A., 2016. Hematopoiesis in bivalvia larvae: cellular origin, differentiation of hemocytes, and neoplasia. *Dev. Comp. Immunol.* 65, 253–257. <https://doi.org/10.1016/j.dci.2016.07.019>.
- Eriksen, M., Mason, S., Wilson, S., Box, C., Zellers, A., Edwards, W., Farley, H., Amato, S., 2013. Microplastic pollution in the surface waters of the Laurentian Great Lakes. *Mar. Pollut. Bull.* 77 (1–2), 177–182. <https://doi.org/10.1016/j.marpolbul.2013.10.007>.
- Faggio, C., Pagano, M., Alampi, R., Vazzana, I., Felice, M.R., 2016. Cytotoxicity, haemolymphatic parameters, and oxidative stress following exposure to sub-lethal concentrations of quaternium-15 in *Mytilus galloprovincialis*. *Aquat. Toxicol.* 180, 258–265. <https://doi.org/10.1016/j.aquatox.2016.10.010>.
- Franzellitti, S., Capolupo, M., Wathsala, R.H.G.R., Valbonesi, P., Fabbri, E., 2019. The multixenobiotic resistance system as a possible protective response triggered by microplastic ingestion in Mediterranean mussels (*Mytilus galloprovincialis*): larvae and adult stages. *Comp. Biochem. Physiol. C: Toxicol. Pharmacol.* 219 (January), 50–58. <https://doi.org/10.1016/j.cbpc.2019.02.005>.
- Fred-Ahmadu, O.H., Ayejuyo, O.O., Benson, N.U., 2020. Dataset on microplastics and associated trace metals and phthalate esters in sandy beaches of tropical Atlantic ecosystems, Nigeria. *Data Brief* 31, 105755. <https://doi.org/10.1016/j.dib.2020.105755>.
- Fu, D., Zhang, Q., Fan, Z., Qi, H., Wang, Z., Peng, L., 2019. Aged microplastics polyvinyl chloride interact with copper and cause oxidative stress towards microalgae *Chlorella vulgaris*. *Aquat. Toxicol.* 216 (July), 105319. <https://doi.org/10.1016/j.aquatox.2019.105319>.
- Gaur, N., Organisation, D., Choudhary, R., 2020. *Handbook of Environmental Materials Management. Handbook of Environmental Materials Management*, January. <https://doi.org/10.1007/978-3-319-58538-3>.
- Giani, D., Bains, M., Galli, M., Casini, S., Fossi, M.C., 2019. Microplastics occurrence in edible fish species (*Mullus barbatus* and *Merluccius merluccius*) collected in three different geographical sub-areas of the Mediterranean Sea. *Mar. Pollut. Bull.* 140 (January), 129–137. <https://doi.org/10.1016/j.marpolbul.2019.01.005>.
- Goldstein, M.C., Titmus, A.J., Ford, M., 2013. Scales of spatial heterogeneity of plastic marine debris in the Northeast Pacific Ocean. *PLoS ONE* 8 (11). <https://doi.org/10.1371/journal.pone.0080020>.

- Hale, R.C., Seeley, M.E., La Guardia, M.J., Mai, L., Zeng, E.Y., 2020. A global perspective on microplastics. *J. Geophys. Res. Oceans* 125 (1). <https://doi.org/10.1029/2018JC014719>.
- Hernandez-Gonzalez, A., Saavedra, C., Gago, J., Covelo, P., Santos, M.B., Pierce, G.J., 2018. Microplastics in the stomach contents of common dolphin (*Delphinus delphis*) stranded on the galician coasts (NW Spain, 2005–2010). *Mar. Pollut. Bull.* 137 (October), 526–532. <https://doi.org/10.1016/j.marpolbul.2018.10.026>.
- Horton, A.A., Barnes, D.K.A., 2020. Microplastic pollution in a rapidly changing world: implications for remote and vulnerable marine ecosystems. *Sci. Total Environ.* 738, 140349 <https://doi.org/10.1016/j.scitotenv.2020.140349>.
- Huang, Y., Ding, J., Zhang, G., Liu, S., Zou, H., Wang, Z., Zhu, W., Geng, J., 2021. Interactive effects of microplastics and selected pharmaceuticals on red tilapia: role of microplastic aging. *Sci. Total Environ.* 752, 142256 <https://doi.org/10.1016/j.scitotenv.2020.142256>.
- Ivar Do Sul, J.A., Costa, M.F., Fillmann, G., 2014. Microplastics in the pelagic environment around oceanic islands of the western Tropical Atlantic Ocean. *Water Air Soil Pollut.* 225 (7) <https://doi.org/10.1007/s11270-014-2004-z>.
- Julienne, F., Delorme, N., Lagarde, F., 2019. From macroplastics to microplastics: role of water in the fragmentation of polyethylene. *Chemosphere* 236, 124409.
- Klasios, N., De Frond, H., Miller, E., Sedlak, M., Rochman, C.M., 2021. Microplastics and other anthropogenic particles are prevalent in mussels from San Francisco Bay, and show no correlation with PAHs. *Environ. Pollut.* 271, 116260 <https://doi.org/10.1016/j.envpol.2020.116260>.
- Kolandhasamy, P., Su, L., Li, J., Qu, X., Jabeen, K., Shi, H., 2018. Adherence of microplastics to soft tissue of mussels: a novel way to uptake microplastics beyond ingestion. *Sci. Total Environ.* 610–611, 635–640. <https://doi.org/10.1016/j.scitotenv.2017.08.053>.
- LeMoine, C.M.R., Kelleher, B.M., Lagarde, R., Northam, C., Elebute, O.O., Cassone, B.J., 2018. Transcriptional effects of polyethylene microplastics ingestion in developing zebrafish (*Danio rerio*). *Environ. Pollut.* 243, 591–600. <https://doi.org/10.1016/j.envpol.2018.08.084>.
- Li, Q., Sun, C., Wang, Y., Cai, H., Li, L., Li, J., Shi, H., 2019. Fusion of microplastics into the mussel byssus. *Environ. Pollut.* 252, 420–426. <https://doi.org/10.1016/j.envpol.2019.05.093>.
- Li, Z., Chang, X., Hu, M., Fang, J.K.H., Huang, W., Xu, E.G., Wang, Y., 2021. Is microplastic an oxidative stressor? Evidence from a meta-analysis on bivalves. *J. Hazard. Mater.* 423, 127211.
- Liu, G., Zhu, Z., Yang, Y., Sun, Y., Yu, F., Ma, J., 2019. Sorption behavior and mechanism of hydrophilic organic chemicals to virgin and aged microplastics in freshwater and seawater. *Environ. Pollut.* 246, 26–33. <https://doi.org/10.1016/j.envpol.2018.11.100>.
- Liu, J., Zhang, T., Tian, L., Liu, X., Qi, Z., Ma, Y., Ji, R., Chen, W., 2019. Aging significantly affects mobility and contaminant-mobilizing ability of nanoplastics in saturated loamy sand. *Environ. Sci. Technol.* 53 (10), 5805–5815. <https://doi.org/10.1021/acs.est.9b00787>.
- Luo, H., Xiang, Y., He, D., Li, Y., Zhao, Y., Wang, S., Pan, X., 2019. Leaching behavior of fluorescent additives from microplastics and the toxicity of leachate to *Chlorella vulgaris*. *Sci. Total Environ.* 678, 1–9. <https://doi.org/10.1016/j.scitotenv.2019.04.401>.
- Magara, G., Elia, A.C., Syberg, K., Khan, F.R., 2018. Single contaminant and combined exposures of polyethylene microplastics and fluoranthene: accumulation and oxidative stress response in the blue mussel, *Mytilus edulis*. *J. Toxicol. Environ. Health Part A* 81 (16), 761–773. <https://doi.org/10.1080/15287394.2018.1488639>.
- Magni, S., Gagné, F., André, C., Della Torre, C., Auclair, J., Hanana, H., Parenti, C.C., Bonasoro, F., Binelli, A., 2018. Evaluation of uptake and chronic toxicity of virgin polystyrene microbeads in freshwater zebra mussel *Dreissena polymorpha* (Mollusca: Bivalvia). *Sci. Total Environ.* 631–632, 778–788. <https://doi.org/10.1016/j.scitotenv.2018.03.075>.
- Moisset, S., Tiam, S.K., Feurtet-Mazel, A., Morin, S., Delmas, F., Mazzella, N., Gonzalez, P., 2015. Genetic and physiological responses of three freshwater diatoms to realistic diuron exposures. *Environ. Sci. Pollut. Res.* 22 (6), 4046–4055. <https://doi.org/10.1007/s11356-014-3523-2>.
- Moore, C.J., 2008. Synthetic polymers in the marine environment: a rapidly increasing, long-term threat. *Environ. Res.* 108 (2), 131–139. <https://doi.org/10.1016/j.envres.2008.07.025>.
- Murphy, F., Quinn, B., 2018. The effects of microplastic on freshwater *Hydra attenuata* feeding, morphology & reproduction. *Environ. Pollut.* 234, 487–494. <https://doi.org/10.1016/j.envpol.2017.11.029>.
- Paul-Pont, I., Lacroix, C., González Fernández, C., Hégaret, H., Lambert, C., Le Goïc, N., Frère, L., Cassone, A.L., Sussarellu, R., Fabioux, C., Guyomarch, J., Albentosa, M., Huvet, A., Soudant, P., 2016. Exposure of marine mussels *mytilus* spp. To polystyrene microplastics: toxicity and influence on fluoranthene bioaccumulation. *Environ. Pollut.* 216, 724–737. <https://doi.org/10.1016/j.envpol.2016.06.039>.
- Phuong, N.N., Poirier, L., Pham, Q.T., Lagarde, F., Zalouk-Vergnoux, A., 2018. Factors influencing the microplastic contamination of bivalves from the french Atlantic coast: location, season and/or mode of life? *Mar. Pollut. Bull.* 129 (2), 664–674. <https://doi.org/10.1016/j.marpolbul.2017.10.054>.
- Pierron, F., Normandeau, E., Defo, M.A., Campbell, P.G.C., Bernatchez, L., Couture, P., 2011. Effects of chronic metal exposure on wild fish populations revealed by high-throughput cDNA sequencing. *Ecotoxicology* 20 (6), 1388–1399. <https://doi.org/10.1007/s10646-011-0696-z>.
- Pollard, T.D., Cooper, J.A., 2009. Actin, a central player in cell shape and movement. *Science* 326 (5957), 1208–1212. <https://doi.org/10.1126/science.1175862>.
- Qian, X., Ba, Y., Zhuang, Q., Zhong, G., 2014. RNA-seq technology and its application in fish transcriptomics. *OMICS* 18 (2), 98–110. <https://doi.org/10.1089/omi.2013.0110>.
- Revel, M., Lagarde, F., Perrein-Ettajani, H., Bruneau, M., Akcha, F., Sussarellu, R., Rouxel, J., Costil, K., Decottignies, P., Cognie, B., Châtel, A., Mouneyrac, C., 2019. Tissue-specific biomarker responses in the blue mussel *Mytilus* spp. exposed to a mixture of microplastics at environmentally relevant concentrations. *Front. Environ. Sci.* 7 (MAR), 1–14. <https://doi.org/10.3389/fenvs.2019.00033>.
- Revel, M., Châtel, A., 2017. MouneyracOmics tools: new challenges in aquatic nanotoxicology? *Aquat. Toxicol.* 193, 72–85. <https://doi.org/10.1016/j.aquatox.2017.10.005>.
- Revel, M., Châtel, A., Perrein-Ettajani, H., Bruneau, M., Akcha, F., Sussarellu, R., Rouxel, J., Costil, K., Decottignies, P., Cognie, B., Lagarde, F., Mouneyrac, C., 2020. Realistic environmental exposure to microplastics does not induce biological effects in the Pacific oyster *Crassostrea gigas*. *Mar. Pollut. Bull.* 150 <https://doi.org/10.1016/j.marpolbul.2019.110627>.
- Ribeiro, F., Garcia, A.R., Pereira, B.P., Fonseca, M., Mestre, N.C., Fonseca, T.G., Ilharco, L.M., Bebianno, M.J., 2017. Microplastics effects in *Scrobicularia plana*. *Mar. Pollut. Bull.* 122, 379–391.
- Rodrigues, M.O., Abrantes, N., Gonçalves, F.J.M., Nogueira, H., Marques, J.C., Gonçalves, A.M.M., 2018. Spatial and temporal distribution of microplastics in water and sediments of a freshwater system (Antua River, Portugal). *Sci. Total Environ.* 633, 1549–1559.
- Romdhani, I., De Marco, G., Cappello, T., Iballa, S., Zitouni, N., Boughattas, I., Banni, M., 2022. Impact of environmental microplastics alone and mixed with benzo(a)pyrene on cellular and molecular responses of *Mytilus galloprovincialis*. *J. Hazard. Mater.* 435 (April), 128952 <https://doi.org/10.1016/j.jhazmat.2022.128952>.
- Savorelli, F., Manfra, L., Croppo, M., Tornambè, A., Palazzi, D., Canepa, S., Trentini, P.L., Cicero, A.M., Faggio, C., 2017. Fitness evaluation of ruditapes philippinarum exposed to ni. *Biol. Trace Elem. Res.* 177 (2), 384–393. <https://doi.org/10.1007/s12011-016-0885-y>.
- Sehonova, P., Svobodova, Z., Dolezelova, P., Vosmerova, P., Faggio, C., 2018. Effects of waterborne antidepressants on non-target animals living in the aquatic environment: a review. *Sci. Total Environ.* 631–632, 789–794. <https://doi.org/10.1016/j.scitotenv.2018.03.076>.
- Singh, B., Sharma, N., 2008. Mechanistic implications of plastic degradation. *Polym. Degrad. Stab.* 93 (3), 561–584. <https://doi.org/10.1016/j.polymdegradstab.2007.11.008>.
- Suhrhoff, T.J., Scholz-Böttcher, B.M., 2016. Qualitative impact of salinity, UV radiation and turbulence on leaching of organic plastic additives from four common plastics - a lab experiment. *Mar. Pollut. Bull.* 102 (1), 84–94. <https://doi.org/10.1016/j.marpolbul.2015.11.054>.
- Sussarellu, R., Suquet, M., Thomas, Y., Lambert, C., Fabioux, C., Pernet, M.E.J., Goïc, N., Le, Quillien, V., Mingant, C., Epelboin, Y., Corporeau, C., Guyomarch, J., Robbes, J., Paul-Pont, I., Soudant, P., Huvet, A., 2016. Oyster reproduction is affected by exposure to polystyrene microplastics. *Proc. Natl. Acad. Sci. U. S. A.* 113 (9), 2430–2435. <https://doi.org/10.1073/pnas.1519019113>.
- Tang, Y., Rong, J., Guan, X., Zha, S., Shi, W., Han, Y., Du, X., Wu, F., Huang, W., Liu, G., 2020. Immunotoxicity of microplastics and two persistent organic pollutants alone or in combination to a bivalve species. *Environ. Pollut.* 258, 113845 <https://doi.org/10.1016/j.envpol.2019.113845>.
- Tomanek, L., Zuzow, M.J., Ivanina, A.V., Beniash, E., Sokolova, I.M., 2011. Proteomic response to elevated PCO2 level in eastern oysters, *Crassostrea virginica*: evidence for oxidative stress. *J. Exp. Biol.* 214 (11), 1836–1844. <https://doi.org/10.1242/jeb.055475>.
- Trestrail, C., Nuggeoda, D., Shimeta, J., 2020. Invertebrate responses to microplastic ingestion: reviewing the role of the antioxidant system. *Sci. Total Environ.* 734, 138559 <https://doi.org/10.1016/j.scitotenv.2020.138559>.
- Trestrail, C., Walpitagama, M., Miranda, A., Nuggeoda, D., Shimeta, J., 2021. Microplastics alter digestive enzyme activities in the marine bivalve, *Mytilus galloprovincialis*. *Sci. Total Environ.* 779, 146418 <https://doi.org/10.1016/j.scitotenv.2021.146418>.
- Van Cauwenbergh, L., Claessens, M., Vandegheuchte, M.B., Janssen, C.R., 2015. Microplastics are taken up by mussels (*Mytilus edulis*) and lugworms (*Arenicola marina*) living in natural habitats. *Environ. Pollut.* 199, 10–17. <https://doi.org/10.1016/j.envpol.2015.01.008>.
- Von Moos, N., Burkhardt-Holm, P., Köhler, A., 2012. Uptake and effects of microplastics on cells and tissue of the blue mussel *Mytilus edulis* L. After an experimental exposure. *Environ. Sci. Technol.* 46 (20), 11327–11335. <https://doi.org/10.1021/es302332w>.
- Vroom, R.J., Koelmans, A.A., Besseling, E., Halsband, C., 2017. Aging of microplastics promotes their ingestion by marine zooplankton. *Environ. Pollut.* 231, 987–996.
- Wang, J., Huang, M., Wang, Q., Sun, Y., Zhao, Y., Huang, Y., 2020. LDPE microplastics significantly alter the temporal turnover of soil microbial communities. *Sci. Total Environ.* 726, 138682 <https://doi.org/10.1016/j.scitotenv.2020.138682>.
- Wang, F., Wu, H., Wu, W., Wang, L., Liu, J., An, L., Xu, Q., 2021. Microplastic characteristics in organisms of different trophic levels from Liaohe Estuary, China. *Sci. Total Environ.* 789, 148027 <https://doi.org/10.1016/j.scitotenv.2021.148027>.
- Webb, H.K., Arnott, J., Crawford, R.J., Ivanova, E.P., 2013. Plastic degradation and its environmental implications with special reference to poly(ethylene terephthalate). *Polymers* 5 (1), 1–18. <https://doi.org/10.3390/polym5010001>.
- Wright, S.L., Rowe, D., Thompson, R.C., Galloway, T.S., 2013. Microplastic ingestion decreases energy reserves in marine worms. *Curr. Biol.* 23 (23), R1031–R1033. <https://doi.org/10.1016/j.cub.2013.10.068>.
- Xiao, Y., Jiang, X., Liao, Y., Zhao, W., Zhao, P., Li, M., 2020. Adverse physiological and molecular level effects of polystyrene microplastics on freshwater microalgae. *Chemosphere* 255, 126914. <https://doi.org/10.1016/j.chemosphere.2020.126914>.

- Xu, X.Y., Lee, W.T., Chan, A.K.Y., Lo, H.S., Shin, P.K.S., Cheung, S.G., 2017. Microplastic ingestion reduces energy intake in the clam *atactodea striata*. *Mar. Pollut. Bull.* 124 (2), 798–802. <https://doi.org/10.1016/j.marpolbul.2016.12.027>.
- Zhang, H., Wang, J., Zhou, B., Zhou, Y., Dai, Z., Zhou, Q., Christie, P., Luo, Y., 2018. Enhanced adsorption of oxytetracycline to weathered microplastic polystyrene: kinetics, isotherms and influencing factors. *Environ. Pollut.* 243, 1550–1557. <https://doi.org/10.1016/j.envpol.2018.09.122>.
- Zhou, W., Tang, Y., Du, X., Han, Y., Shi, W., Sun, S., Zhang, W., Zheng, H., Liu, G., 2021. Fine polystyrene microplastics render immune responses more vulnerable to two veterinary antibiotics in a bivalve species. *Mar. Pollut. Bull.* 164 (January), 111995 <https://doi.org/10.1016/j.marpolbul.2021.111995>.
- Ziajahromi, S., Kumar, A., Neale, P.A., Leusch, F.D.L., 2018. Environmentally relevant concentrations of polyethylene microplastics negatively impact the survival, growth and emergence of sediment-dwelling invertebrates. *Environ. Pollut.* 236, 425–431. <https://doi.org/10.1016/j.envpol.2018.01.094>.

ARTICLES FOR FACULTY MEMBERS

MICROPLASTICS AND MARINE ENVIRONMENT

Title/Author	Effects of acute microplastic exposure on physiological parameters in Tubastrea aurea corals / Liao, B., Wang, J., Xiao, B., Yang, X., Xie, Z., Li, D., & Li, C.
Source	<i>Marine Pollution Bulletin</i> Volume 165 (2021) 112173 Pages 1 –7 https://doi.org/10.1016/J.MARPOLBUL.2021.112173 (Database: ScienceDirect)



Effects of acute microplastic exposure on physiological parameters in *Tubastrea aurea* corals

Baolin Liao^a, Junjie Wang^{a,1}, Baohua Xiao^{a,*}, Xiaodong Yang^{a,b}, Ziqiang Xie^a, Dongdong Li^a, Chengyong Li^{a,b,**}

^a Shenzhen Institute of Guangdong Ocean University, Shenzhen, Guangdong 518114, PR China

^b School of Chemistry and Environment, Guangdong Ocean University, Zhanjiang 524088, China

ARTICLE INFO

Keywords:

Microplastics
Tubastrea aurea
Antioxidant capacity
Immune system
Calcification
Energy metabolism

ABSTRACT

Pollution of marine environments with microplastic particles has increased rapidly during the last few decades and its impact on marine lives have recently gained attention in both public and scientific community. Scleractinian corals are the foundation species of coral reef ecosystems that are greatly affected by the microplastics (MPs), yet little is known about the effects of microplastics on the coral azooxanthellate. In the present study, effects of the exposure and ingestion of polyvinyl chloride (PVC), polyethylene (PE), polyethylene terephthalate (PET), and polyamide 66 (PA66) were studied on the physiological responses of *Tubastrea aurea*. Our results shows that coral ingested microplastics in four treatment groups and the exposure of microplastics inhibited the antioxidant capacity, immune system, calcification and energy metabolism of the coral *Tubastrea aurea*. Super-oxide dismutase (SOD), catalase (CAT), alkaline phosphatase (AKP), and total antioxidant capacity (TAC) were reduced by 29.4%, 35.5%, 73.9%, and 52.2% in the corals exposed to PVC, respectively. PET microplastics impacted more severely on pyruvate kinase (PK), Na, K-ATPase (Na, K-ATP), Ca-ATPase (Ca-ATP), Mg-ATPase (Mg-ATP), Ca-Mg-ATPase (Ca, Mg-ATP), and glutathione (GSH). Activity of these enzymes decreases to 89.6%, 66.7%, 63.6%, 60.4%, 48.4%, and 50.5% respectively. We anticipate that this work will provide important preliminary data for better understanding the effects of MPs on stony corals azooxanthellate.

1. Introduction

Plastics are extensively used nearly in all aspects of our daily life and plastic debris is causing devastating effects on the marine ecosystem (Browne et al., 2011; Galgani et al., 2013; Isobe et al., 2017; Rocha-Santos and Duarte, 2015; Setaelae et al., 2014; Waller et al., 2017; Woodall et al., 2014). Plastics decompose very slowly due to their chemical properties, so they remain in the water, air, or soil/sediment for hundreds or even thousands of years (Auta et al., 2017), this leads to some serious ecological and environmental problems. Solar UV radiation (Andrady, 2011), physical abrasion including waves, oxygen availability (Cole et al., 2011), and turbulence (Barnes et al., 2009) can promote the production of microplastics (MPs, plastic particles of size <5 mm). MPs have become an emerging global problem (Caruso, 2015; Wang et al., 2016) due to their easy and extensive dispersal to remote locations via hydrodynamic processes and ocean currents (Neto et al.,

2016).

MPs are ubiquitous in the ocean environment, especially PVC, PE, PET, and PA are in higher abundance, due to the frequent human activities (Andrady, 2011; Andrady and Neal, 2009; Thompson et al., 2005). Lately, people have paid attention to the hazards caused by MPs to corals and there are many reports concerning the risk of MPs ingestion (Allen et al., 2017; Hall et al., 2018; Hankins et al., 2018; Rotjan et al., 2019; Savinelli et al., 2020). In addition, corals also suffered from bleaching (Syakti et al., 2019), stress response (Tang et al., 2018), or tissue damage (Reichert et al., 2018) when exposed to the MPs environment. Furthermore, exposure to the MPs may cause slow growth of the corals' skeleton (Chapron et al., 2018). Previous investigations have mainly been done on zooxanthellate staghorn corals and studies on azooxanthellate corals have not been conducted before in this regard. So, the study regarding the physiological responses of stony corals azooxanthellate to different MPs is largely important. The goal of the

* Corresponding author.

** Correspondence to: C. Li, Shenzhen Institute of Guangdong Ocean University, Shenzhen, Guangdong 518114, PR China.

E-mail addresses: xiaobh@gdou.edu.cn (B. Xiao), cylil@gdou.edu.cn (C. Li).

¹ These authors contributed equally to this work.

<https://doi.org/10.1016/j.marpolbul.2021.112173>

Received 7 June 2020; Received in revised form 9 February 2021; Accepted 10 February 2021

Available online 20 February 2021

0025-326X/© 2021 Elsevier Ltd. All rights reserved.

current study is to characterize the physiological responses of stony corals azooxanthellate to several MPs exposure.

The scleractinian coral *Tubastrea aurea* (a coral devoid of zooxanthellate, family: Dendrophylliidae) is common in temperate and tropical waters and its polyps can be as long as 2-3 cm. Moreover, it usually grows on the dead coral substratum (Bakus, 1975) and can form small colonies on coral reefs or rocks (Fusetani et al., 1986). In the present study, biochemical stress response and the ingestion of MPs (PVC, PE, PET, and PA66) were tested on coral species after being exposed to microplastics for 24 h. It provides important preliminary data for MPs exposure in stony corals azooxanthellate. To the best of our knowledge, this is the first report about the effects of MPs on the *T. aurea*.

2. Materials and methods

2.1. Chemicals and reagents

All the chemicals were purchased from MACKLIN (Shanghai, China). The commercial kits of PK, SOD, AK P, CAT, Na, K-ATP, Ca-ATP, Mg-ATP, Ca, Mg-ATP, TAC, and GSH assay in the supernatants were obtained from Nanjing Jianchen Bioengineering Institute (A001, A007, A059, A076, A016, A016, A016, A016, A015 and A006, Nanjing, China).

2.2. Coral collection and rearing

Samples of the coral *Tubastrea aurea* were purchased from Shenzhen Zhihai Marine Biological Technology Co., Ltd., indigenous to the Indo-Pacific, then transferred and cultured in flow-through aquaria (Shenzhen Institute of Guangdong Ocean University) filled with filtered seawater. Aquarium facilities were kept at a temperature of 26.0 ± 1.0 °C and salinity of 35.0 ± 0.3 ppt with metal halide lights on a 14:10 light:dark cycle. The corals need to be fed artificially with frozen *Artemia salina* three times a week because *T. aurea* must catch food from the environment. Prior to the treatment, corals were placed in the tank for at least 3 weeks to adapt to the environment.

2.3. Characteristics of MPs

MPs of PVC, PE, PET, and PA66 (diameters ranging from 1 to 10 μm) were purchased from Yineng Platic Materials CO., Ltd. (Dongguan, China). Four MPs were analyzed by Raman Spectroscopy (RS, SR-510 Pro, Ocean optics Asia) according to the previously published methods (Araujo et al., 2018; Elert et al., 2017; Ribeiro-Claro et al., 2017). The shape and size distribution of MPs were characterized by using a fluorescence microscope (TI2-U, Nikon) combined with the software Image J.

2.4. Experimental design

The MPs containing seawater was prepared by adding MPs to the tank (15 L) and the final concentration was 300 mg/L. Continuous gentle aeration was necessary to keep the homogeneous distribution and avoid aggregations of MPs. Then 40 coral polyps were transferred into the four tanks with different MPs, while another 10 coral polyps were put into the tank having only the filtered seawater. All the coral polyps were fed 2 days before putting into the tank.

2.5. Biochemical analysis

For enzyme activity assays, the three coral nubbins were randomly selected from each treatment group after 24 h treatment. Corals were separated into coral soft tissues and coral skeletal fractions under the anatomical microscope (OLYMPUS-SZXP, Japan). The coral soft tissues were moved into a new tube after weighed precisely and added 9 times

the volume saline into the tube respectively. Homogenate was made by Automatic Sample Rapid Grinding Instrument (JXFSTPRP-24 L, Shanghai Jingxin Industrial Development CO., Ltd) and centrifuged for 10 min (3500 g , 4 °C). The supernatant was transferred to a new centrifuge tube for the following analysis.

The detailed procedure for the determination of GSH, TAC, SOD, CAT, AKP, PK, and four ATPases in the supernatant were carried according to the product instructions. The detection instrument used in this study is enzyme-labeled instrument (Synergy HT, BioTek) and ultraviolet spectrophotometer (SP-754PC, Shanghai Spectrum Instruments Co., Ltd.).

2.6. Histopathology

The method of histopathology was according to the article (Downs et al., 2009). Polyp samples from each treatment group were fixed in 4% formalin in seawater for 24 h then rinsed in filtered seawater. The polyps were maintained in 70% ethanol/30% seawater. The decalcified reagents contained 1:1 (v/v) solution of 50% formic acid and 20% sodium citrate. The tissue was embedded in paraffin and sectioned (5 μm) by a Kede Tissue Slicer (KD-2260, Jinhua, China). Each slice came from a different area and depth of the tissue. The slice sections were stained with hematoxylin/eosin and observed and photographed.

2.7. Statistical analysis

Data in this study is presented as means \pm SD from three biological replicates. All of the data were subjected to a two-way analysis of variance (two-way ANOVA) followed by multiple comparisons (S-N-K) using SPSS v22.0 (SPSS Inc., Chicago, Illinois). Significant differences were presented at $p < 0.05$ (letter refers to $p < 0.05$, capital letter refers to $p < 0.01$).

3. Results and discussion

3.1. The characteristic of MPs

The characterization of MPs is shown in Figs. 1 and 2.

Fig. 1 shows the characteristic Raman vibrations of MPs (PVC, PE, PET, and PA66) used in this study. The shape of these MPs is nearly circular with the size ranging from 1 μm to 10 μm (Fig. 2).

3.2. Histology

Microscopic images from the slices of coral polyps showed the presence of MPs after their exposure for 24 h, suggesting the ingestion of MPs in *T. aurea* (Fig. 3).

3.3. Detecting antioxidant enzyme activity of TAC, GSH, SOD, and CAT after microplastic exposure

The changes of TAC, GSH, SOD, and CAT were determined in the whole *T. aurea* nubbins after the acute MPs exposure for 24 h. For the GSH concentration, all kinds of MPs had a significant impact on it. The lowest GSH concentration was 45.42 ± 3.8 $\mu\text{mol/gprot}$ in the PVC group, it decreased by 50.5% as compared to the control group (Fig. 4A). TAC level was also decreased from 0.23 ± 0.04 mmol/gprot (control group) to 0.11 ± 0.02 mmol/gprot (PET group), about 52.2% (Fig. 4B). As for SOD activity, a significant decrease occurred at all the MPs group and the impacts of four MPs on coral were similar, but the lowest activity was obtained in PVC group with a 29.4% decrease (Fig. 4C). CAT activity decreased significantly in the MPs group except for the PA66 group, in which CAT changed slightly (Fig. 4D). The PET had the highest toxicity to the CAT activity due to the activity decreased by 35.5%.

In this study, TAC, GSH, SOD, and CAT enzymic activity were decreased significantly after MPs exposure. This suggests that acute MPs

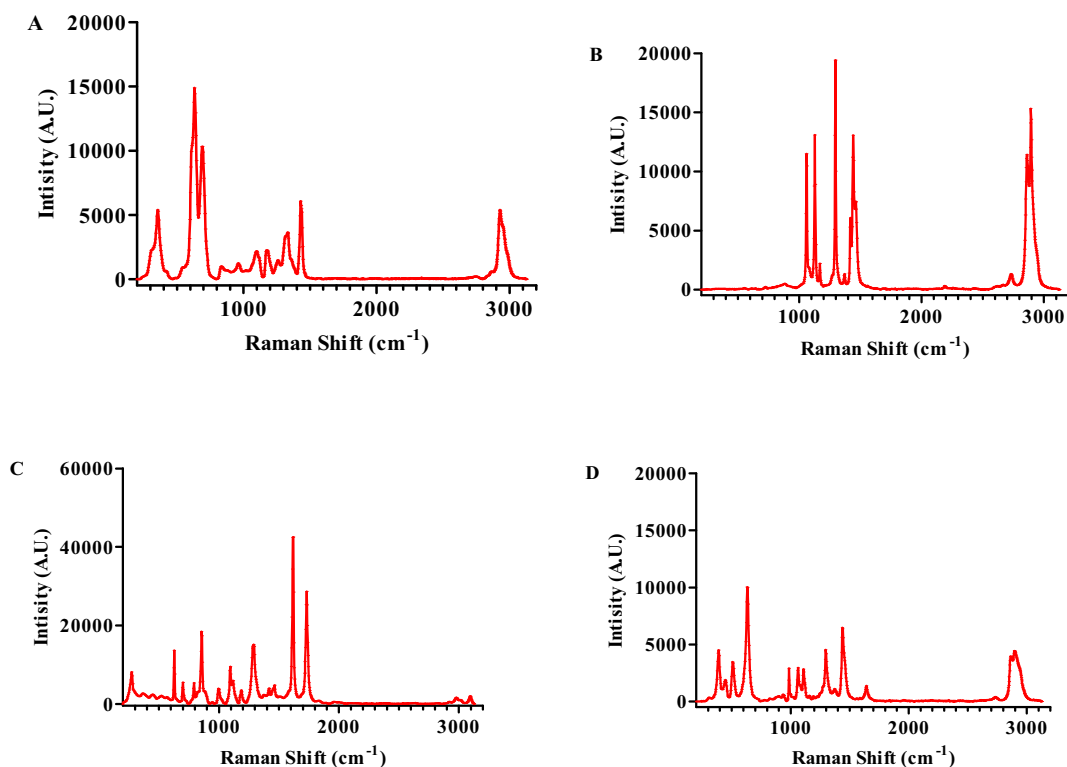


Fig. 1. The Raman spectrum of MPs. (A) PVC, (B) PE, (C) PET, and (D) PA66.

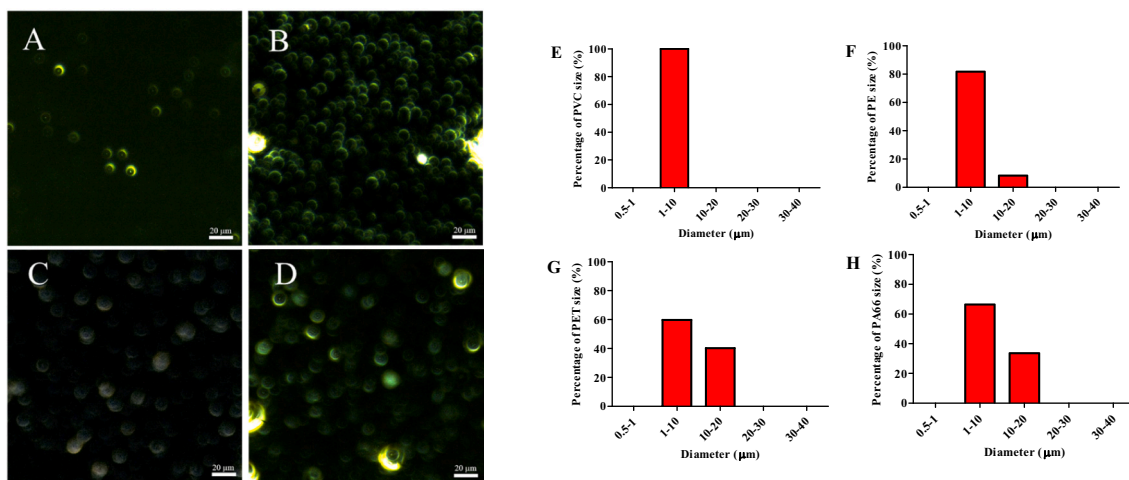


Fig. 2. The microscope images and size distribution of four types of MPs. (A, E) PVC, (B, F) PE, (C, G) PET, (D, H) PA66.

stress inhibited the total antioxidant capacity of the coral *T. aurea*. Wan has also suggested SOD, CAT, and GSH were decreased when larval zebrafishes were exposed to polystyrene MPs (1000 μg/L) (Wan et al., 2019). The possible reason for this result might be the damage to the ROS-sensitive enzymes caused due to the MPs (Dias et al., 2019; Hermes-Lima and Storey, 1993). Roberty also reported that the lower antioxidant capacity can be associated with the damages of ROS-sensitive enzymes in *Symbiodinium* (Roberty et al., 2016). So it was possible that the MPs would cause damage to the ROS-sensitive enzymes and ultimately lead to a reduction in the corals antioxidant capacity, but the underlying mechanism of the antioxidant abilities suppression in this study still needs further study.

3.4. Activity of AKP after microplastic exposure

Compared with the control group, the lower activity of AKP was observed in the MPs group (Fig. 5). All kinds of MPs resulted in a significant decrease in enzymatic activity. Especially, the AKP activity seemed to be more sensitive to PVC, as it decreased by 73.9%.

The immune system, a mechanism of host defense, is responsible to identify and eliminate exogenous substances. Corals can employ both natural and inducible humoral defenses. The natural humoral defenses include lysozyme and lysosomal enzymes in corals. Lysosomal enzymes, encapsulated in lysosomes, are granules containing bactericidal and hydrolytic substances (Sutherland et al., 2004). AKP is an important part of lysosomal enzymes, so it plays a role in the corals' immune. The decrease of AKP activity suggested that MPs might inhibit the immune

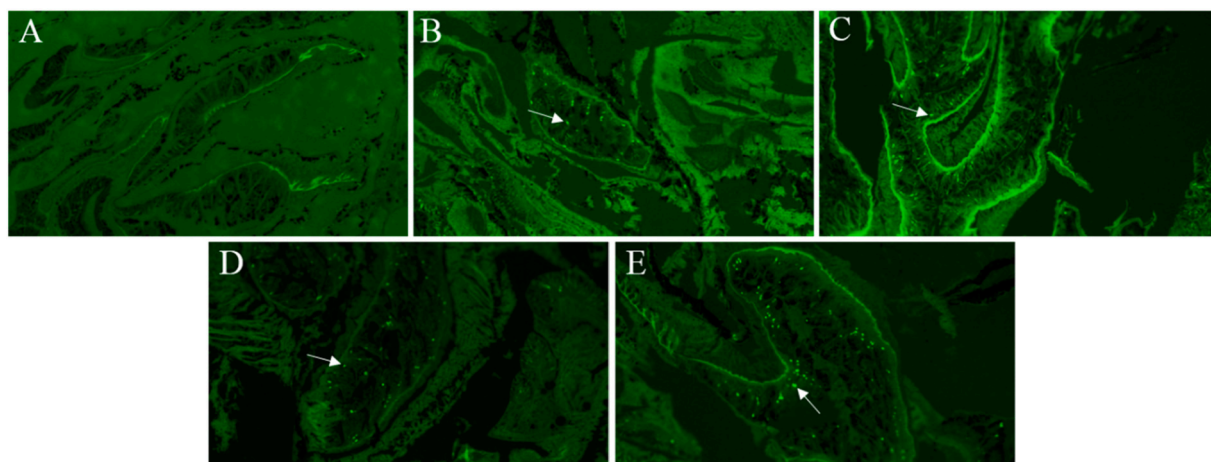


Fig. 3. Histology of coral after microplastic exposure for 24 h. (A) Control, (B) PVC, (C) PE, (D) PET, (E) PA66.

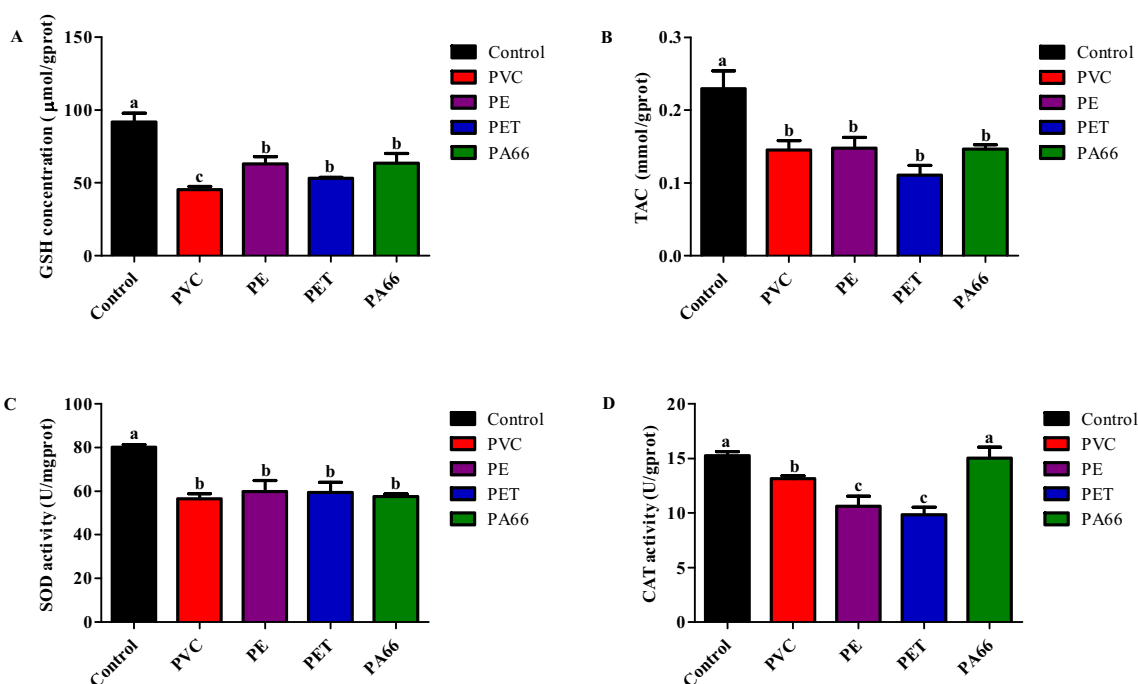


Fig. 4. Changes in (A) GSH, (B) TAC, (C) SOD, and (D) CAT in the coral *Tubastrea aurea* after acute MPs exposure for 24 h. Letter indicates significantly different mean values (letter refers to $p < 0.05$, capital letter refers to $p < 0.01$) between two groups.

system in *T. aurea*. Tang proposed acute MPs exposure suppressed immune capacities in the coral *Pocillopora damicornis* (Tang et al., 2018), and similar reports have been reported in other species like a mussel (Detree and Gallardo-Escarate, 2018). The possible reason for the effect of MPs on immunity capacities is that they could disturb pathways or genes of the immune system in coral. It has been reported that MPs could impact the immune system in corals by regulating the MAPK signal pathways (Tang et al., 2018). In addition, in the presence of MPs, the immune-related gene expressions were up-regulated in the digestive gland while they were down-regulated in the mantle of a mussel (Detree and Gallardo-Escarate, 2018). But the underlying mechanism of the immune system suppression in this study still needs further study.

3.5. Detection energy metabolism enzyme activity of PK and Na, K-ATP after microplastic exposure

A significant decrease in PK activity was observed in all the samples

treated with MPs and tested after 24 h (Fig. 6A). PVC showed the strongest toxicity to the activity by decreasing it from 15.16 ± 2.77 U/L to 1.58 ± 0.95 U/L, overall, the activity was reduced by 89.6%. The activity of Na, K-ATP in the control group was 0.45 ± 0.02 μmolPi/mgprot/h, it was higher than that in the MPs group (Fig. 6B). And the lowest activity of Na, K-ATP was obtained in PVC group, it decreased by 66.7%.

PK catalyzes the transfer of a phosphate group from phosphoenolpyruvate to ADP, producing pyruvate and ATP (da Silva Fonseca et al., 2019). The function of Na, K-ATP is to maintain the normal physiological metabolism and energy metabolism of the organism, Na, K-ATP transforms chemical energy in ATP to osmotic work (Jorgensen and Pedersen, 2001). Ellis et al. also reported that Na, K-ATP plays a critical role in energy metabolism and ion fluxes (Ellis et al., 2003). The reduced enzymatic activity of PK and Na, K-ATP indicated that energy metabolism was inhibited in *T. aurea*. Wan reported that polystyrene had a significant impact on glucose metabolism in larval zebrafish (Wan et al.,

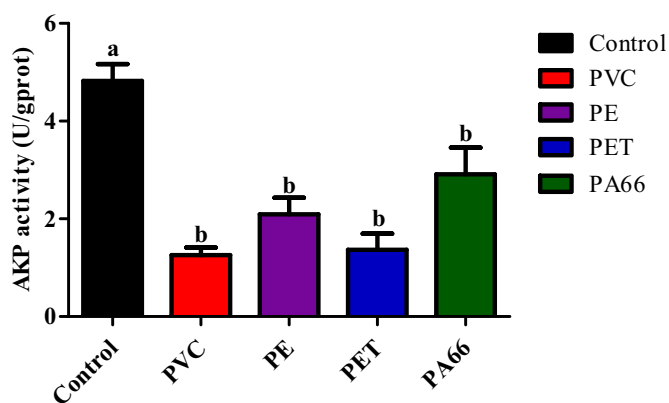


Fig. 5. Variation in the activity of AKP in the coral *Tubastrea aurea* after acute MPs exposure for 24 h. Letter indicates significantly different mean values (letter refers to $p < 0.05$, capital letter refers to $p < 0.01$) between two groups.

2019). The reason explained for this result might be the changes in energy metabolism-related metabolites. MPs could change the metabolomic profiles and metabolites in larval zebrafish (da Silva Fonseca et al., 2019). Polystyrene (1000 mg/L, 50 mm) induced changes in metabolites, which are involved in energy metabolism (Wan et al., 2019), but the exact causes are still unclear and this require further research.

3.6. Detection calcification enzyme activity of Ca-ATP, Mg-ATP and Ca, Mg-ATP after microplastic exposure

As shown in Fig. 7, the activities of Ca-ATP, Mg-ATP, and Ca, Mg-ATP were significantly affected by the MPs. For Ca-ATP, MPs led to a significant decrease of the activity except for the PET, and PVC had the most serious effect on enzymatic activity. As for Mg-ATP and Ca, Mg-ATP, PE did not have a significant impact on them, while PVC resulted in the lowest activity. For these three ATPases, PVC always had the maximum toxicity to Ca-ATP, Mg-ATP, and Ca, Mg-ATP, representing the 63.6%, 60.4%, and 48.4% decrease respectively.

Ca-ATP, an essential enzyme in the calcification process of corals,

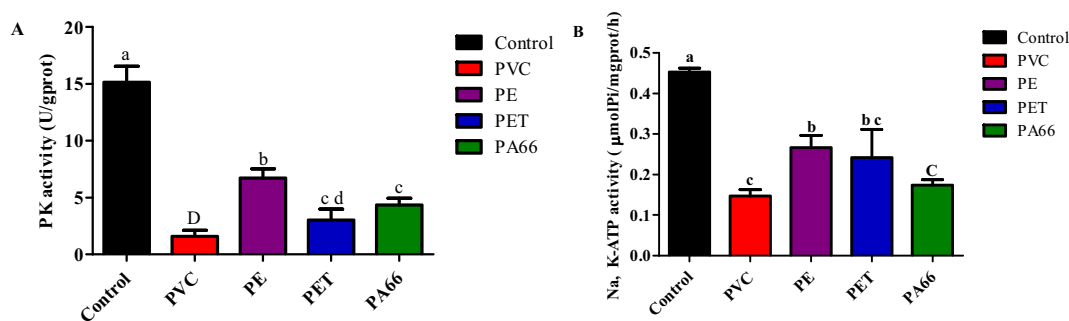


Fig. 6. Variation in the activity of (A) PK and (B) Na, K-ATP, in the coral *Tubastrea aurea* after acute MPs exposure for 24 h. Letter indicates significantly different mean values (letter refers to $p < 0.05$, capital letter refers to $p < 0.01$) between two groups.

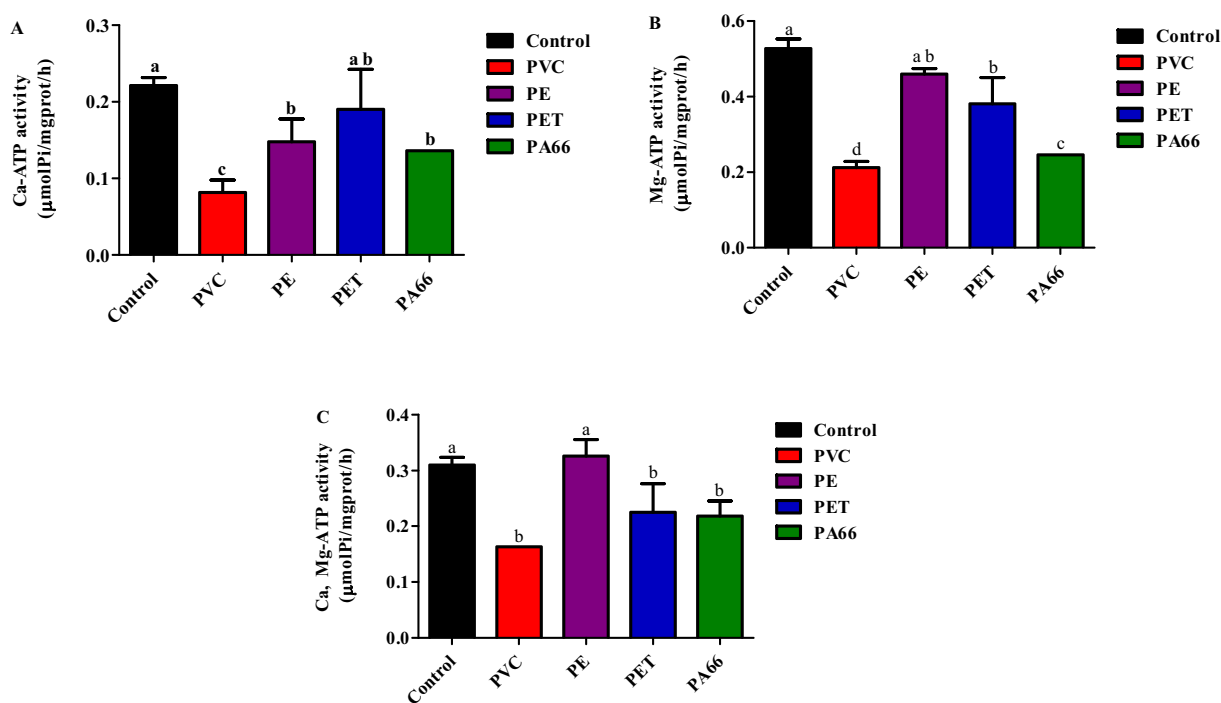


Fig. 7. Variation in the activity of (A) Ca-ATP, (B) Mg-ATP, (C) Ca, Mg-ATP in the coral *Tubastrea aurea* after acute MPs exposure for 24 h. Letter indicates significantly different mean values (letter refers to $p < 0.05$, capital letter refers to $p < 0.01$) between two groups.

can facilitate the formation of CaCO_3 by transporting Ca^{2+} and removing protons (H^+) in the calcification site (Al-Horani et al., 2003; Allemand et al., 2011). Mg-ATP has a relationship with the growth of corals skeleton by releasing Mg^{2+} to the mineralizing surface (Allison et al., 2011). Due to the interaction between Ca-ATP and Mg-ATP in the organism, the Ca, Mg-ATP was regarded as an appropriate indicator for explaining the calcification response of the organism (Allison et al., 2011). Therefore, the significantly decreased activities of Ca-ATP, Mg-ATP, and Ca, Mg-ATP indicated that MPs could interfere with the process of calcification in the coral *T. aurea*. Chapron proposed MPs could reduce calcification compared to control in cold-water corals (Chapron et al., 2018). The most likely explanation is that the MPs might lead to energy metabolism damage, and the significant decreases of PK and Na, K-ATP also confirmed this. Naumann reported that zooplankton exclusion led to the reduction of energy and then had a negative impact on the calcification of coral *Desmophyllum dianthus* in the cold water (Naumann et al., 2011). But the exact causes are still unclear and this require further study.

Based on the above results of biochemical analysis, the most affected treatments are PVC among treated corals showing the lower level markers of several physiological parameters, it means that MPs of PVC had the highest toxicity to *T. aurea*. The same result was discovered in the study, which reported that PVC resulted in the most toxic than PP, PE, and PE + PVC on *Lepidium sativum* (Pignattelli et al., 2019). The possible reasons might be the characteristics and type of MPs. PVC has been identified as the most hazardous plastic, because of the high contents of chloride and additives and the generation of dioxins (PhD and Lent, 2006). The size of PVC also was a vital factor, PVC had the smallest size among the four kinds of MPs. There were reports about the size-dependent toxicity (An et al., 2021; Jeong et al., 2016; Lili et al., 2018). The smaller size MPs had a longer retention time and greater interference in the digestive tract. PET had a higher toxicity on coral than PE and PA66 MPs. The possible reason was the characteristic and type of PET, in addition, PET can release endocrine-disrupting chemicals, such as bisphenol A, estradiol (Soto et al., 1991; Wagner and Oehlmann, 2009, 2011). All in all, Weber reported MPs toxicity was possibly dependent on the polymer type as well as an organism (Weber et al., 2018), it may be a vital aspect that resulted in completely different toxicity of four different types of MPs. However, the mechanism of MPs toxicity still needs to investigate further.

4. Conclusion

In the present study, we evaluated changes in biomarkers and the ingestion of MPs in the coral *T. aurea* after exposure to MPs. The results showed that MPs led to the significant decreases in activities of SOD, CAT, AKP, PK, Ca-ATP, Mg-ATP, Na, K-ATP, Ca, Mg-ATP, and concentrations of TAC and GSH. In addition, coral *T. aurea* ingested MPs.

In summary, high concentration of MPs after short-term exposure caused negative effects on physiological responses of *T. aurea*, including the energy metabolism, antioxidant status, immune system, and calcification process. However, more study is to be required to uncover the effect of MPs at low concentrations after long-term treatment as well as the combined effects with other pollutants on corals.

CRedit authorship contribution statement

Baolin Liao: Conceptualization, Methodology, Investigation, Writing – original draft, Writing – review & editing. **Junjie Wang:** Conceptualization, Methodology, Investigation, Writing – original draft, Writing – review & editing. **Baohua Xiao:** Validation, Methodology, Formal analysis, Funding acquisition. **Xiaodong Yang:** Investigation, Methodology. **Ziqiang Xie:** Methodology. **Dongdong Li:** Methodology. **Chengyong Li:** Formal analysis, Writing – review & editing, Supervision, Funding acquisition.

Declaration of competing interest

The authors declare that there are no conflicts of interest.

Acknowledgments

The authors were grateful to all of the laboratory members for their continuous technical advice and helpful discussions. The study was funded by the Guangdong Oceanic and Fishery Administration (project number: A201708D06), China Guangdong MEPP Fund (project number: GDOE [2019]A01), Shenzhen Science and Technology R&D Fund (project number: KJYY20180213182720347), Shenzhen Science and Technology R&D Fund (project number: JCYJ20200109144803833), Shenzhen Science and Technology R&D Fund (project number: KCXFZ202002011011057), Guangdong Key Area R & D Program Project (Project number:2020B1111030002) and China Guangdong OEDP Fund (project number: GDNRC [2020]040).

References

- Al-Horani, F.A., Al-Moghrabi, S.M., Beer, D.D., 2003. The mechanism of calcification and its relation to photosynthesis and respiration in the scleractinian coral *Galaxea fascicularis*. *Mar. Biol.* 142, 419–426.
- Allemand, D., Tambutté, É., Zoccola, D., Tambutté, S., 2011. Coral calcification, cells to reefs. *An Ecosystem in Transition, Coral Reefs*, pp. 119–150.
- Allen, A.S., Seymour, A.C., Rittschof, D., 2017. Chemoreception drives plastic consumption in a hard coral. *Mar. Pollut. Bull.* 124, 198–205.
- Allison, N., Cohen, I., Finch, A.A., Erez, J., 2011. Controls on Sr/Ca and Mg/Ca in scleractinian corals: the effects of Ca-ATPase and transcellular Ca channels on skeletal chemistry. *Geochim. Cosmochim. Acta* 75, 6350–6360.
- An, D., Na, J., Song, J., Jung, J., 2021. Size-dependent chronic toxicity of fragmented polyethylene microplastics to *Daphnia magna*. *Chemosphere* 271.
- Andrady, A.L., 2011. Microplastics in the marine environment. *Mar. Pollut. Bull.* 1596–1605.
- Andrady, A.L., Neal, M.A., 2009. Applications and societal benefits of plastics. *Philosophical transactions of the Royal Society of London. Series B, Biological sciences* 364, 1977–1984.
- Araujo, C.F., Nolasco, M.M., Ribeiro, A.M.P., Ribeiro-Claro, P.J.A., 2018. Identification of microplastics using Raman spectroscopy: latest developments and future prospects. *Water Res.* 142, 426–440.
- Auta, H.S., Emenike, C.U., Fauziah, S.H., 2017. Distribution and importance of microplastics in the marine environment: a review of the sources, fate, effects, and potential solutions. *Environ. Int.* 102, 165–176.
- Bakus, G.J., 1975. Marine zonation and ecology of Cocos island. *Off Central America. Atoll Research Bulletin* 179.
- Barnes, D.K.A., Galgani, F., Thompson, R.C., Barlaz, M., 2009. Accumulation and fragmentation of plastic debris in global environments. *Philos Trans R Soc Lond B Biol* 364, 1985–1998.
- Browne, M.A., Crump, P., Niven, S.J., Teuten, E., Tonkin, A., Galloway, T., Thompson, R., 2011. Accumulation of microplastic on shorelines worldwide: sources and sinks. *Environ. Sci. Technol.* 45, 9175–9179.
- Caruso, G., 2015. Plastic degrading microorganisms as a tool for bioremediation of plastic contamination in aquatic environments. *Journal of Pollution Effects & Control* 03, 3.
- Chapron, L., Peru, E., Engler, A., Ghiglione, J.F., Meistertzheim, A.L., Pruski, A.M., Purser, A., Vétion, G., Galand, P.E., Lartaud, F., 2018. Macro- and microplastics affect cold-water corals growth, feeding and behaviour. *Sci. Rep.* 8, 15299.
- Cole, M., Lindeque, P., Halsband, C., Galloway, T.S., 2011. Microplastics as contaminants in the marine environment: a review. *Mar. Pollut. Bull.* 62, 2588–2597.
- da Silva Fonseca, J., de Barros Marangoni, L.F., Marques, J.A., Bianchini, A., 2019. Energy metabolism enzymes inhibition by the combined effects of increasing temperature and copper exposure in the coral *Mussismilia harttii*. *Chemosphere* 236, 124420.
- Detree, C., Gallardo-Escarate, C., 2018. Single and repetitive microplastics exposures induce immune system modulation and homeostasis alteration in the edible mussel *Mytilus galloprovincialis*. *Fish Shellfish Immunol* 83, 52–60.
- Dias, M., Madeira, C., Jøgee, N., Ferreira, A., Gouveia, R., Cabral, H., Diniz, M., Vinagre, C., 2019. Oxidative stress on scleractinian coral fragments following exposure to high temperature and low salinity. *Ecol. Indic.* 107, 105586.
- Downs, C.A., Kramarsky-Winter, E., Woodley, C.M., Downs, A., Winters, G., Loya, Y., Ostrander, G.K., 2009. Cellular pathology and histopathology of hypo-salinity exposure on the coral *Stylophora pistillata*. *Sci. Total Environ.* 407, 4838–4851.
- Elert, A.M., Becker, R., Duemichen, E., Eisentraut, P., Falkenhagen, J., Sturm, H., Braun, U., 2017. Comparison of different methods for MP detection: what can we learn from them, and why asking the right question before measurements matters? *Environ. Pollut.* 231, 1256–1264.
- Ellis, D.Z., Rabe, J., Sweadner, K.J., 2003. Global loss of Na,K-ATPase and its nitric oxide-mediated regulation in a transgenic mouse model of amyotrophic lateral sclerosis. *J. Neurosci.* 23, 43–51.

- Fusetani, N., Asano, M., Matsunaga, S., Hashimoto, K., 1986. Bioactive marine metabolites—XV. Isolation of aplysinopsin from the scleractinian coral *Tubastrea aurea* as an inhibitor of development of fertilized sea urchin eggs. *Comparative Biochemistry & Physiology Part B Comparative Biochemistry* 85, 845–846.
- Galgani, F., Hanke, G., Werner, S., De, V.L., 2013. Marine litter within the European marine strategy framework directive. *ICES J. Mar. Sci.* 70, 1055–1064.
- Hall, N.M., Berry, K.L.E., Rintoul, L., Hoogenboom, M.O., 2018. Microplastic ingestion by scleractinian corals. *Mar. Biol.* 162, 725–732.
- Hankins, C., Duffy, A., Drisco, K., 2018. Scleractinian coral microplastic ingestion: potential calcification effects, size limits, and retention. *Mar. Pollut. Bull.* 135, 587–593.
- Hermes-Lima, M., Storey, K.B., 1993. In vitro oxidative inactivation of glutathione S-transferase from a freeze tolerant reptile. *Mol. Cell. Biochem.* 124, 149–158.
- Isobe, A., Uchiyama-Matsumoto, K., Uchida, K., Tokai, T., 2017. Microplastics in the Southern Ocean. *Mar. Pollut. Bull.* 114, 623–626.
- Jeong, C.B., Won, E.J., Kang, H.M., Lee, M.C., Hwang, D.S., Hwang, U.K., Zhou, B., Souissi, S., Lee, S.J., Lee, J.S., 2016. Microplastic size-dependent toxicity, oxidative stress induction, and p-JNK and p-p38 activation in the monogonont rotifer (*Brachionus koreanus*). *Environ. Sci. Technol.* 50, 8849.
- Jorgensen, P.L., Pedersen, P.A., 2001. Structure-function relationships of Na(+), K(+), ATP, or Mg(2+) binding and energy transduction in Na,K-ATPase. *Biochim. Biophys. Acta* 1505, 57–74.
- Lili, L., Mengting, L., Yang, S., Shibo, L., Jiani, H., Chengjin, C., Bing, X., Huahong, S., Defu, H., 2018. Polystyrene (Nano)Microplastics Cause Size-dependent Neurotoxicity, Oxidative Damage and Other Adverse Effects in *Caenorhabditis elegans* (Environmental Science Nano).
- Naumann, M.S., Orejas, C., Wild, C., Ferrier-Pages, C., 2011. First evidence for zooplankton feeding sustaining key physiological processes in a scleractinian cold-water coral. *J. Exp. Biol.* 214, 3570–3576.
- Neto, B., Antonio, J., Carvalho, D., Gomes, D., 2016. Microplastic pollution of the beaches of Guanabara Bay, Southeast Brazil. *Ocean Coast. Manag.* 128, 10–17.
- PhD, M.R., Lent, T., 2006. *Creating Safe and Healthy Spaces: Selecting Materials That Support Healing* (The Center for Health Design).
- Pignattelli, S., Broccoli, A., Renzi, M., 2019. Physiological responses of garden cress (*L. sativum*) to different types of microplastics. *Science of The Total Environment* 727.
- Reichert, J., Schellenberg, J., Schubert, P., Wilke, T., 2018. Responses of reef building corals to microplastic exposure. *Environ. Pollut.* 237, 955–960.
- Ribeiro-Claro, P., Nolasco, M.M., Araújo, C., 2017. Characterization of microplastics by Raman spectroscopy. *Compr. Anal. Chem.* 75, 119–151.
- Roberty, S., Furla, P., Plumier, J.C., 2016. Differential antioxidant response between two Symbiodinium species from contrasting environments. *Plant Cell Environ.* 39, 2713–2724.
- Rocha-Santos, T., Duarte, A.C., 2015. A critical overview of the analytical approaches to the occurrence, the fate and the behavior of microplastics in the environment. *TrAC Trends Anal. Chem.* 65, 47–53.
- Rotjan, R.D., Sharp, K.H., Gauthier, A.E., Yelton, R., Lopez, E.M.B., Carilli, J., Kagan, J. C., Urban-Rich, J., 2019. Patterns, dynamics and consequences of microplastic ingestion by the temperate coral, *Astrangia poculata*. *Proc. Biol. Sci.* 286, 20190726.
- Savinelli, B., Vega Fernandez, T., Galasso, N.M., D'Anna, G., Pipitone, C., Prada, F., Zenone, A., Badalamenti, F., Musco, L., 2020. Microplastics impair the feeding performance of a Mediterranean habitat-forming coral. *Mar. Environ. Res.* 155, 104887.
- Setaelae, O., Fleming-Lehtinen, V., Lehtiniemi, M., 2014. Ingestion and transfer of microplastics in the planktonic food web. *Environ. Pollut.* 185, 77–83.
- Soto, A.M., Justicia, H., Wray, J.W., Sonnenschein, C., 1991. p-Nonyl-phenol: an estrogenic xenobiotic released from “modified” polystyrene. *Environ. Health Perspect.* 92, 167–173.
- Sutherland, K.P., Porter, J.W., Torres, C., 2004. Disease and immunity in Caribbean and Indo-Pacific zooxanthellate corals. *Marine Ecology Progress* 266, 273–302.
- Syakti, A.D., Jaya, J.V., Rahman, A., Hidayati, N.V., Raza'i, T.S., Idris, F., Trenggono, M., Doumenq, P., Chou, L.M., 2019. Bleaching and necrosis of staghorn coral (*Acropora formosa*) in laboratory assays: immediate impact of LDPE microplastics. *Chemosphere* 228, 528–535.
- Tang, J., Ni, X., Zhou, Z., Wang, L., Lin, S., 2018. Acute microplastic exposure raises stress response and suppresses detoxification and immune capacities in the scleractinian coral *Pocillopora damicornis*. *Environ. Pollut.* 243, 66–74.
- Thompson, Richard, Moore, Charles, Andrady, Anthony, Gregory, Murray, Takada, Hideshige, 2005. New directions in plastic debris. *Environ. Sci. Technol.* 39, 1117–1117.
- Wagner, M., Oehlmann, J., 2009. Endocrine disruptors in bottled mineral water: total estrogenic burden and migration from plastic bottles. *Environ. Sci. Pollut. Res. Int.* 16, 278–286.
- Wagner, M., Oehlmann, J., 2011. Endocrine disruptors in bottled mineral water: estrogenic activity in the E-screen. *J. Steroid Biochem. Mol. Biol.* 127, 128–135.
- Waller, C.L., Griffiths, H.J., Waluda, C.M., Thorpe, S.E., Loaiza, I., Moreno, B., Pachterres, C.O., Hughes, K.A., 2017. Microplastics in the Antarctic marine system: an emerging area of research. *Sci. Total Environ.* 598, 220–227.
- Wan, Z., Wang, C., Zhou, J., Shen, M., Wang, X., Fu, Z., Jin, Y., 2019. Effects of polystyrene microplastics on the composition of the microbiome and metabolism in larval zebrafish. *Chemosphere* 217, 646–658.
- Wang, J., Tan, Z., Peng, J., Qiu, Q., Li, M., 2016. The behaviors of microplastics in the marine environment. *Mar. Environ. Res.* 113, 7–17.
- Weber, A., Scherer, C., Brennholt, N., Reifferscheid, G., Wagner, M., 2018. PET microplastics do not negatively affect the survival, development, metabolism and feeding activity of the freshwater invertebrate *Gammarus pulex*. *Environ. Pollut.* 234, 181–189.
- Woodall, L.C., Sanchez-Vidal, A., Canals, M., Paterson, G.L.J., Coppock, R., Sleight, V., Calafat, A., Rogers, A.D., Narayanaswamy, B.E., Thompson, R.C., 2014. The deep sea is a major sink for microplastic debris. *R. Soc. Open Sci.* 1, 140317.










ARTICLES FOR FACULTY MEMBERS

MICROPLASTICS AND MARINE ENVIRONMENT

Title/Author	Exposure of <i>Mytilus galloprovincialis</i> to Microplastics: Accumulation, Depuration and Evaluation of the Expression Levels of a Selection of Molecular Biomarkers / Pizzurro, F., Nerone, E., Ancora, M., Domenico, M. Di, Mincarelli, L. F., Cammà, C., Salini, R., Renzo, L. Di, Giacinto, F. Di, Corbau, C., Bokan, I., Ferri, N., & Recchi, S.
Source	<i>Animals</i> Volume 14 Issue 4 (2023) 103110 Pages 1-18 https://doi.org/10.3390/ANI14010004 (Database: MDPI)

Article

Exposure of *Mytilus galloprovincialis* to Microplastics: Accumulation, Depuration and Evaluation of the Expression Levels of a Selection of Molecular Biomarkers

Federica Pizzurro ¹, Eliana Nerone ^{1,*}, Massimo Ancora ¹, Marco Di Domenico ¹, Luana Fiorella Mincarelli ¹, Cesare Cammà ¹, Romolo Salini ¹, Ludovica Di Renzo ¹, Federica Di Giacinto ¹, Corinne Corbau ², Itana Bokan ³, Nicola Ferri ¹ and Sara Recchi ¹

¹ Istituto Zooprofilattico Sperimentale dell'Abruzzo e Molise (IZSAM), 64100 Teramo, Italy; f.pizzurro@izs.it (F.P.); m.ancora@izs.it (M.A.); m.didomenico@izs.it (M.D.D.); c.camma@izs.it (C.C.); r.salini@izs.it (R.S.); l.direnzo@izs.it (L.D.R.); f.digiacinto@izs.it (F.D.G.); n.ferri@izs.it (N.F.); s.recchi@izs.it (S.R.)

² Dipartimento di Scienze dell'Ambiente e della Prevenzione, Università di Ferrara, 44122 Ferrara, Italy; cbc@unife.it

³ Teaching Institute of Public Health (TIPH), 51000 Rijeka, Croatia; itanabokan@yahoo.co.uk

* Correspondence: e.nerone@izs.it; Tel.: +39-0-87581343

Simple Summary: Microplastics are an environmental pollutant increasingly present in seawater, the spread of which also represents a threat to food safety. In fact, these particles can be ingested through various foods, among the most at risk are bivalve molluscs, as they filter large quantities of seawater and enter the diet of consumers ingested entirely. Purification studies of bivalves could allow us to understand in a more precise way the ability of organisms to eliminate microplastics, in order to test this process as a potential method of removing such contaminants from bivalves intended for human consumption.



Citation: Pizzurro, F.; Nerone, E.; Ancora, M.; Di Domenico, M.; Mincarelli, L.F.; Cammà, C.; Salini, R.; Di Renzo, L.; Di Giacinto, F.; Corbau, C.; et al. Exposure of *Mytilus galloprovincialis* to Microplastics: Accumulation, Depuration and Evaluation of the Expression Levels of a Selection of Molecular Biomarkers. *Animals* **2024**, *14*, 4. <https://doi.org/10.3390/ani14010004>

Academic Editors: Beniamino T. Cenci-Goga and Sonia Tassone

Received: 9 October 2023

Revised: 11 December 2023

Accepted: 15 December 2023

Published: 19 December 2023

Abstract: Microplastic contamination is a growing marine environmental issue with possible consequences for seafood safety. Filter feeders are the target species for microplastic (MPs) pollution because they filter large quantities of seawater to feed. In the present study, an experimental contamination of *Mytilus galloprovincialis* was conducted using a mixture of the main types of MPs usually present in the seawater column (53% filaments, 30% fragments, 3% granules) in order to test the purification process as a potential method for removing these contaminants from bivalves intended for human consumption. A set of molecular biomarkers was also evaluated in order to detect any variations in the expression levels of some genes associated with biotransformation and detoxification, DNA repair, cellular response, and the immune system. Our results demonstrate that: (a) the purification process can significantly reduce MP contamination in *M. galloprovincialis*; (b) a differential expression level has been observed between mussels tested and in particular most of the differences were found in the gills, thus defining it as the target organ for the use of these biomarkers. Therefore, this study further suggests the potential use of molecular biomarkers as an innovative method, encouraging their use in next-generation marine monitoring programs.

Keywords: *Mytilus galloprovincialis*; shellfish; microplastics; depuration; marine pollution



Copyright: © 2023 by the authors. Licensee MDPI, Basel, Switzerland. This article is an open access article distributed under the terms and conditions of the Creative Commons Attribution (CC BY) license (<https://creativecommons.org/licenses/by/4.0/>).

1. Introduction

Global ever-increasing production of plastic is expected to reach 33 billion tons by 2050, and they are constantly poured out in terrestrial and aquatic environments worldwide. Plastic debris, as a result of their fragmentation, produces microplastics (MPs), plastic particles with a diameter of less than 5 mm. MPs, to date, are extensively recognized as ubiquitous contaminants in aquatic environments [1–5] and at the same time as a worrying

contaminant for human health [6–9]. Indeed, these particles easily disperse in the seawater column and are frequently found in marine biota [10–12]. Moreover, MPs have a high capacity for adsorbing organic pollutants from surrounding water, which can then be released into the organisms upon ingestion [13–16]. Benthic filter feeders, such as mussels, are prone to ingest microplastic particles [17–22] due to their filtering capacity allowing them to feed on planktonic organisms that have a similar size to MPs [6]. Indeed, several studies highlight the presence of MPs in many species of filter-feeding bivalves [23–27]. Among the detected MPs in bivalves, fibers are the most abundant independent of the location and species [28,29].

Mussels, i.e., *Mytilus galloprovincialis*, are an excellent species both as sentinel organisms in MPs pollution monitoring and for MPs experimental studies. Indeed, they are filter-feeding organisms worldwide distributed [24], very tolerant to salinity changes and other stressors, and also able to accumulate particulate pollutants, having a high-water filtration rate and low metabolic activity [12,30].

Specifically, MPs enter bivalves through the gills, being the first entry point for particulate pollutants and associated chemical and microbiological contaminants, then move towards the mouth and enter into the digestive gland [31–33]. These two organs have been the subject of some recent studies related to biomolecular biomarkers, which were intended to detect gene expression variations caused by pollutants' exposure, including MPs, in aquatic organisms [34–36].

Although to date there are several papers related to the presence of MPs in bivalves there is still a lack of data and more detailed studies are needed about their depuration capacity. The depuration process, which consists of placing bivalves in clean seawater in an aquarium where filtration rates are maximized, reduces contaminant levels in these organisms [37].

This practice is commonly used in the shellfish aquaculture industry to remove microbiological contaminants such as *Escherichia coli* from bivalves cultivated in areas where such microbes might occur in harmful amounts [5]. Similarly, it has been demonstrated that this technique could be able to reduce the presence of MPs from bivalves [33,38–43]. It is, therefore, necessary to examine in depth the use of this practice in the shellfish purification centers (CDM) in order to release on the market a product as healthy as possible.

The present work aims to study accumulation and depuration in *M. galloprovincialis* after exposure of bivalves to known concentrations of an MP's mixture under controlled conditions, in order to test the depuration process as a potential method for removing MPs from bivalves intended for human consumption. Furthermore, tested mussels' digestive glands and gills were examined by reverse transcription quantitative PCR (RT-qPCR) to evaluate the gene expression levels of a selection of molecular biomarkers. These indicators are usually involved in bivalves' response to stress due to microplastic pollutants and specifically are associated with different processes such as biotransformation and detoxification (cytochrome P450-3-like-2, cytochrome P450-1-like-1, π -glutathione-S-transferase), DNA repair (tumor protein, p53), cellular response (heat shock protein 70), and innate immunity (cathepsin and lysozyme).

2. Materials and Methods

2.1. Experimental Design

The experiments were conducted at the laboratories of Marine Ecosystem and Fisheries Centre of the Istituto Zooprofilattico Sperimentale dell'Abruzzo e del Molise "G. Caporale", in the NET4mPLASTIC project [44]. Although we have treated animals that do not require authorization by an ethical committee for animal testing, we have however asked for information from the Ethics Committee of University of Teramo (Italy), which declared that our experiment was out of Directive 63/2010 of the European Parliament and of the Council on the protection of animals used for scientific purposes (transposed into Italian law by Legislative Decree 26/2014).

Mussels (total number: 360 organisms) used for the experiments of exposure to MPs and depuration were collected from the Defmar mussel farm located at Termoli (Italy), selected based on the commercial size class, i.e., 4–7 cm in shell height. Three replicates were conducted, and each experimental group was made up of 120 individuals (divided into 2 groups of 60). The experimental setup consisted of two 50 L glass aquariums containing filtered artificial seawater (Instant Ocean; 0.8 mm membrane filter, Supor® 800) placed in a climatic room at constant temperature of 18 ± 1 °C. (Figure 1).

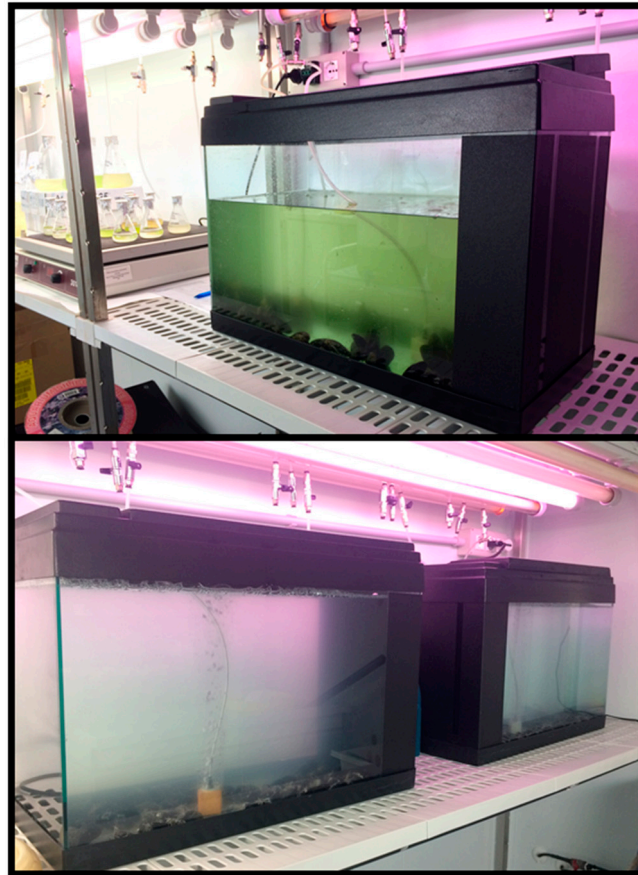


Figure 1. Experimental setup including the two 50 L glass aquariums containing filtered artificial seawater, placed in thermostatic chamber at 20 °C, with inside mussels tested.

The experimental protocol lasted 17 days and it included the following consequential phases: (a) acclimatization (7 days) (control group), (b) exposure phase (3 days) (T0 group), (c) 2 days depuration (T2 group), and (d) 7 days depuration (T7 group). At the end of each phase, 20 mussels were collected (10 for each aquarium) for MPs' qualitative–quantitative analysis (see Section 2.3). Moreover, 5 mussels were sampled for gene expression analysis (see Section 2.4).

First, once arrived in the laboratory, mussels were scrubbed to remove biofouling and then acclimated for 7 days in two 50 L glass aquarium systems containing filtered artificial seawater. During this acclimatization phase, mussels were maintained under photoperiod regime of 12 h light–12 h dark, and water's chemical–physical parameters were monitored (temperature of 18 ± 1 °C, salinity 32–35‰, dissolved oxygen $\geq 80\%$, and pH 7.5–8.5). Furthermore, filtered artificial seawater used was continuously aerated and changed daily. No food was supplied for the entire duration of acclimatization. This phase is necessary to allow the clearance of the mussels' gut. After the acclimatization period, 20 mussels (control group—not treated mussels) were collected for the digestion and MPs' qualitative–quantitative analysis, while the remaining organisms were used for a 3-day exposure phase.

For the exposure phase, three main types of microplastics, usually found in seawater columns, were used: 53% fibers, 30% fragments, and 3% granules [45], with 10^4 particles/L as frequently reported in marine environment [46] (see the following paragraph 2.2). The experiments were performed at constant salinity of 32–35‰, temperature of 18 ± 1 °C, and a 12 h light–dark regime. The mortality of mussels was monitored daily, and the water was renewed to ensure that previously ingested material, including microplastic particles, would not be ingested again.

Furthermore, during the whole period, mussels were fed daily with algal cultures of *Isochrysis galbana* and *Tetraselmis suecica* with a dose equal to 3% of mussels' dry weight, ration considered enough to fulfill mussels' daily energy requirements [47]. The algae were cultured using filtered seawater starting from small volume (50 mL) until massive algal production (150–200 L), via intermediate volumes. Before feeding, algal cell densities were measured using Bürker chamber, to ensure the right concentration to add to each experimental tank.

At the end of the 3-day exposure phase, mussels were removed from the exposure tanks and thoroughly rinsed to avoid any transfer of microplastics. Twenty mussels (0-time group) were removed and prepared for digestion and MPs' qualitative–quantitative analysis, while other organisms were moved to another tank with clean seawater and subsequently underwent depuration process.

Depuration phase lasted a total of 7 days during which monitoring of mortality, water renewal, and feeding of organisms was carried out on a daily basis. At the end of the 2-day depuration period, 20 mussels (2-time group) were removed and prepared for digestion and MPs' qualitative–quantitative analysis, while other organisms continued purification for up to 7 days. At the end of the 7-day depuration period, 20 mussels (7-time group) were removed and prepared for digestion and MPs' qualitative–quantitative analysis. Two different depuration times were chosen:

- (a) A “microbiological” depuration lasting 2 days, corresponding to the time usually applied for microbiological depuration in shellfish purification plants;
- (b) An “experimental” depuration lasting 7 days, assuming that increasing the dwell time in the shellfish purification plants could allow a better depuration from these contaminants. The same experiment in its entirety was repeated in triplicate.

Furthermore, considering that airborne particle contamination in laboratories can be very high if precautions are not taken [48], laboratory access was restricted to researchers who wore distinctive (for subsequent particle identification) blue cotton coveralls whenever working in the room. The same attire was worn during sample processing.

2.2. Preparation of the Microplastic Mixture

Microplastics used for the exposure phase of the *M. galloprovincialis* samples were polystyrene (EPS) granules with a diameter of 100 and 200 µm, polypropylene (PP) filaments with a size range from 50 to 4000 µm, and polyethylene terephthalate (PET) fragments with a size range from 2 to 300 µm.

Filaments and fragments were industrial by-products; therefore, to know the number of particles present in 1 mg, we weighed, ten replicates of 1 mg of particles, and after we counted them with a stereomicroscope. Instead, granules were purchased (ChromoSphere Dry Dyed Polymer Particles; ThermoScientific™ Waltham, MA, USA) with a certification regarding their concentration.

Defined the concentration of microplastics (200 filaments/g; 300 fragments/g and 2.2×10^6 granules/g), 1 L stock suspensions of the three polymers' mixture, inside glass bottles, were prepared in filtered sea water with a concentration of 5×10^5 particles/L.

Lastly, in order to obtain the MPs mixture's final concentration of 10^4 particles/L in the aquariums, 1 L of stock solution was poured daily for the total duration of 3 days of the contamination phase, after each water replacement.

2.3. MPs' Qualitative-Quantitative Analysis

Before their dissection, mussel height (cm) was measured. Digestion of mussel's soft body was performed for each individual separately by filling a glass bottle with 20 mL of 15% H₂O₂ per gram of soft tissues, according to the Mathalon and Hill procedure [49] and Bessa et al. [50] with minor modifications (digestion time increased until 7 days; elimination of density separation by NaCl's phase). Bottles with samples were covered and placed in an incubator at 60–65 °C for 5–7 days.

For each experimental group, three blank samples (consisting of water plus 15% H₂O₂) were also performed using the same analytical methods. Blank correction was made by subtracting the mean MP particle for each size, shape, and color counted in the blanks from those found in the matching samples.

Following digestion, each sample was vacuum filtered through 47 mm diameter, 2.7 µm pore size glass microfiber filters (Whatman[®] glass microfiber filters, Grade GF/D, GE HealthCare, Chicago, IL, USA). The filters thus obtained were then placed in glass Petri dishes and left to dry at room temperature.

Finally, filters were observed under a stereomicroscope (Leika MZ6, Leica Microsystem Ltd., Heerbrugg, Switzerland), images were taken using a digital camera (JVC-C1381, JVC, Yokohama, Japan) (Figure 2) and each particle was measured along its longest dimension, using Leica IM500 software (Leica Microsystem Ltd., Heerbrugg, Switzerland). A visual assessment was applied to recognize and classify the spiked microplastics according to the rules of [51] and the hot needle test [52].

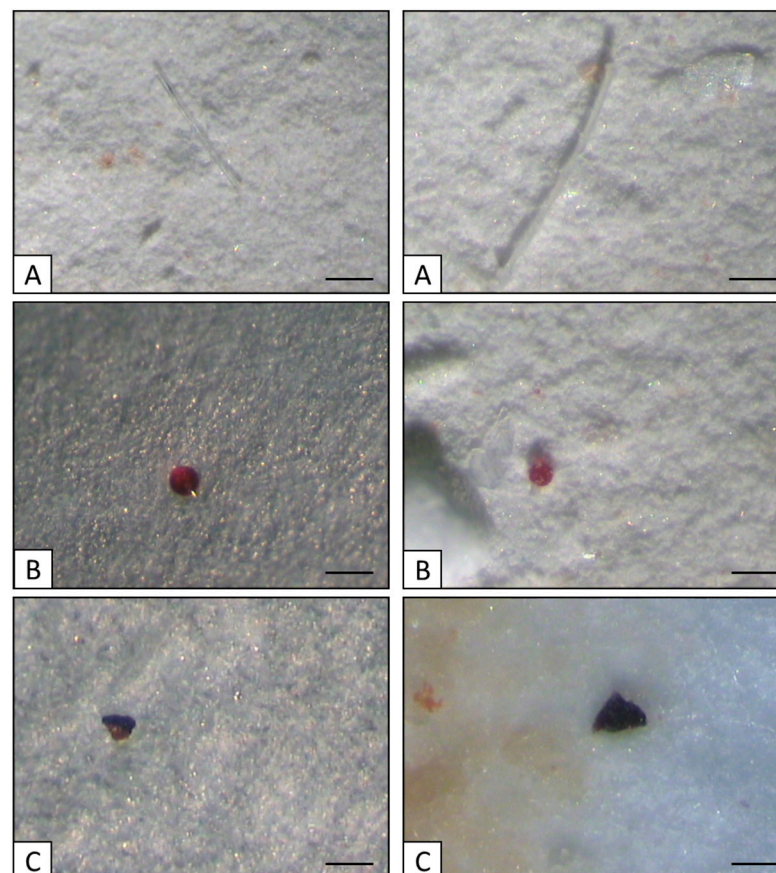


Figure 2. Images of microplastics used in the experiment: fibers (A), granules (B), and fragments (C). (Scale bar: 50 µm).

The blue cotton fibers produced by the outer clothing worn by laboratory workers were easily recognized during visual microscopy due to their unique color and structure and were subsequently ignored during particle counting.

2.4. Gene Expression Analysis

For each sampling time (control group, 0-time group, 2-time group, and 7-time group) five organisms were taken. From each bivalve, separate gills and digestive glands were taken and pools were created, then samples were submitted to biomolecular investigations in order to evaluate a set of target genes, through the analysis of gene expression with RT-qPCR, to evaluate the response of bivalves to stress from microplastic pollutants.

As organs were randomly divided into each pool and sex and gametogenesis status cannot be determined through external morphology of the body, only by histological analysis of the gonads, for this experiment there was no possibility to recognize the sexual traits of each animal belonging to the pool. The molecular analysis was therefore conducted considering the biological responses of the mussel population as a natural collection of both males and females.

The steps performed for the gene expression analysis are as follows: (a) RNA extraction and cDNA synthesis, (b) primers and PCR efficiency (*Eff*); (c) qPCR Sybr Green.

2.4.1. RNA Extraction and cDNA Synthesis

For each sampling time, digestive glands and gills were dissected and quickly snap-frozen in RNA later™ Stabilization Solution (ThermoScientific™ Waltham, MA, USA) and stored individually at -80°C . Digestive glands and gills were then pooled (4–5 individuals per pool) according to sampling time and, for each pool, total RNA was subsequently extracted using Quick-RNA™ MiniPrep Plus kit (Zymo Research, Irvine, CA, USA), following the manufacturer's recommendations. Briefly, 50 mg of each sample was submerged into 600 μL of DNA/RNA Shield™ and homogenized. For every 300 μL of sample, was added 15 μL Proteinase K and 30 μL PK Digestion Buffer, mixed and incubated at room temperature ($20\text{--}30^{\circ}\text{C}$) for 5 h. To remove particulate debris, sample was centrifuged and the cleared supernatant was transferred into a nuclease-free tube. An equal volume of RNA Lysis Buffer was added to the supernatant and mixed well. The lysed sample was transferred into a Spin-Away™ Filter and centrifuged at $16,000\times g$ per 30 s to remove the majority of genomic DNA. One volume of ethanol (95–100%) was added to the flow-through and mixed well. Then the mixture was transferred into a Zymo-Spin™ IICG Column, centrifuged and the flow-through was discarded. An amount of 400 μL RNA Prep Buffer was added to the column, centrifuged and the flow-through was discarded. An amount of 700 μL RNA Wash Buffer was added to the column, centrifuged, and the flow-through was discarded. An amount of 400 μL RNA Wash Buffer was added, centrifuged the column, and the flow-through was discarded. Lastly, 100 μL DNase/RNase-Free Water was added to the column matrix, centrifuged and the eluted RNA was harvested.

RNA extracted from all samples was quantified by the Qubit 2.0 fluorometer (ThermoFisher Scientific), using the Qubit™ RNA High Sensitivity (HS) kit, according to manufacturer's instructions. Concerning purity, all RNA samples showed absorbance ratios ($A_{260\text{nm}}/A_{280\text{nm}}$ and $A_{260\text{nm}}/A_{230\text{nm}}$) above 1.9, indicating a high level of purity.

cDNA synthesis reverse transcription (RT) was performed using 2.5 μg of the total RNA using RevertAid H Minus First Strand cDNA Synthesis Kit (Thermo Fisher Scientific) with random hexamers and according to the manufacturer's instructions. A control cDNA sample was made for each organ by pooling the same volume of each cDNA sample.

2.4.2. Primers and PCR Efficiency (*Eff*)

The genes to be tested as biomarkers, listed in Table 1, were chosen in agreement with the recent scientific bibliography [34–36]. Two genes, β -actin and tubulin, were selected as stable housekeeping already described in the literature by [36].

Primers were synthesized by Eurofins Genomics GmbH (Ebersberg, Germany)). PCR efficiency (*Eff*) was calculated for each primer pair in both organs by making standard curves from serial dilutions of reference cDNA (from 1/50 to 1/800) and using the following formula [53]: $\text{Eff} = 10^{-1/\text{slope}}$.

Efficiency of the amplification was determined for each primer pair using serial 5-fold dilutions of pooled cDNA and calculated as $E = 10^{-1/s}$, where s is the slope generated from the serial dilutions [53]. Primer pairs specificities were checked both in silico and empirically by BLAST analysis and using melting profiles. BLAST analyses indicated all primers were specific, which was confirmed by melting profiles.

Table 1. Gene name, abbreviation, pathway/function, primer pair, GenBank accession numbers, and references, for target genes analyzed in digestive gland and gills of *Mytilus galloprovincialis*.

Gene Name	Abbreviation	Pathway/Function	Forward (5'-3')	Reverse (5'-3')	Accession Number	Reference
β -Actin	<i>act</i>	Housekeeping gene	CGACTCTGGAGATGGTGCA	GCGGTGGTTGTGAATGAGTA	AF157491.1	[36]
α -Tubulin	<i>tub</i>	Housekeeping gene	CTTCGGTGGTGGTACTGGAT	AGTGCTCAAGGGTGGTATGG	HM537081.1	[36]
Cytochrome P450-1-like-1	<i>cyp11</i>	Phase I biotransformation	TGGTTGCGATTGTTATGCCCTGGA	GGCGGAAAGCAATCCATCCGTA	JX885878	[34]
Cytochrome P450-3-like-2	<i>cyp32</i>	Phase I biotransformation	CAGACGCGCCAAAAGTGATA	GTCCAAGCCAAAAGGAAGG	AB479539	[34]
π -glutathione-S-transferase	<i>π-gst</i>	Phase II biotransformation	CCTGAAACCAACCAAGGGTTACAT	TGGACTCCTGGTCTAGCCAACACT	AF227977/ AF527010	[34]
<i>p</i> -53 tumor suppressor-like	<i>p53</i>	Cellular stress response	CAACAACCTGCCCAATCCGA	GGCGGCTGGTATATGGATCT	AY579472/ DQ158079	[34]
Heat shock protein 70	<i>hsp70</i>	Cellular tissue repair	CCCTTTCTTCAAGCACACAAGCA	AACTGGTTCCATGGTTCTCTGAA	AF172607	[36]
Cathepsin	<i>cat</i>	Immune system	CGCAGCTAATGTTGGCGCC	CTACGGCGATTGGTCCCTG	AF172607	[36]
Lysozyme	<i>lys</i>	Immune system	TCGACTGTGGACAACCAAAA	GTGACCAATGTACCTCGCCA	AF334662/ AF334665	[35]

2.4.3. qPCR Sybr Green

qPCR Sybr Green was performed using the Applied Biosystems 7500 Real-time System. Assays were performed in triplicate using PowerUp™ SYBR™ Green Master Mix (ThermoFisher Scientific) according to the manufacturer's instructions. Briefly, 2 μ L of each sample's cDNA was used at the concentration of 5 ng. Each PCR reaction (20 μ L/well) contained 10 μ L of PowerUp™ SYBR™ Green Master Mix (2X), 1.5 μ L of forward and reverse primers (500 nM for each primer) and 5 μ L of Nuclease-Free Water. The PCR program consisted of 2 min of Dual-Lock DNA polymerase activation at 95 °C followed by 40 cycles of 15 s of denaturation at 95 °C, 15 s of annealing at 55–60 °C and 1 min of elongation at 72 °C. For each sample a melting curve program was performed having the following conditions: 1 cycle 95 °C for 15 s, 60 °C for 1 min, and 95 °C for 15 s. To minimize technical variation, all samples were analyzed on the same run for one gene. Each PCR run included the control cDNA sample and water controls. Relative gene expression was calculated with the $2^{-\Delta\Delta C_t}$ method, extensively used as a relative quantification strategy for quantitative real-time polymerase chain reaction (qPCR) data analysis [54].

2.5. Statistical Analysis

The statistical analyses of data were performed using R v4.0.5 (R Core Team, 2021, R Foundation for Statistical Computing, Vienna, Austria) and Excel 2016 (Microsoft, Silicon Valley, CA, USA). Normality of data set was tested with Shapiro–Wilk test. Then, non-parametric tests were used if the data were not normally distributed.

Beta distribution with 95% confidence intervals was used to verify the variability between the three experimental replicates with respect to the percentages of organisms contaminated by microplastics. A Kruskal–Wallis test was also applied to verify any differences between the experimental groups with respect to the variables “size” and “n. particles MPs/g”. When the Kruskal–Wallis test was significant, Dunn's post hoc tests were

carried out for comparisons between all possible pairs, and Bonferroni's correction was applied.

Linear regression analysis was used to verify the possible existence of a linear relationship between the number of MP particles per gram and time. The Spearman rank correlation test was performed to test any correlation between size of the mussels and the number of MPs.

For the analysis of gene expression data, to assess variations in transcript levels across different sampling times, we employed the non-parametric Mann–Whitney test. The analysis with $p < 0.05$ was considered statistically different.

3. Results

3.1. MPs' Accumulation and Depuration

In all experiments conducted in T0 groups, 100% of mussels were contaminated with a number of MPs between 182 and 217 MPs/individuals total number. The average of MPs particles/g ranged from 1.97 to 2.4. In T2 groups, the percentage of contaminated organisms was, respectively, 95, 70, and 75 with a number of MPs between 26 and 63. The average of MPs particles/g ranged from 0.24 to 2.4. In T7 groups, the percentage of contaminated organisms ranged from 55 to 75, the average of MPs particles/g ranged from 0.26 to 1 (Table 2).

Table 2. Summary table of the bivalves contaminated by MPs in the three experimental replicates with u.c.l. (upper control limit) and l.c.l. (lower control limit) at 95%. Group T0: 20 organisms collected at the end of the 3 days of exposure to MPs; Group T2: 20 organisms collected at the end of the 2 days of depuration (microbiological depuration); Group T7: 20 organisms collected at the end of the 7 days of depuration (experimental depuration for MPs).

	N. Organisms Found Contaminated	N. Organisms Found Contaminated (%)	l.c.l.	u.c.l.	N. MPs/Individuals' Total Number \pm SD	Average MPs Particles/g \pm SD	Granules (%)	Fibers (%)	Fragments (%)
EXPERIMENTAL GROUPS (replicate 1)									
Group T0	20/20	100%	87%	100%	182 \pm 8.69	2.40 \pm 1.10	36	60	4
Group T2	19/20	95%	76%	99%	63 \pm 2.40	0.79 \pm 0.64	11	87	2
Group T7	15/20	75%	53%	89%	28 \pm 1.23	0.39 \pm 0.35	7	89	4
EXPERIMENTAL GROUPS (replicate 2)									
Group T0	20/20	100%	87%	100%	217 \pm 5.58	2.15 \pm 1.24	37	61	2
Group T2	14/20	70%	48%	85%	38 \pm 1.76	0.45 \pm 0.31	16	71	13
Group T7	13/20	65%	43%	82%	20 \pm 0.97	0.17 \pm 0.15	0	95	5
EXPERIMENTAL GROUPS (replicate 3)									
Group T0	20/20	100%	87%	100%	203 \pm 8.29	1.97 \pm 1.32	17	83	0
Group T2	14/20	95%	48%	85%	26 \pm 8.19	0.24 \pm 0.11	8	88	4
Group T7	11/20	55%	34%	74%	27 \pm 0.78	0.26 \pm 0.20	0	89	11

By analyzing the percentages of organisms contaminated by microplastics (Table 2), with the relative 95% confidence interval, calculated using the Beta distribution, it is possible to observe for each of the three replicates a variability between the replicates that is not statistically significant, as the 95% confidence intervals are comparable. This means that the presence of the experimental error did not interfere with the results obtained during our experiments.

On the values relating to "n. particles MPs/g" a linear regression analysis was performed to verify the possible existence of a linear relationship between the number of MPs particles per gram and sampling times (T0, T2, and T7 group). From the regression plot (Figure 3, Table 3), it is possible to observe a statistically significant decrease (p Value 2.5×10^{-14}) in the number of MPs found per gram of soft tissue of the analyzed mussels after 7 days of depuration process (group T0: average 2.17 MPs/g; group T2: average 0.49 MPs/g; group T7: average 0.27 MPs/g). This decrease, although already present after 2 days, was not statistically significant, but instead, it became so after 7 days of depuration.

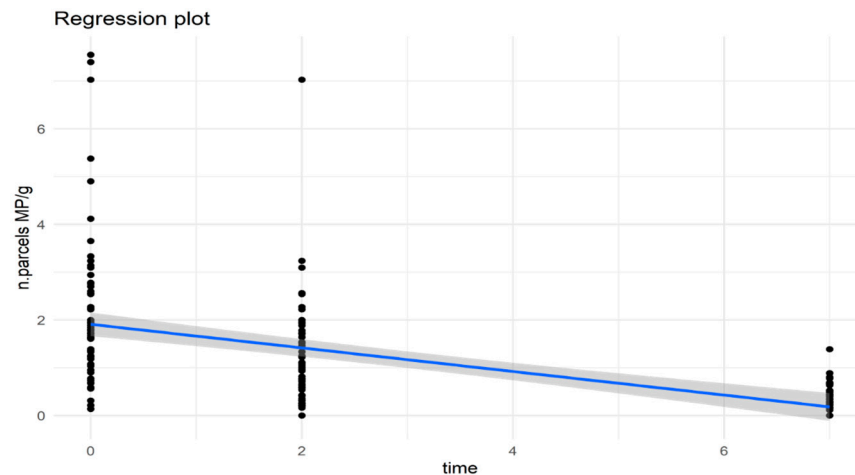


Figure 3. Regression plot of n. particles MP/g trend in three experimental replicates.

Table 3. Table of coefficients of the linear regression analysis to verify a linear relationship between the “n. particles MP/g” and the “time expressed in days”.

	Coefficients	Standard Error	Stat t	Significance Value	Lower 95%	Upper 95%
Intercept	1.91	0.12	15.28	3×10^{-34}	1.66	2.16
TIME	−0.25	0.03	−8.30	2×10^{-14}	−0.31	−0.19

Furthermore, to verify the differences in the experimental groups (control, T0, T2, and T7 group) with respect to the variable “n. particles MP/g” (Figure 4), the Kruskal–Wallis test was performed, followed by related Dunn’s post hoc tests (with Bonferroni correction). This comparison showed a statistically significant difference between: (a) the control group vs. T0 group (p Value: 1.23336×10^{-6}), indicating that T0 group was correctly contaminated experimentally with MPs compared to the control group; (b) T0 group vs. T7 group (p Value: 0.007125783), highlighting a good capacity of the mussels after 7 days of depuration to properly remove the microplastics accumulated within their soft tissue.

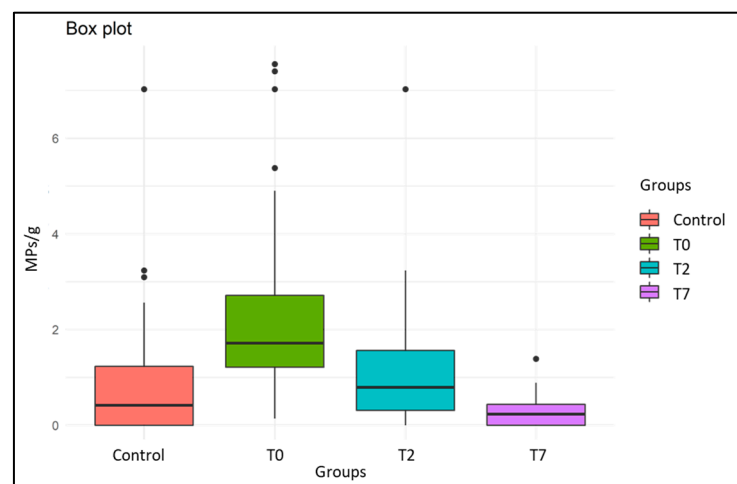


Figure 4. Box plot representing the number particles MP/g differences in experimental groups. Control group: organisms collected at the end of the 7 days of acclimatization phase; Group T0: organisms collected at the end of the 3 days of exposure to MPs; Group T2: organisms collected at the end of the 2 days of depuration (microbiological depuration); Group T7: organisms collected at the end of the 7 days of depuration (experimental depuration for MPs).

For the variable “size” of the MPs (Table 4), the statistical analysis carried out on the experimental groups highlighted statistically significant differences between the control group vs. T0 group (p Value: 4.42×10^{-7}) and control group vs. T2 group (p Value: 0.0001). This comparison suggests that the frequency in the control group of microplastic particles of size 50–100 μm (most represented size class) is statistically different from that found in groups T0 (most present size class: 1000–2000 μm) and T2 (class most present dimensional: <1000 μm). In addition, statistically significant differences were found between the T0 group vs. T7 group (p Value: 0.007048), pointing that the frequency in the T0 group of MPs of size 1000–2000 μm (most represented size class) is statistically different from that present in the T7 group (most present size class: <1000 μm).

Table 4. Summary table of the percentage presence of the various size classes of microplastic particles in the comparison groups (control, T0, T2, and T7 groups).

	10–50 μm	50–100 μm	200 μm	100–500 μm	<1000 μm	1000–2000 μm	2000–3000 μm	>3000 μm
Control group	1%	70%	0%	1%	15%	7%	3%	3%
T0 group	0%	0%	6%	1%	18%	43%	24%	7%
T2 group	2%	13%	2%	0%	33%	17%	31%	2%
T7 group	1%	5%	0%	3%	51%	20%	11%	9%

The results of the variable “type of microplastics” is reported in Figure 5, which shows the different decrease for each type of microplastic chosen in the three experimental replicates. Granule seems to be eliminated more effectively by mussels, both after 2 and 7 days of depuration, followed by filament and fragment.

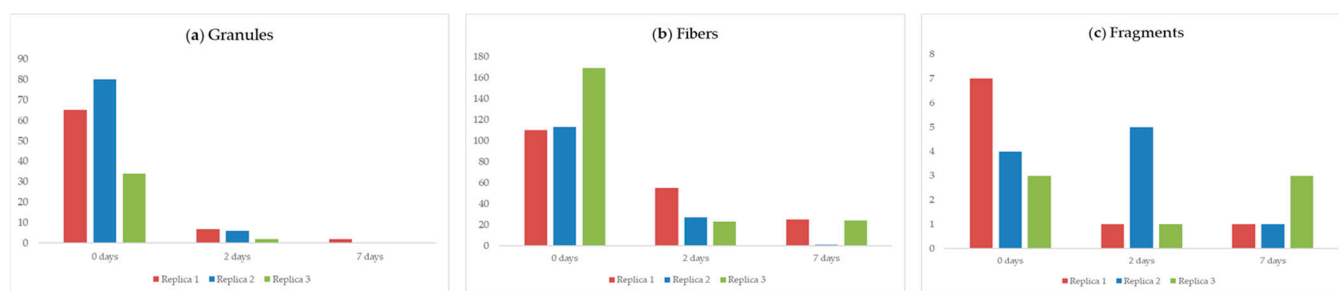


Figure 5. Graphical representation of the number of granules (a), fibers (b), and fragments (c) in the three experimental replicates. Error bars = Standard deviation.

Finally, the Spearman’s rank correlation rho test was performed to evaluate a possible positive correlation between the size of mussels (expressed in soft tissue weight) and the number of microplastic particles found. The results indicate that there was no significant correlation between the two variables (p Value = 0.6313).

3.2. Gene Expression Analysis

Molecular biomarkers, already known from other studies to be involved in the response to pollutants [34–36] were tested in analyzed mussels’ gills and digestive glands. The digestive gland and gills are both tissues of relevant interest for the analysis of the change in the expression of target genes. The first has been described as the organ in which pollutants accumulate in higher concentrations, while gills are the dominant site of interaction with the environment [36].

Overall, a differential expression was observed (Figure 6) between the groups of mussels tested, in particular, most of the differences were found in the gills, thus defining it as the target organ for the use of these biomarkers [34,55].

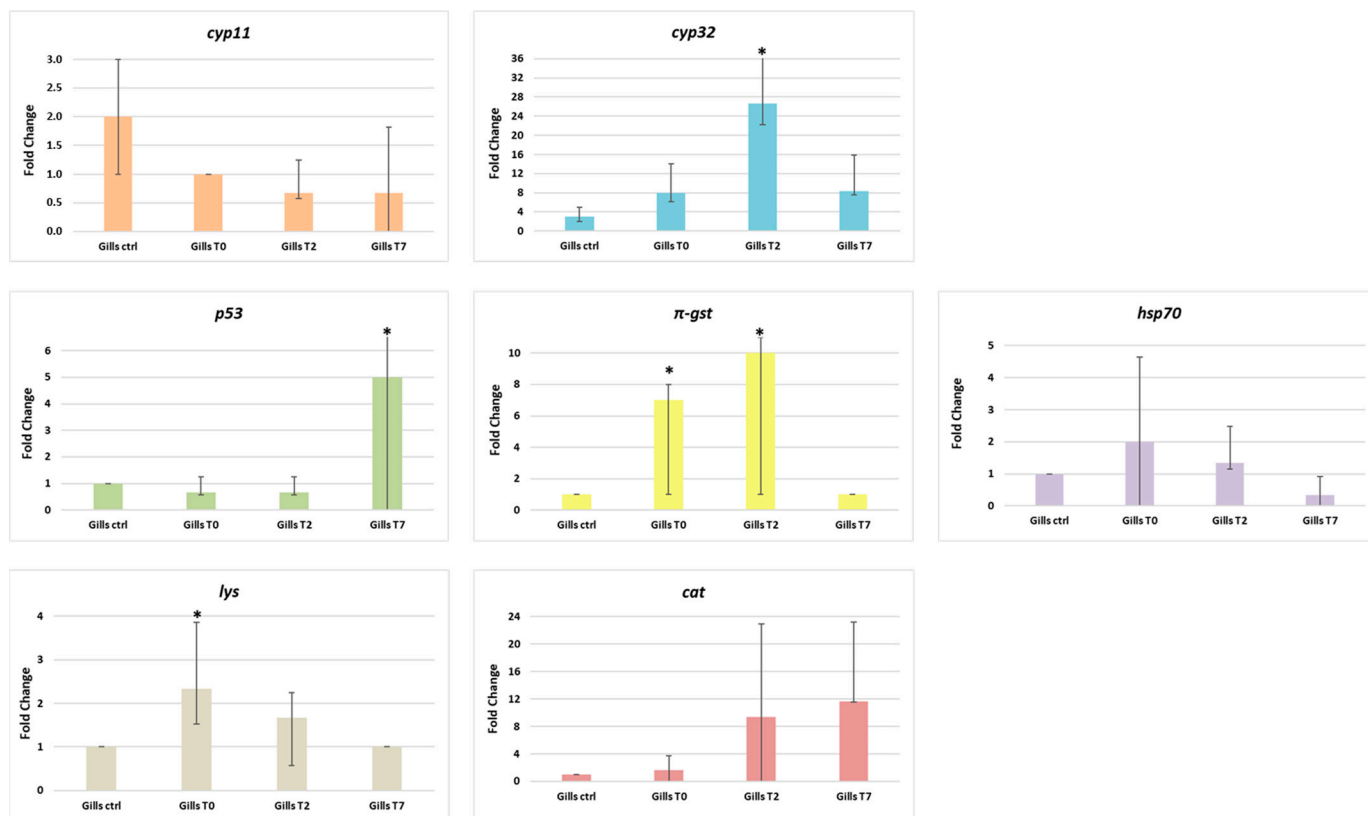


Figure 6. Gene expression results calculated with the $2^{-\Delta\Delta CT}$ method [54]. Bar graph presentation of the fold change in target genes analyzed (*cyp11*, *cyp32*, *p53*, *π-gst*, *hsp70*, *lys*, and *cat*) as a function of sampling times in gills of *M. galloprovincialis* after 3 days MP exposure phase (Gills T0), after 2 days depuration phase (Gills T2) and after 7 days depuration phase (Gills T7). All RT-PCR results are normalized to β -actin and tubulin, the housekeeping genes, and expressed as change from their respective controls. The average values were obtained from three experiments. Significant difference < 0.05 is indicated by an asterisk. Values represent the means \pm standard deviation (SD).

In gills, a significant increase ($p = 0.001$) in mRNA abundance of *cyp32* was found after 2 days of depuration (Gills T2) when compared to the control group, whereas *cyp11* mRNA levels were basically unaltered in relation to the control group, as described by [34].

Transcriptional levels of the *p53* gene in gills significantly increased ($p = 0.001$) in mussels after 7 days of depuration (Gills T7) compared to the control group, whereas mRNA levels of *π-gst* significantly increased ($p = 0.001$) in mussels both after 2 and 7 days of depuration (Gills T2 and Gills T7). In the gills, the expression levels of *hsp70* were upregulated in the mussels exposed (Gills T0) in comparison to the mussels subjected to 7 days of depuration (Gills T7).

Finally, always in gills, mRNA abundance of the *lys* gene in mussels exposed (Gills T0) is statistically upregulated ($p = 0.002$), whereas the expression levels of the *cat* gene showed no significant increase in both groups subjected to depuration compared to the control group. Concerning the target genes' expression in the digestive glands of *M. galloprovincialis* (Figure 7), our results highlight no statistically significant increase in the level of mRNA of *cyp11* in the digestive glands of mussels exposed for 3 days to MPs (Digestive gland T0) compared to mussels subjected to depuration. Furthermore, in the digestive gland, transcriptional levels of genes *cyp32* e *π-gst*, associated with biotransformation and detoxification processes, were unaltered in all mussel groups.

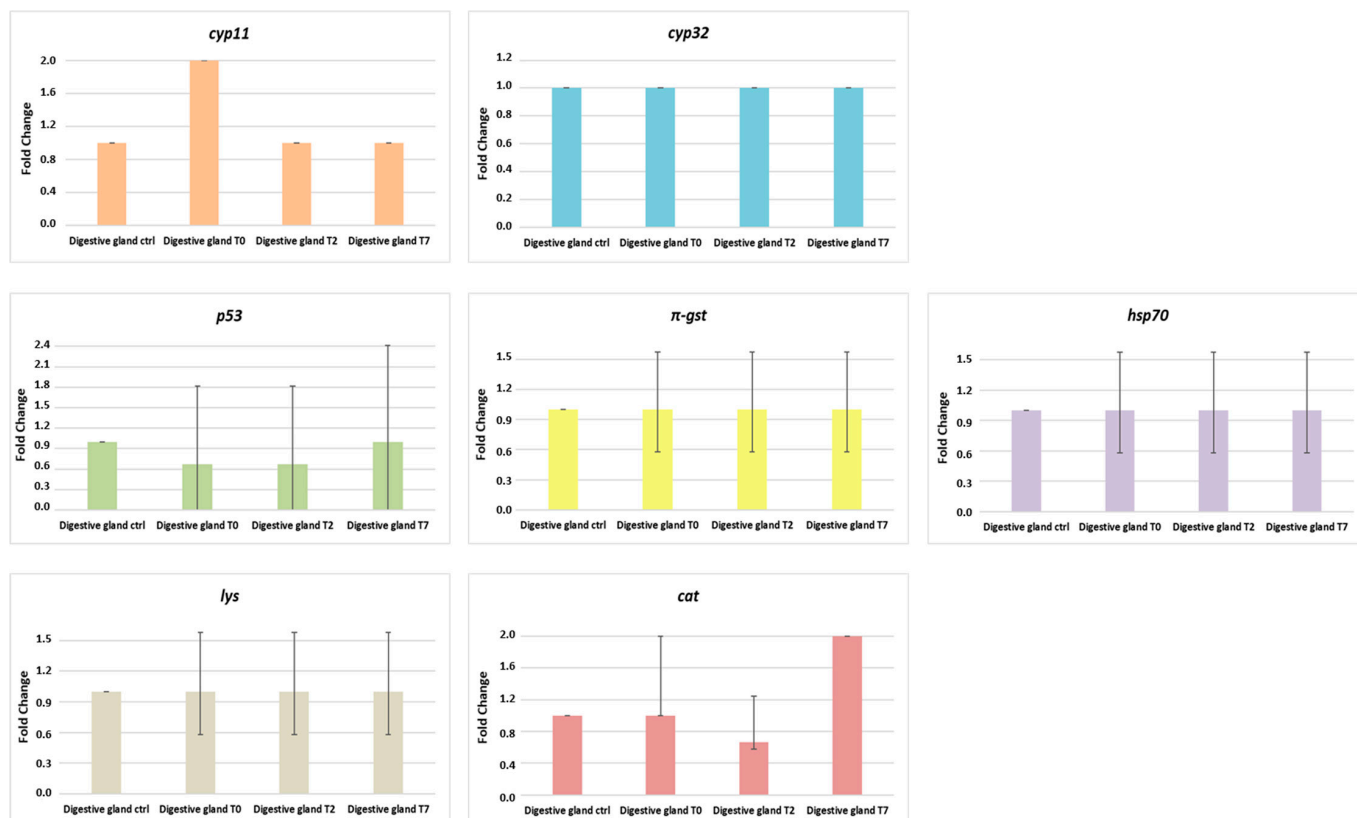


Figure 7. Gene expression results calculated with the $2^{-\Delta\Delta CT}$ method [54]. Bar graph presentation of the fold change in target genes analyzed (*cyp11*, *cyp32*, *p53*, π -*gst*, *hsp70*, *lys*, and *cat*) as a function of sampling times in digestive gland of *M. galloprovincialis* after 3 days MP exposure phase (Digestive gland T0), after 2 days depuration phase (Digestive gland T2) and after 7 days depuration phase (Digestive gland T7). All RT-PCR results are normalized to β -actin and tubulin, the housekeeping genes, and expressed as change from their respective controls. The average values were obtained from three experiments. Significant difference <0.05 is indicated by an asterisk. Values represent the means \pm standard deviation (SD).

Regarding the *p53* gene, the expression was slightly decreased in the digestive gland of mussels after both the exposure phase (Digestive gland T0) and 2 days of depuration (Digestive gland T2) compared to the control group. Cell tissue repair-related gene *hsp70*, presented an unaltered transcriptional level in the digestive gland of all mussels groups.

Lastly, regarding immune genes in the digestive gland, mRNA levels of *lys* were unaltered, whereas the transcriptional levels of the *cat* gene appeared upregulated in the depurated group (Digestive gland T7) when compared to other groups.

4. Discussion

Exposure experiments are effective methods to study the uptake of contaminants. The ingestion and biological effects of microplastics have been tested in numerous previous studies [12,33,38–40,42,43,52,56,57]. Considering the limitations imposed by the common approach of using a single type of microplastic, the present study instead used three types of microplastic particles (i.e., fibers, fragments, and granules) usually found in the marine environment to simulate as much as possible the microplastic pollution [45,46]. This approach allows us to obtain more detailed information about MP accumulation and depuration processes in mussels.

In our exposure experiments, we tried to recreate a condition of microplastic pollution, using the main types of microplastics found in seawater columns with a final concentration frequently reported in the marine environment, however, we encountered limitations given

by our experimental design. This could be due to (a) microplastics present in marine environments could have different physical–chemical properties such as shapes, sizes, colors, compositions, and additives [58]; (b) microplastic accumulation in the marine environment occurs over a long period while the exposure experiments are shorter [20]. Therefore, great efforts are needed to simulate these aspects in exposure studies [20].

The linear regression analysis used to verify a possible relationship between the variables “number of MPs particles per gram” and “time” showed considerable variability in terms of the presence of microplastics in mussels’ soft tissue at the end of the 3-day exposure phase (T0). This variability confirmed by a low corrected R-squared value (0.275) could be explained by too short contamination times, so that all mussels did not bioaccumulate microplastics uniformly. In fact, our observations are in agreement with other studies [42] where short exposure times (10, 20, and 40 min) were performed and a higher number of microplastics, used for contamination, was found in the exposure water when compared to those found in bivalves’ soft tissue.

The mussels were able to remove most MPs within 7 days, with about an 80% reduction in average MPs’ concentration occurring between days 0 and 7, highlighting a statistically significant decrease (p Value 2.5×10^{-14}) in microplastic particles found per gram in analyzed mussels’ soft tissue. Our results are in agreement with previous studies [5,33] performed on both mussels and oysters, which demonstrated that a longer purification time (5–7 days) could give a significant reduction in MPs’ concentration of bivalves intended for human consumption. An example is the study conducted by Covert et al. [5], which observed in specimens of *Crassostrea gigas*, 5 days after the start of the depuration process, a reduction in the concentration of MPs’ particles equal to 73%. Comparing T0 and T2 groups (mussels at the end of 2-day depuration), where we found 2.17 MPs/g and 0.49 MPs/g, respectively, no statistically significant differences emerged (p Value 1). This result suggests that the two-day depuration time is not long enough to ensure the complete elimination of microplastic particles. Similarly, a previous study conducted by [59] highlights that differences in depuration rates among various particles probably reflect the differences in particle fate within bivalves. There is a fast elimination (between 0 and 1 h of depuration process) of those particles associated with the gills, or those recently rejected by the gills and labial palps and incorporated into mucous for ejection as pseudofeces. There is, instead, a long retention time for particles associated with a variety of tissues, including the digestive tract, mantle, and muscle [59].

Other studies [39] also suggest that the short depuration times are not sufficient to completely eliminate MPs in bivalves. In addition, longer depuration times (7 days) have been tested in other studies [60,61] suggesting that even a longer depuration period would not be enough to completely remove MPs accumulated in bivalves. Therefore, it is noteworthy that depuration can minimize the effects caused by MP contamination, even if it does not reach a 100% reduction [39].

Concerning microplastics’ size class found in analyzed mussels, our results showed a statistically significant difference between the T0 and T7 groups (p Value: 0.007048). In the T0 group, the most represented size class was 1000–2000 μm , unlike in the T7 group where microplastics <1000 μm in size were more present. These results could be explained by the ability of bivalves to eliminate larger microplastic particles more easily and in a shorter time. In fact, even in other bivalves, such as *Mytilus edulis* and *Crassostrea gigas*, a greater depuration capacity of larger microplastic particles has been found [38–62]. On the other hand, Fernandez and Albetosa [33] demonstrated that mussels (*M. galloprovincialis*) were unable to eliminate smaller particles (<6 μm) as well as larger ones, which remained in digestive glands.

The type of microplastics that seems to be eliminated more effectively by mussels, both after 2 and 7 days of depuration, are granules, followed by filaments and fragments. Probably granules’ spherical shape allows them to be less retained within the mussels, and are therefore able to get rid of them more easily [39–52]. In fact, we observed an almost total absence of this type of microplastic in all analyzed organisms after 7 days of depuration.

Fibers instead, due to their geometry, may be better trapped in mussels' gills and digestive glands, resulting in a longer depuration time compared with other microplastic types [23,39,52,63,64]. Regarding the fragments, we did not observe a typical trend during the overall duration of the experiment. Furthermore, no significant correlation was highlighted between variables "mussels' weight" and "number of MPs particles per gram". As also reported in other experiments, mussels' ability to accumulate microplastics, as well as to eliminate them, is not strictly correlated with the organisms' size [39]. Other studies, instead, showed a negative correlation between microfiber levels and mussel weight, which could be explained by the fact that in the *Mytilus* species, pumping and filtration rates decrease with higher soft tissue mass [65,66].

In addition to MPs' bioaccumulation and depuration experiments, seven biomarkers, known to be involved in pollutant response [34–36] were tested in *M. galloprovincialis*' gills and digestive glands.

A differential gene expression was observed between the groups of mussels tested and in particular, most of the differences were found in the gills, thus defining it as the target organ for the use of these biomarkers. Indeed, the gills are a key organ for the uptake during filtration processes of pollutants present in the marine environment and are known to temporarily accumulate the contaminants before their probable transfer to the digestive gland and other tissues [67].

Our results give further proof of the involvement of the *cyp32* gene in mussel bio-transformation processes [34–68] and of its potential as a biomarker since we observed a significantly higher *cyp32* mRNA level in the gills of mussels after 2-day depuration (T2) compared to the control group.

Variations of expression were observed for the *p53* gene, which plays an important role in apoptosis signaling [55] and therefore it is considered a cellular stress marker in mussels [69]. In particular, *p53* transcriptional levels in contaminated mussels (T0) showed a downregulation compared to other groups. This data could highlight, as described by Lacroix et al. (2014) [34], that inhibition of apoptosis processes is activated in contaminated mussels rather than an enhancement, most probably due to the existence of a powerful anti-apoptotic system in bivalves. This could explain their high resilience to pollution as suggested by Wang et al. [70].

Concerning the π -*gst* isoform, which plays a role in the antioxidant defense system [34], a statistically significantly higher mRNA level was observed in the gills exposed to MPs for 3-day mussels (T0) compared to other mussels. Also, other authors [34,71] observed in general higher π -*gst* mRNA levels in the gills of mussels sampled in polluted sites compared to control sites, which highlights the potential role of π -*gst* as a pollution biomarker. This same gene, instead, in the digestive glands of *M. galloprovincialis*, shows unaltered transcriptional levels, which has also been described by Brandts et al. [36] and Zanette et al. [68].

In gills, the observed increased expression of the *hsp70* gene after the exposure phase (T0) has also been described in other studies regarding the contamination with MPs [36,71,72], and it may indicate an induction of de novo synthesis of these proteins as an attempt to cope with pollutants.

Concerning the gene *cat*, our results showed an upregulation of this gene in the two mussel groups subjected to the two depuration times (T2 and T7). As reported by other recent studies [36,73,74], an upregulation of the *cat* gene transcript after exposure to MPs suggested that this cathepsin would play a role in an intracellular apoptotic pathway.

Lastly, the mRNA levels of *lys* noticeably increased in in mussels' group exposed to MPs for 3 days (T0), as also described by Brandts et al. [36], whose study reported such an increase in nanoplastic-exposed organisms.

5. Conclusions

Our evidence suggests that depuration processes can significantly reduce MP contamination in *M. galloprovincialis*, even if, as also indicated by Covernton et al. [5], it would be

difficult to completely remove all MPs from mussels under commercial depuration conditions. Indeed, in order to obtain a significantly reduced MP contamination in bivalves it is necessary (a) to use a “clean” facility (filtering water, covering tanks, and longer depuration time); and (b) to practice a depuration process for longer times than those already in use (Reg. UE 627/2019). Unfortunately, a longer depuration period (5–7 days) could implicate more cost to the industry, and consequently increase shellfish’s cost to the consumer [5]. Therefore, it is necessary to conduct more research to refine the depuration time that allows for good results in terms of cost/benefit.

Concerning molecular biomarkers analysis, several genes were found differentially expressed between sample mussel groups. However, further studies are necessary to confirm the diagnostic ability of this set of biomolecular biomarkers in marine environmental monitoring programs to be used as a supplement to traditional chemical and biomarker measures. Furthermore, it is known that sex and gametogenesis cycle could influence contaminant uptake and elimination or biomarkers levels in molluscs [75–77], as well as the *Mytilus* gene expressions involved in natural biological rhythms [78] or when the animals are exposed to endocrine disruptors [79–81]. Considering this, further investigations are needed involving histological observation of gonadal samples alongside gills and digestive glands, in order to analyze whether these molecular responses would be influenced by sex or the gametogenesis cycle in which the animals are found.

Author Contributions: Conceptualization, F.P., S.R., M.A. and M.D.D.; methodology, F.P., S.R., M.A. and M.D.D.; formal analysis, F.P., S.R. and M.A.; investigation, F.P., S.R. and E.N.; data curation, F.P., S.R., E.N. and R.S.; writing—original draft preparation, F.P., S.R., E.N., C.C. (Corinne Corbau), I.B., L.D.R. and F.D.G.; writing—review and editing, F.P., S.R., E.N., C.C. (Corinne Corbau), I.B., M.A., M.D.D. and L.F.M.; supervision, C.C. (Cesare Cammà) and N.F.; project administration, C.C. (Cesare Cammà) and N.F. All authors have read and agreed to the published version of the manuscript.

Funding: This research was supported by the European Regional Development Fund 2014–2020 Interreg V-A Italy-Croatia CBC Programme, New Technologies for Macro and Microplastic Detection and Analysis in the Adriatic Basin (project acronym: NET4mPLASTIC; CUP F76C19000000007).

Institutional Review Board Statement: Not applicable.

Informed Consent Statement: Not applicable.

Data Availability Statement: Data are presented in this article in the form of figures and tables.

Conflicts of Interest: The authors declare no conflict of interest.

References

1. Taylor, M.L.; Gwinnett, C.; Robinson, L.F.; Woodall, L.C. Plastic microfibre ingestion by deep-sea organisms. *Sci. Rep.* **2016**, *6*, 33997. [[CrossRef](#)] [[PubMed](#)]
2. Barrows, A.P.W.; Cathey, S.E.; Petersen, C.W. Marine environment microfiber contamination: Global patterns and the diversity of microparticle origins. *Environ. Pollut.* **2018**, *237*, 275–284. [[CrossRef](#)] [[PubMed](#)]
3. Stanton, T.; Johnson, M.; Nathanail, P.; MacNaughtan, W.; Gomes, R.L. Freshwater and airborne textile fibre populations are dominated by ‘natural’, not microplastic, fibres. *Sci. Total Environ.* **2019**, *666*, 377–389. [[CrossRef](#)] [[PubMed](#)]
4. Vivekanand, A.C.; Mohapatra, S.; Tyagi, V.K. Microplastics in aquatic environment: Challenges and perspectives. *Chemosphere* **2021**, *282*, 131151. [[CrossRef](#)] [[PubMed](#)]
5. Covernton, G.A.; Dietterle, M.; Pearce, C.M.; Gurney-Smith, H.J.; Dower, J.F.; Dudas, S.E. Depuration of anthropogenic particles by Pacific oysters (*Crassostrea gigas*): Feasibility and efficacy. *Mar. Pollut. Bull.* **2022**, *181*, 113886. [[CrossRef](#)] [[PubMed](#)]
6. Browne, M.A.; Galloway, T.; Thompson, R. Microplastic an emerging contaminant of potential concern? *Integr. Environ. Assess. Manag.* **2007**, *3*, 559–561. [[CrossRef](#)] [[PubMed](#)]
7. Sedlak, D. Three Lessons for the Microplastics Voyage. *Environ. Sci. Technol.* **2017**, *51*, 7747–7748. [[CrossRef](#)] [[PubMed](#)]
8. Sharma, S.; Chatterjee, S. Microplastic pollution, a threat to marine ecosystem and human health: A short review. *Environ. Sci. Pollut. Res.* **2017**, *24*, 21530–21547. [[CrossRef](#)]
9. Huang, W.; Song, B.; Liang, J.; Niu, Q.; Zeng, G.; Shen, M.; Deng, J.; Luo, Y.; Wen, X.; Zhang, Y. Microplastics and associated contaminants in the aquatic environment: A review on their ecotoxicological effects, trophic transfer, and potential impacts to human health. *J. Hazard. Mater.* **2021**, *405*, 124187. [[CrossRef](#)]
10. Rezanian, S.; Park, J.; Md Din, M.F.; Mat Taib, S.; Talaiekhosani, A.; Kumar Yadav, K.; Kamyab, H. Microplastics pollution in different aquatic environments and biota: A review of recent studies. *Mar. Pollut. Bull.* **2018**, *133*, 191–208. [[CrossRef](#)]

11. Ugwu, K.; Herrera, A.; Gómez, M. Microplastics in marine biota: A review. *Mar. Pollut. Bull.* **2021**, *169*, 112540. [[CrossRef](#)]
12. Von Hellfeld, R.; Zarzuelo, M.; Zaldibar, B.; Cajaraville, M.P.; Orbea, A. Accumulation, Depuration, and Biological Effects of Polystyrene Microplastic Spheres and Adsorbed Cadmium and Benzo(a)pyrene on the Mussel *Mytilus galloprovincialis*. *Toxics* **2022**, *10*, 18. [[CrossRef](#)] [[PubMed](#)]
13. Cole, M.; Lindeque, P.; Halsband, C.; Galloway, T.S. Microplastics as contaminants in the marine environment: A review. *Mar. Pollut. Bull.* **2011**, *62*, 2588–2597. [[CrossRef](#)] [[PubMed](#)]
14. Lee, H.; Shim, W.J.; Kwon, J.H. Sorption capacity of plastic debris for hydrophobic organic chemicals. *Sci. Total Environ.* **2014**, *470–471*, 1545–1552. [[CrossRef](#)] [[PubMed](#)]
15. Smith, M.; Love, D.C.; Rochman, C.M.; Neff, R.A. Microplastics in Seafood and the Implications for Human Health. In *Current Environmental Health Reports*; Springer: Berlin/Heidelberg, Germany, 2018; Volume 5, pp. 375–386. [[CrossRef](#)]
16. Xia, Y.; Niu, S.; Yu, J. Microplastics as vectors of organic pollutants in aquatic environment: A review on mechanisms, numerical models, and influencing factors. *Sci. Total Environ.* **2023**, *887*, 164008. [[CrossRef](#)] [[PubMed](#)]
17. Setälä, O.; Norkko, J.; Lehtiniemi, M. Feeding type affects microplastic ingestion in a coastal invertebrate community. *Mar. Pollut. Bull.* **2016**, *102*, 95–101. [[CrossRef](#)] [[PubMed](#)]
18. Phuong, N.N.; Zalouk-Vergnoux, A.; Kamari, A.; Mouneyrac, C.; Amiard, F.; Poirier, L.; Lagarde, F. Quantification and characterization of microplastics in blue mussels (*Mytilus edulis*): Protocol setup and preliminary data on the contamination of the French Atlantic coast. *Environ. Sci. Pollut. Res.* **2018**, *25*, 6135–6144. [[CrossRef](#)] [[PubMed](#)]
19. Li, H.X.; Ma, L.S.; Lin, L.; Ni, Z.X.; Xu, X.R.; Shi, H.H.; Yan, Y.; Zheng, G.M.; Rittschof, D. Microplastics in oysters *Saccostrea cucullata* along the Pearl River Estuary, China. *Environ. Pollut.* **2018**, *236*, 619–625. [[CrossRef](#)] [[PubMed](#)]
20. Qu, X.; Su, L.; Li, H.; Liang, M.; Shi, H. Assessing the relationship between the abundance and properties of microplastics in water and in mussels. *Sci. Total Environ.* **2018**, *621*, 679–686. [[CrossRef](#)]
21. Stamataki, N.; Hatzonikolakis, Y.; Tsiaras, K.; Tsangaris, C.; Petihakis, G.; Sofianos, S.; Triantafyllou, G. Modelling mussel (*Mytilus* spp.) microplastic accumulation. *Ocean Sci.* **2020**, *16*, 927–949. [[CrossRef](#)]
22. Laubscher, A.; Hamm, T.; Lenz, M. Where have all the beads gone? Fate of microplastics in a closed exposure system and their effects on clearance rates in *Mytilus* spp. *Mar. Pollut. Bull.* **2023**, *187*, 114474. [[CrossRef](#)] [[PubMed](#)]
23. Renzi, M.; Guerranti, C.; Blašković, A. Microplastic contents from maricultured and natural mussels. *Mar. Pollut. Bull.* **2018**, *131*, 248–251. [[CrossRef](#)] [[PubMed](#)]
24. Beyer, J.; Green, N.W.; Brooks, S.; Allan, I.J.; Ruus, A.; Gomes, T.; Bråte, I.L.N.; Schøyen, M. Blue mussels (*Mytilus edulis* spp.) as sentinel organisms in coastal pollution monitoring: A review. *Mar. Environ. Res.* **2017**, *130*, 338–365. [[CrossRef](#)] [[PubMed](#)]
25. Baechler, B.R.; Stienbarger, C.D.; Horn, D.A.; Joseph, J.; Taylor, A.R.; Granek, E.F.; Brander, S.M. Microplastic occurrence and effects in commercially harvested North American finfish and shellfish: Current knowledge and future directions. *Limnol. Oceanogr. Lett.* **2020**, *5*, 113–136. [[CrossRef](#)]
26. Daniel, D.B.; Ashraf, P.M.; Thomas, S.N.; Thomson, K.T. Microplastics in the edible tissues of shellfishes sold for human consumption. *Chemosphere* **2021**, *264*, 128554. [[CrossRef](#)] [[PubMed](#)]
27. Lozano-Hernández, E.A.; Ramírez-Álvarez, N.; Rios Mendoza, L.M.; Macías-Zamora, J.V.; Sánchez-Osorio, J.L.; Hernández-Guzmán, F.A. Microplastic concentrations in cultured oysters in two seasons from two bays of Baja California, Mexico. *Environ. Pollut.* **2021**, *290*, 118031. [[CrossRef](#)] [[PubMed](#)]
28. Sendra, M.; Sparaventi, E.; Novoa, B.; Figueras, A. An overview of the internalization and effects of microplastics and nanoplastics as pollutants of emerging concern in bivalves. *Sci. Total Environ.* **2021**, *753*, 142024. [[CrossRef](#)]
29. Santonicola, S.; Volgare, M.; Cocca, M.; Dorigato, G.; Giaccone, V.; Colavita, G. Impact of Fibrous Microplastic Pollution on Commercial Seafood and Consumer Health: A Review. *Animals* **2023**, *13*, 1736. [[CrossRef](#)]
30. Rosa, M.; Ward, J.E.; Shumway, S.E. Selective Capture and Ingestion of Particles by Suspension-Feeding Bivalve Molluscs: A Review. *J. Shellfish Res.* **2018**, *37*, 727–746. [[CrossRef](#)]
31. Browne, M.A.; Chapman, M.G.; Thompson, R.C.; Amaral Zettler, L.A.; Jambeck, J.; Mallos, N.J. Spatial and Temporal Patterns of Stranded Intertidal Marine Debris: Is There a Picture of Global Change? *Environ. Sci. Technol.* **2015**, *49*, 7082–7094. [[CrossRef](#)]
32. von Moos, N.; Burkhardt-Holm, P.; Köhler, A. Uptake and Effects of Microplastics on Cells and Tissue of the Blue Mussel *Mytilus edulis* L. after an Experimental Exposure. *Environ. Sci. Technol.* **2012**, *46*, 11327–11335. [[CrossRef](#)] [[PubMed](#)]
33. Fernández, B.; Albentosa, M. Insights into the uptake, elimination and accumulation of microplastics in mussel. *Environ. Pollut.* **2019**, *249*, 321–329. [[CrossRef](#)] [[PubMed](#)]
34. Lacroix, C.; Coquillé, V.; Guyomarch, J.; Auffret, M.; Moraga, D. A selection of reference genes and early-warning mRNA biomarkers for environmental monitoring using *Mytilus* spp. as sentinel species. *Mar. Pollut. Bull.* **2014**, *86*, 304–313. [[CrossRef](#)] [[PubMed](#)]
35. Paul-Pont, I.; Lacroix, C.; González Fernández, C.; Hégaret, H.; Lambert, C.; le Goïc, N.; Frère, L.; Cassone, A.L.; Sussarellu, R.; Fabioux, C.; et al. Exposure of marine mussels *Mytilus* spp. to polystyrene microplastics: Toxicity and influence on fluoranthene bioaccumulation. *Environ. Pollut.* **2016**, *216*, 724–737. [[CrossRef](#)] [[PubMed](#)]
36. Brandts, I.; Teles, M.; Gonçalves, A.P.; Barreto, A.; Franco-Martinez, L.; Tvarijonaviciute, A.; Martins, M.A.; Soares, A.M.V.M.; Tort, L.; Oliveira, M. Effects of nanoplastics on *Mytilus galloprovincialis* after individual and combined exposure with carbamazepine. *Sci. Total Environ.* **2018**, *643*, 775–784. [[CrossRef](#)]

37. Lee, R.; Lovatelli, A.; Ababouch, L. Bivalve depuration: Fundamental and practical aspects. In *FAO Fisheries Technical Paper*; Arabic edition; Food and Agriculture Organization of the United Nations: Rome, Italy, 2008.
38. van Cauwenberghe, L.; Janssen, C.R. Microplastics in bivalves cultured for human consumption. *Environ. Pollut.* **2014**, *193*, 65–70. [[CrossRef](#)]
39. Birnstiel, S.; Soares-Gomes, A.; da Gama, B.A.P. Depuration reduces microplastic content in wild and farmed mussels. *Mar. Pollut. Bull.* **2019**, *140*, 241–247. [[CrossRef](#)]
40. Fernández, B.; Albertosa, M. Dynamic of small polyethylene microplastics ($\leq 10 \mu\text{m}$) in mussel's tissues. *Mar. Pollut. Bull.* **2019**, *146*, 493–501. [[CrossRef](#)]
41. Graham, P.; Palazzo, L.; Andrea de Lucia, G.; Telfer, T.C.; Baroli, M.; Carboni, S. Microplastics uptake and egestion dynamics in Pacific oysters, *Magallana gigas* (Thunberg, 1793), under controlled conditions. *Environ. Pollut.* **2019**, *252*, 742–748. [[CrossRef](#)]
42. Rist, S.; Steensgaard, I.M.; Guven, O.; Nielsen, T.G.; Jensen, L.H.; Møller, L.F.; Hartmann, N.B. The fate of microplastics during uptake and depuration phases in a blue mussel exposure system. *Environ. Toxicol. Chem.* **2019**, *38*, 99–105. [[CrossRef](#)]
43. Chae, Y.; An, Y.J. Effects of food presence on microplastic ingestion and egestion in *Mytilus galloprovincialis*. *Chemosphere* **2020**, *240*, 124855. [[CrossRef](#)] [[PubMed](#)]
44. Pizzurro, F.; Recchi, S.; Nerone, E.; Barile, N.B. Evaluation of Clearance Gut Rate in Bivalves for Risk Assessment Associated with Their Consumption. Istituto Zooprofilattico Sperimentale dell'Abruzzo e Molise, Teramo, Italy. June 2022, Final Report-Activity 4.4-D 4.4.3. Unpublished work.
45. Burns, E.E.; Boxall, A.B.A. Microplastics in the aquatic environment: Evidence for or against adverse impacts and major knowledge gaps. *Environ. Toxicol. Chem.* **2018**, *37*, 2776–2796. [[CrossRef](#)] [[PubMed](#)]
46. Gardon, T.; Morvan, L.; Huvet, A.; Quillien, V.; Soyeux, C.; le Moullac, G.; le Luyer, J. Microplastics induce dose-specific transcriptomic disruptions in energy metabolism and immunity of the pearl oyster *Pinctada margaritifera*. *Environ. Pollut.* **2020**, *266*, 115180. [[CrossRef](#)] [[PubMed](#)]
47. Albertosa, M.; Sánchez-Hernández, M.; Campillo, J.A.; Moyano, F.J. Relationship between physiological measurements (SFG-scope for growth-) and the functionality of the digestive gland in *Mytilus galloprovincialis*. *Comp. Biochem. Physiol. Part A Mol. Integr. Physiol.* **2012**, *163*, 286–295. [[CrossRef](#)] [[PubMed](#)]
48. Woodall, L.C.; Gwinnett, C.; Packer, M.; Thompson, R.C.; Robinson, L.F.; Paterson, G.L.J. Using a forensic science approach to minimize environmental contamination and to identify microfibrils in marine sediments. *Mar. Pollut. Bull.* **2015**, *95*, 40–46. [[CrossRef](#)] [[PubMed](#)]
49. Mathalon, A.; Hill, P. Microplastic fibers in the intertidal ecosystem surrounding halifaxharbor, nova scotia. *Mar. Pollut. Bull.* **2014**, *81*, 69–79. [[CrossRef](#)] [[PubMed](#)]
50. Bessa, F.; Barría, P.; Neto, J.M.; Frias, J.P.G.L.; Otero, V.; Sobral, P.; Marques, J.C. Occurrence of microplastics in commercial fish from a natural estuarine environment. *Mar. Pollut. Bull.* **2018**, *128*, 575–584. [[CrossRef](#)] [[PubMed](#)]
51. Hidalgo-Ruz, V.; Gutow, L.; Thompson, R.C.; Thiel, M. Microplastics in the Marine Environment: A Review of the Methods Used for Identification and Quantification. *Environ. Sci. Technol.* **2012**, *46*, 3060–3075. [[CrossRef](#)]
52. de Witte, B.; Devriese, L.; Bekaert, K.; Hoffman, S.; Vandermeersch, G.; Cooreman, K.; Robbens, J. Quality assessment of the blue mussel (*Mytilus edulis*): Comparison between commercial and wild types. *Mar. Pollut. Bull.* **2014**, *85*, 146–155. [[CrossRef](#)]
53. Pfaffl, M.W. A new mathematical model for relative quantification in real-time RT-PCR. *Nucleic Acids Res.* **2001**, *29*, e45. [[CrossRef](#)]
54. Livak, K.J.; Schmittgen, T.D. Analysis of Relative Gene Expression Data Using Real-Time Quantitative PCR and the $2^{-\Delta\Delta\text{CT}}$ Method. *Methods* **2001**, *25*, 402–408. [[CrossRef](#)] [[PubMed](#)]
55. Sokolova, I.M. Apoptosis in molluscan immune defense. *Invertebr. Surviv. J.* **2009**, *6*, 49–58.
56. Avio, C.G.; Gorbi, S.; Milan, M.; Benedetti, M.; Fattorini, D.; D'Errico, G.; Pauletto, M.; Bargelloni, L.; Regoli, F. Pollutants bioavailability and toxicological risk from microplastics to marine mussels. *Environ. Pollut.* **2015**, *198*, 211–222. [[CrossRef](#)] [[PubMed](#)]
57. van Cauwenberghe, L.; Claessens, M.; Vandegheuchte, M.B.; Janssen, C.R. Microplastics are taken up by mussels (*Mytilus edulis*) and lugworms (*Arenicola marina*) living in natural habitats. *Environ. Pollut.* **2015**, *199*, 10–17. [[CrossRef](#)] [[PubMed](#)]
58. Lambert, S.; Scherer, C.; Wagner, M. Ecotoxicity testing of microplastics: Considering the heterogeneity of physicochemical properties. In *Integrated Environmental Assessment and Management*; Wiley-Blackwell: Hoboken, NJ, USA, 2017; Volume 13, pp. 470–475.
59. Weinstein, J.E.; Ertel, B.M.; Gray, A.D. Accumulation and depuration of microplastic fibers, fragments, and tire particles in the eastern oyster, *Crassostrea virginica*: A toxicokinetic approach. *Environ. Pollut.* **2022**, *308*, 119681. [[CrossRef](#)]
60. Ribeiro, F.; Garcia, A.R.; Pereira, B.P.; Fonseca, M.; Mestre, N.C.; Fonseca, T.G.; Ilharco, L.M.; Bebianno, M.J. Microplastics effects in *Scrobicularia plana*. *Mar. Pollut. Bull.* **2017**, *122*, 379–391. [[CrossRef](#)]
61. Xu, X.Y.; Lee, W.T.; Chan, A.K.Y.; Lo, H.S.; Shin, P.K.S.; Cheung, S.G. Microplastic ingestion reduces energy intake in the clam *Atactodea striata*. *Mar. Pollut. Bull.* **2017**, *124*, 798–802. [[CrossRef](#)]
62. Browne, M.A.; Dissanayake, A.; Galloway, T.S.; Lowe, D.M.; Thompson, R.C. Ingested Microscopic Plastic Translocates to the Circulatory System of the Mussel, *Mytilus edulis* (L.). *Environ. Sci. Technol.* **2008**, *42*, 5026–5031. [[CrossRef](#)]
63. Ward, J.E.; Zhao, S.; Holohan, B.A.; Mladinich, K.M.; Griffin, T.W.; Wozniak, J.; Shumway, S.E. Selective Ingestion and Egestion of Plastic Particles by the Blue Mussel (*Mytilus edulis*) and Eastern Oyster (*Crassostrea virginica*): Implications for Using Bivalves as Bioindicators of Microplastic Pollution. *Environ. Sci. Technol.* **2019**, *53*, 8776–8784. [[CrossRef](#)]

64. Li, J.; Wang, Z.; Rotchell, J.M.; Shen, X.; Li, Q.; Zhu, J. Where are we? Towards an understanding of the selective accumulation of microplastics in mussels. *Environ. Pollut.* **2021**, *286*, 117543. [[CrossRef](#)]
65. Catarino, A.I.; Macchia, V.; Sanderson, W.G.; Thompson, R.C.; Henry, T.B. Low levels of microplastics (MP) in wild mussels indicate that MP ingestion by humans is minimal compared to exposure via household fibres fallout during a meal. *Environ. Pollut.* **2018**, *237*, 675–684. [[CrossRef](#)]
66. Volgare, M.; Santonicola, S.; Cocca, M.; Avolio, R.; Castaldo, R.; Errico, M.E.; Gentile, G.; Raimo, G.; Gasperi, M.; Colavita, G. A versatile approach to evaluate the occurrence of microfibers in mussels *Mytilus galloprovincialis*. *Sci. Rep.* **2022**, *12*, 21827. [[CrossRef](#)]
67. Bustamante, P.; Luna-Acosta, A.; Clemens, S.; Cassi, R.; Thomas-Guyon, H.; Warnau, M. Bioaccumulation and metabolisation of ¹⁴C-pyrene by the Pacific oyster *Crassostrea gigas* exposed via seawater. *Chemosphere* **2012**, *87*, 938–944. [[CrossRef](#)]
68. Zanette, J.; Jenny, M.J.; Goldstone, J.V.; Parente, T.; Woodin, B.R.; Bairy, A.C.D.; Stegeman, J.J. Identification and expression of multiple CYP1-like and CYP3-like genes in the bivalve mollusk *Mytilus edulis*. *Aquat. Toxicol.* **2013**, *128–129*, 101–112. [[CrossRef](#)]
69. Estévez-Calvar, N.; Romero, A.; Figueras, A.; Novoa, B. Genes of the Mitochondrial Apoptotic Pathway in *Mytilus galloprovincialis*. *PLoS ONE* **2013**, *8*, e61502. [[CrossRef](#)]
70. Wang, J.; Zhang, G.; Fang, X.; Guo, X.; Li, L.; Luo, R.; Xu, F.; Yang, P.; Zhang, L.; Wang, X.; et al. The oyster genome reveals stress adaptation and complexity of shell formation. *Nature* **2012**, *490*, 49–54. [[CrossRef](#)]
71. Rola, R.C.; Monteiro, M.d.C.; Reis, S.R.d.S.; Sandrini, J.Z. Molecular and biochemical biomarkers responses in the mussel *Mytilus edulis* collected from Southern Brazil coast. *Mar. Pollut. Bull.* **2012**, *64*, 766–771. [[CrossRef](#)]
72. Gomes, T.; Chora, S.; Pereira, C.G.; Cardoso, C.; Bebianno, M.J. Proteomic response of mussels *Mytilus galloprovincialis* exposed to CuO NPs and Cu²⁺: An exploratory biomarker discovery. *Aquat. Toxicol.* **2014**, *155*, 327–336. [[CrossRef](#)]
73. Pinsino, A.; Bergami, E.; della Torre, C.; Vannuccini, M.L.; Addis, P.; Secci, M.; Dawson, K.A.; Matranga, V.; Corsi, I. Amino-modified polystyrene nanoparticles affect signalling pathways of the sea urchin (*Paracentrotus lividus*) embryos. *Nanotoxicology* **2017**, *11*, 201–209. [[CrossRef](#)]
74. Bergami, E.; Pugnolini, S.; Vannuccini, M.L.; Manfra, L.; Faleri, C.; Savorelli, F.; Dawson, K.A.; Corsi, I. Long-term toxicity of surface-charged polystyrene nanoplastics to marine planktonic species *Dunaliella tertiolecta* and *Artemia franciscana*. *Aquat. Toxicol.* **2017**, *189*, 159–169. [[CrossRef](#)]
75. Blanco-Rayón, E.; Ivanina, A.v.; Sokolova, I.M.; Marigómez, I.; Izagirre, U. Sex and sex-related differences in gamete development progression impinge on biomarker responsiveness in sentinel mussels. *Sci. Total Environ.* **2020**, *740*, 140178. [[CrossRef](#)]
76. Kapranov, S.V.; Karavantseva, N.V.; Bobko, N.I.; Ryabushko, V.I.; Kapranova, L.L. Sex- and sexual maturation-related aspects of the element accumulation in soft tissues of the bivalve *Mytilus galloprovincialis* Lam. collected off coasts of Sevastopol (southwestern Crimea, Black Sea). *Environ. Sci. Pollut. Res. Int.* **2021**, *28*, 21553–21576. [[CrossRef](#)]
77. Matozzo, V.; Marin, M.G. First Evidence of Gender-Related Differences in Immune Parameters of the Clam *Ruditapes philippinarum* (Mollusca, Bivalvia). *Mar. Biol.* **2010**, *157*, 1181–1189. [[CrossRef](#)]
78. Chapman, E.C.; O'Dell, A.R.; Meligi, N.M.; Parsons, D.R.; Rotchell, J.M. Seasonal expression patterns of clock-associated genes in the blue mussel *Mytilus edulis*. *Chronobiol. Int.* **2017**, *34*, 1300–1314. [[CrossRef](#)]
79. Ciocan, C.M.; Cubero-Leon, E.; Puinean, A.M.; Hill, E.M.; Minier, C.; Osada, M.; Fenlon, K.; Rotchell, J.M. Effects of estrogen exposure in mussels, *Mytilus edulis*, at different stages of gametogenesis. *Environ. Pollut.* **2010**, *158*, 2977–2984. [[CrossRef](#)]
80. Mincarelli, L.F.; Rotchell, J.M.; Chapman, E.C.; Turner, A.P.; Wollenberg Valero, K.C. Consequences of combined exposure to thermal stress and the plasticiser DEHP in *Mytilus* spp. differ by sex. *Mar. Pollut. Bull.* **2021**, *170*, 112624. [[CrossRef](#)]
81. Mincarelli, L.F.; Chapman, E.C.; Rotchell, J.M.; Turner, A.P.; Wollenberg Valero, K.C. Sex and gametogenesis stage are strong drivers of gene expression in *Mytilus edulis* exposed to environmentally relevant plasticiser levels and pH 7.7. *Environ. Sci. Pollut. Res. Int.* **2023**, *30*, 23437–23449. [[CrossRef](#)]

Disclaimer/Publisher's Note: The statements, opinions and data contained in all publications are solely those of the individual author(s) and contributor(s) and not of MDPI and/or the editor(s). MDPI and/or the editor(s) disclaim responsibility for any injury to people or property resulting from any ideas, methods, instructions or products referred to in the content.

ARTICLES FOR FACULTY MEMBERS

MICROPLASTICS AND MARINE ENVIRONMENT

Title/Author	<p>Microplastic exposure represses the growth of endosymbiotic dinoflagellate <i>Cladocopium goreau</i> in culture through affecting its apoptosis and metabolism / Su, Y., Zhang, K., Zhou, Z., Wang, J., Yang, X., Tang, J., Li, H., & Lin, S.</p>
Source	<p><i>Chemosphere</i> Volume 244 (2020) 125485 Pages 1-8 https://doi.org/10.1016/J.CHEMOSPHERE.2019.125485 (Database: ScienceDirect)</p>



Microplastic exposure represses the growth of endosymbiotic dinoflagellate *Cladocopium goreau* in culture through affecting its apoptosis and metabolism

Yilu Su^a, Kaidian Zhang^{b,c}, Zhi Zhou^{a,c,*}, Jierui Wang^b, Xiaohong Yang^b, Jia Tang^a, Hongfei Li^b, Senjie Lin^{c,**}

^a State Key Laboratory of Marine Resource Utilization in South China Sea, Hainan University, Haikou, Hainan, China

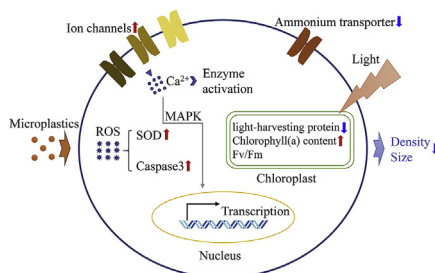
^b State Key Laboratory of Marine Environmental Science, Xiamen University, Xiamen, Fujian, China

^c Department of Marine Sciences, University of Connecticut, Groton, CT, USA

HIGHLIGHTS

- The growth and density of algal cells were repressed by microplastic exposure.
- Microplastics declined detoxification activity, nutrient uptake, and photosynthesis.
- Microplastics raised oxidative stress, apoptosis level and ion transport.

GRAPHICAL ABSTRACT



ARTICLE INFO

Article history:

Received 26 July 2019

Received in revised form

29 October 2019

Accepted 26 November 2019

Available online 27 November 2019

Handling Editor: Tamara S. Galloway

Keywords:

Microplastic

Symbiodiniaceae

Apoptosis

Assimilation metabolism

Adaptation

ABSTRACT

Microplastics are widespread emerging marine pollutants that have been found in the coral reef ecosystem. In the present study, using *Cladocopium goreau* as a symbiont representative, we investigated cytological, physiological, and molecular responses of a Symbiodiniaceae species to weeklong microplastic exposure (Polystyrene, diameter 1.0 μm , 9.0×10^9 particles L^{-1}). The density and size of algal cells decreased significantly at 7 d and 6–7 d of microplastic exposure, respectively. Chlorophyll *a* content increased significantly at 7 d of exposure, whereas Fv/Fm did not change significantly during the entire exposure period. We observed significant increases in superoxide dismutase activity and caspase3 activation level, significant decrease in glutathione S-transferase activity, but no change in catalase activity during the whole exposure period. Transcriptomic analysis revealed 191 significantly upregulated and 71 significantly downregulated genes at 7 d after microplastic exposure. Fifteen GO terms were overrepresented for these significantly upregulated genes, which were grouped into four categories including transmembrane ion transport, substrate-specific transmembrane transporter activity, calcium ion binding, and calcium-dependent cysteine-type endopeptidase activity. Thirteen of the significantly upregulated genes encode metal ion transporter and ammonium transporter, and five light-harvesting protein genes were among the significantly downregulated genes. These results demonstrate that microplastics can act as an exogenous stressor, suppress detoxification activity, nutrient uptake, and photosynthesis, elevate oxidative stress, and raise the apoptosis level through upregulating ion transport

* Corresponding author. State Key Laboratory of Marine Resource Utilization in South China Sea, Hainan University, Haikou, Hainan, China.

** Corresponding author.

E-mail addresses: zhouzhi@hainanu.edu.cn (Z. Zhou), senjie.lin@uconn.edu (S. Lin).

and apoptotic enzymes to repress the growth of *C. goreau*. These effects have implications in negative impacts of microplastics on coral-Symbiodiniaceae symbiosis that involves *C. goreau*.

© 2019 Elsevier Ltd. All rights reserved.

1. Introduction

Microplastics are defined as plastic particles or fragments smaller than 5 mm, and have been considered a potential threat to marine ecosystems globally (Galloway et al., 2017). Microplastic debris has also been observed in the seawater, sediment, and organisms in many marine ecosystems, including coral reef and deep-sea ecosystems (Woodall et al., 2014; Sharma and Chatterjee, 2017). Microplastic are ingested at multiple trophic levels to enter into the marine food web (Setälä et al., 2014; Sun et al., 2017; Rotjan et al., 2019), and may be bioaccumulated. In organisms microplastics can cause adverse effects through the blockage of alimentary tract, owing to the inability of the organisms to degrade them or the toxicity of mixed additives and adsorbed marine pollutants on them. Different types of additives such as bisphenol A, phthalates and flame retardants can be mixed into plastic monomers during the manufacturing process, while microplastics with large surface area-to-volume ratio can easily adsorb marine pollutants such as trace metal and persistent organic pollutants (Ivar do Sul and Costa, 2014; Tsang et al., 2017; Guo and Wang, 2019). Adsorbed additives and pollutants have severe toxic effects on the consumer organisms, and can also function as environmental hormones to negatively modulate physiological activities of marine organisms (Panti et al., 2015; Jeong et al., 2017).

Marine phytoplankton and protists are among the victims of microplastic pollution in the ocean. It has been reported that microplastics can be hetero-aggregated with diatom *Chaetoceros neogracile* and single-cell green alga *Chlamydomonas reinhardtii* (Lagarde et al., 2016; Long et al., 2017), adhered to *Skeletonema marinoi* and dinoflagellate *Lingulodinium polyedrum* (Casabianca et al., 2019), and ingested by the heterotrophic dinoflagellate *Oxyrrhis marina* (Cole et al., 2013). These microplastics have different effects on the growth of different phytoplankton species. For example, exposure to microplastics seems to enhance growth of the microalga *Raphidocelis subcapitata* (Canniff and Hoang, 2018) yet depress that of *C. reinhardtii* (Lagarde et al., 2016). In addition, it has been suggested that microplastics has a negative effect on the photosynthesis activity of phytoplankton through reducing chlorophyll content and photochemical efficiency, yet it increases the expression level of genes involved in the sugar biosynthesis pathways during a long-term exposure (Zhang et al., 2017; Mao et al., 2018; Prata et al., 2019; Wu et al., 2019). Overall, the mechanism underlying the contradicting effects of microplastics on phytoplankton is not well understood.

Dinoflagellates of the family Symbiodiniaceae are the most prevalent photosynthetic symbionts in tropical and subtropical coral reef ecosystems. The mutualisms of Symbiodiniaceae with scleractinian corals are fundamental to the existence of coral reef ecosystems worldwide, because they supply their coral hosts with photosynthates that can meet up to 95% of the corals' energy requirements (Houlbreque and Ferrier-Pages, 2009; Gonzalez-Pech et al., 2019). Symbiodiniaceae has evolved into diverse lineages of symbionts of corals and other invertebrates, including genera of *Symbiodinium* (Clade A), *Breviolum* (Clade B), *Cladocopium* (Clade C), *Durusdinium* (Clade D) and *Fugacium* (Clade F) (Lajeunesse et al., 2018). In the coral-Symbiodiniaceae relationship, Symbiodiniaceae cells are recognized by scleractinian corals presumably through the

interaction between coral lectin and algal glycan, and the flagellated motile form of Symbiodiniaceae cells will be transformed into the nonmotile coccoid form (equivalent to the symbiotic stage) (Jimbo et al., 2010). The community composition and density of symbiotic Symbiodiniaceae in scleractinian corals can change dynamically in response to changes in the internal and external environment (Cooper et al., 2011).

In this study, we used *Cladocopium goreau* as a representative species to gain understanding on microplastic effects on Symbiodiniaceae and underlying mechanisms. *C. goreau* belongs to clade C, the most abundant clade of Symbiodiniaceae in the coral reef ecosystem in the Pacific. To understand the potential effects of microplastic exposure on survival and reproduction of this species, growth and photosynthesis parameters, crucial enzyme activities, and transcriptomic profiles of *C. goreau* were investigated after an exposure to microplastics. Our results provide insights for further understanding the response mechanisms of Symbiodiniaceae to microplastic pollution and its potential influence on scleractinian coral hosts.

2. Materials and methods

2.1. Algal culture and microplastic exposure

C. goreau strain CCMP 2466 originally isolated from the anemone *Discosoma sancti-thomae* was provided by the National Center for Marine Algae and Microbiota. Cells were cultured in sterilized oceanic seawater, which was filtered through 0.22 μm membranes, enriched with the full nutrient regime of the L1 medium. The cultures were incubated at 26 °C and under a 14:10 h light:night cycle, with a photons of 110 $\mu\text{E m}^{-2} \text{s}^{-1}$.

Polystyrene microplastics (diameter 1.0 μm , density 1.05 g cm^{-3} , Saierqun, China) with smooth surface were used in the microplastic exposure experiment. Algal cells were cultured until its density exceeded 1.0×10^5 cells mL^{-1} , and the culture was divided equally into ten culture bottles, each one containing 250 mL of L1 medium. Microplastics were added into five cultures at the final concentration of 5.0 mg L^{-1} (9.0×10^9 particles L^{-1}), while the other five cultures received no microplastic additions serve as the control group. Twenty-seven milliliters of algal cells were sampled daily from each culture to determine cell density, cell size, chlorophyll content, photochemical efficiency, and major enzyme activities. When the cell density in the microplastic group changed significantly (cultured for a week), 50 mL of algal cells from each culture were harvested by centrifugation at 5000 g 4 °C for 10 min and resuspended in 1 mL TRI-Reagent (Molecular Research Center, Inc., Cincinnati, OH, USA) and stored at -80 °C for subsequent RNA extraction.

2.2. Measurement of cell density and size

One mL samples were fixed in Lugol's solution, and cell density was determined by directed counting three times using a Sedgwick-Rafter counting chamber under the microscope, and the growth curves were plotted (Lin et al., 2012). The average cell size was measured as equivalent spherical diameter using Z2-Coulter Particle Counter (Beckman Coulter, USA). The mean cell diameter

was calculated with a particle count and size analyzer ranging from 5 μm to 15 μm (Li et al., 2016).

2.3. Determination of chlorophyll content and photochemical efficiency

Five mL samples were filtered onto a 25 mm GF/F glass micro-fiber filter (Whatman, USA) to obtain the cells. The algae-containing filters were each immersed into 90% acetone separately and kept in the dark for 48 h at 4 °C to extract chlorophyll *a*, which was determined using Turner Trilogy (Turner Designs fluorometer, USA) following the non-acidification method (EJ and GB, 1997) and averaged to content per cell. Photochemical efficiency was measured using Xe-PAM (Walz, Germany) after 30 min of incubation in the dark.

2.4. Activity assay of antioxidases and detoxification enzyme

Cells were harvested from a 10 mL sample from each culture using centrifugation at 5000 g 4 °C for 10 min. Cell pellets were resuspended in PBS (phosphate buffered saline, PH 7.4) and homogenized using 0.5 mm diameter ceramic beads and a bead-beater (FastPrep® –24 Sample Preparation System, MP Bio-medicals, USA). The homogenate was centrifuged at 12000 g 4 °C for 10 min to obtain the supernatant (crude protein extract). The activities of superoxide dismutase (SOD), catalase (CAT), and glutathione S-transferase (GST) in the supernatants were measured using commercial kits (A001, A007 and A004, JIANCHENG, China), following the manufacturer's recommendations. Then, the concentration of total protein in the supernatant was quantified with BCA Protein Assay kit (Sangon Biotech, China), and used to normalize the measured activities of SOD, CAT and GST to U mg^{-1} protein.

2.5. Activity assay of caspase3

Caspase3 activity in the protein extract was measured using Caspase-3 Colorimetric Assay Kit (KeyGEN BioTECH) according to the manufacturer's protocol. Briefly, 50 μL reaction buffer and 5 μL substrate were added to 50 μL protein extract, which was then incubated for 4 h in the dark at 37 °C. Next, the activity of caspase3 was measured spectrophotometrically at 405 nm (A_{405}), and the activation level of caspase3 in algal cells was defined as the ratio of A_{405} in samples to that of the control group at 1 d.

2.6. RNA extraction and transcriptome sequencing

RNA extraction was carried out using TRI-Reagent combined with the Qiagen RNeasy Mini kit (Qiagen) following a previously reported protocol (Lin et al., 2010). The RNA concentrations of samples were measured using NanoDrop ND-2000 spectrophotometer (Thermo Scientific), and the RNA quality was evaluated using the RNA 6000 Nano LabChip Kit (Agilent 2100 Bioanalyzer, Agilent Technologies, Australia). The extracted RNA from the microplastics-treated and the control, 3 replicates in each, was used for RNA-seq (transcriptome sequencing). Six paired-end fragment libraries (2×100 bp) were constructed and sequenced on the BGISEQ-500 platform (BGI, Shenzhen, China). The generated raw sequencing reads were deposited at the NCBI (National Center for Biotechnology Information) Short Read Archive under BioProject **No. PRJNA510646**.

2.7. Reads mapping and identification of differentially expressed genes (DEGs)

The genome sequences and annotation of *C. goreau* (<http://symbis.reefgenomics.org/>) (Liu et al., 2018) were used as reference. The alignment of the paired-end reads to the reference was performed using the HISAT2 software (Pertea et al., 2016). StringTie and DESeq2 software were used to estimate transcript abundances and identify DEGs between the microplastic and control groups (Love et al., 2014). FDR <0.05 was used to call statistically significant DEGs.

2.8. Functional annotation of differentially expressed genes

After the identification of significantly upregulated and down-regulated DEGs, their protein sequences were retrieved from the reference database mentioned above to align to Non-redundant protein database (Nr) using the online BLASTP program (<https://blast.ncbi.nlm.nih.gov/Blast.cgi>). Furthermore, the domains of these proteins were further predicted through Simple Modular Architecture Research Tool 8.0 (SMART, <http://smart.embl-heidelberg.de/>). The functions of the DEGs were annotated based on the functions of the best-hit homologous proteins and domains.

2.9. GO overrepresentation of differentially expressed genes

For GO analysis, sequences of all 35,913 Symbiodiniaceae proteins were aligned using local BLASTP search to the Uniport-sprot database with *e*value <0.001, and analyzed using InterProScan software to predict their domains. The obtained results were parsed by Blast2GO software (<https://www.blast2go.com/>) for assigning GO terms. GO overrepresentation analysis was implemented via the hypergeometric test with filter value of 0.05. The significantly upregulated or downregulated DEGs were selected as test set, while all genes were used as the reference set. The BiNGO tool was employed to calculate the overrepresented GO terms and display the network of significant GO terms (Maere et al., 2005).

2.10. Statistical analysis

All data were presented as means \pm standard deviation (SD) obtained from all replicates for each experimental condition. All of the data were subjected to two-way analysis of variance (two-way ANOVA) followed by multiple comparisons (S-N-K and Duncan) using SPSS v22.0 to determine significant differences between the microplastic treatment group and the control group. Differences were considered significant at $p < 0.05$.

3. Results

3.1. Algal cell density and cell size after microplastic exposure

As shown in Fig. 1, cell density increased slowly in both the microplastic and control groups. No significant difference was observed between these two groups during 1–6 d after microplastic exposure, but on the 7th d, the cell density in the microplastic group ($2.37 \pm 0.10 \times 10^5$ cells mL^{-1} , $p < 0.05$) was significantly lower than that in the control group ($2.83 \pm 0.16 \times 10^5$ cells mL^{-1}). Similarly, cell size in the microplastic group was significantly smaller than that in the control group during 6–7 d after exposure, reaching the lowest level at 7 d ($6.43 \pm 0.18 \mu\text{m}$) (Fig. 1B).

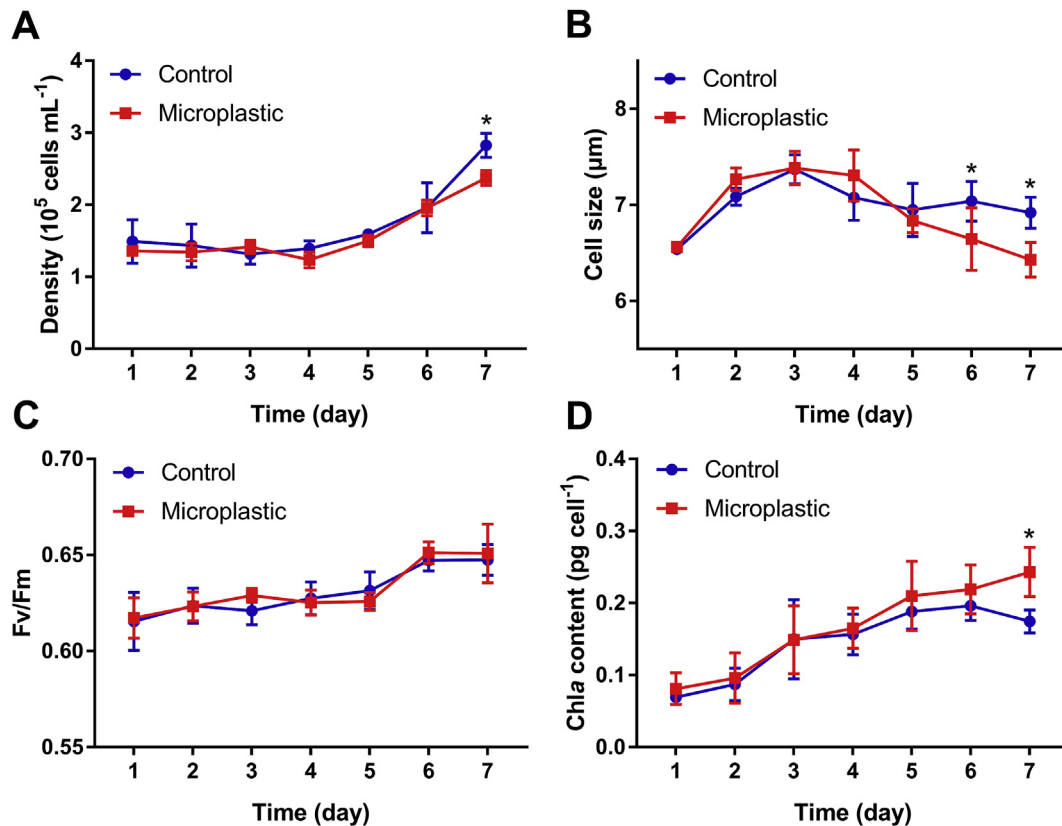


Fig. 1. Variations of cell density (A), cell size (B), photochemical efficiency Fv/Fm (C), and chlorophyll *a* content (D) in cultured *Cladocopium goreau* after microplastic exposure. Data points represent means and error bars represent standard deviations ($N = 5$). Asterisks depict significant differences between the microplastic and control groups ($p < 0.05$).

3.2. Photochemical efficiency and chlorophyll *a* content after microplastic exposure

There was no significant difference in the photochemical efficiency Fv/Fm between the microplastic and the control groups for the entire duration of the experiment (Fig. 1C). In contrast, chlorophyll *a* content increased in the microplastic exposure group, and became significantly higher at 7 d of the exposure (0.17 ± 0.02 pg cell⁻¹, $p < 0.05$) than that in the control group (Fig. 1D).

3.3. Activity alterations of SOD, CAT, and GST after microplastic exposure

SOD, CAT, and GST activities in the algal cells were determined after microplastic exposure. The SOD activity began to increase significantly at 1 d of exposure (97.12 ± 13.01 U mg⁻¹, $p < 0.05$), in comparison to the control group. After reaching the peak at 2 d exposure (114.99 ± 19.37 U mg⁻¹, $p < 0.05$), the SOD activity in the microplastic group returned to the control level (Fig. 2A). No significant difference was observed in CAT activity between the microplastic and control groups during the whole period of microplastic exposure (Fig. 2B). For the GST activity, there was no significant difference throughout the experiment except at 4 d exposure, when the activity (1024.62 ± 260.71 U mg⁻¹) in the microplastic group was lower than that in the control group ($p < 0.05$) (Fig. 2C).

3.4. Activation level change of caspase3 after microplastic exposure

The activation level of caspase3 was measured in the algal cells after the exposure to microplastics. Its activation level in the

microplastic group increased significantly during 2–3 d exposure, compared to those in the control group. Furthermore, the highest activation level was observed at 3 d of the exposure (1.71 ± 0.29 -fold, $p < 0.05$), and then it decreased to the control level (Fig. 2D).

3.5. Gene expression of *C. goreau* after microplastic exposure

A total of six paired-end (2×100 bp) transcriptome libraries were constructed, including three libraries in the control group and three libraries in the microplastic exposure group, and sequenced to saturated level to compare the transcript abundances and characterize transcriptomic response to microplastic exposure. A total of 210,756,476 high-quality reads were obtained after quality control, comprising 33,886,745, 32,531,926 and 35,860,663 reads from the three control libraries, and 35,342,075, 34,305,438 and 38,829,629 reads from the three microplastic libraries, respectively (Table 1).

The high-quality clean paired-end reads obtained from all six transcriptome libraries were mapped to the reference genome of *C. goreau* using HISAT2 software, and the mapping rates and detected genes were very consistent among the six libraries, ranging from 87.08% to 87.69% and from 22,332 to 22,449, respectively (Table 1). StringTie software was employed to analyze all gene expression levels and export the counts of mapped reads for each gene to be fed into the DESeq2 software to identify DEGs (Supplementary Table S1). After library calibration, the expression levels of all algal genes were compared between the microplastic and control groups. A total 262 DEGs were obtained, which accounted for 0.73% of total number of the algal genes, comprising 191 significantly upregulated and 71 significantly downregulated DEGs (Supplementary Table S2).

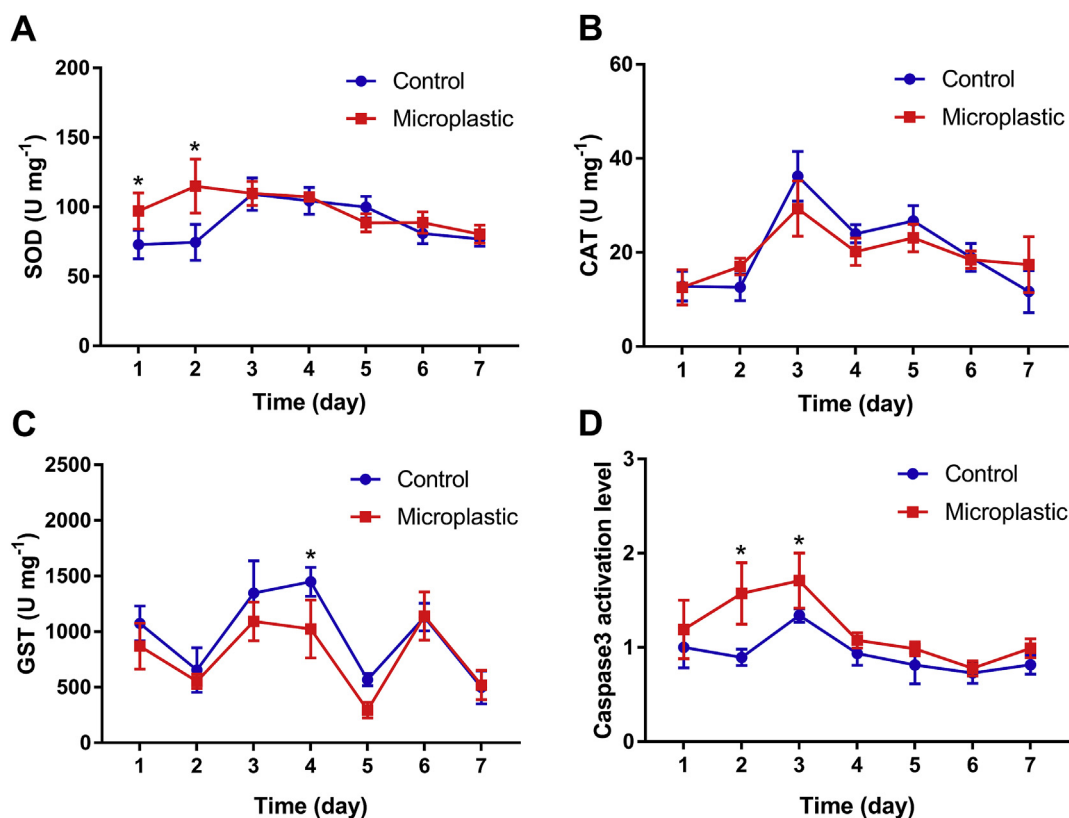


Fig. 2. Temporal patterns of SOD, CAT, GST activities, and caspase3 activation level in cultured *Cladocopium goreau* after microplastic exposure. (A) Superoxide dismutase (SOD). (B) Catalase (CAT). (C) Glutathione S-transferase (GST). (D) Caspase3 activation level. Data points represent means and error bars represent standard deviations (N = 5). Asterisks depict significant differences between the microplastic and control groups ($p < 0.05$).

Table 1
Transcriptome mapping statistics.

Library	Total reads	Mapped rate	Detected genes
Control_1	33,886,745	87.23%	22,332
Control_2	32,531,926	87.08%	22,362
Control_3	35,860,663	87.48%	22,338
Microplastic_1	35,342,075	87.58%	22,338
Microplastic_2	34,305,438	87.31%	22,365
Microplastic_3	38,829,629	87.69%	22,449

3.6. Functional annotation of DEGs after microplastic exposure

For the 191 significantly upregulated and 71 significantly downregulated DEGs identified from 7 d after exposure, functional annotation was carried out through homologous searching and domain prediction. Furthermore, GO overrepresentation analysis was conducted at multiple GO levels in the whole categories. The amino acid sequences encoded by the significantly upregulated DEGs were aligned to the Nr and SMART database, and the information of the returned homologous molecules and domains were retrieved (Supplementary Table S3). Predicted domains that appeared more than three times included ANK (28 times), Efh (23), WD40 (19), Ion_trans (14), CysPc (4), and EZ_HEAT (3), which were contained in 6, 9, 3, 13, 4, and 1 genes, respectively (Table 2). Furthermore, a total of 15 major GO terms were overrepresented for the significantly upregulated DEGs (Fig. 3A, Supplementary Table S4). According to the dependency relationship, these GO terms were classified into four groups: transmembrane ion transport, substrate-specific transmembrane transporter activity, calcium-dependent cysteine-type endopeptidase activity, and

Table 2
Domain statistics (three or more) of proteins encoded by significantly upregulated genes of *Cladocopium goreau* after microplastic exposure.

ID	Domain Name	Domain Number	Gene Number
1	ANK	28	6
2	Efh	23	9
3	WD40	19	3
4	Ion_trans	14	13
5	CysPc	4	4
6	EZ_HEAT	3	1

calcium ion binding (Fig. 3B).

The homologous molecules and protein domains of 71 significantly downregulated DEGs are shown in Table S4. Eight domains appeared three times or more, including LRR (22 times, in 2 genes), Chloroa_b-bind (9 times, 5 genes), WD40 (8 times, 1 gene), HMG (6 times, 1 gene), VCBS (4 times, 2 genes), Pumilio (4 times, 1 gene), ANK (3 times, 1 gene) and Ammonium_transp (3 times, 1 gene) (Table 3). These significantly downregulated DEGs did not particularly enrich any GO terms.

4. Discussion

Microplastic pollution poses a serious threat to marine ecosystems such as coral reef (Avio et al., 2017), and has toxic effects on at least some marine microalgae (Zhang et al., 2017). Little information is available about effects and their molecular underpinnings of microplastic exposure in Symbiodiniaceae, the endosymbionts of scleractinian corals. In the present study, we found that microplastic exposure caused significant increase in SOD activity and

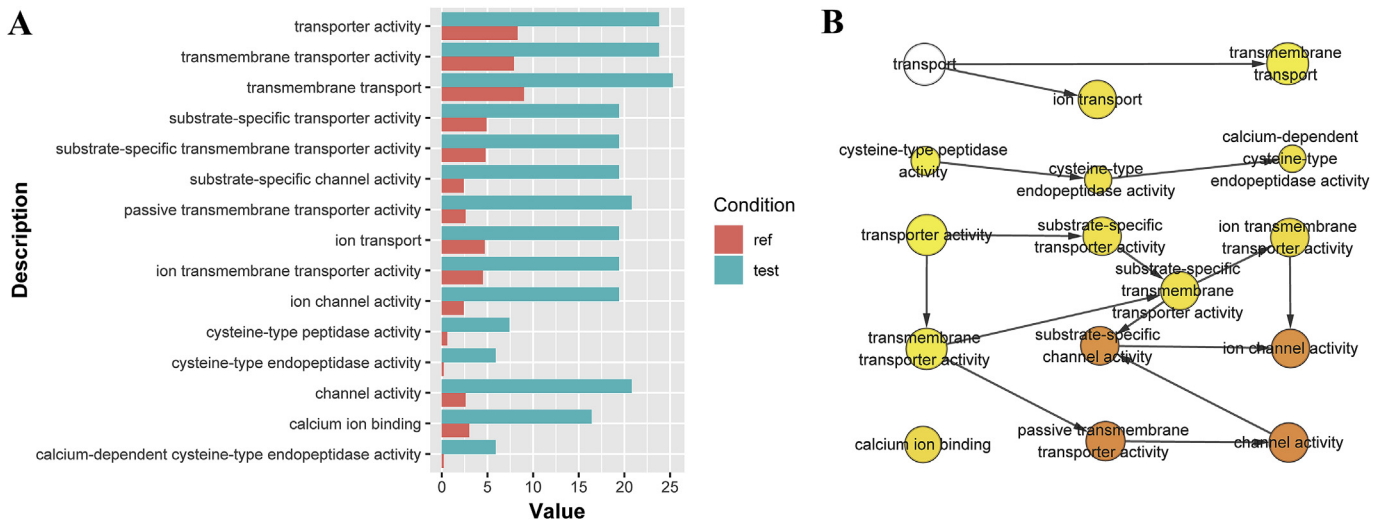


Fig. 3. Overrepresented GO terms of the significantly upregulated DEGs of cultured *Cladocopium goreau* in the microplastic group at 7 d after microplastic exposure. (A) Fifteen GO terms were found overrepresented for these significantly upregulated DEGs. "Ref" refers to the proportion of genes functionally assigned a GO term out of all genes existing in the reference genome, while "test" refers to the proportion of genes assigned to that GO term out of the significantly upregulated DEGs. (B) grouping of fifteen overrepresented GO terms after microplastic exposure.

Table 3

Domain statistics (three or more) of proteins encoded by significantly down-regulated genes of *Cladocopium goreau* after microplastic exposure.

ID	Domain Name	Domain Number	Gene Number
1	LRR	22	2
2	Chloroa_b-bind	9	5
3	WD40	8	1
4	HMG	6	1
5	VCBS	4	2
6	Pumilio	4	1
7	ANK	3	1
8	Ammonium_transp	3	1

caspase3 activation level in the coral endosymbiont *C. goreau*, and significant decrease in GST activity at the early period of exposure. At extended exposure, *C. goreau* cell concentration and size both exhibited a significant decrease, whereas the content of chlorophyll *a* increased significantly. Transcriptomic analysis further revealed the regulation of ion transport, calcium-dependent cysteine-type endopeptidase activity and light-harvesting protein, suggesting elevated apoptosis and depressed photosynthesis.

4.1. The suppression of algal growth by microplastic exposure

In order to understand the response of Symbiodiniaceae to microplastic exposure, growth and cell size of *C. goreau* was determined under microplastic and control conditions. Both cell yield and cell size in the microplastic group significantly decreased relative to the control group at 7 d and during 6–7 d of microplastic exposure, respectively. This demonstrates that the microplastic exposure could suppress the growth and cell size of cultured (aposymbiotic) *C. goreau*. Similar negative effects have previously been observed in the microalgae *C. reinhardtii* and *Skeletonema costatum* after microplastic exposure, and the negative effects were mainly attributed to the hetero-aggregation between microplastics and algal cells (Lagarde et al., 2016; Zhang et al., 2017). This might not apply to our study, however, because self-aggregation of *C. goreau* also occurred in the control culture. The suppressing effect on cell yield and cell size of cultured *C. goreau* might have derived from ingestion of microplastics or effects of toxic

substances released by microplastics. It has been reported that the dinoflagellate *O. marina* could ingest microplastics during 1 h of exposure (Cole et al., 2013). The decrease in cell size and yield might have resulted from the apoptosis promoting or proliferation and nutrient uptake inhibiting effects of microplastics. This is consistent with the results of our transcriptomic analysis, which are elaborated below.

4.2. The induction of apoptosis and impacts on photosynthesis and ion transport in *C. goreau* by microplastic exposure

We monitored the activities of several enzymes in cultured *C. goreau* to characterize physiological responses of *C. goreau* to microplastic exposure. Caspase3 is a key enzyme associated with apoptosis, and increase in its activation level observed in cultured *C. goreau* during 2–3 d after microplastic exposure indicated that microplastic exposure induced the apoptosis level of algal cells. Meanwhile, we observed a rise of SOD activity during 1–2 d and a decline of GST activity at 4 d after the exposure, suggesting the induction of ROS in cultured *C. goreau* by microplastic exposure in the early stage. Both SOD and CAT are main functional antioxidants in dinoflagellates (Leitao et al., 2003). The increase of SOD activity demonstrates that microplastics activates the stress response of the algal cells. GST is a crucial phase II metabolic enzymes in the detoxification process of all eukaryotes (Nicosia et al., 2014), and the decrease of GST activity indicates that detoxification response can be suppressed by microplastics, which together with the activation of stress response can bring about increasing apoptosis. These results suggest in concert that microplastics as an exogenous stressor could induce oxidative stress and repress the detoxification response, possibly raising the apoptosis level of Symbiodiniaceae and leading to the decline of their growth.

Meanwhile, several physiological parameters related to the assimilation metabolism were measured to further understand the repression of Symbiodiniaceae growth after microplastic exposure. With respect to photosynthesis, the content of chlorophyll *a* increased significantly at 7 d of microplastic exposure, whereas the photochemical efficiency showed no significant change during the entire exposure period. The results seem to be inconsistent with the growth depressing and stress inducing effects discussed above and

with other reports in *Chlorella pyrenoidosa* and *S. costatum* that microplastics could reduce algal photosynthesis through decreasing chlorophyll content and photochemical efficiency (Zhang et al., 2017; Mao et al., 2018). However, five light-harvesting protein genes were observed to be among the 71 significantly downregulated DEGs in the present study, corresponding to 9 Chloroa_b-bind domains. These results together suggest that microplastics can depress photosynthesis of cultured *C. goreau* through decreasing the formation of light-harvesting complex without decreasing chlorophyll content and photochemical efficiency. The increase of chlorophyll *a* might have been a response to the shading of microplastics, because increased chlorophyll content is a common response in algae to reduction of light availability (Falkowski and Owens, 1980). The inhibited photosynthesis would cause the reduction of photosynthate and the lack of energy in *C. goreau* after microplastic exposure. In addition, we also documented the decreased expression of ammonium transporter gene, indicative of decreased ability of cultured *C. goreau* to take up ammonium as a result of microplastic exposure. Ammonium is the main nitrogen nutrient for symbiotic Symbiodiniaceae (Pernice et al., 2012; Tanaka et al., 2018), but the L1 medium used in this study contains nitrate instead of ammonium as the source of nitrogen nutrient. The decline in the expression of ammonium transporter is likely to signal a lowered requirement of nitrogen as a result of decreased photosynthesis. Therefore, microplastic exposure seemed to exert inhibitory effects on assimilation metabolism of carbon dioxide and inorganic nitrogen, which could result in the lack of organic carbon and nitrogen nutrients in algal cells. This might have contributed to the induction of apoptosis and the repression of growth.

The transcriptomes of cultured *C. goreau* at 7 d of microplastic exposure further reveals the molecular response mechanism of Symbiodiniaceae to microplastic. The significantly upregulated DEGs under microplastic exposure were mainly related to ion transport and utilization. Among all 191 significantly upregulated DEGs, 13 genes encode ion channel proteins for potassium, sodium and calcium. This suggests that microplastic exposure activates these ion channels. To our knowledge, no similar results have been reported in other organisms. The transmembrane ion flux has been reported to be associated with the change of cell state and cell cycle in dinoflagellates (Gordeeva et al., 2004; Yeung et al., 2006; Smith et al., 2011), and therefore the increased expression of these ion channel genes might be evidence of heightened cellular response to microplastic exposure. Furthermore, the calcium flux might have induced the transcriptome alteration in *C. goreau* after exposing to microplastics, such as the decreased expression of light-harvesting proteins, because calcium channels are implicated in calcium-based signaling in photosynthetic eukaryotes (Verret et al., 2010). Calcium ion is both essential secondary messenger and the substrate of calcification, and its influx into the symbiotic *C. goreau* in coral association might further affect the form of host carbonate exoskeleton. In sum, our results presented in this paper suggest that microplastics as an exogenous stressor could repress detoxification activity and assimilatory metabolism, trigger ion transport and raise apoptosis level resulting in the decline of growth of the endosymbiotic dinoflagellate *C. goreau*. Previous studies have documented contradicting effects of microplastics on phytoplankton, which could have resulted from the disaccordance of tested physiological variables and the lack of molecular analysis. In this study, concerted effects of microplastic exposure on stress response, detoxification, apoptosis and ion transport were observed through biochemical and molecular methods, underscoring the value of the combined methods in studying Symbiodiniaceae response to environmental stress.

Declaration of interest statement

This manuscript is original and it has not been previously published or submitted in part or whole. All authors have agreed to be listed and have seen the manuscript, and approved the submission to *Chemosphere*. This manuscript has no conflicts of interest. Our study does not involve human subjects.

Acknowledgements

The authors were grateful to all of the laboratory members for their continuous technical advice and helpful discussions. Z.Z. gratefully acknowledges the financial support from China Scholarship Council (201708460042) to enable his visit to the University of Connecticut. This research was supported by the National Key R&D Program of China (Grant 2018YFC1406504), the National Natural Science Foundation of China (Grants 31772460 and 31661143029) and the Scientific Research Foundation of Hainan University (kyqd1554).

Appendix A. Supplementary data

Supplementary data to this article can be found online at <https://doi.org/10.1016/j.chemosphere.2019.125485>.

References

- Avio, C.G., Gorbi, S., Regoli, F., 2017. Plastics and microplastics in the oceans: from emerging pollutants to emerged threat. *Mar. Environ. Res.* 128, 2–11.
- Canniff, P.M., Hoang, T.C., 2018. Microplastic ingestion by *Daphnia magna* and its enhancement on algal growth. *Sci. Total Environ.* 633, 500–507.
- Casabianca, S., Capellacci, S., Penna, A., Cangiotti, M., Fattori, A., Corsi, I., Ottaviani, M.F., Carloni, R., 2019. Physical interactions between marine phytoplankton and PET plastics in seawater. *Chemosphere* 238, 124560.
- Cole, M., Lindeque, P., Fileman, E., Halsband, C., Goodhead, R., Moger, J., Galloway, T.S., 2013. Microplastic ingestion by zooplankton. *Environ. Sci. Technol.* 47, 6646–6655.
- Cooper, T.F., Berkelmans, R., Ulstrup, K.E., Weeks, S., Radford, B., Jones, A.M., Doyle, J., Canto, M., O'Leary, R.A., van Oppen, M.J., 2011. Environmental factors controlling the distribution of symbiodinium harboured by the coral *Acropora millepora* on the Great Barrier Reef. *PLoS One* 6, e25536.
- EJ, A., GB, C., 1997. Method 445.0: In Vitro Determination of Chlorophyll *a* and Pheophytin *a* in Marine and Freshwater Algae by Fluorescence. Revision 1.2. National Exposure Research Laboratory Office of Research and development, U.S. Environmental Protection Agency, Cincinnati, OH.
- Falkowski, P.G., Owens, T.G., 1980. Light-shade adaptation: two strategies in marine phytoplankton. *Plant Physiol.* 66, 592–595.
- Galloway, T.S., Cole, M., Lewis, C., 2017. Interactions of microplastic debris throughout the marine ecosystem. *Nat Ecol Evol* 1, 116.
- Gonzalez-Pech, R.A., Bhattacharya, D., Ragan, M.A., Chan, C.X., 2019. Genome evolution of coral reef symbionts as intracellular residents. *Trends Ecol. Evol.* 34, 799–806.
- Gordeeva, A.V., Labas, Y.A., Zvyagil'skaya, R.A., 2004. Apoptosis in unicellular organisms: mechanisms and evolution. *Biochemistry (Mosc.)* 69, 1055–1066.
- Guo, X., Wang, J., 2019. The chemical behaviors of microplastics in marine environment: a review. *Mar. Pollut. Bull.* 142, 1–14.
- Houlbreque, F., Ferrier-Pages, C., 2009. Heterotrophy in tropical scleractinian corals. *Biol. Rev. Camb. Philos. Soc.* 84, 1–17.
- Ivar do Sul, J.A., Costa, M.F., 2014. The present and future of microplastic pollution in the marine environment. *Environ. Pollut.* 185, 352–364.
- Jeong, C.B., Kang, H.M., Lee, M.C., Kim, D.H., Han, J., Hwang, D.S., Souissi, S., Lee, S.J., Shin, K.H., Park, H.G., Lee, J.S., 2017. Adverse effects of microplastics and oxidative stress-induced MAPK/Nrf2 pathway-mediated defense mechanisms in the marine copepod *Paracyclops nana*. *Sci. Rep.* 7, 41323.
- Jimbo, M., Yamashita, H., Koike, K., Sakai, R., Kamiya, H., 2010. Effects of lectin in the scleractinian coral *Ctenactis echinata* on symbiotic zooxanthellae. *Fish. Sci.* 76, 355–363.
- Lagarde, F., Olivier, O., Zanella, M., Daniel, P., Hiard, S., Caruso, A., 2016. Microplastic interactions with freshwater microalgae: hetero-aggregation and changes in plastic density appear strongly dependent on polymer type. *Environ. Pollut.* 215, 331–339.
- Lajeunesse, T.C., Parkinson, J.E., Gabrielson, P.W., Jeong, H.J., Reimer, J.D., Voolstra, C.R., Santos, S.R., 2018. Systematic revision of Symbiodiniaceae highlights the antiquity and diversity of coral endosymbionts. *Curr. Biol.* 28, 2570–2580 e2576.
- Leitao, M.A., Cardozo, K.H., Pinto, E., Colepicolo, P., 2003. PCB-induced oxidative

- stress in the unicellular marine dinoflagellate *Lingulodinium polyedrum*. *Arch. Environ. Contam. Toxicol.* 45, 59–65.
- Li, M., Shi, X., Guo, C., Lin, S., 2016. Phosphorus deficiency inhibits cell division but not growth in the dinoflagellate amphidinium carterae. *Front. Microbiol.* 7, 826.
- Lin, S., Zhang, H., Zhuang, Y., Tran, B., Gill, J., 2010. Spliced leader-based metatranscriptomic analyses lead to recognition of hidden genomic features in dinoflagellates. *Proc. Natl. Acad. Sci. U. S. A.* 107, 20033–20038.
- Lin, X., Zhang, H., Huang, B., Lin, S., 2012. Alkaline phosphatase gene sequence characteristics and transcriptional regulation by phosphate limitation in *Karenia brevis* (Dinophyceae). *Harmful Algae* 17, 14–24.
- Liu, H., Stephens, T.G., Gonzalez-Pech, R.A., Beltran, V.H., Lapeyre, B., Bongaerts, P., Cooke, I., Aranda, M., Bourne, D.G., Foret, S., Miller, D.J., van Oppen, M.J.H., Voolstra, C.R., Ragan, M.A., Chan, C.X., 2018. Symbiodinium genomes reveal adaptive evolution of functions related to coral-dinoflagellate symbiosis. *Commun Biol* 1, 95.
- Long, M., Paul-Pont, I., Hegaret, H., Moriceau, B., Lambert, C., Huvet, A., Soudant, P., 2017. Interactions between polystyrene microplastics and marine phytoplankton lead to species-specific hetero-aggregation. *Environ. Pollut.* 228, 454–463.
- Love, M.I., Huber, W., Anders, S., 2014. Moderated estimation of fold change and dispersion for RNA-seq data with DESeq2. *Genome Biol.* 15, 550.
- Maere, S., Heymans, K., Kuiper, M., 2005. BiNGO: a Cytoscape plugin to assess overrepresentation of gene ontology categories in biological networks. *Bioinformatics* 21, 3448–3449.
- Mao, Y., Ai, H., Chen, Y., Zhang, Z., Zeng, P., Kang, L., Li, W., Gu, W., He, Q., Li, H., 2018. Phytoplankton response to polystyrene microplastics: perspective from an entire growth period. *Chemosphere* 208, 59–68.
- Nicosia, A., Celi, M., Vazzana, M., Damiano, M.A., Parrinello, N., D'Agostino, F., Avellone, G., Indelicato, S., Mazzola, S., Cuttitta, A., 2014. Profiling the physiological and molecular response to sulfonamidic drug in *Procamburus clarkii*. *Comp. Biochem. Physiol. C Toxicol. Pharmacol.* 166, 14–23.
- Panti, C., Giannetti, M., Bainsi, M., Rubegni, F., Minutoli, R., Fossi, M.C., 2015. Occurrence, relative abundance and spatial distribution of microplastics and zooplankton NW of sardinia in the pelagos sanctuary protected area, mediterranean sea. *Environ. Chem.* 12, 618–626.
- Pernice, M., Meibom, A., Van Den Heuvel, A., Kopp, C., Domart-Coulon, I., Hoegh-Guldberg, O., Dove, S., 2012. A single-cell view of ammonium assimilation in coral-dinoflagellate symbiosis. *ISME J.* 6, 1314–1324.
- Perteau, M., Kim, D., Perteau, G.M., Leek, J.T., Salzberg, S.L., 2016. Transcript-level expression analysis of RNA-seq experiments with HISAT, StringTie and Ballgown. *Nat. Protoc.* 11, 1650–1667.
- Prata, J.C., da Costa, J.P., Lopes, I., Duarte, A.C., Rocha-Santos, T., 2019. Effects of microplastics on microalgae populations: a critical review. *Sci. Total Environ.* 665, 400–405.
- Rotjan, R.D., Sharp, K.H., Gauthier, A.E., Yelton, R., Lopez, E.M.B., Carilli, J., Kagan, J.C., Urban-Rich, J., 2019. Patterns, dynamics and consequences of microplastic ingestion by the temperate coral, *Astrangia poculata*. *Proc Biol Sci* 286, 20190726.
- Setälä, O., Fleming-Lehtinen, V., Lehtiniemi, M., 2014. Ingestion and transfer of microplastics in the planktonic food web. *Environ. Pollut.* 185, 77–83.
- Sharma, S., Chatterjee, S., 2017. Microplastic pollution, a threat to marine ecosystem and human health: a short review. *Environ. Sci. Pollut. Res. Int.* 24, 21530–21547.
- Smith, S.M., Morgan, D., Musset, B., Cherny, V.V., Place, A.R., Hastings, J.W., Decoursey, T.E., 2011. Voltage-gated proton channel in a dinoflagellate. *Proc. Natl. Acad. Sci. U. S. A.* 108, 18162–18167.
- Sun, X., Li, Q., Zhu, M., Liang, J., Zheng, S., Zhao, Y., 2017. Ingestion of microplastics by natural zooplankton groups in the northern South China Sea. *Mar. Pollut. Bull.* 115, 217–224.
- Tanaka, Y., Suzuki, A., Sakai, K., 2018. The stoichiometry of coral-dinoflagellate symbiosis: carbon and nitrogen cycles are balanced in the recycling and double translocation system. *ISME J.* 12, 860–868.
- Tsang, Y.Y., Mak, C.W., Liebich, C., Lam, S.W., Sze, E.T., Chan, K.M., 2017. Microplastic pollution in the marine waters and sediments of Hong Kong. *Mar. Pollut. Bull.* 115, 20–28.
- Verret, F., Wheeler, G., Taylor, A.R., Farnham, G., Brownlee, C., 2010. Calcium channels in photosynthetic eukaryotes: implications for evolution of calcium-based signalling. *New Phytol.* 187, 23–43.
- Woodall, L.C., Sanchez-Vidal, A., Canals, M., Paterson, G.L., Coppock, R., Sleight, V., Calafat, A., Rogers, A.D., Narayanaswamy, B.E., Thompson, R.C., 2014. The deep sea is a major sink for microplastic debris. *R Soc Open Sci* 1, 140317.
- Wu, Y., Guo, P., Zhang, X., Zhang, Y., Xie, S., Deng, J., 2019. Effect of microplastics exposure on the photosynthesis system of freshwater algae. *J. Hazard Mater.* 374, 219–227.
- Yeung, P.K., Lam, C.M., Ma, Z.Y., Wong, Y.H., Wong, J.T., 2006. Involvement of calcium mobilization from caffeine-sensitive stores in mechanically induced cell cycle arrest in the dinoflagellate *Cryptocodinium cohnii*. *Cell Calcium* 39, 259–274.
- Zhang, C., Chen, X., Wang, J., Tan, L., 2017. Toxic effects of microplastic on marine microalgae *Skeletonema costatum*: interactions between microplastic and algae. *Environ. Pollut.* 220, 1282–1288.

ARTICLES FOR FACULTY MEMBERS

MICROPLASTICS AND MARINE ENVIRONMENT

Title/Author	Physiological stress response of the scleractinian coral <i>Stylophora pistillata</i> exposed to polyethylene microplastics / Lanctôt, C. M., Bednarz, V. N., Melvin, S., Jacob, H., Oberhaensli, F., Swarzenski, P. W., Ferrier-Pagès, C., Carroll, A. R., & Metian, M.
Source	<i>Environmental Pollution</i> Volume 263 Part A (2020) 114559 Pages 1-9 https://doi.org/10.1016/J.ENVPOL.2020.114559 (Database: ScienceDirect)



Physiological stress response of the scleractinian coral *Stylophora pistillata* exposed to polyethylene microplastics[☆]

Chantal M. Lanctôt^{a, b, *}, Vanessa N. Bednarz^c, Steven Melvin^b, Hugo Jacob^a, François Oberhaensli^a, Peter W. Swarzenski^a, Christine Ferrier-Pagès^c, Anthony R. Carroll^{d, e}, Marc Metian^a

^a Environment Laboratories, International Atomic Energy Agency, 4a, Quai Antoine 1er, 98000, Monaco

^b Australian Rivers Institute, Griffith University, Southport, QLD, 4215, Australia

^c CSM – Centre Scientifique de Monaco, Equipe Ecophysiologie corallienne, 8 Quai Antoine 1er, 98000, Monaco

^d Environmental Futures Research Institute, School of Environment and Science, Griffith University, Southport, QLD, 4222, Australia

^e Griffith Institute for Drug Discovery, Griffith University, Brisbane, QLD, 4111, Australia

ARTICLE INFO

Article history:

Received 12 November 2019

Received in revised form

30 March 2020

Accepted 6 April 2020

Available online 12 April 2020

Keywords:

Microplastic

Coral

Calcification

Photosynthetic activity

Metabolomics

ABSTRACT

We investigated physiological responses including calcification, photosynthesis and alterations to polar metabolites, in the scleractinian coral *Stylophora pistillata* exposed to different concentrations of polyethylene microplastics. Results showed that at high plastic concentrations (50 particles/mL nominal concentration) the photosynthetic efficiency of photosystem II in the coral symbiont was affected after 4 weeks of exposure. Both moderate and high (5 and 50 particles/mL nominal) concentrations of microplastics caused subtle but significant alterations to metabolite profiles of coral, as determined by Nuclear Magnetic Resonance (NMR) spectroscopy. Specifically, exposed corals were found to have increased levels of phosphorylated sugars and pyrimidine nucleobases that make up nucleotides, scyllo-inositol and a region containing overlapping proline and glutamate signals, compared to control animals. Together with the photo-physiological stress response observed and previously published literature, these findings support the hypothesis that microplastics disrupt host-symbiont signaling and that corals respond to this interference by increasing signaling and chemical support to the symbiotic zooxanthellae algae. These findings are also consistent with increased mucus production in corals exposed to microplastics described in previous studies. Considering the importance of coral reefs to marine ecosystems and their sensitivity to anthropogenic stressors, more research is needed to elucidate coral response mechanisms to microplastics under realistic exposure conditions.

© 2020 Elsevier Ltd. All rights reserved.

1. Introduction

Marine plastic pollution has garnered considerable public, media and scientific attention in recent years and is now recognized as an important threat to ocean health. It is estimated that over 5 million metric tonnes of plastic waste entered the oceans annually

over the last decade alone (Jambeck et al., 2015). Plastic debris is consequently ubiquitous in the marine environment, with coastal waters including coral reefs considered particularly vulnerable since they are subjected to plastic pollution from both land and open ocean (Lebreton et al., 2017; UNEP, 2016). A recent study estimated the number of plastic items entangled on coral reefs across the Asia-Pacific to be 11.1 billion, and this will increase if current usage and disposal trends remain unchanged (Lamb et al., 2018). Much of the concern surrounding marine plastic debris is associated with macro plastics, but microplastics (MPs), which originate either from the fragmentation of larger plastic pieces (i.e., secondary MPs) or are manufactured into fragments, beads or fibers (i.e., primary MPs) also pose a threat to coral reefs (Connors, 2017; UNEP, 2019). Understanding how MPs impact important marine species like coral is therefore an international research

[☆] This paper has been recommended for acceptance by Maria Cristina Fossi.

* Corresponding author. Australian Rivers Institute, Griffith University Gold Coast, Building G51, Southport, QLD, 4215, Australia.

E-mail addresses: c.lanctot@griffith.edu.au (C.M. Lanctôt), vbednarz@centrescientifique.mc (V.N. Bednarz), s.melvin@griffith.edu.au (S. Melvin), h.jacob@iaea.org (H. Jacob), f.oberhaensli@iaea.org (F. Oberhaensli), p.swarzenski@iaea.org (P.W. Swarzenski), ferrier@centrescientifique.mc (C. Ferrier-Pagès), a.carroll@griffith.edu.au (A.R. Carroll), m.metian@iaea.org (M. Metian).

priority (UNEP, 2019).

Ingestion of MPs has been reported in several marine species and, in some instances, linked to adverse effects like gut blockage, false satiation and reduced energy reserves (reviewed by Avio et al., 2017; Bouwmeester et al., 2015; Ivar Do Sul and Costa, 2014; Wright et al., 2013). However, relatively few studies have focused on the impacts of MPs on corals (reviewed in Table S1), despite their high likelihood of encountering MPs in coastal environments (UNEP, 2019). It has only recently been reported that corals can ingest plastic particles, including fragments, fibers and microbeads ranging from 3 to 5000 μm in size, and that they can retain ingested plastics for over 24 h (Allen et al., 2017; Axworthy and Padilla-Gamiño, 2019; Connors, 2017; Hall et al., 2015; Hankins et al., 2018; Martin et al., 2019; Rotjan et al., 2019). Plastic debris has also recently been shown to have damaging effects on coral reefs through suffocation, shading and tissue abrasion, and these impacts can lead to declines in coral communities (Connors, 2017; Lamb et al., 2018; Richards and Beger, 2011). For example, MPs can increase the susceptibility of corals to disease by hosting and promoting pathogen colonization, and facilitate the dispersion of pathogens by causing physical injury or reducing immune responses during wound-healing processes by diminishing resources (Kirstein et al., 2016; Lamb et al., 2018; Rotjan et al., 2019).

Under natural circumstances, corals possess a variety of cleaning mechanisms, including ciliary action and mucus production, which allow them to reject or eliminate non-nutritional particles (Riegl, 1995; Stafford-Smith and Ormond, 1992). It is however currently unknown if corals respond similarly to MPs (i.e., if they are able to mitigate harmful impacts of MPs through these mechanisms). In recent studies, corals were observed to selectively ingest different types of plastics over natural food and sand particles (Allen et al., 2017; Rotjan et al., 2019), while in other cases plastic exposure resulted in mucus formation (Connors, 2017; Hall et al., 2015), which may consequently be associated with increased energetic demands (Riegl and Branch, 1995). Recent studies report a range of negative effects in corals exposed to high concentrations of MPs, including bleaching and necrosis (Reichert et al., 2019, 2018; Syakti et al., 2019), reduced growth and prey capture rate (Chapron et al., 2018; Mouchi et al., 2019; Reichert et al., 2019; Savinelli et al., 2020), disruption of symbionts uptake into host cells (Okubo et al., 2018), as well as induced stress response and suppressed detoxification and immune functions (Rocha et al., 2020; Tang et al., 2018). Considering the apparent sensitivity of coral to a diverse range of environmental stressors and their importance to marine ecosystems, research aimed at improving our understanding of the physiological responses of coral to discrete stressors like MPs is warranted.

Here we characterized a range of sub-lethal effects including calcification, photosynthesis, and changes to polar metabolites in the scleractinian coral *Stylophora pistillata* exposed to moderate (5 particles/mL) and high (50 particles/mL) concentrations of polyethylene MPs under controlled laboratory conditions.

2. Material and method

2.1. Experimental design

S. pistillata (Esper 1797) colonies were initially collected in the Gulf of Aqaba, Red Sea (original Cites n°DCI 89/32) and maintained under controlled conditions at the Centre Scientifique de Monaco, before being transferred to the IAEA laboratories (ca. 100 $\mu\text{moles photon/m}^2/\text{s}$ 12/12 light/dark and 25 °C). Sixty-five fragments (2 cm) were cut from at least 3 parent colonies and suspended with nylon threads in a 70-L open-circuit aquarium supplied with filtered seawater (FSW) during acclimation (filtered 1 μm and

maintained at 25 \pm 0.5 °C). Corals were fed three times per week with *Artemia salina* nauplii.

After 7 weeks, tissue completely covered the exposed skeletons, and nubbins were randomly distributed into nine 5-L glass beakers containing 4.5 L FSW ($n = 6$ nubbins per beaker, total of 54 nubbins; Fig. S1 shows a schematic of the experimental setup and timeline). Beakers were placed in a flow-through water bath to maintain constant water temperature (25.4 °C \pm 0.4; $n = 2689$; monitored continuously using an IKS Aquastar system throughout the experiment). Each beaker was equipped with a submersible pump (Aquarium system®, Maxi-Jet Micro) placed 2 cm below the water surface to generate water flow (ca. 140 L/h). Light intensity (provided by Giesemann REFLEXX T5 4 \times 54 W lamps) was kept consistent to rearing conditions with a 12:12 h photoperiod and did not differ between treatments (measured using a Li-COR Li-250A light meter with an underwater quantum sensor, Biosciences; Fig. S2).

2.2. Microplastic exposure

Corals were exposed to pristine polyethylene MP (Fluorescent Green Microspheres, Cospheric; density: 1.025 g/cc; size 106–125 μm) at nominal concentrations of 5 or 50 particles/mL (5000 and 50,000 $\mu\text{g/L}$, respectively; $n = 3$ replicates per concentration, with 6 nubbins each) for 28 days. The lower concentration (5 MP/mL) is within the range commonly applied to study the effects of MPs and the higher concentration (50 MP/L) represents a worst-case scenario concentration that is unlikely to occur in natural systems. The two concentrations are hereafter referred to as moderate and high, respectively. MP stock solutions were prepared using 0.001% Tween 80 (CAS 9005-65-6, Sigma-Aldrich, USA), resulting in a final exposure concentration of 0.000005% surfactant. A control group was exposed to FSW with the equivalent surfactant concentration ($n = 3$, with 6 nubbins each). Treatments were renewed 3 times per week after a complete water change. Nubbins were fed *Artemia salina* nauplii (0.2 nauplii/mL) 1 h before each water renewal. Water samples (20 mL) were taken from each replicate once per week before and after treatment renewal to verify particle concentrations. Since a large proportion of the plastic particles were observed to float over time, we quantified the temporal change in particles remaining in the water column (at the height of the coral) over a 48-h period in one replicate per treatment in the absence of coral (Fig. S3). MP concentrations were determined by counting 4 aliquots from each sample under a microscope using a 1 mL cell counting chamber. Water quality parameters (temperature, pH, dissolved oxygen, salinity, ammonium, nitrate, nitrite and phosphate) were measured weekly throughout the experiment.

2.3. Calcification

Gross calcification rates were assessed according to a protocol adapted from Tambutté et al. (1995). After 8 and 28 days of exposure, one nubbins per replicate ($n = 3$ per treatment and time point) were suspended individually in incubation chambers containing 3.0 kBq of ^{45}Ca (as $^{45}\text{CaCl}_2$, 10 Bq/mL, PerkinElmer, Italy) dissolved in 300 mL FSW. At each time point, three nubbins skeletons (tissue removed using NaOH as described below) were incubated individually as a control for isotopic exchange and one incubation chamber was left without nubbins to serve as a FSW control. Each incubation chamber contained a magnetic stir bar and gentle water motion was provided using a magnetic plate. To determine the specific activity, 1 mL aliquots were taken at the beginning and end of each incubation period.

After 6 h of incubation in ^{45}Ca , nubbins were rinsed in 11 L FSW

in a flow-through aquarium for 30 min. Nubbins were then drip-dried for a few seconds to remove any excess water and transferred to 50 mL Falcon tubes. Coral tissue was removed using 11 mL 1 M NaOH (CAS 1310-73-2, PanReac, Spain) for 30 min at 90 °C. Following tissue hydrolysis, the NaOH-soluble fraction was transferred to a 15 mL Falcon tube and skeleton rinse with an additional 1 mL NaOH, which was added to the NaOH fraction. Skeletons were then rinsed with 10 mL deionized water. The rinsate was discarded and skeletons dried at 60 °C. Dried skeletons were weighed and dissolved in pure HCl (37%; CAS 7647-01-0, ACROS Organics, Germany). To dissolve the skeletons, HCl was added in small increments (2–3 mL total volume) over two days. Once completely dissolved, the HCl-soluble fraction was weighed and three 200 μ L aliquots taken from each sample. The remaining digest was dried on a hot plate. Once dried, 1 mL of deionized water was added to each evaporated sample and sonicated for 45 min to dissolve the dried skeleton.

Scintillation liquid (10 mL, Ultima Gold AB) was added to each coral and water samples that were then vortexed and β -emissions measured using a liquid scintillation counter (PerkinElmer Tricarb 6300 TR). Standards with known activity were made for each type of sample (FSW, 200 μ L aliquots and evaporated sample).

Total protein concentration was measured from the NaOH fraction of each nubbin assessed for calcification using the commercially available BC Assay Protein Quantification kit (Interchim Uptima, France) and a spectrophotometer (Epoch 2, BioTek, USA).

2.4. Photosynthetic efficiency

Chlorophyll *a* fluorescence of photosystem II was assessed weekly (on day 0, 9, 14, 21 and 28) by Pulse Amplitude Modulated (PAM) fluorometry, using an underwater diving-PAM (Walz GmbH, Germany) on two nubbins per replicate ($n = 3$ replicates per treatment (3); total 18 nubbins). Each nubbin was rinsed twice in clean FSW to remove any attached MPs and individually transferred to glass beakers containing 80 mL FSW. Nubbins were dark-adapted for 15 min prior to measurements. The relative electron transport rate (rETR), as well as the maximal (F_v/F_m) quantum yields of photosystem II of the coral symbionts, were determined as a measure of the photosynthetic efficiency. For this, rapid light curves (RLCs) were generated by illuminating each nubbin for 10 s periods to eight light intensities (from 0 to 1952 μ mol/m²/s). Non-photochemical quenching (NPQ), which is a measure of the heat dissipation of the excess absorbed excitation energy, was also calculated during the RLC. Values of F_v/F_m , obtained at the lowest light intensity, and values of ETR_{max} and NPQ_{max} , obtained at the highest light intensity, were compared between treatments.

2.5. Symbiodiniaceae, chlorophyll and protein content

After 28 days of exposure, a small fragment (1 cm) was cut from 2 nubbin per replicate ($n = 3$ per treatment, total 18 nubbins) and preserved at –20 °C for Symbiodiniaceae, chlorophyll and protein content measurements. The nubbins used for these analyses were the same used for the fluorometry measurement throughout the experiment. The tissue was removed from the skeleton using a Water-Pic and homogenized using a tissue Potter grinder. The homogenate was divided into three aliquots for the determination of Symbiodiniaceae cell number, chlorophyll and protein content, respectively. Symbiont cell number was counted using a Coulter Counter (Beckman Coulter, France). For chlorophyll analysis, the homogenate was centrifuged to separate symbiont cells from the host tissue. The supernatant was decanted and the chlorophyll *a* and *c*₂ in the pellet (containing the symbiont cells) were extracted

in 99% acetone (24 h at 4 °C). The extracts were then centrifuged and the absorbances measured at 630, 663, and 750 nm (Jeffrey and Humphrey, 1975). The protein content was assessed according to Smith et al. (1985) by the use of a BC Assay Protein Quantification Kit (Uptima, Interchim) and a Xenius spectrofluorometer (SAFAS, Monaco). All parameters were normalized to the skeletal surface area of the coral fragments which was determined using the single wax-dipping technique (Veal et al., 2010).

2.6. Metabolomics

On day 28, 4 nubbins from each replicate ($n = 3$ per treatment; 36 nubbins total) were sampled for NMR-based metabolomic analysis. Each nubbin was quickly weighed (wet weight; mg) and snap-frozen in liquid nitrogen in a pre-weighed 15 mL Falcon tube. The samples were subsequently lyophilized and stored at –80 °C prior to metabolite extraction.

2.7. Extraction of polar metabolites

Prior to extractions the lyophilized nubbins were weighed (dry weight; mg). Metabolites were extracted using a modified methanol:chloroform extraction (Bligh and Dyer, 1959; Melvin et al., 2017). Individual nubbins were first submerged in 4 mL chloroform and ultra-sonicated (VWR Ultrasonic cleaner, USA) for 15 min. This step was repeated 4 times to remove non-polar compounds common to marine organisms, and was based on preliminary extraction trials with coral samples. Nubbins were next submerged in 4 mL 70% v/v methanol/water and ultra-sonicated for 15 min. The methanol/water extraction was repeated 2 times to ensure full recovery of extractable polar metabolites and the resulting yields were combined (total 12 mL). Polar extracts were evaporated using a Series II centrifugal vacuum concentrator (GeneVac Technologies, England) and the samples were lyophilized to ensure removal of any residual water. To purify the polar extract, the samples were resuspended in 1 mL methanol (vortexed and sonicated for 15 min) and 2 mL chloroform was added followed by 0.75 mL water (Bligh and Dyer, 1959). Samples were vortexed and centrifuged at 3500 rpm for 10 min at 4 °C. The upper phase of the purification step was transferred to a glass vial, dried using a Series II centrifugal vacuum concentrator (GeneVac Technologies, England).

2.8. ¹H NMR spectroscopy

NMR spectra were acquired using an 800 MHz Bruker® Avance III HDX spectrometer equipped with a Triple (TCI) Resonance 5 mm Cryoprobe with Z-gradient and automatic tuning and matching. Polar metabolites were re-suspended in 200 μ L phosphate buffer made with deuterium oxide (D₂O) which contained 0.05% sodium-3-(trimethylsilyl)-2,2,3,3-tetradeuteriopropionate (TSP) as an internal reference. Individual samples were transferred to 3 mm NMR tubes using a Hamilton® zero dead volume glass syringe (Hamilton Company, Reno, Nevada).

The NMR was controlled via IconNMR™ software paired to a SampleJet auto-sampler (Bruker Pty Ltd., Victoria, Australia). Spectra were acquired at 298 K with the internal reference used for field locking (Proton ¹H chemical shift for TSP at δ 0.00 ppm). Proton spectra were acquired using zg30 pulse program with 0.8 relaxation delay, 7.83 pulse width and a spectral width of 16 kHz and using 128 scans. An edited ¹H–¹³C heteronuclear single quantum coherence (HSQC) spectra was also acquired for a representative sample, with 350 scans, 0.8 relaxation delay, 7.83 μ s 90° pulse width, and spectral widths of 12.8 kHz (¹H δ –3.23–12.79) and 33.1 kHz (¹³C δ –9.40–155.2).

Post-processing of NMR data was carried out with MestReNova

v11.0.3 (Mestrelab Research S.L., Spain). The ^1H FIDs were Fourier transformed with a 0.3 Hz line broadening, manually phase-corrected and automatically baseline adjusted (ablative), and finally referenced to the internal standard (TSP at ^1H δ 0.00 ppm). Spectra were stacked and individual features were integrated using the advanced data analysis tool in MestReNova, and this data was copied into an excel file for final processing prior to statistical analysis. The ^1H – ^{13}C HSQC spectra was processed with default Bruker parameters and referenced to the internal standard (TSP at ^1H δ 0.00 ppm and ^{13}C δ 0.00 ppm). The HSQC data was used to verify metabolite identification in conjunction with the Chenomx NMR suite v8.4 (ChenomxInc., Edmonton, Canada) and comparison to reference spectra housed in the Human Metabolome Database (www.hmdb.ca).

2.9. Statistical analysis

Differences in relative calcification rates were analyzed using one-way ANOVAs at each time point ($n = 3$ replicates per treatment; 1 coral nubbin sampled per replicate at each time point). Symbiodiniaceae, chlorophyll and protein content of nubbins sampled on day 28 was analyzed by one-way ANOVAs ($n = 3$ replicates per treatment; 2 nubbins per replicate). Differences in PAM measurements (maximal Fv/Fm, ETR and NPQ) were analyzed using one-way ANOVAs at each time point followed by Tukey's multiple comparison tests ($n = 3$ replicates per treatment; 2 nubbins per replicate at each time point). All data met assumptions of normality and homogeneity of variance and were analyzed using GraphPad Prism 8.0.

Multivariate analysis of metabolite profiles ($n = 3$ replicates per treatment; 4 nubbins per replicate) were performed with Metaboanalyst 4.0 (Chong et al., 2019). Data were normalized to the skeletal surface area, Log transformed and pareto-scaled, and Principal Components Analysis (PCA) was performed to explore differences between treatments. Sparse Partial Least Squares Discriminant Analysis (sPLS-DA) was used to highlight differences identified via PCA. Metabolites driving the response were identified with Significance Analysis of Metabolites (SAM).

3. Results and discussion

3.1. Microplastic concentrations in experimental setup

Concentrations of MP were measured to evaluate fluctuations in bioavailable particles (i.e., in suspension at the height of the coral) throughout the exposure. Measured concentrations were 5 ± 1 particles/mL (mean \pm SD; median = 4.67) and 70 ± 33 particles/mL (mean \pm SD; median = 53.8) immediately following MP-spike in moderate and high treatments, respectively (Fig. S3A). Measurements over a 48-h period (representing the time between treatment renewals) in a separate experiment without coral showed that relatively few particles remained in suspension after 24 h (Fig. S3B), and none were detected after 48 h. This highlights the importance of quantifying the concentration of bioavailable plastics within the experimental beakers, as this can vary greatly over time (Karami, 2017). Nevertheless, this information is rarely documented in published studies. In fact, less than half the published studies on MP effects in coral under laboratory conditions have verified particle concentrations (Table S1) and those that have, report heterogeneous distributions of MP in the water column, with the majority of particles either floating or sinking (Allen et al., 2017; Reichert et al., 2019, 2018). This is especially important for sessile organisms like coral since nominal concentrations may be much higher or lower than the bioavailable fraction, which would depend on the position of the coral in relation to the bulk of the

particles.

3.2. Growth response of coral to microplastics

Microplastics had no significant effect on coral gross calcification rates after 8 ($F_{(2,6)} = 0.86$, $p = 0.47$) and 28 days ($F_{(2,6)} = 3.36$, $p = 0.11$) of exposure (Fig. 1). To-date, four other studies have assessed the effects of MP on coral growth, but the magnitude of observed responses varied greatly between studies. Similar to our study, Hankins et al. (2018) found no significant differences in calcification of two species (*Montastraea cavernosa* and *Orbicella faveolata*) after a 2-d exposure to PE beads (90–100 μm). A longer duration study (6 months), however, reported a significant 3% reduction in calcification of the reef-building coral *Heliopora coerulea* exposed to HDPE fragments (65–410 μm), but found no significant changes in the three other species tested (Reichert et al., 2019). This species-specific sensitivity to MPs is consistent with other studies that compared the effects on MPs on growth rates among coral species and reported significant growth reductions in some species but not others (Chapron et al., 2018; Mouchi et al., 2019). Though several factors differed between these studies, it seems most likely that exposure duration and coral species were the driving factor and therefore a longer exposure duration may have resulted in a greater effect size in our study.

3.3. Photophysiological response of coral to microplastics

Photosynthetic yields of photosystem II of zooxanthellae were measured as an indicator of photophysiological stress in the coral nubbins. After 4 weeks of exposure to the high MP treatment, nubbins exhibited increased photosynthetic efficiency (Fv/Fm_{max}) and non-photochemical quenching (NPQ_{max}) and decreased electron transport rate (ETR_{max}) compared to those in control or moderate MP treatments (Fig. 2; $p < 0.05$, Tukey's multiple comparison test). A similar response was observed after 3 weeks, but to a lesser extent (Fig. S4; $p > 0.05$). An increased photosynthetic efficiency (Fv/Fm) was also observed in corals exposed to MPs for

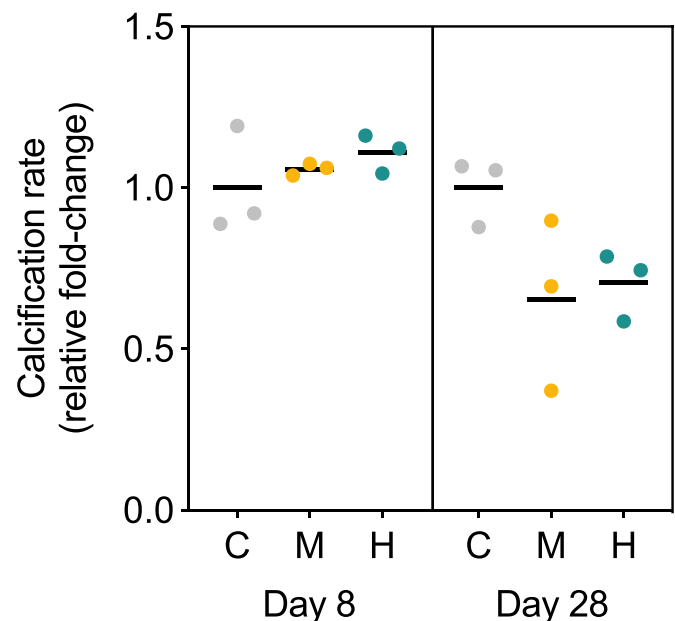


Fig. 1. Gross calcification rates of the coral *Stylophora pistillata* (per dry mass) exposed to moderate (5 particles/mL) or high (50 particles/mL) microplastics relative to controls after 8 and 28 days. Lines are means of $n = 3$ replicates. Dots are individual data for each replicate (1 coral nubbin per replicate).

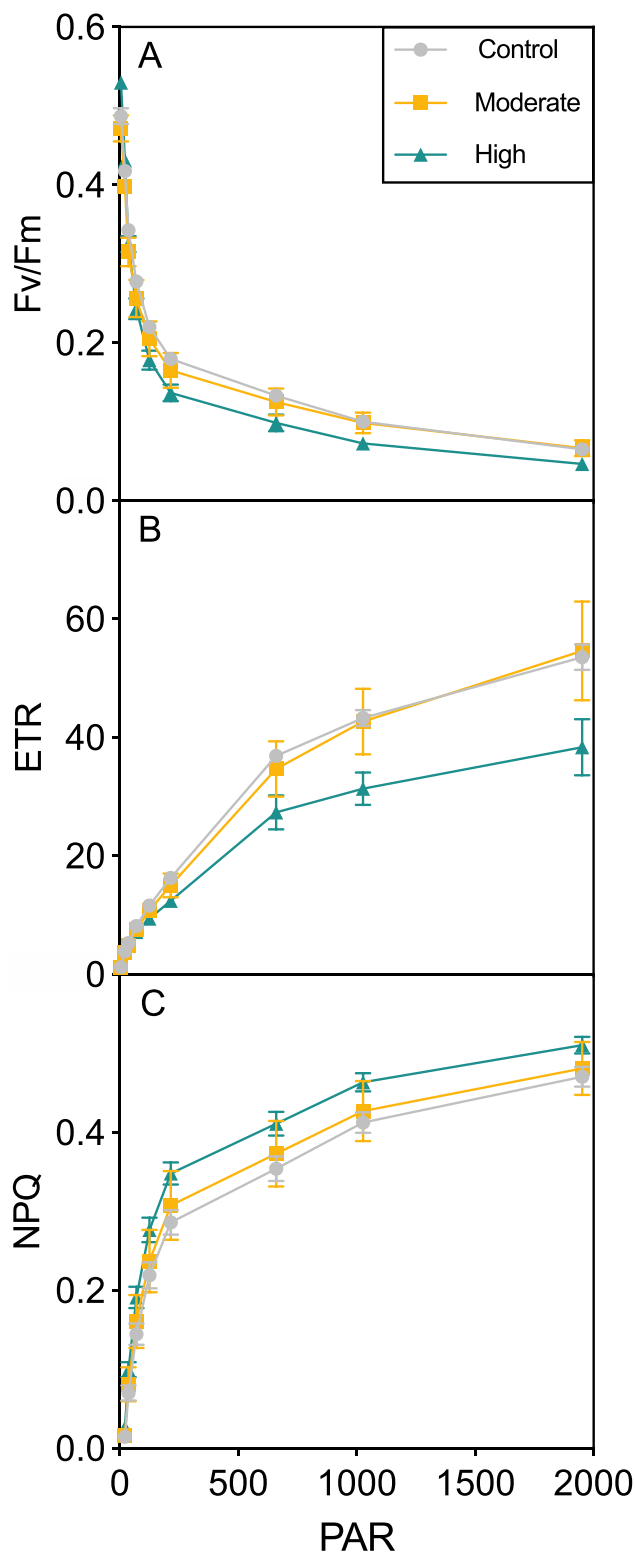


Fig. 2. Photosynthetic efficiency (Fv/Fm, A), electron transport rate (ETR, B) and non-photochemical quenching (NPQ, C) of the coral *Stylophora pistillata* after 4 weeks of exposure to control, moderate (5 particles/mL) or high (50 particles/mL) microplastic concentrations. Values are means \pm s.e.m., n = 3.

24 weeks at a concentration similar to the moderate MP treatment used here (Reichert et al., 2019). This up-regulation in photosynthesis may be an initial strategy of the corals to counteract energy deficits and reduced growth rates evolving from MP ingestion and subsequent impaired heterotrophic feeding rates (Reichert et al., 2019). Interestingly, that study also observed that the up-regulation of photosynthesis ceased after 24 weeks of exposure suggesting that this process will not provide the required energy to the corals on the long term.

Despite an increased Fv/Fm in the present study, the ETR_{max} decreased in corals exposed to the high MP treatment. A reduced ETR_{max} is indicative of potential photodamage and photoinhibition of photosystem II, which suggests that MPs can cause photo-physiological stress in coral. Similar negative effects of MP exposure on photosynthesis parameters have previously been reported for free-living marine microalgae as well as for another reef-building coral species (Long et al., 2017; Mao et al., 2018; Reichert et al., 2019; Zhang et al., 2017). Reduced ETR rates may result in electron accumulation of photosystem II potentially leading to the accumulation of reactive oxygen species (ROS). Excessive ROS levels can subsequently induce oxidative stress and membrane lipid peroxidation (Chen et al., 2015; Mao et al., 2018; Qian et al., 2010). Oxidative stress of corals is known to occur under environmental stressors such as high temperatures, eutrophication and UV radiation, but MPs were also suggested to function as an environmental parameter to modulate coral physiological activities (Tang et al., 2018). Indeed, transcriptome analysis identified an up-regulated antioxidant capacity and overall stress response in the coral *Pocillopora damicornis* when exposed to 9.0×10^{10} microbeads/L (Tang et al., 2018). While MPs cause membrane and cell damage in free-living algae possibly due to the direct cell contact and the formation of MP-algae-aggregates (Mao et al., 2018), in corals it is the host that is primarily in contact with MP particles. Thus, damaging effects on the photosystem II of coral symbionts residing within the host tissue may not result from a direct contact with MPs, but potentially result from a disrupted host-symbiont signaling (see details in next section) that will require further investigation. This has proven to be a sensitive endpoint, since effects were observed prior to any other physiological changes in the coral symbiont. Specifically, coral from our study showed no significant differences in pigment content (Fig. 3A; $F_{(2,6)} = 2.19$, $p = 0.19$ and Fig. 3B; $F_{(2,6)} = 1.12$, $p = 0.39$) or symbiont density (Fig. 3C; $F_{(2,6)} = 0.18$, $p = 0.84$) following MP exposure. Trends did suggest a slight (1.2-fold), but non-statistically significant, decrease in chlorophyll *a* concentration when exposed to the high concentration, which is consistent with the photosynthetic response.

Similar to our observations, recent studies have also found no significant changes in the density of symbiotic zooxanthellae in five other species of reef-building coral exposed to MPs (Reichert et al., 2019; Tang et al., 2018). This is contrary to findings from other recent studies which reported that MP exposure suppressed the infectivity of Symbiodiniaceae into host cells in both the sea anemone, *Aiptasia* sp., and primary polyps of the scleractinian coral *Favites chinensis* (Okubo et al., 2018), as well as increased the release of zooxanthellae from the scleractinian coral *Acropora formosa* (Syakti et al., 2019). It is therefore possible that differences in sensitivity exist between species, which would help explain the discrepancies between studies. Effects of MPs on the initiation of symbiosis merits further investigation since corals rely heavily on symbionts for energy and this could potentially increase their vulnerability.

3.4. Metabolite profiles of corals exposed to microplastics

Microplastic exposure had a significant effect on metabolite

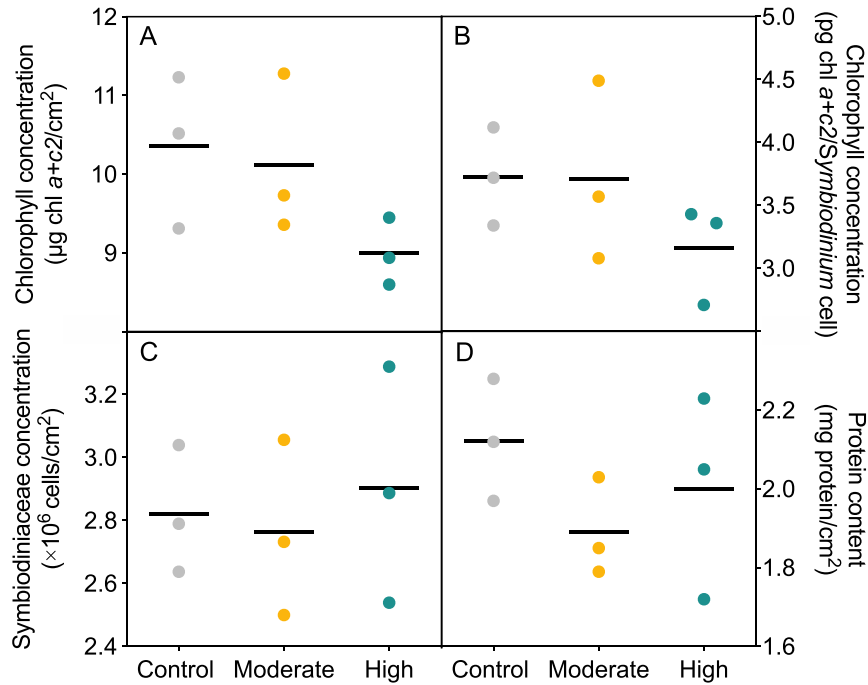


Fig. 3. Chlorophyll *a* concentration (A), chlorophyll *a* concentration per Symbiodiniaceae cell (B), Symbiodiniaceae density (C) and protein content (D) of the coral *Stylophora pistillata* exposed to control, moderate (5 particles/mL) or high (50 particles/mL) microplastic concentrations for 4 weeks. Lines are means of $n = 3$ replicates. Dots are means of 2 coral nubbins per replicate.

profiles extracted from coral nubbins. Preliminary analysis with PCA identified separation between control nubbins and those exposed to moderate and high MP particle densities (Fig. S5); a pattern that was further highlighted by supervised sPLS-DA (Fig. 4A). Significance Analysis of Metabolites (SAM) following sPLS-DA identified 5 spectral features as being significantly

different between control and treatment groups (Fig. 4B). Three of these were identified as corresponding to the anomeric proton of phosphorylated sugars (5.50–5.43 ppm; Fig. 5A), the pyrimidine protons of nucleobases (5.89–5.85 ppm; Fig. 5B), and the anomeric proton of the sugar moiety in nucleosides (5.99–5.90 ppm; Fig. 5C). The latter two features are present in nucleosides and nucleotides.

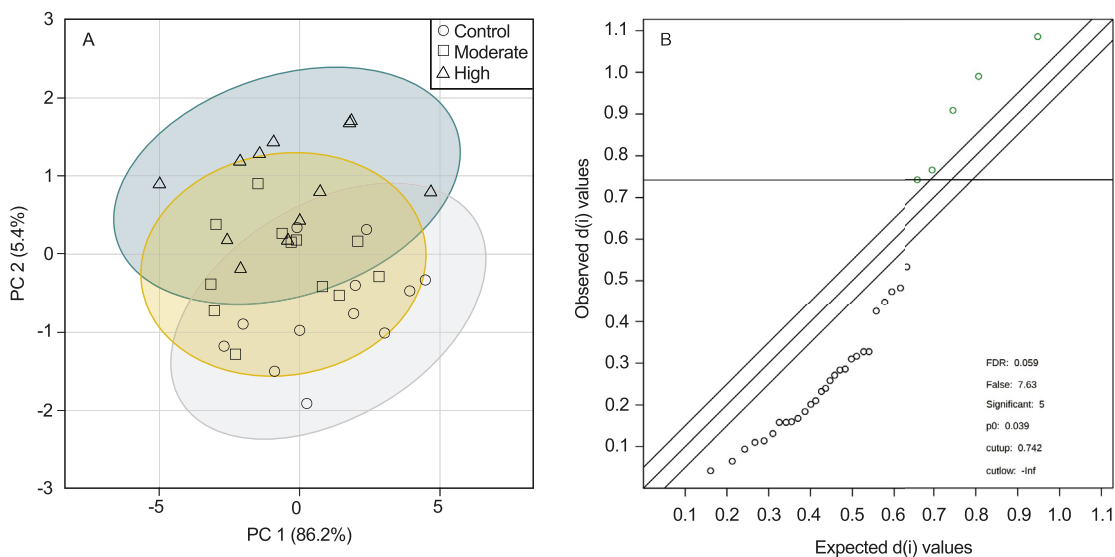


Fig. 4. (A) Results of sPLS-DA of polar metabolites from the coral *Stylophora pistillata* after 4 weeks of exposure to control, moderate (5 particles/mL) or high (50 particles/mL) microplastic concentrations. (B) Results of Significance Analysis of Metabolites (SAM) associated with the sPLS-DA identifying five key features as significantly different between treatment groups.

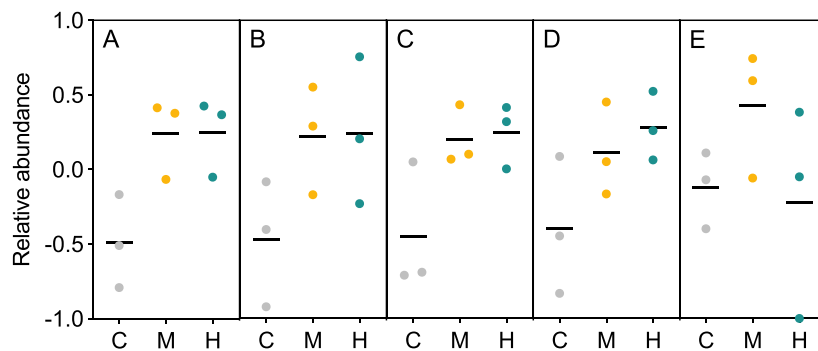


Fig. 5. Relative abundance of select metabolites: (A) anomeric proton of phosphorylated sugars (5.50–5.43 ppm), (B) the pyrimidine protons of nucleobases (5.89–5.85 ppm), (C) and the anomeric proton of the sugar moiety in nucleosides (5.99–5.90 ppm), (D) scyllo-inositol (3.38–3.33 ppm), and (E) a region containing overlapping proline and glutamate signals (2.30–2.33 ppm) of the coral *Stylophora pistillata* exposed to control, moderate (5 particles/mL) or high (50 particles/mL) microplastic concentrations for 4 weeks. Lines are means of $n = 3$ replicates. Dots are means of 4 coral nubbins per replicate.

The pyrimidine and nucleoside anomeric protons are consistent with uracil and uridine, respectively, but may represent unique analogs since marine species are known for modifying both the base and ribose sugar of nucleosides (Huang et al., 2014). The other two features corresponded to scyllo-inositol (3.38–3.33 ppm; Fig. 5D) and a region of the ^1H spectra with overlapping signals from proline, glutamate and other metabolites (2.30–2.33 ppm; Fig. 5E). Despite the relatively small number of metabolites being significantly altered, these findings offer supporting biochemical data consistent with what is already known (or hypothesized) about how corals respond to MP exposure.

Recent studies have found that MPs can interfere with the host-symbiont relationship between coral (host) and photosynthetic zooxanthellae algae (symbiont); an interference that leads to the phenomenon known as coral bleaching when it results in the loss of the symbionts (Okubo et al., 2018; Syakti et al., 2019). Under normal circumstances, the coral supplies basic nutrients and other metabolites to the symbiont. One such class of metabolites is the pyrimidine bases, including uracil, which was recently found to be essential in at least one algal symbiont species (Ishii et al., 2018). The observed increase in the nucleobase uracil (or uracil analog) in the present study may therefore reflect a compensatory response by the coral aimed at supporting the algal symbiont by providing limiting resources. The increase in uracil (or analog) is also likely linked to the observed increased abundance of other nucleotide moieties in MP-exposed coral, including a phosphate sugar and nucleoside, which itself is made up of a pentose sugar (e.g., ribose) bound to a nucleobase. Besides supporting the symbiont through the provision of a limiting pyrimidine bases, it has been suggested that corals use chemical signaling to support the host-symbiont relationship (Hillyer et al., 2016). Nucleosides and nucleotides are common cellular signaling molecules (Giuliani et al., 2019; Vijayamahantesh and Vijayalaxmi, 2019), and increases in nucleotide precursors nicotinamide adenine dinucleotide (NAD) and nicotinamide adenine dinucleotide phosphate (NADP) have indeed been described in stressed corals (Hillyer et al., 2016).

At this stage, the signaling relationship between coral and symbiont and the impact of MPs on this relationship are areas needing further research attention. Aside from nucleotides, the metabolite scyllo-inositol was recently identified as a possible signaling molecule in corals. A recent study described appreciable levels of scyllo-inositol in coral but had no explanation as to the role of this metabolite (Yancey et al., 2010). More recently, Hillyer et al. (2017) observed increased scyllo-inositol in coral undergoing

thermal stress – another factor known to cause coral bleaching (Skirving et al., 2019). Emerging evidence suggests that the inositols are indeed involved with host-symbiont signaling between corals and algae (Matthews et al., 2018). The observation of increased scyllo-inositol, along with uracil (or an analog nucleobase) and other components of nucleosides/nucleotides in the present study, are consistent with reports of disrupted host-symbiont signaling described in other studies (Okubo et al., 2018). Specifically, these responses support the hypothesis that MPs disrupt host-symbiont signaling, and that corals respond to this interference by ramping up signaling and chemical support to the zooxanthellae algae.

While the increased abundance of scyllo-inositol and nucleotide constituents (i.e., nucleobase, pentose sugar and phosphate sugar moieties) suggest a response that involves host-symbiont signaling, the latter is also consistent with increased mucus production in corals exposed to MPs (Hadaidi et al., 2019). The chemical makeup of mucus varies between coral species, but carbohydrate polymers are the major component (Meikle et al., 1988; Wild et al., 2010). Nucleotide sugars play a key role as sugar donors in carbohydrate metabolism and polysaccharide synthesis across taxa (Bar-Peled and O'Neill, 2011), and would therefore be expected to increase to facilitate mucus production. Indeed, individuals of the cnidarian *Exaiptasia pallida* exhibiting signs of bleaching (loss of symbiont) were recently shown to have a greater abundance of the phosphate sugar glucose-3-phosphate compared to non-bleached individuals (Molina et al., 2017). The increase in NMR signals corresponding to phosphate sugars (free or incorporated into sugar nucleotides) in corals exposed to MPs therefore offers supporting evidence of a general stress response involving increased mucus production.

4. Conclusions

Coral reefs are suffering from anthropogenic pressures on a global scale (Hughes et al., 2018; Sweet and Brown, 2016), and plastic pollution may pose an added stress. Response mechanisms in coral exposed to MPs are poorly understood, in part due to significant knowledge gaps regarding actual MP concentrations expected to occur in coral reef ecosystems (Connors, 2017; Saliu et al., 2018). Reports of MPs in waters surrounding coral reefs are generally low (<1 MP/m³ in relatively pristine reefs [Saliu et al., 2019; Jensen et al., 2019] and up to 45,200 MP/m³ in polluted reefs [Ding et al., 2019]), but the sparsity of data and variations in sampling procedures and plastic characterisation make it difficult to evaluate the actual abundance of MPs in coral habitats. MPs have

been shown to elicit a range of negative effects in coral at relatively high concentrations under laboratory conditions (Chapron et al., 2018; Mouchi et al., 2019; Okubo et al., 2018; Reichert et al., 2018; Syakti et al., 2019; Tang et al., 2018), demonstrating the potential for MPs to affect coral health. Our study observed significant changes to metabolite profiles of coral exposed to comparable or even lower MP concentrations, contributing to the mechanistic understanding of how MPs influence coral at the higher concentrations commonly tested. However, the likelihood of particle concentration in coral reef ecosystems reaching levels that have been shown to elicit responses in the laboratory remains doubtful and information on realistic impacts of plastics on the reef environment is needed (UNEP, 2019). The question then arises as to how corals will respond to a chronic exposure to environmental MP concentrations and whether this can influence the susceptibility of corals to other anthropogenic and global-change related stressors.

Declaration of interests

The authors declare that they have no known competing financial interests or personal relationships that could have appeared to influence the work reported in this paper.

CRediT authorship contribution statement

Chantal M. Lancôt: Conceptualization, Methodology, Validation, Formal analysis, Data curation, Investigation, Writing - original draft, Visualization. **Vanessa N. Bednarz:** Methodology, Validation, Formal analysis, Investigation, Writing - review & editing, Visualization. **Steven Melvin:** Methodology, Validation, Formal analysis, Data curation, Writing - original draft, Visualization. **Hugo Jacob:** Investigation, Writing - review & editing. **François Oberhaensli:** Conceptualization, Methodology, Resources. **Peter W. Swarzenski:** Writing - review & editing, Supervision, Funding acquisition. **Christine Ferrier-Pagès:** Methodology, Writing - review & editing, Resources, Supervision. **Anthony R. Carroll:** Methodology, Formal analysis, Writing - review & editing. **Marc Metian:** Conceptualization, Methodology, Data curation, Writing - review & editing, Supervision, Project administration, Funding acquisition.

Acknowledgment

This research work has been funded by the US through the Peaceful Uses Initiatives (PUI) program under the project of "Implementation of a comprehensive sampling and analytical methodology to determine and trace oil pollution in marine waters (Phase II – Marine plastics: tackling the challenge using nuclear applications)". The IAEA is grateful to the Government of the Principality of Monaco for the support provided to its Environment Laboratories. VB and CFP are grateful to the Prince Albert II of Monaco Foundation for their financial support. CL is supported by an Australian Research Council Discovery Early Career Award (DE180101286) funded by the Australian Government. We thank Mr. Miguel Gomez Batista (Centro de Estudios Ambientales de Cienfuegos, Cuba) for assistance with protein and ⁴⁵Ca analysis. Coral illustration in graphical abstract is courtesy of the Integration and Application Network, University of Maryland Centre for Environmental Science (ian.umces.edu/symbols/).

Appendix A. Supplementary data

Supplementary data to this article can be found online at <https://doi.org/10.1016/j.envpol.2020.114559>.

References

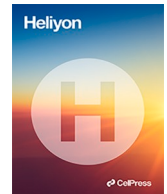
- Allen, A.S., Seymour, A.C., Rittschof, D., 2017. Chemoreception drives plastic consumption in a hard coral. *Mar. Pollut. Bull.* 124, 198–205. <https://doi.org/10.1016/j.marpolbul.2017.07.030>.
- Avio, C.G., Gorb, S., Regoli, F., 2017. Plastics and microplastics in the oceans: from emerging pollutants to emerged threat. *Mar. Environ. Res.* 128, 2–11. <https://doi.org/10.1016/j.marenvres.2016.05.012>.
- Axworthy, J.B., Padilla-Gamiño, J.L., 2019. Microplastics ingestion and heterotrophy in thermally stressed corals. *Sci. Rep.* 9, 18193. <https://doi.org/10.1038/s41598-019-54698-7>.
- Bar-Peled, M., O'Neill, M.A., 2011. Plant nucleotide sugar formation, interconversion, and salvage by sugar recycling. *Annu. Rev. Plant Biol.* 62, 127–155. <https://doi.org/10.1146/annurev-arplant-042110-103918>.
- Bligh, E.G., Dyer, W.J., 1959. A rapid method of total lipid extraction and purification. *Can. J. Biochem. Physiol.* 37, 911–917. <https://doi.org/10.1139/o59-099>.
- Bouwmeester, H., Hollman, P.C.H., Peters, R.J.B., 2015. Potential health impact of environmentally released micro- and nanoplastics in the human food production chain: experiences from nanotoxicology. *Environ. Sci. Technol.* 49, 8932–8947. <https://doi.org/10.1021/acs.est.5b01090>.
- Chapron, L., Peru, E., Engler, A., Ghiglione, J.-F.F., Meistertzheim, A.-L.L., Pruski, A.M., Purser, A., Vétion, G., Galand, P.E., Lartaud, F., 2018. Macro- and microplastics affect cold-water corals growth, feeding and behaviour. *Sci. Rep.* 8, 1–8. <https://doi.org/10.1038/s41598-018-33683-6>.
- Chen, L., Mao, F., Kirumba, G.C., Jiang, C., Manefield, M., He, Y., 2015. Changes in metabolites, antioxidant system, and gene expression in *Microcystis aeruginosa* under sodium chloride stress. *Ecotoxicol. Environ. Saf.* 122, 126–135. <https://doi.org/10.1016/j.ecoenv.2015.07.011>.
- Chong, J., Wishart, D.S., Xia, J., 2019. Using MetaboAnalyst 4.0 for comprehensive and integrative metabolomics data analysis. *Curr. Protoc. Bioinf.* 68, e86. <https://doi.org/10.1002/cpbi.86>.
- Connors, E.J., 2017. Distribution and biological implications of plastic pollution on the fringing reef of Mo'orea, French Polynesia. *PeerJ.* 5, e3733. <https://doi.org/10.7717/peerj.3733>.
- Ding, J., Jiang, F., Li, J., Wang, Z., Sun, C., Wang, Z., Fu, L., Ding, N.X., He, C., 2019. Microplastics in the coral reef systems from xisha islands of south China sea. *Environ. Sci. Technol.* 53, 8036–8046. <https://doi.org/10.1021/acs.est.9b01452>.
- Giuliani, A.L., Sarti, A.C., Di Virgilio, F., 2019. Extracellular nucleotides and nucleosides as signalling molecules. *Immunol. Lett.* 205, 16–24. <https://doi.org/10.1016/j.imlet.2018.11.006>.
- Hadaidi, G., Gegner, H.M., Ziegler, M., Voolstra, C.R., 2019. Carbohydrate composition of mucus from scleractinian corals from the central Red Sea. *Coral Reefs* 38, 21–27. <https://doi.org/10.1007/s00338-018-01758-5>.
- Hall, N.M., Berry, K.L.E., Rintoul, L., Hoogenboom, M., 2015. Microplastic ingestion by scleractinian corals. *Mar. Biol.* 162, 725–732. <https://doi.org/10.1007/s00227-015-2619-7>.
- Hankins, C., Duffy, A., Drisco, K., 2018. Scleractinian coral microplastic ingestion: potential calcification effects, size limits, and retention. *Mar. Pollut. Bull.* 135, 587–593. <https://doi.org/10.1016/j.marpolbul.2018.07.067>.
- Hillyer, K.E., Dias, D.A., Lutz, A., Roessner, U., Davy, S.K., 2017. Mapping carbon fate during bleaching in a model cnidarian symbiosis: the application of 13C metabolomics. *New Phytol.* 214, 1551–1562. <https://doi.org/10.1111/nph.14515>.
- Hillyer, K.E., Tumanov, S., Villas-Bóas, S., Davy, S.K., 2016. Metabolite profiling of symbiont and host during thermal stress and bleaching in a model cnidarian-dinoflagellate symbiosis. *J. Exp. Biol.* 219, 516–527. <https://doi.org/10.1242/jeb.128660>.
- Huang, R.M., Chen, Y.N., Zeng, Z., Gao, C.H., Su, X., Peng, Y., 2014. Marine nucleosides: structure, bioactivity, synthesis and biosynthesis. *Mar. Drugs* 12, 5817–5838. <https://doi.org/10.3390/md12125817>.
- Hughes, T.P., Anderson, K.D., Connolly, S.R., Heron, S.F., Kerry, J.T., Lough, J.M., Baird, A.H., Baum, J.K., Berumen, M.L., Bridger, T.C., Claar, D.C., Eakin, C.M., Gilmour, J.P., Graham, N.A.J., Harrison, H., Hobbs, J.P.A., Hoey, A.S., Hoogenboom, M., Lowe, R.J., McCulloch, M.T., Pandolfi, J.M., Pratchett, M., Schoepf, V., Torda, G., Wilson, S.K., 2018. Spatial and temporal patterns of mass bleaching of corals in the Anthropocene. *Science* 80 (359), 80–83. <https://doi.org/10.1126/science.aan8048>.
- Ishii, Y., Maruyama, S., Fujimura-Kamada, K., Kutsuna, N., Takahashi, S., Kawata, M., Minagawa, J., 2018. Isolation of uracil auxotroph mutants of coral symbiont alga for symbiosis studies. *Sci. Rep.* 8, 3237. <https://doi.org/10.1038/s41598-018-21499-3>.
- Ivar Do Sul, J.A., Costa, M.F., 2014. The present and future of microplastic pollution in the marine environment. *Environ. Pollut.* 185, 352–364. <https://doi.org/10.1016/j.envpol.2013.10.036>.
- Jambeck, J.R., Geyer, R., Wilcox, C., Siegler, T.R., Perryman, M., Andrady, A.L., Narayan, R., Law, K.L., 2015. Plastic waste inputs from land into the ocean. *Science* 80 (347), 768–771. <https://doi.org/10.1126/science.1260352>.
- Jeffrey, S.W., Humphrey, G.F., 1975. New spectrophotometric equations for determining chlorophylls a, b, c1 and c2 in higher plants, algae and natural phytoplankton. *Biochem. Physiol. Pflanz. (BPP)* 167, 191–194. [https://doi.org/10.1016/s0015-3796\(17\)30778-3](https://doi.org/10.1016/s0015-3796(17)30778-3).
- Jensen, L.H., Motti, C.A., Garm, A.L., Tonin, H., Kroon, F.J., 2019. Sources, distribution and fate of microfibres on the great barrier reef, Australia. *Sci. Rep.* 9, 1–15. <https://doi.org/10.1038/s41598-019-45340-7>.
- Karami, A., 2017. Gaps in aquatic toxicological studies of microplastics.

- Chemosphere 184, 841–848. <https://doi.org/10.1016/j.chemosphere.2017.06.048>.
- Kirstein, I.V., Kirmizi, S., Wichels, A., Garin-Fernandez, A., Erler, R., Löder, M., Gerdt, G., 2016. Dangerous hitchhikers? Evidence for potentially pathogenic *Vibrio* spp. on microplastic particles. *Mar. Environ. Res.* 120, 1–8. <https://doi.org/10.1016/j.marenvres.2016.07.004>.
- Lamb, J.B., Willis, B.L., Fiorenza, E.A., Couch, C.S., Howard, R., Rader, D.N., True, J.D., Kelly, L.A., Ahmad, A., Jompa, J., Harvell, C.D., 2018. Plastic waste associated with disease on coral reefs. *Science* 80 (359), 460–462. <https://doi.org/10.1126/science.aar3320>.
- Lebreton, L.C.M., van der Zwet, J., Damsteeg, J.-W., Slat, B., Andrady, A.L., Reisser, J., 2017. River plastic emissions to the world's oceans. *Nat. Commun.* 8, 15611. <https://doi.org/10.1038/ncomms15611>.
- Long, M., Paul-Pont, I., Hégaret, H., Moriceau, B., Lambert, C., Huvet, A., Soudant, P., 2017. Interactions between polystyrene microplastics and marine phytoplankton lead to species-specific hetero-aggregation. *Environ. Pollut.* 228, 454–463. <https://doi.org/10.1016/j.envpol.2017.05.047>.
- Mao, Y., Ai, H., Chen, Y., Zhang, Z., Zeng, P., Kang, L., Li, W., Gu, W., He, Q., Li, H., 2018. Phytoplankton response to polystyrene microplastics: perspective from an entire growth period. *Chemosphere* 208, 59–68. <https://doi.org/10.1016/j.chemosphere.2018.05.170>.
- Martin, C., Corona, E., Mahadik, G.A., Duarte, C.M., 2019. Adhesion to coral surface as a potential sink for marine microplastics. *Environ. Pollut.* 255, 113281. <https://doi.org/10.1016/j.envpol.2019.113281>.
- Matthews, J.L., Oakley, C.A., Lutz, A., Hillyer, K.E., Roessner, U., Grossman, A.R., Weis, V.M., Davy, S.K., 2018. Partner switching and metabolic flux in a model cnidarian–dinoflagellate symbiosis. *Proc. R. Soc. B Biol. Sci.* 285, 20182336. <https://doi.org/10.1098/rspb.2018.2336>.
- Meikle, P., Richards, G.N., Yellowlees, D., 1988. Structural investigations on the mucus from six species of coral. *Mar. Biol.* 99, 187–193.
- Melvin, S.D., Habener, L.J., Leusch, F.D.L., Carroll, A.R., 2017. 1H NMR-based metabolomics reveals sub-lethal toxicity of a mixture of diabetic and lipid-regulating pharmaceuticals on amphibian larvae. *Aquat. Toxicol.* 184, 123–132. <https://doi.org/10.1016/j.aquatox.2017.01.012>.
- Molina, V.H., Castillo-Medina, R.E., Thomé, P.E., 2017. Experimentally induced bleaching in the sea anemone *Exaiptasia* supports glucose as a main metabolite associated with its symbiosis. *J. Mar. Biol.* 2017, 1–7. <https://doi.org/10.1155/2017/3130723>.
- Mouchi, V., Chapron, L., Peru, E., Pruski, A.M., Meistertzheim, A.L., Vétion, G., Galand, P.E., Lartaud, F., 2019. Long-term aquaria study suggests species-specific responses of two cold-water corals to macro- and microplastics exposure. *Environ. Pollut.* 253, 322–329. <https://doi.org/10.1016/j.envpol.2019.07.024>.
- Okubo, N., Takahashi, S., Nakano, Y., 2018. Microplastics disturb the anthozoan-algae symbiotic relationship. *Mar. Pollut. Bull.* 135, 83–89. <https://doi.org/10.1016/j.marpolbul.2018.07.016>.
- Qian, H., Yu, S., Sun, Z., Xie, X., Liu, W., Fu, Z., 2010. Effects of copper sulfate, hydrogen peroxide and N-phenyl-2-naphthylamine on oxidative stress and the expression of genes involved in photosynthesis and microcystin disposition in *Microcystis aeruginosa*. *Aquat. Toxicol.* 99, 405–412. <https://doi.org/10.1016/j.aquatox.2010.05.018>.
- Reichert, J., Arnold, A.L., Hoogenboom, M.O., Schubert, P., Wilke, T., 2019. Impacts of microplastics on growth and health of hermatypic corals are species-specific. *Environ. Pollut.* 254, 113074. <https://doi.org/10.1016/j.envpol.2019.113074>.
- Reichert, J., Schellenberg, J., Schubert, P., Wilke, T., 2018. Responses of reef building corals to microplastic exposure. *Environ. Pollut.* 237, 955–960. <https://doi.org/10.1016/j.envpol.2017.11.006>.
- Richards, Z.T., Beger, M., 2011. A quantification of the standing stock of macro-debris in Majuro lagoon and its effect on hard coral communities. *Mar. Pollut. Bull.* 62, 1693–1701. <https://doi.org/10.1016/j.marpolbul.2011.06.003>.
- Riegl, B., 1995. Effects of sand deposition on scleractinian and alcyonacean corals. *Mar. Biol.* 121, 517–526. <https://doi.org/10.1007/BF00349461>.
- Riegl, B., Branch, G.M., 1995. Effects of sediment on the energy budgets of four scleractinian (Bourne 1900) and five alcyonacean (Lamouroux 1816) corals. *J. Exp. Mar. Biol. Ecol.* 186, 259–275. [https://doi.org/10.1016/0022-0981\(94\)00164-9](https://doi.org/10.1016/0022-0981(94)00164-9).
- Rocha, R.J.M., Rodrigues, A.C.M., Campos, D., Cicero, L.H., Costa, A.P.L., Silva, D.A.M., Oliveira, M., Soares, A.M.V.M., Patrício Silva, A.L., 2020. Do microplastics affect the zoanthid *Zoanthus sociatus*? *Sci. Total Environ.* 713, 136659. <https://doi.org/10.1016/j.scitotenv.2020.136659>.
- Rotjan, R.D., Sharp, K.H., Gauthier, A.E., Yelton, R., Lopez, E.M.B., Carilli, J., Kagan, J.C., Urban-Rich, J., 2019. Patterns, dynamics and consequences of microplastic ingestion by the temperate coral, *Astrangia poculata*. *Proc. R. Soc. B Biol. Sci.* 286, 20190726. <https://doi.org/10.1098/rspb.2019.0726>.
- Saliu, F., Montano, S., Garavaglia, M.G., Lasagni, M., Seveso, D., Galli, P., 2018. Microplastic and charred microplastic in the Faafu Atoll, Maldives. *Mar. Pollut. Bull.* 136, 464–471. <https://doi.org/10.1016/j.marpolbul.2018.09.023>.
- Saliu, F., Montano, S., Leoni, B., Lasagni, M., Galli, P., 2019. Microplastics as a threat to coral reef environments: detection of phthalate esters in neuston and scleractinian corals from the Faafu Atoll, Maldives. *Mar. Pollut. Bull.* 142, 234–241. <https://doi.org/10.1016/j.marpolbul.2019.03.043>.
- Savinelli, B., Vega Fernández, T., Galasso, N.M., D'Anna, G., Pipitone, C., Prada, F., Zenone, A., Badalamenti, F., Musco, L., 2020. Microplastics impair the feeding performance of a Mediterranean habitat-forming coral. *Mar. Environ. Res.* 155, 104887. <https://doi.org/10.1016/j.marenvres.2020.104887>.
- Skirving, W.J., Heron, S.F., Marsh, B.L., Liu, G., De La Cour, J.L., Geiger, E.F., Eakin, C.M., 2019. The relentless march of mass coral bleaching: a global perspective of changing heat stress. *Coral Reefs* 38, 547–557. <https://doi.org/10.1007/s00338-019-01799-4>.
- Smith, P.K., Krohn, R.I., Hermanson, G.T., Mallia, A.K., Gartner, F.H., Provenzano, M.D., Fujimoto, E.K., Goeke, N.M., Olson, B.J., Klenk, D.C., 1985. Measurement of protein using bicinchoninic acid. *Anal. Biochem.* 150, 76–85. [https://doi.org/10.1016/0003-2697\(85\)90442-7](https://doi.org/10.1016/0003-2697(85)90442-7).
- Stafford-Smith, M.G., Ormond, R.F.G., 1992. Sediment-rejection mechanisms of 42 species of Australian scleractinian corals. *Mar. Freshw. Res.* 43, 683–705. <https://doi.org/10.1071/MF9920683>.
- Sweet, M.J., Brown, B.E., 2016. Coral responses to anthropogenic stress in the twenty-first century: an ecophysiological perspective. In: *Oceanography and Marine Biology: an Annual Review*. CRC Press, pp. 271–314. <https://doi.org/10.1201/9781315368597>.
- Syakti, A.D., Jaya, J.V., Rahman, A., Hidayati, N.V., Raza'i, T.S., Idris, F., Trenggono, M., Doumenq, P., Chou, L.M., 2019. Bleaching and necrosis of staghorn coral (*Acropora formosa*) in laboratory assays: immediate impact of LDPE microplastics. *Chemosphere* 228, 528–535. <https://doi.org/10.1016/j.chemosphere.2019.04.156>.
- Tambutté, É., Allemand, D., Bourge, I., Gattuso, J.P., Jaubert, J., 1995. An improved ⁴⁵Ca protocol for investigating physiological mechanisms in coral calcification. *Mar. Biol.* 122, 453–459. <https://doi.org/10.1007/BF00350879>.
- Tang, J., Ni, X., Zhou, Z., Wang, L., Lin, S., 2018. Acute microplastic exposure raises stress response and suppresses detoxification and immune capacities in the scleractinian coral *Pocillopora damicornis*. *Environ. Pollut.* 243, 66–74. <https://doi.org/10.1016/j.envpol.2018.08.045>.
- UNEP, 2019. *Plastics and Shallow Water Coral Reefs. Synthesis of the Science for Policy-Makers*.
- UNEP, 2016. *Marine Plastic Debris and Microplastics - Global Lessons and Research to Inspire Action and Guide Policy Change*.
- Veal, C.J., Carmi, M., Fine, M., Hoegh-Guldberg, O., 2010. Increasing the accuracy of surface area estimation using single wax dipping of coral fragments. *Coral Reefs* 29, 893–897. <https://doi.org/10.1007/s00338-010-0647-9>.
- Vijayamahantesh, Vijayalaxmi, 2019. Tinkering with targeting nucleotide signaling for control of intracellular *Leishmania* parasites. *Cytokine* 119, 129–143. <https://doi.org/10.1016/j.cyto.2019.03.005>.
- Wild, C., Naumann, M., Niggel, W., Haas, A., 2010. Carbohydrate composition of mucus released by scleractinian warm- and cold-water reef corals. *Aquat. Biol.* 10, 41–45. <https://doi.org/10.3354/ab00269>.
- Wright, S.L., Thompson, R.C., Galloway, T.S., 2013. The physical impacts of microplastics on marine organisms: a review. *Environ. Pollut.* 178, 483–492. <https://doi.org/10.1016/j.envpol.2013.02.031>.
- Yancey, P.H., Heppenstall, M., Ly, S., Andrell, R.M., Gates, R.D., Carter, V.L., Hagedorn, M., 2010. Betaines and dimethylsulfoniopropionate as major osmolytes in Cnidaria with endosymbiotic dinoflagellates. *Physiol. Biochem. Zool.* 83, 167–173. <https://doi.org/10.1086/644625>.
- Zhang, C., Chen, X., Wang, J., Tan, L., 2017. Toxic effects of microplastic on marine microalgae *Skeletonema costatum*: interactions between microplastic and algae. *Environ. Pollut.* 220, 1282–1288. <https://doi.org/10.1016/j.envpol.2016.11.005>.

ARTICLES FOR FACULTY MEMBERS

MICROPLASTICS AND MARINE ENVIRONMENT

Title/Author	Spatiotemporal characterisation of microplastics in the coastal regions of Singapore / Curren, E., & Yew Leong, S. C.
Source	<i>Helicon</i> Volume 9 Issue 1 (2023) e12961 Pages 1-14 https://doi.org/10.1016/J.HELIYON.2023.E12961 (Database: ScienceDirect)



Research article

Spatiotemporal characterisation of microplastics in the coastal regions of Singapore

Emily Curren^{*}, Sandric Chee Yew Leong*St. John's Island National Marine Laboratory, Tropical Marine Science Institute, National University of Singapore, 18 Kent Ridge Road, Singapore 119227, Singapore*

ARTICLE INFO

Keywords:
Microplastics
Distribution
Marine
Seawater

ABSTRACT

In the 21st century, plastic production continues to increase at an unprecedented rate, leading to the global issue of plastic pollution. In marine environments, a significant fraction of plastic litter are microplastics, which have a wide range of effects in marine ecosystems. Here, we examine the spatiotemporal distribution of microplastics along the Johor and Singapore Straits, at surface and at depth. Generally, more microplastics were recorded from the surface waters across both Straits. Fragments were the dominant microplastic type (70%), followed by film (25%) and fiber (5%). A total of seven colours of microplastics were identified, with clear microplastics as the most abundant (64.9%), followed by black (25.1%) and blue (5.5%). Microplastics under 500 μm in size accounted for 98.9%, followed by particles 500–1000 μm (1%) and 1–5 mm (0.1%). During the monsoon season, the abundance of microplastics across various sites were observed to be > 1.1 times when compared to the inter-monsoon period. Rainfall was a closely related to the increased microplastic abundance across various sites in the Singapore Strait. This suggests that weather variations during climate change can play critical roles in modulating microplastic availability. Beach sediments facing the Singapore Strait recorded an abundance of 13.1 particles/kg, with polypropylene fragments, polyethylene pellets and thermoplastic polyester foam identified via Fourier transform infrared spectroscopy. Hence, it is crucial to profile the spatiotemporal variation of microplastic abundance in both the surface and in the water column to gain a better understanding of the threat caused by microplastic pollution in the coastal regions of Singapore.

1. Introduction

Plastic pollution is a pertinent problem of the 21st century. This issue has gained significant attention in the recent decade among scientists and the public as plastic litter is increasingly abundant in many terrestrial and aquatic ecosystems. To date, there are an estimated 296,000 tonnes of plastic that exist in the oceans. This number is expected to increase, with hotspots of microplastics around the world with abundances of 30,000–38,000 particles/kg in marine sand sediments [1]. Approximately 11% of total ocean plastics are microplastics [2]. Microplastics are small plastic particles of less than 5 mm in length and exist in two forms—primary and secondary [3]. Primary microplastics are small plastic pieces designed for various uses, such as cosmetics, clothing and plastic production [4]. Resin pellet beads and facial microbeads are some examples of primary microplastics. Secondary microplastics originate from the

^{*} Corresponding author.

E-mail address: e0013223@u.nus.edu (E. Curren).

<https://doi.org/10.1016/j.heliyon.2023.e12961>

Received 2 August 2022; Received in revised form 7 December 2022; Accepted 10 January 2023

Available online 13 January 2023

2405-8440/© 2023 The Authors. Published by Elsevier Ltd. This is an open access article under the CC BY-NC-ND license (<http://creativecommons.org/licenses/by-nc-nd/4.0/>).

breakdown of larger plastic pieces, such as styrofoam buoys, derelict fishing gear, due to physical and biological processes over time [5]. The rate and extent of plastic degradation depends on various physical (age and type of polymer) and environmental (surrounding temperature and pH) factors [6].

Microplastics enter the marine environment through various ways. Urban sources such as agricultural [7] and stormwater runoff [8] are pathways where terrestrial microplastics enter the oceans. In addition, synthetic textiles release microfibers during washing processes and these are not fully eliminated by filtration systems in wastewater treatments plants. As a result, they are released into marine waters [9]. A study by Ref. [10] showed that an average wash load of 6 kg released approximately 700 000 acrylic fibers from domestic washing machines. Sea-based industries such as shipping and fishing also contribute to microplastic pollution [11]. Gray water (wastewater) from showers, basins and laundry of ships have recorded a high abundance of 2000–50 000 microplastics/L [12].

Due to the small size of these particles, microplastics are easily mistaken as food by marine animals. This has been clearly observed in pelagic and benthic organisms such as bivalve mollusks [13] and shrimp [14]. Although some microplastics will be egested by these organisms, many plastic particles are still retained for an extended period. Microplastic particles have been observed in organs such as gills and stomach and are found to remain in the hemolymph for as long as 48 days [15]. Larger marine animals such as the common mink and sei whales are also recorded to ingest microplastics through their prey species [16]. These whales commonly feed on fish species from the Scombridae and Gadidae families, which contain large amounts of microplastics [16].

Microplastics have a large surface area to volume ratio, which enhances their capacity to adsorb harmful pollutants in marine waters [17]. Studies have examined how microplastics can accumulate and release harmful compounds such as polybrominated diphenyl ethers and dichlorodiphenyltrichloroethane (DDT; [18,19]). Microplastics are known to be biologically inert. However, once these particles are ingested, pollutants that have been adsorbed onto their surfaces can enter the cells of organisms and disrupt their physiological processes. Ingestion of DDT-treated microspheres has resulted in poorer growth in larval fish *Menidia beryllina* [20]. Exposure of the Japanese medaka fish (*Oryzias latipes*) to microplastics and its associated chemicals have disrupted endocrine genes [21].

In marine environments, microplastics can exist for hundreds of years [22]. As a result, they form a suitable habitat for the colonization of many microorganisms, including harmful or non-native ones. A wide range of phyla have been found colonizing the surfaces of microplastics, including Annelida, Bryozoa, Cnidaria and Mollusca [23]. Pathogens such as *Vibrio parahaemolyticus* and *Vibrio vulnificus* have been identified from polyethylene (PE) fragment and fibers from the Baltic Sea [24]. [25] identified the toxic bacterium *Photobacterium rosenbergii* from beach sediment microplastics located near coral reefs. This bacterium is associated with coral bleaching and its proliferation can be detrimental to existing coral reef ecosystems [26]. The bloom-forming dinoflagellate *Pfiesteria piscicida* was also identified on microplastics from the Baltic Sea [27]. This dinoflagellate *P. piscicida* is known to be toxic and has caused major fish kills in previous blooms [28,29]. The long-range transport of these harmful organisms can be damaging to marine ecosystems. Although the numbers of these organisms may be few on these microplastics, blooms of these organisms in new locations can be triggered with suitable nutrient and environmental conditions [30].

In Southeast Asia, the problem of plastic pollution in marine environments is highly pertinent, with concentrations of microplastics ranging from 0.1 to 1.1×10^4 pieces/L [31]. However, there have only been 36 studies in this region investigating microplastic pollution across various matrices such as beach and marine sediments, seawater, and marine organisms [31]. In Singapore, studies related to marine microplastics are relatively limited, with a few reports of microplastic pollution in mangroves [32], seagrasses [33] and beach sediments [25]. The Johor Strait is known to be eutrophic and highly polluted, with high inputs of nitrogen sources, ranging from 2.04 to 6.47 $\mu\text{M-N}$ for nitrate and nitrite [34]. The Johor Strait is also characterized by many aquaculture fisheries carrying seafood from farm to table. Various beaches in the Johor and Singapore Straits were previously found to contain high levels of sand sediment microplastics (9.2–59.9 pieces/kg; [25]). Hence, it is important to elucidate the presence of microplastics in seawater as a high level of microplastics in seawater could be assimilated in seafood and be transferred to the consumer. This will in turn harm human health and threaten food security. In this study, we aimed to characterize the spatial and temporal distribution of microplastics isolated from the Johor and Singapore Straits. Surface and depth samples were obtained to examine for any differences in microplastic

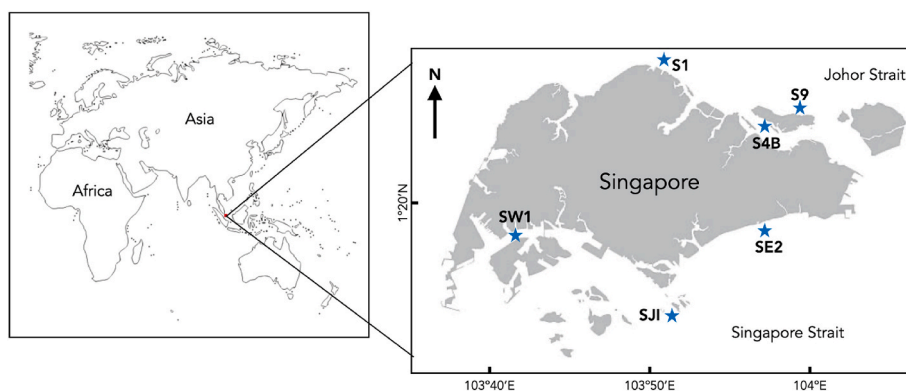


Fig. 1. Sampling area and stations for microplastics in the Johor and Singapore Straits in this study. A total of six stations were evaluated. The stars indicate the sampling points.

abundance. Environmental variables such as temperature, rainfall and wind speed were also collected to explore any association with microplastic abundance at various sampling sites.

2. Materials and methods

2.1. Sampling stations and collection

In this study, sampling was conducted within the Johor and Singapore Straits from 2021 to 2022. Monthly seawater sampling was conducted across six stations around Singapore from August 2021 to January 2022 (Fig. 1). A bucket was used to collect surface seawater samples and a Niskin bottle was used to collect seawater at 5 m depth. A single beach sediment sample was collected at Se2 in April 2022 for comparison purposes (Fig. 1). Singapore is a tropical island nation (728 km²) located in Southeast Asia. The country is characterized by a wet equatorial climate with relatively high rainfall (~2200 mm) and annual average temperatures around 27.5 °C. The Johor Strait is a 50 km-long narrow international strait that separates Singapore and Peninsular Malaysia. This strait connects to the Singapore Strait on the southeast and to the Straits of Malacca on the western side. Sampling stations S1, S9 and S4B were facing the Johor Strait. The Singapore Strait is a channel that lies between Singapore and Riau Islands, Indonesia. This Strait is also an international commercial shipping route. The remaining sampling stations, SW1, SJI and Se2 were located on the Singapore Strait. Sampling of microplastics were conducted in the Johor due to the high abundance of microplastics observed in beach sediments of these areas [25]. Furthermore, the Johor Strait is characterized by multiple aquaculture farms which increases the level of anthropogenicity in the region. Commercial shipping routes are known to be hotspots of microplastic pollution, with container ships being great microplastic contributors [35] and hence the Singapore Strait was chosen for sampling purposes. The western part of the country was not sampled due to restricted access. Surface seawater samples were collected using a large bucket and sealed in 500 mL collection bottles for further analysis. At 5 m depth, seawater samples were obtained using Niskin bottles. A 100 m stretch of beach was chosen for sand sediment collection at site Se2 to provide a basis of comparison against seawater microplastic samples. Sampling was done on the high-strand line, at the zone of vegetation, 3 m from the shoreline. Beach samples were collected according to the protocol of Curren et al. (2018). For sand sediment samples, collected microplastics were resuspended in a sterile filtered 1.2 g/cm³ sodium chloride solution to separate microplastics from the sand particles. Sterile stainless-steel tweezers were used to obtain microplastic samples for microscopy.

Microplastics from seawater samples were analysed by pipetting 1 mL of seawater onto a Sedgewick rafter slide and viewed under the inverted microscope (Nikon, Ti-S). Microplastics were separated from organic matter using the hot-needle test according to the protocol by Ref. [36]. Microplastic abundances were determined from triplicate counts. A blank control was conducted before analysing each seawater sample to ensure that no microplastics were present before examination. All microplastics were characterized and recorded according to size (<500 µm, 500–1000 µm and 1–5 mm), colour and type (fiber, foam, pellet, fragment or film).

2.2. Quality control

In this study, glass and metal labware were used wherever possible. All labware (forceps, glass bottles, petri dishes, metal sieve) were sterilized and pre-rinsed with milliQ water twice. During analysis, all containers were covered with aluminum foil or glass lids to prevent microplastic contamination from the air. Microplastic particles identified for spectroscopy were individually rinsed with milliQ water and dried at room temperature before analysis. Contamination protocols follow that of Curren et al. (2018).

2.3. Collection of meteorological variables

Meteorological variables such as average temperature, rainfall and wind speed for water samples were obtained from the Meteorological Service Singapore (MSS) (<http://www.weather.gov.sg/home/>) from various weather stations around Singapore.

2.4. Fourier Transform Infrared spectrometer (FTIR)

Beach sediment microplastics were analysed using an Alpha II Fourier Transform Infrared spectrometer (FTIR) equipped with a diamond ATR crystal (Bruker, Germany). Individual microplastic samples were transferred to the diamond using sterilized forceps. IR spectral data were collected across a wavelength of 4000 cm⁻¹ to 450 cm⁻¹ with an interval of 1 cm⁻¹, with reference to Bruker's material database.

2.5. Data analysis

The differences in microplastic abundances across sampling stations were tested using one-way analysis of variance (ANOVA) and Tukey's Honestly Significant Difference (HSD) *post hoc* pairwise comparisons. For all statistical tests, a significance level of 0.05 was chosen. The 'multcomp' package in R studio (version 4.1.3) was used to run various statistical analyses. Principal component analysis (PCA) was used to analyse the clustering between various sampling sites and environmental variables in R. Reported results were given as means ± SD and corrected to three significant figures wherever required.

3. Results

Microplastics were detected in both surface and seawater samples at 5 m depth across all sampling stations in both the Johor and Singapore Straits. The concentration of microplastics ranged from 106 to 238 particles/mL in the Johor Strait and 143–196 particles/mL in the Singapore Strait (Table 1). During the monsoon season, many sites recorded an increase in microplastic abundance across the Johor and Singapore Straits. Sites S1, S9, SW1 and SE2 had 1.1–1.7 times more microplastics during the monsoon season compared to the inter-monsoon period. Site SE2 had the greatest increase observed (1.7 \times) during the monsoon season. In December, the microplastic abundance at site S9 was almost three times that of the average abundance in the Johor Strait across the sampling months. Similarly, sites SW1 and SE2 had 1.3 and 1.8 times more microplastics than the average abundance in the Singapore Strait across the sampling months.

Overall, microplastic fragments, film and fibers were observed (Fig. 2). Fragments accounted for the majority of the microplastics, at 70%, followed by film and fiber at 25% and 5%, respectively (Fig. 2). Fragments were the most dominant at each sampling location, with site SJI recording the most fragments of 100% at depth (Fig. 3). However, at surface, site SJI had film pieces being the most dominant at 34% (Fig. 3). The three types of microplastics—fragments, film and fibers were detected at all sites, except for site SJI, where only fragments were detected at depth (Fig. 3). Microplastic types were significantly different within each site across both the Johor and Singapore Straits (Table 2; $p < 0.05$). Across all the sites, there were significant differences in the microplastic abundances for fragments and fibers (Table 3; $p < 0.05$). At sites S4B and SW1, microplastic abundances were significantly different between the three comparison categories (film vs fragment, film vs fiber and fragment vs fiber; Table 3; $p < 0.05$).

Generally, the abundance of microplastics were greater at the surface in the Johor Straits (sites S1 and S9), compared to the Singapore Strait (sites SJI, SW1 and SE2), where the abundance of microplastics was greater at depth (Table 1). Across the sites at both surface and depth, the abundance of microplastics were not significantly different (ANOVA, Tukey's HSD, $p > 0.05$). Between surface and depth samples, there were significant differences observed between microplastic film collected across sites (Table 4; ANOVA, $p = 4.75 \times 10^{-2}$ and 1.55×10^{-2} , respectively). The abundance of film collected at the surface waters of site SJI and SE2 were significantly different (Tukey's HSD, $Q = 4.51$, $p = 3.78 \times 10^{-2}$). At depth, the abundance of film microplastics were significantly different across site S1 and SJI (Tukey's HSD, $Q = 5.53$, $p = 6.68 \times 10^{-3}$).

Besides accounting for microplastic type, the colour of plastic particles were also recorded. Across the various microplastics, a total of seven colours were observed from all sites (Fig. 4). From all microplastic types, clear microplastics were the most abundant (64.9%), followed by black (25.1%), blue (5.5%), purple (2.3%), pink (1.7%), red (0.5%) and brown (0.04%). For fragments, black was the dominant fragment colour (75%) and 12% were transparent (Fig. 4A). Other colours, purple (7%), blue (5%) and red (1%) were recorded (Fig. 4A). For microplastic film, 89% were transparent, 9% were blue and 2% were red (Fig. 4B). The majority of microplastic fibers were transparent (94%), 3% red and 3% were blue (Fig. 4C).

Microplastics in this study were categorised into three size fractions—smaller than 500 μm , 500–1000 μm and 1–5 mm (Fig. 5). Across the stations, microplastics smaller than 500 μm were the most abundant, at 98.9%, followed by pieces of size 500–1000 μm and 1–5 mm at 1% and 0.1% respectively (Fig. 5). Microplastics of size 1–5 mm were only observed from the surface waters of S1 (Fig. 5). In this study, 42% of sites only recorded microplastics smaller than 500 μm in size. Across all sites, the size of microplastics were significantly different (ANOVA, $p < 0.0001$). The abundance of microplastics were significantly different across pairs <500 μm and 500–1000 μm and <500 μm and 1–5 mm (Tukey's HSD, $Q = 321$ and 324 , respectively $p < 0.0001$).

Patterns of microplastic composition across sites against environmental variables such as rainfall, temperature, salinity and windspeed were visualized through a PCA plot (Fig. 6). The first two axes amount to 49.4% of the variation between the stations (Fig. 6). Rainfall was closely associated with surface and depth samples of sites SJI and SE2 during the month of November (Fig. 6).

A single beach sediment sample was obtained at site SE2, where the microplastic abundance recorded was a total of 13.1 particles/kg. Microplastic fragments, foam, pellets, film and fibers were observed with the abundance of 3.27, 4.58, 3.27, 0.654 and 1.31 particles/kg of sand, respectively. Fragment microplastics were identified to be polypropylene (PP; Fig. 7). Microplastic foam pieces were identified to be thermoplastic copolyester (TPC; Fig. 7) and pellets were identified to be polyethylene (PE; Fig. 7). Fragments were observed to be green (40%), white (40%) and blue (20%). Foam microplastics were white (85.7%) and pink (14.3%). The remaining pellet, film, and fiber microplastic particles were all white in colour. On the same day, the surface waters of SE2 were sampled and were

Table 1
Microplastic abundance and type at surface and depth seawater of various locations of the Johor and Singapore Straits.

	S1		S9		S4B		SJI		SW1		SE2	
	S	D	S	D	S	D	S	D	S	D	S	D
Film/mL	21.2 \pm 28.2	32.2 \pm 33.5	28.8 \pm 25.1	17.9 \pm 14.4	24.1 \pm 5.85	19.6 \pm 14.6	50.7 \pm 16.7	0	34.1 \pm 19.3	19.1 \pm 11.6	15.2 \pm 11.5	96.7 \pm 14.4
Fragment/mL	66.2 \pm 79.8	58.6 \pm 24.6	83.8 \pm 47.0	97.8 \pm 48.7	46.3 \pm 22.7	49.8 \pm 36.2	44.4 \pm 19.2	62.5 \pm 28.5	41.2 \pm 24.7	43.6 \pm 30.8	86.0 \pm 58.4	76.7 \pm 18.7
Fiber/mL	8.15 \pm 7.66	12.4 \pm 19.1	5.97 \pm 7.83	4.03 \pm 4.90	0.925 \pm 2.27	0.556 \pm 1.36	5.66 \pm 9.62	0	0.833 \pm 1.67	3.74 \pm 4.36	6.11 \pm 6.50	2.15 \pm 4.81
Total across types/mL	95.5	10.3	119	120	71.4	70.0	101	62.5	76.2	66.5	107	88.5
Total per site/mL	106		238		141		163		143		196	

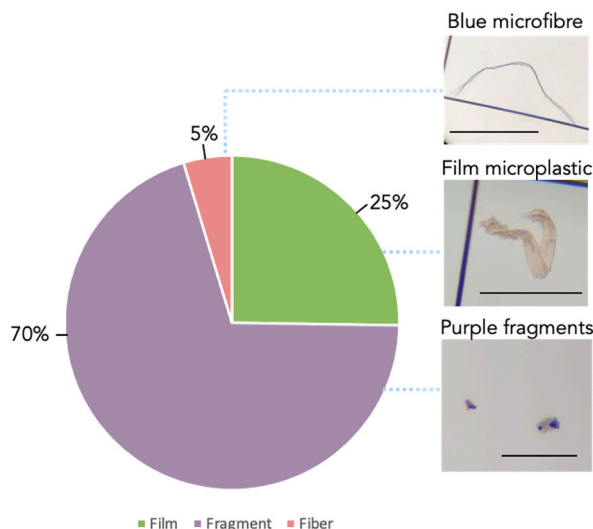


Fig. 2. Composition of microplastic types found in this study. Three types of microplastics were observed: film, fragment and fiber. Examples of blue microfibers, film microplastics and purple microplastic fragments were shown on the right of the pie chart. The scale bars on each picture indicate 5 µm.

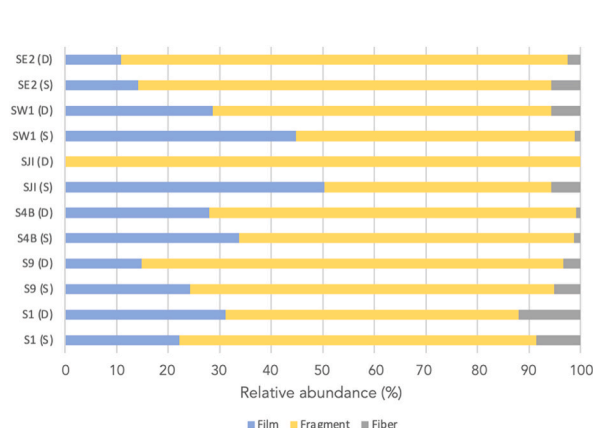


Fig. 3. Composition of each microplastic type recorded from surface and depth samples of sampling sites. The colours in the chart correspond to the legend above.

Table 2

One-way ANOVA test results showing the differences in composition of microplastic types within each sampling site.

	SS	df	MS	F statistic	P-value
S1	17.1	2	8.53	5.96	0.00615*
S9	49	2	24.5	28.3	<0.0001*
S4B	13.8	2	6.74	21.2	<0.0001*
SJI	5.92	2	2.96	7.56	0.00537*
SW1	6.53	2	3.27	10.2	0.000815*
SE2	35.9	2	18.0	28.5	<0.0001*

The * indicates significant differences ($p < 0.01$).

recorded to have 206 microplastic particles/mL, consisting of fragments (84%), film (8%) and fiber (8%). Majority of the microplastic fragments were black (74.2%) and the remaining transparent (12.9%), pink (6.45%) and blue (6.45%). Fibers observed were blue (66.7%) and transparent (33.3%). At depth, microplastic abundance was observed to be 22.2 particles/mL and consisted of fragments (50%) and film (50%). At this site, all the fragment and film microplastics collected were recorded to be black and pink, respectively.

Table 3
Output of Tukey's HSD *Post hoc* test on the composition of microplastic types found within each site.

	S1		S9		S4B		SJI		SW1		SE2	
	Q-statistic	P-value	Q-statistic	P-value	Q-statistic	P-value	Q-statistic	P-value	Q-statistic	P-value	Q-statistic	P-value
Film vs. fragment	3.27	0.0680	7.95	0.0001*	5.08	0.00294*	2.75	0.161	2.49	0.206*	8.68	<0.0001*
Film vs fiber	1.51	0.542	2.16	0.292	4.11	0.0175*	2.75	0.161	3.84	0.0334*	1.05	0.742
Fragment vs fiber	4.78	0.00522*	10.11	<0.0001*	9.19	<0.0001*	5.50	0.00391*	6.33	0.00058*	9.73	<0.0001*

The * indicates significant differences ($p < 0.01$).

Table 4
One-way ANOVA test results showing the differences in composition of microplastic types between surface and depth samples.

Surface	SS	df	MS	F statistic	P-value
Film	4.04	5	0.808	2.61	0.0475*
Fragment	9.56	5	1.91	0.880	0.508
Fiber	0.184	5	36.8	1.22	0.325
Depth					
Film	5.05	5	1.01	3.45	0.0155*
Fragment	10.6	5	2.13	2.05	0.102
Fiber	0.533	5	107	1.37	0.267

The * indicates significant differences ($p < 0.01$).

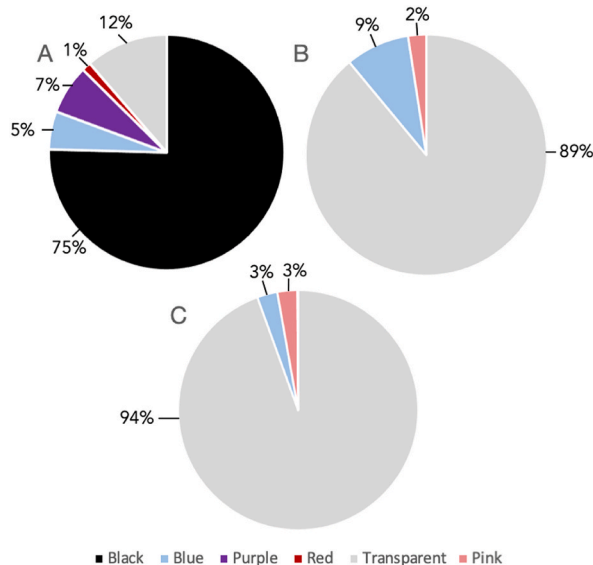


Fig. 4. Colour composition of microplastic fragments, fiber and film across sites. A total of seven colours were observed. (A) Colour composition of microplastic fragments. (B) Colour composition of microplastic fiber. (C) Colour composition of microplastic film. The colours in the chart correspond to the legend above.

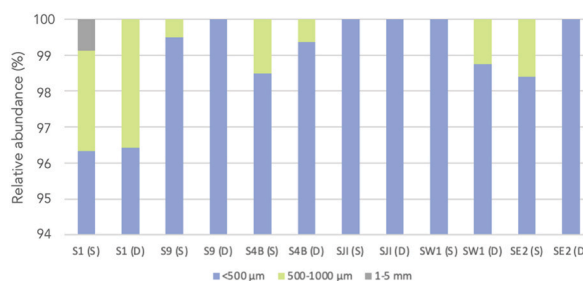


Fig. 5. Size distribution of microplastics across sampling locations. The colours in the chart correspond to the legend above.

4. Discussion

In this study, it is evident that microplastic pollution is present in the coastal waters of Singapore. The microplastic concentration in the Johor and Singapore Straits is comparable to that of the Northeastern Pacific Ocean (Table 5 [17,19,37–39], [37]; and is higher than that of the Northeastern Atlantic Ocean (Table 5; Lusher et al., 2014) and the coastal waters of Tarragona, Spain [39]; Table 5). Microplastic abundances across both straits were lower than that in the neighbouring region of the Terengganu estuary, Malaysia (Table 5; [38]. From the Johor Strait, site S9 recorded the highest microplastic abundance from surface and depth samples (Table 1). This site is the closest to the mouth of the Johor River, which is highly polluted due to agricultural activities [40] and waste from plastic and rubber industries [41]. It is generally observed that more polluted waters result in higher microplastic abundances in various locations [42,43]. For beach sediments, it was also observed that sites in the Johor Strait recorded a higher microplastic abundance

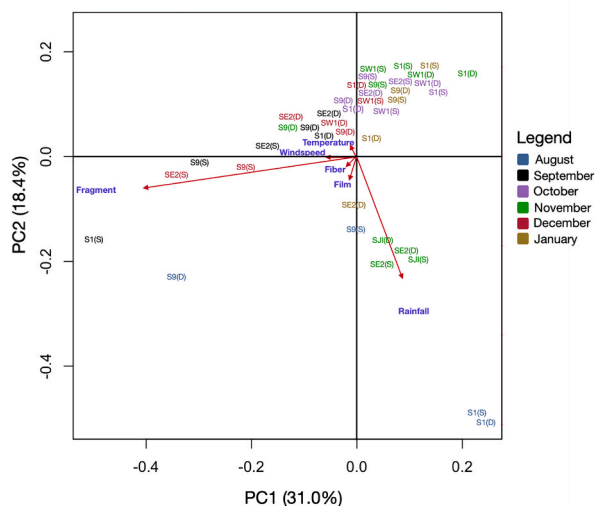


Fig. 6. Principal component analysis displaying the variation in microplastic composition across the sites in relation to environmental variables: temperature, salinity, rainfall and windspeed. The (S) and (D) in site labels correspond to surface and depth, respectively. Colours in the chart refer to the months of sampling according to the legend on the right.

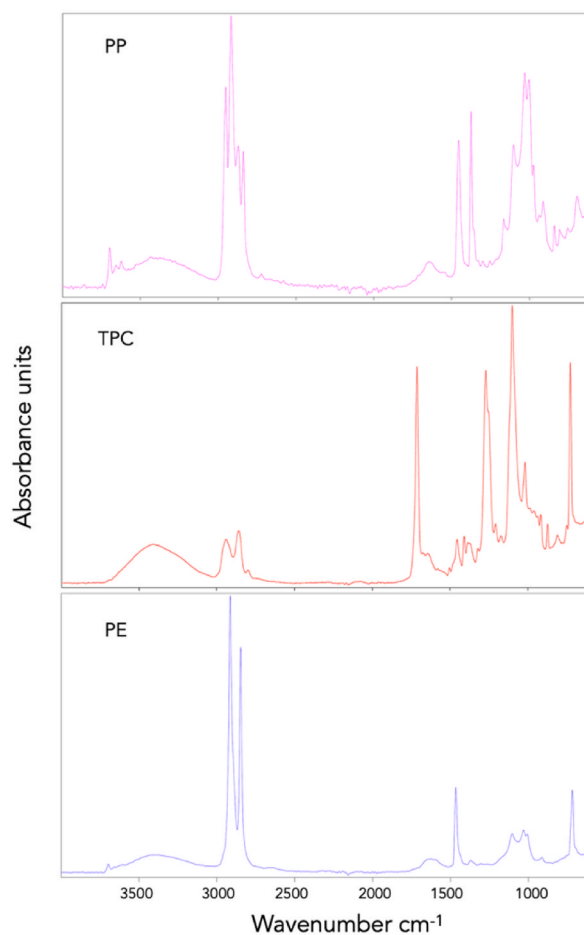


Fig. 7. FTIR spectra of different microplastic polymer types isolated from beach sediments.

Table 5
Comparison of seawater microplastic abundance across various regions around the world.

Region	Microplastic abundance (particles/L)	Reference
Hangzhou Bay, China	1.4×10^{-3}	[19]
Northeastern Atlantic Ocean	2.4×10^3	Lusher et al. (2014)
Northeastern Pacific Ocean	27.9×10^4	[37]
Arrábida, Portugal	450	[17]
Terengganu estuary, Malaysia	5.46×10^5	[38]
Tarragona, Spain	1.3×10^3	[39]
Johor Strait	$14.3\text{--}19.6 \times 10^4$	This study
Singapore Strait	$10.6\text{--}23.8 \times 10^4$	

(31.1–59.9 particles/kg of sand sediment) compared to sites in the Singapore Strait (9.2 particles/kg of sand sediment; [25]). From surface waters, the Johor Strait had a higher average concentration of microplastics compared to the Singapore Strait. This could also be due to the lower flow of water in the Johor Strait, because of the causeway which separates Singapore and Johor Bahru, Malaysia [44]. A lower water flow would mean a greater accumulation of microplastics, resulting in a higher abundance observed in the Johor Strait. Across the sites, the average microplastic concentrations were about 1.4 times greater at surface waters (95 pieces/mL) compared to at depth (69.6 pieces/mL). This concurs with other reports which showed a decrease in microplastic abundance with depth of sampling [45,46]. Many studies have investigated the presence of microplastics from surface seawater [47,48] or sediments [49]. However, there are few reports on the vertical distribution of microplastics along the water column. This distribution can be altered by various physical and environmental factors such as particle size, density and water flow [50,51].

Microplastic distribution along the water column is known to be inhomogeneous [52]. Hence in this study, the concentration of microplastics were measured in milliliters instead of liters, to prevent overestimation of the results. In this study, surface, and water at depth of 5 m were examined and provided evidence about the variation in microplastics at two different depths. However, more layers along the water column could be sampled to provide a greater resolution of microplastic distribution in the water column. This is especially so for microplastics of smaller sizes (10 μm), which were found to be more abundant in the water column and more easily transported vertically, due to the pycnocline [53]. The improved depth profiling will allow better understanding of vertical migration of microplastics, regarding upwelling events [37]. In this study, the sediment concentration of microplastics were not examined in both Straits. The understanding of sediment microplastic concentration will provide a better understanding of the vertical gradient, from surface to water column and sediment [52].

Across the sites, microplastic film, fragments and fibers were identified, with fragments being the dominant microplastic type. This is similar to other works conducted in the Baltic Sea [54], the Mediterranean [55] and Korea [56], which had microplastic fragments as the major fraction. Overall, black was the main colour identified for microplastic fragments in this study. Along the Johor Strait, many aquaculture farms were observed to use black plastic drums and carboys as floatation devices. Over time, exposure to high temperatures and light intensities can result in physical degradation of these large items, releasing microplastic particles into the marine environment. In addition, given that Singapore is a busy shipping port, it is likely that many of these black fragments are paint particles from ships and boats [57]. The weathering of the ships' hulls and flaking of anti-fouling coatings are known to be significant sources of marine microplastic fragments [58].

At site SE2, beach sediment and seawater samples were taken on the same day to examine the differences in microplastic abundances and types. As both measurement units were different (particles/kg and particles/mL), their abundances cannot be directly compared. However, the microplastic composition for beach and seawater samples were different. TPC foam microplastics were the dominant microplastic type present and is commonly used in tubing and insulation [59]. Fragments were still the dominant microplastic type from seawater. White polyester pellets present on the beach could have been part of the plastic pre-production process and originate from spillages from container ships carrying these items. As site SE2 is a popular recreation beach, brightly coloured propylene fragments from beach sediments could have come from the degradation of larger items such as toys and plastic bottles.

Studies in other locations have reported rainfall to be a significant environmental contributor to microplastic pollution [60,61]. Greater rainfall has resulted in a larger surface runoff from terrestrial sources, which ultimately enter marine environments. Furthermore, microplastics floating in the atmosphere can adhere to raindrops and be transferred to marine waters during periods of heavy rain [62]. Besides rainfall, other environmental variables such as temperature have also been studied to determine its impact on microplastic pollution. The formation of specific bacterial assemblages on microplastics in the Baltic Sea have been shaped by temperature [63]. Furthermore, temperature changes have also increased the toxicity of microplastics to *Daphnia magna* and *Daphnia pulex* [64].

Biofilms naturally develop on the surfaces of microplastics after long periods of time in the marine environment. This 'conditioning film' further enables the attachment of larger organisms such as mussels, algae and barnacles [65]. As a result, their densities increase, exceeding that of the surrounding seawater and they descend the water column [66]. The seafloor is thought to be the ultimate sink for most microplastics in oceans [67]. Many of these particles settle in marine sediments and become more available to benthic organisms such as jellyfish [68], starfish and bivalves [66]. Furthermore, benthic organisms such as shrimp and mussels are popular seafood consumed by man and are reported to contain microplastics across various studies [69,70]. In the Singapore Straits, pathogenic bacteria have been found colonizing the surfaces of microplastics [25]. The genus *Photobacterium rosenbergii* was identified and this species can cause coral bleaching [26]. As the Singapore Strait is characterized by many coral reefs in marine parks, proliferation of this species on microplastics can hamper conservation efforts.

In recent years, the presence of microplastic contaminants in seafood has been heavily discussed as a route of exposure to humans [71]. This is especially so if the organism is consumed whole, without removing the digestive organs. Previous studies have detailed the egestion of some microplastics from marine organisms during depuration [72]. However, selective accumulation of microplastics still exists and is dependent on many factors such as the microplastic type and feeding characteristic of the organism [73]. Contaminated seafood adds to the existing ways which microplastics can enter the human body. To date, microplastics have been found in bottled [74] and tap water [75], tea bags [76] and even air [62]. It is for a fact that microplastics enter and are present in the human body, as these particles have been found in human placenta [77], lung [78] and stool samples [79]. However, the long-term effects of these contaminants on the human body are yet to be fully understood.

Microplastics not only threaten human health and food security, but has other effects on coastal water quality, potentially reducing the aesthetic value of recreational areas. The socio-economic impact of microplastic pollution has been studied in various locations [80,81]. Given the multi-faceted implications of microplastic pollution, a greater call is needed to manage this issue on an individual and regional scale.

5. Conclusion

In this study, the spatiotemporal variation of marine microplastics from the Johor and Singapore Straits were examined at surface and at depth. The Johor Strait had a higher abundance of microplastics compared to the Singapore Strait. This is likely due to the Johor Strait being more polluted and having a lower water flow. There were no significant differences observed in average microplastic abundances across surface and depth seawater samples. However, it is still critical to elucidate the vertical distribution of microplastics as only sampling the surface waters could result in an over- or underestimation of true microplastic quantities. From seawater samples, microplastic fragments, fibers and film particles were observed, with black microplastic fragments being the most dominant. From the beach sediment, TPC foam, PP fragments and PE pellets were recorded. Rainfall was closely associated with increased microplastic abundances across some sites during the Northeast monsoon season. This suggests that weather variations during climate change can play critical roles in modulating the microplastic availability in marine environments and should continue to be explored in future studies. Efforts to combat plastic pollution should continue, starting from individuals to national policies, to reduce plastic waste and hence microplastic pollution as a whole.

Author contribution statement

Emily Curren: Wrote the paper, analysed and interpreted the data.

Sandric Chee Yew Leong: Supervised data analysis and interpretation of data. Contributed data analysis tools.

Funding statement

This research did not receive any specific grant from funding agencies in the public, commercial, or not-for-profit sectors.

Data availability statement

Data is all included or referenced in the article.

Declaration of interest's statement

The authors declare that they have no known competing financial interests or personal relationships that could have appeared to influence the work reported in this paper.

Acknowledgements

This work was partially supported by funds awarded to Dr. Sandric Leong through the National University of Singapore and was made possible because of the support from members of Team HABS, St. John Island National Marine Laboratory. We would like to thank Bruker, Singapore for the FTIR analysis conducted in this study.

References

- [1] G. Kibria, D. Nugegoda, A.K. Haroon, Microplastic (MP) pollution in the context of occurrence, distribution, composition and concentration in surface waters and sediments: a global overview, *Microplast. Pollut.* (2022) 133–166.
- [2] W. Lau, M. Murphy, Microplastics are a big- and growing- part of global pollution, in: *Preventing Ocean Plastics*, 2021. <https://www.pewtrusts.org/en/research-and-analysis/articles/2021/03/30/microplastics-are-a-big-and-growing-part-of-global-pollution>. (Accessed 13 October 2022). accessed.
- [3] A.L. Andrady, The plastic in microplastics: a review, *Mar. Pollut. Bull.* 119 (1) (2017) 12–22.
- [4] J. Boucher, D. Friot, *Primary Microplastics in the Oceans: a Global Evaluation of Sources*, vol. 43, Iucn, Gland, Switzerland, 2017.
- [5] W.R. Waldman, M.C. Rillig, Microplastic Research Should Embrace the Complexity of Secondary Particles, 2020.
- [6] İ.K. Akbay, T. Ozdemir, Monomer migration and degradation of polycarbonate via UV-C irradiation within aquatic and atmospheric environments, *J. Macromol. Sci., Part A* 53 (6) (2016) 340–345.
- [7] L. Nizzetto, M. Futter, S. Langaas, Are Agricultural Soils Dumps for Microplastics of Urban Origin?, 2016.

- [8] J. Grbić, P. Helm, S. Athey, C.M. Rochman, Microplastics entering northwestern Lake Ontario are diverse and linked to urban sources, *Water Res.* 174 (2020), 115623.
- [9] R. Qiu, Y. Song, X. Zhang, B. Xie, D. He, Microplastics in urban environments: sources, pathways, and distribution, *Microplast. Terrest. Environ.* (2020) 41–61.
- [10] I.E. Napper, R.C. Thompson, Release of synthetic microplastic plastic fibres from domestic washing machines: effects of fabric type and washing conditions, *Mar. Pollut. Bull.* 112 (1–2) (2016) 39–45.
- [11] H. Yang, G. Chen, J. Wang, Microplastics in the marine environment: sources, fates, impacts and microbial degradation, *Toxics* 9 (2) (2021) 41.
- [12] O. Mikkola, Estimating Microplastic Concentrations and Loads in Cruise Ship Grey Waters, 2020.
- [13] L. Van Cauwenberghe, M. Claessens, M.B. Vandegehuchte, C.R. Janssen, Microplastics are taken up by mussels (*Mytilus edulis*) and lugworms (*Arenicola marina*) living in natural habitats, *Environ. Pollut.* 199 (2015) 10–17.
- [14] E. Curren, C.P. Leaw, P.T. Lim, S.C.Y. Leong, Evidence of marine microplastics in commercially harvested seafood, *Front. Bioeng. Biotechnol.* 8 (2020), 562760.
- [15] M.A. Browne, A. Dissanayake, T.S. Galloway, D.M. Lowe, R.C. Thompson, Ingested microscopic plastic translocates to the circulatory system of the mussel, *Mytilus edulis* (L.), *Environ. Sci. Tech.* 42 (13) (2008) 5026–5031.
- [16] P. Burkhardt-Holm, A. N'Guyen, Ingestion of microplastics by fish and other prey organisms of cetaceans, exemplified for two large baleen whale species, *Mar. Pollut. Bull.* 144 (2019) 224–234.
- [17] D. Rodrigues, J. Antunes, V. Otero, P. Sobral, M.H. Costa, Distribution patterns of microplastics in seawater surface at a Portuguese estuary and marine park, *Front. Environ. Sci.* 8 (2020) 254.
- [18] W. Zhang, X. Ma, Z. Zhang, Y. Wang, J. Wang, J. Wang, D. Ma, Persistent organic pollutants carried on plastic resin pellets from two beaches in China, *Mar. Pollut. Bull.* 99 (1–2) (2015) 28–34.
- [19] F. Wang, M. Zhang, W. Sha, Y. Wang, H. Hao, Y. Dou, Y. Li, Sorption behavior and mechanisms of organic contaminants to nano and microplastics, *Molecules* 25 (8) (2020) 1827.
- [20] S.N. Athey, S.D. Albotra, C.A. Gordon, B. Montealeone, P. Seaton, A.L. Andrady, A.R. Taylor, S.M. Brander, Trophic transfer of microplastics in an estuarine food chain and the effects of a sorbed legacy pollutant, *Limnology and Oceanography Letters* 5 (1) (2020) 154–162.
- [21] C.M. Rochman, T. Kurobe, I. Flores, S.J. Teh, Early warning signs of endocrine disruption in adult fish from the ingestion of polyethylene with and without sorbed chemical pollutants from the marine environment, *Sci. Total Environ.* 493 (2014) 656–661.
- [22] W.M. Wu, J. Yang, C.S. Criddle, Microplastics pollution and reduction strategies, *Front. Environ. Sci. Eng.* 11 (1) (2017) 1–4.
- [23] S. Oberbeckmann, M.G. Löder, M. Labrenz, Marine microplastic-associated biofilms—a review, *Environ. Chem.* 12 (5) (2015) 551–562.
- [24] I.V. Kirstein, S. Kirmizi, A. Wichels, A. Garin-Fernandez, R. Erler, M. Löder, G. Gerdt, Dangerous hitchhikers? Evidence for potentially pathogenic *Vibrio* spp. on microplastic particles, *Mar. Environ. Res.* 120 (2016) 1–8.
- [25] E. Curren, S.C.Y. Leong, Profiles of bacterial assemblages from microplastics of tropical coastal environments, *Sci. Total Environ.* 655 (2019) 313–320.
- [26] F.L. Thompson, C.C. Thompson, S. Naser, B. Hoste, K. Vandemeulebroecke, C. Munn, D. Bourne, J. Swings, *Photobacterium rosenbergii* sp. nov. and *Enterovibrio coralli* sp. nov., vibrios associated with coral bleaching, *Int. J. Syst. Evol. Microbiol.* 55 (2) (2005) 913–917.
- [27] M.T. Kettner, Microbial Colonization of Microplastic Particles in Aquatic Systems, Doctoral dissertation, Universität Potsdam, 2018.
- [28] P.D. Moeller, K.R. Beauchesne, K.M. Huncik, W.C. Davis, S.J. Christopher, P. Riggs-Gelasco, A.K. Gelasco, Metal complexes and free radical toxins produced by *Pfiesteria piscicida*, *Environ. Sci. Tech.* 41 (4) (2007) 1166–1172.
- [29] H.B. Glasgow, J.M. Burkholder, M.A. Mallin, N.J. Deamer-Melia, R.E. Reed, Field ecology of toxic *Pfiesteria* complex species and a conservative analysis of their role in estuarine fish kills, *Environ. Health Perspect.* 109 (suppl 5) (2001) 715–730.
- [30] M. Pal, P.J. Yesankar, A. Dwivedi, A. Qureshi, Biotic control of harmful algal blooms (HABs): a brief review, *J. Environ. Manag.* 268 (2020), 110687.
- [31] E. Curren, V.S. Kuwahara, T. Yoshida, S.C.Y. Leong, Marine microplastics in the ASEAN region: a review of the current state of knowledge, *Environ. Pollut.* 288 (2021), 117776.
- [32] N.H.M. Nor, J.P. Obbard, Microplastics in Singapore's coastal mangrove ecosystems, *Mar. Pollut. Bull.* 79 (1–2) (2014) 278–283.
- [33] N. Seng, S. Lai, J. Fong, M.F. Saleh, C. Cheng, Z.Y. Cheok, P.A. Todd, Early evidence of microplastics on seagrass and macroalgae, *Mar. Freshw. Res.* 71 (8) (2020) 922–928.
- [34] J.W.K. Kok, S.C.Y. Leong, Nutrient conditions and the occurrence of a *Karenia mikimotoi* (kareniaecae) bloom within east johor straits, Singapore, *Regional Stud. Marine Sci.* 27 (2019), 100514.
- [35] G. Peng, B. Xu, D. Li, Gray water from ships: a significant sea-based source of microplastics? *Environ. Sci. Technol.* 56 (1) (2021) 4–7.
- [36] J.C. Prata, J.P. da Costa, A.V. Girão, I. Lopes, A.C. Duarte, T. Rocha-Santos, Identifying a quick and efficient method of removing organic matter without damaging microplastic samples, *Sci. Total Environ.* 686 (2019) 131–139.
- [37] J.P.W. Desforges, M. Galbraith, N. Dangerfield, P.S. Ross, Widespread distribution of microplastics in subsurface seawater in the NE Pacific Ocean, *Mar. Pollut. Bull.* 79 (1–2) (2014) 94–99.
- [38] Z.D. Taha, R.M. Amin, S.T. Anuar, A.A.A. Nasser, E.S. Sohaimi, Microplastics in seawater and zooplankton: a case study from Terengganu estuary and offshore waters, Malaysia, *Sci. Total Environ.* 786 (2021), 147466.
- [39] N. Expósito, J. Rovira, J. Sierra, J. Folch, M. Schuhmacher, Microplastics levels, size, morphology and composition in marine water, sediments and sand beaches. Case study of Tarragona coast (western Mediterranean), *Sci. Total Environ.* 786 (2021), 147453.
- [40] H. Hamza, Water Quality Trend at the Upper Part of Johor River in Relation to Rainfall and Runoff Pattern, Doctoral dissertation, Universiti Teknologi Malaysia, 2009.
- [41] H.Y. Pak, C.J. Chuah, E.L. Yong, S.A. Snyder, Effects of land use configuration, seasonality and point source on water quality in a tropical watershed: a case study of the Johor River Basin, *Sci. Total Environ.* 780 (2021), 146661.
- [42] V.E. Alves, G.M. Figueiredo, Microplastic in the sediments of a highly eutrophic tropical estuary, *Mar. Pollut. Bull.* 146 (2019) 326–335.
- [43] H.Y. Yuan, L. Hou, Q.B. Liang, J.C. Li, J. Ren, Correlation between microplastics pollution and eutrophication in the near shore waters of dianchi lake, *Huan Jing ke Xue* = *Huanjing Kexue* 42 (7) (2021) 3166–3175.
- [44] S.C.Y. Leong, L.P. Lim, S.M. Chew, J.W.K. Kok, S.L.M. Teo, Three new records of dinoflagellates in Singapore's coastal waters, with observations on environmental conditions associated with microalgal growth in the Johor Straits, *Raffles Bull. Zool.* 31 (2015) 24–36.
- [45] J. Reisser, B. Slat, K. Noble, K. Du Plessis, M. Epp, M. Proietti, J. de Sonneville, T. Becker, C. Pattiaratchi, The vertical distribution of buoyant plastics at sea: an observational study in the North Atlantic Gyre, *Biogeosciences* 12 (4) (2015) 1249–1256.
- [46] Y.K. Song, S.H. Hong, S. Eo, M. Jang, G.M. Han, A. Isobe, W.J. Shim, Horizontal and vertical distribution of microplastics in Korean coastal waters, *Environ. Sci. Tech.* 52 (21) (2018) 12188–12197.
- [47] M. Russell, L. Webster, Microplastics in sea surface waters around Scotland, *Mar. Pollut. Bull.* 166 (2021), 112210.
- [48] J. Bikker, J. Lawson, S. Wilson, C.M. Rochman, Microplastics and other anthropogenic particles in the surface waters of the Chesapeake Bay, *Mar. Pollut. Bull.* 156 (2020), 111257.
- [49] N.N. Phuong, V. Fauvelle, C. Grenz, M. Ourgaud, N. Schmidt, E. Strady, R. Sempéré, Highlights from a review of microplastics in marine sediments, *Sci. Total Environ.* 777 (2021), 146225.
- [50] M. Cole, P.K. Lindeque, E. Fileman, J. Clark, C. Lewis, C. Halsband, T.S. Galloway, Microplastics alter the properties and sinking rates of zooplankton faecal pellets, *Environ. Sci. Tech.* 50 (6) (2016) 3239–3246.
- [51] N. Kowalski, A.M. Reichardt, J.J. Waniek, Sinking rates of microplastics and potential implications of their alteration by physical, biological, and chemical factors, *Mar. Pollut. Bull.* 109 (1) (2016) 310–319.
- [52] P.L. Lenaker, A.K. Baldwin, S.R. Corsi, S.A. Mason, P.C. Reneau, J.W. Scott, Vertical distribution of microplastics in the water column and surficial sediment from the Milwaukee River Basin to Lake Michigan, *Environ. Sci. Tech.* 53 (21) (2019) 12227–12237.
- [53] K. Enders, R. Lenz, C.A. Stedmon, T.G. Nielsen, Abundance, size and polymer composition of marine microplastics $\geq 10 \mu\text{m}$ in the Atlantic Ocean and their modelled vertical distribution, *Mar. Pollut. Bull.* 100 (1) (2015) 70–81.

- [54] B. Urban-Malinga, M. Zalewski, A. Jakubowska, T. Wodzinowski, M. Malinga, B. Patys, A. Dąbrowska, Microplastics on sandy beaches of the southern Baltic Sea, *Mar. Pollut. Bull.* 155 (2020), 111170.
- [55] N. Digka, C. Tsangaris, H. Kaberi, A. Adamopoulou, C. Zeri, Microplastic abundance and polymer types in a Mediterranean environment, in: *Proceedings of the International Conference on Microplastic Pollution in the Mediterranean Sea*, Springer, Cham, 2018, pp. 17–24.
- [56] O.Y. Kwon, J.H. Kang, S.H. Hong, W.J. Shim, Spatial distribution of microplastic in the surface waters along the coast of Korea, *Mar. Pollut. Bull.* 155 (2020), 110729.
- [57] C.C. Gaylarde, J.A.B. Neto, E.M. da Fonseca, Paint fragments as polluting microplastics: a brief review, *Mar. Pollut. Bull.* 162 (2021), 111847.
- [58] H. Savelli, UN Environment Assembly Process on Marine Litter and Microplastics, 2018.
- [59] S. Amin, M. Amin, Thermoplastic elastomeric (TPE) materials and their use in outdoor electrical insulation, *Rev. Adv. Mater. Sci.* 29 (1) (2011) 15–30.
- [60] W. Xia, Q. Rao, X. Deng, J. Chen, P. Xie, Rainfall is a significant environmental factor of microplastic pollution in inland waters, *Sci. Total Environ.* 732 (2020), 139065.
- [61] A.I.S. Purwiyanto, T. Prartono, E. Riani, Y. Naulita, M.R. Cordova, A.F. Koropitan, The deposition of atmospheric microplastics in Jakarta-Indonesia: the coastal urban area, *Mar. Pollut. Bull.* 174 (2022), 113195.
- [62] J. Gasperi, S.L. Wright, R. Dris, F. Collard, C. Mandin, M. Guerrouache, V. Langlois, F.J. Kelly, B. Tassin, Microplastics in air: are we breathing it in? *Curr. Opin. Environ. Sci. Health* 1 (2018) 1–5.
- [63] S. Oberbeckmann, B. Kreikemeyer, M. Labrenz, Environmental factors support the formation of specific bacterial assemblages on microplastics, *Front. Microbiol.* 8 (2018) 2709.
- [64] G. Jaikumar, J. Baas, N.R. Brun, M.G. Vijver, T. Bosker, Acute sensitivity of three Cladoceran species to different types of microplastics in combination with thermal stress, *Environ. Pollut.* 239 (2018) 733–740.
- [65] D. Lobelle, M. Cunliffe, Early microbial biofilm formation on marine plastic debris, *Mar. Pollut. Bull.* 62 (1) (2011) 197–200.
- [66] D. Kaiser, N. Kowalski, J.J. Waniek, Effects of biofouling on the sinking behavior of microplastics, *Environ. Res. Lett.* 12 (12) (2017), 124003.
- [67] H. Zhang, Transport of microplastics in coastal seas, *Estuar. Coast Shelf Sci.* 199 (2017) 74–86.
- [68] S.M. Liff, E.R. Wilczek, R.J. Harris, R. Bouldin, E.W. Stoner, Evidence of microplastics from benthic jellyfish (*Cassiopea xamachana*) in Florida estuaries, *Mar. Pollut. Bull.* 159 (2020), 111521.
- [69] M.F. Severini, N.S. Buzzi, A.F. López, C.V. Colombo, G.C. Sartor, G.N. Rimondino, D.M. Truchet, Chemical composition and abundance of microplastics in the muscle of commercial shrimp *Pleoticus muelleri* at an impacted coastal environment (Southwestern Atlantic), *Mar. Pollut. Bull.* 161 (2020), 111700.
- [70] J. Li, A.L. Lusher, J.M. Rotchell, S. Deudero, A. Turra, I.L. Bråte, C. Sun, M.S. Hossain, Q. Li, P. Kolandhasamy, H. Shi, Using mussel as a global bioindicator of coastal microplastic pollution, *Environ. Pollut.* 244 (2019) 522–533.
- [71] M. Smith, D.C. Love, C.M. Rochman, R.A. Neff, Microplastics in seafood and the implications for human health, *Curr. Environ. Health Reports* 5 (3) (2018) 375–386.
- [72] C.O. Egbeocha, S. Malek, C.U. Emenike, P. Milow, Feasting on microplastics: ingestion by and effects on marine organisms, *Aquat. Biol.* 27 (2018) 93–106.
- [73] J. Li, Z. Wang, J.M. Rotchell, X. Shen, Q. Li, J. Zhu, Where are we? Towards an understanding of the selective accumulation of microplastics in mussels, *Environ. Pollut.* 286 (2021), 117543.
- [74] S.A. Mason, V.G. Welch, J. Neratko, Synthetic polymer contamination in bottled water, *Front. Chem.* 407 (2018).
- [75] H. Tong, Q. Jiang, X. Hu, X. Zhong, Occurrence and identification of microplastics in tap water from China, *Chemosphere* 252 (2020), 126493.
- [76] L.M. Hernandez, E.G. Xu, H.C. Larsson, R. Tahara, V.B. Maisuria, N. Tufenkji, Plastic teabags release billions of microparticles and nanoparticles into tea, *Environ. Sci. Tech.* 53 (21) (2019) 12300–12310.
- [77] A. Ragusa, A. Svelato, C. Santacroce, P. Catalano, V. Notarstefano, O. Carnevali, F. Papa, M.C. Rongioletti, F. Baiocco, S. Draghi, E. D'Amore, Plasticenta: first evidence of microplastics in human placenta, *Environ. Int.* 146 (2021), 106274.
- [78] L.F. Amato-Lourenço, R. Carvalho-Oliveira, G.R. Júnior, L. dos Santos Galvão, R.A. Ando, T. Mauad, Presence of airborne microplastics in human lung tissue, *J. Hazard Mater.* 416 (2021), 126124.
- [79] P. Schwabl, S. Köppel, P. Königshofer, T. Bucsis, M. Trauner, T. Reiberger, B. Liebmann, Detection of various microplastics in human stool: a prospective case series, *Ann. Intern. Med.* 171 (7) (2019) 453–457.
- [80] J. Lee, *Economic Valuation of Marine Litter and Microplastic Pollution in the Marine Environment: an Initial Assessment of the Case of the United Kingdom*, SOAS-CeFiMS, London, UK, 2015, pp. 1–16.
- [81] M. Mofijur, S.F. Ahmed, S.A. Rahman, S.Y.A. Siddiki, A.S. Islam, M. Shahabuddin, H.C. Ong, T.I. Mahlia, F. Djanaroodi, P.L. Show, Source, distribution and emerging threat of micro-and nanoplastics to marine organism and human health: socio-economic impact and management strategies, *Environ. Res.* 195 (2021), 110857.

ARTICLES FOR FACULTY MEMBERS

MICROPLASTICS AND MARINE ENVIRONMENT

Title/Author	Spatiotemporal microplastic occurrence study of Setiu Wetland, South China Sea / Ibrahim, Y. S., Hamzah, S. R., Khalik, W. M. A. W. M., Ku Yusof, K. M. K., & Anuar, S. T.
Source	<i>Science of The Total Environment</i> Volume 788 (2021) 147809 Pages 1-12 https://doi.org/10.1016/J.SCITOTENV.2021.147809 (Database: ScienceDirect)



Spatiotemporal microplastic occurrence study of Setiu Wetland, South China Sea



Yusof Shuaib Ibrahim^{a,b,*}, Siti Rabaah Hamzah^b, Wan Mohd Afiq Wan Mohd Khalik^{a,b},
Ku Mohd Kalkausar Ku Yusof^{a,b}, Sabiqah Tuan Anuar^{a,b}

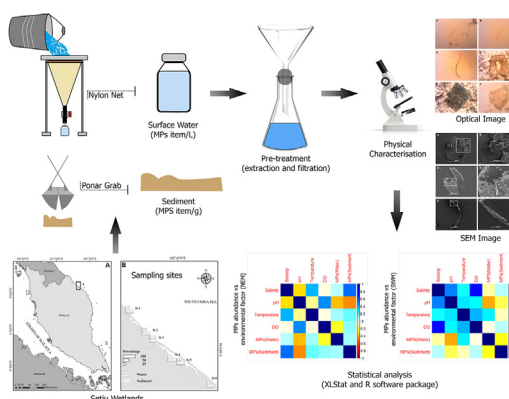
^a Microplastic Research Interest Group (MRIG), Faculty of Science and Marine Environment, University Malaysia Terengganu, 21030 Kuala Nerus, Terengganu, Malaysia

^b Faculty of Science and Marine Environment, University Malaysia Terengganu, 21030 Kuala Nerus, Terengganu, Malaysia

HIGHLIGHTS

- Microplastics were detected in both water surface and sediment of a pristine area.
- Filaments and transparent microplastics were the most abundant in both matrices.
- Seasonality was the most important variable explaining the distribution of microplastics.
- The presence of microplastics could be related to environmental physical parameters and water intrusion.

GRAPHICAL ABSTRACT



ARTICLE INFO

Article history:

Received 31 December 2020

Received in revised form 3 May 2021

Accepted 13 May 2021

Available online 17 May 2021

Editor: Ouyang Wei

Keywords:

Malaysia

Microplastic distribution

Monsoon

Microfibres

ABSTRACT

This study reports the distribution of microplastics (MPs) in surface water and estuarine sediments in South and North Setiu Wetland in the South China Sea. Sampling was conducted bimonthly for one year from November 2016 to November 2017, including the northeast and southwest monsoons. Water surface and sediment samples were collected from six different sampling stations (STs). Samples were sorted based on physical analysis (optical observation) and selected particles were further analyzed by chemical characterizations. The findings of this study indicate that a total of 0.36 items/L and 5.97 items/g particles of MPs were found from characterizations surface water and dry sediment, respectively. Among the selected stations included in this research, ST3 (1.375 ± 0.347 items/L) and ST2 (14.250 ± 4.343 items/g) were individually identified as high potential MP sinking areas, exacerbated during the northeast and southwest monsoons. Transparent, film, and filament MP types were consistently found across all stations. Microplastic filaments revealed a functional group of polypropylenes based on the main peak spectrum at $2893\text{--}2955\text{ cm}^{-1}$ (C–H alkyl stretching), 1458 cm^{-1} (C–H₂ bending), and 1381 cm^{-1} (CH₃ bending). Microplastic materials were thermally decomposed by pyrolysis–gas chromatography–mass spectrometry (Pyr–GC/MS) and identified as cyclohexane and cyclohexene derivatives, as well as precursors of polymer blends. The distribution of MPs in both matrices varied according to different seasons. These findings provide useful baseline information on the distribution of MPs from the estuarine area in Malaysia and South China Sea waters.

© 2021 Elsevier B.V. All rights reserved.

* Corresponding author.

E-mail addresses: yusofshuaib@umt.edu.my (Y.S. Ibrahim), p3078@pps.umt.edu.my (S.R. Hamzah), wan.afiq@umt.edu.my (W.M.A.W.M. Khalik), kukausar@umt.edu.my (K.M.K. Ku Yusof), sabiqahanuar@umt.edu.my (S.T. Anuar).

1. Introduction

Microplastics (MPs) are small synthetic polymer particles less than 5 mm in size (Arthur et al., 2009). In the aquatic environment, MPs can be classified into primary and secondary types, representing the originally manufactured sizes of polymer products and the plastic fragmented into smaller sizes, respectively (Cole et al., 2011). Microplastics have been found in freshwater (Alam et al., 2019) and marine environments (Maes et al., 2017; Khalik et al., 2018), as well as in mangrove ecosystems (Mohamed Nor and Obbard, 2014; Peng et al., 2017). Previous studies indicated that filaments/fibers, films, and fragments were the most frequently isolated MP types, among which filaments were the most abundant based on a variety of environmental matrices (Xu et al., 2018; Maes et al., 2017; Peng et al., 2017). For example, filaments originated from different anthropogenic activities such as sewage and aquaculture activities. Once MPs enter the aquatic environment, a wide variety of organisms become susceptible to their presence, sometimes in high abundance. Previously, Rochman et al. (2016) revealed that if plastic debris were to ecologically impact an ecosystem, and sublethal (suborganismal changes) or lethal effects could result. Ingested MPs have been proven to cause weight loss and low energy in marine organisms, a slow egestion process, and their transfer within the trophic level (Besseling et al., 2013; Farrell and Nelson, 2013; Ory et al., 2018).

International statistics in 2017 showed that 50.1% of global plastic production has originated in Asia, with 29.4% from China (which has the most significant global plastic industry globally), 3.9% from Japan, and 16.8% from the rest of Asia, including Malaysia (PlasticsEurope, 2018). The increase in plastic manufacturing has been accompanied by an increase in plastic waste because of the lack of public awareness and plastic dumping into the marine environment, both directly and indirectly. This has become an emerging topic among researchers, and MP distribution has been studied globally, and more specifically in Asian countries such as Indonesia (Alam et al., 2019), Korea (Eo et al., 2018), China (Li et al., 2018), and the Philippines (Kalnasa et al., 2019). Malaysia ranked as the eighth country in terms of the mismanaged plastic waste problem in 2010, contributing up to 0.37 million metric tons per year (Jambeck et al., 2015). To deal with this problem, the Ministry of Environment and Water in Malaysia created a strategy roadmap for achieving zero single-use plastic production between 2018 and 2030 (Ministry of Energy, Science, Technology, Environment and Climate Change, 2018; Ma et al., 2020).

Previous research documented the presence and analysis of MPs in Malaysian coastal areas, beaches, marine water, and rivers (Barasarathi et al., 2014; Fauziah et al., 2015; Khalik et al., 2018; Sarijan et al., 2018). Microplastics from personal care and cosmetic products were discharged as part of treated and untreated waste into the environment (Praveena et al., 2018). Recently, the presence of MPs was detected in marine species of commercial fish from a local market in Malaysia (Karbalaei et al., 2019; Jaafar et al., 2020) and in zooplankton in the South China Sea (Amin et al., 2020). Studies presented the characterization of MPs found in marine organisms collected from Setiu Wetland, e.g., filter feeder bivalve (*Scapharca cornea*) and estuarine fish (*Lates calcarifer*) (Ibrahim et al., 2016, 2017). However, there remain a limited number of related publications on the distribution and occurrence of MPs in surface water and sediments, hampering a true perspective of the current situation of this emergent issue in Malaysia.

The Setiu Wetland is officially recognized as a protected area that has become an important region for ecotourism activities. Furthermore, it is considered a representative of a natural officially recognized area in Malaysia for investigating a baseline level of MP abundance. Therefore, this research focuses on documenting the spatiotemporal variation of MP abundance along the Setiu Wetland, located in the South China Sea, particularly in sediment and surface water matrices. Physical and chemical characterizations were defined to identify the surface morphology and composition of polymers.

2. Materials and methods

2.1. Study area and sample collection

Prior to sample collection, physicochemical data of water (temperature, dissolved oxygen (DO)), salinity, and pH were taken in situ using a hand-held multiparameter hydro-lab (Quanta, Hydrolab Corp., USA) instrument. Triplicates of all parameter readings at both water and sediment were taken at various sampling stations (STs). The sample collections were completed during high tide to ensure boat accessibility. Sample collections were conducted bi-monthly at six different stations (STs) and during seven different events, separated into two main different monsoonal seasons called as Northeast Monsoon (NEM) and Southwest Monsoon (SWM) across a year-long period (November 2016 to November 2017), covering the northern and southern parts of the Setiu Wetland (Fig. 1, Supplementary 1). For each sampling event, a total of 20 pails (120L) of surface water samples were taken using a metal pail at a depth of 50 cm, which was then poured into a 20 μ m nylon net. All visible organic materials such as leaves, wood, and plant fragments were removed by hand from the net. The filtered residue together with solid material at the bottom of the net was consistently transferred through the valve connected to the net, that can be transferred directly into a 500 mL glass bottle for each ST. Filter paper and a glass bottle of Milli-Q water (blank) were placed side-by-side (left open to the air), during the transfer of residues for the contamination control procedure. Meanwhile, sediment samples were taken using a Ponar grab (229 \times 229 mm dimensions with a volume of 2 kg per grab) (approximately 2–3 m water depth). Subsequently, the sediment samples were transferred into a stainless steel pail using a metal shovel before they were placed into containers covered with aluminum foil to avoid contamination. All devices and tools were pre-washed with Milli-Q water and 80% ethanol in situ before proceeding to the next ST. Whenever possible, the metal pail and Ponar grab were covered with aluminum foil before being used at subsequent STs. The glass bottles containing water samples were stored carefully in a sterile storage area at room temperature, and the sediment samples were kept cold at 4 $^{\circ}$ C until further analysis.

2.2. Microplastic extraction

Water samples were transferred into a sterile beaker covered with aluminum foil. Meanwhile, five spatulas of wet sediment were transferred into three different glass petri dishes and covered with aluminum foil. Sediment samples were dried in a desiccator for two days to avoid airborne contamination. Once completely dried, three replicates of 4 g of dry sediment were weighed and put into different glass beakers. For the extraction process, the samples (water and sediments) were mixed with 500 mL of saline water (NaCl prepared in Milli-Q water) in a 500 mL beaker. The samples were left for 15 min so that the impurities could settle. The upper part of the water sample was pumped out using a vacuum pump through a 0.45 μ m cellulose nitrate membrane filter. Then, filter papers were placed in a glass petri dish and dried overnight in a desiccator.

2.3. Contamination control

All laboratory tools and glassware were frequently rinsed after and before usage with Milli-Q water and 80% ethanol. Furthermore, only metal and glass equipment was prepared during the sampling process. The bench and table were pre-cleaned with clean laboratory tissue, ultra-pure water and 80% ethanol before handling the samples in a closed and clean chamber during the laboratory analysis. The researchers wore a clean cotton laboratory coat, and latex gloves were worn in the laboratory. Control filter papers were placed next to the sorting zone beside the microscope during the handling, observing,

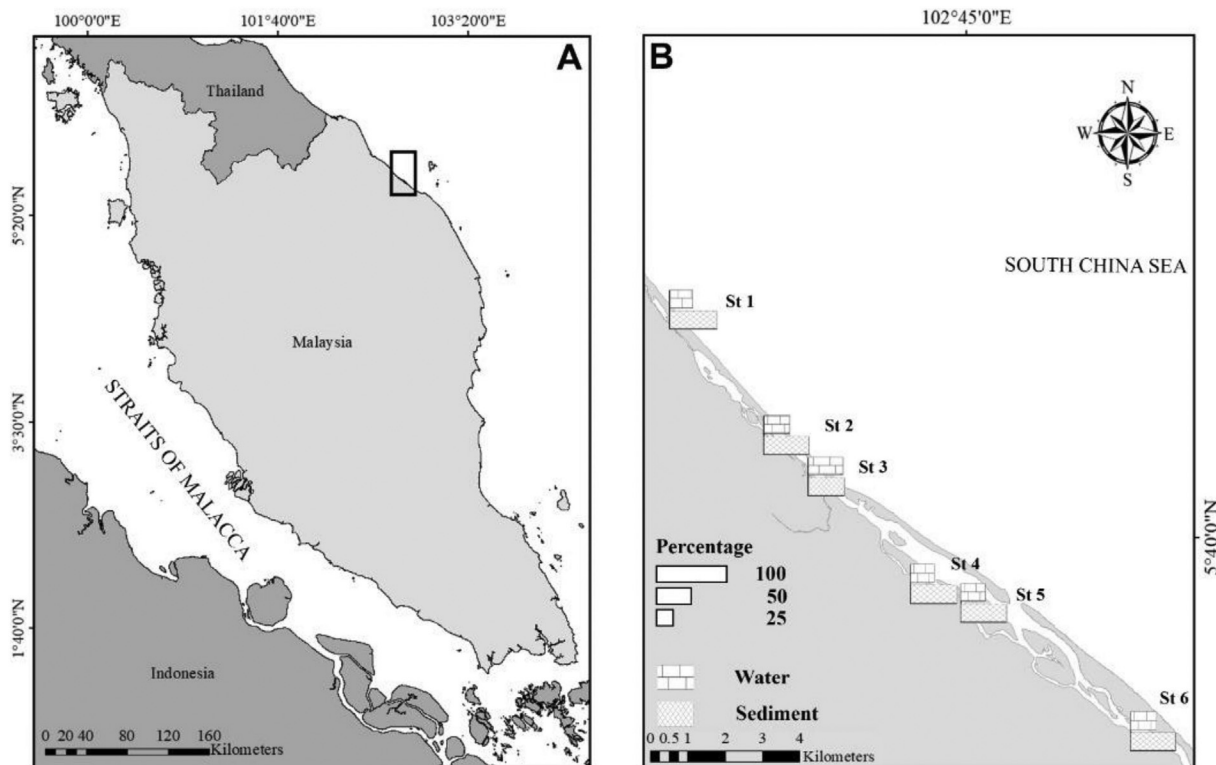


Fig. 1. Map of STs: (A) Peninsular Malaysia; (B) Setiu Wetland, Terengganu. *Percentage bars shown in (B) represent percentage of microplastic distribution in surface water and sediment by different sampling station.

and analysis of MPs to avoid any airborne contamination and over-quantification. All blanks from the sampling and laboratory procedures were analyzed for any possible type of MP, where particles with similar morphologies were excluded from subsequent sample processing following the same procedure as for the environmental samples.

2.4. Physical characterization

The isolation of MPs was conducted based on the gravimetric method (Masura et al., 2015). Filter papers were screened under a dissecting microscope (Olympus SZX-ZB7, Olympus Corp., Tokyo, Japan). The MPs were sorted and classified based on their different shapes (filament, fragment, film, and styrofoam) and colors (transparent, red, blue, green, black, and brown) (Hidalgo-Ruz et al., 2012). During this process, a melting behaviour test (hot needle test) was conducted to observe the plastic melting behaviour and reaction toward the heat (Enders et al., 2015). Then, the sorted MPs were immediately transferred into a 10 mL vial containing Milli-Q water using fine-tip stainless steel forceps. All MP particles were measured by scale on the lens of microscope and Dyno-eye camera with measurement software (DinoCapture 2.0 version 1.5.19), and particles with a size larger than 5 mm were removed during the sorting process. In total, 1813 and 3011 particles of MPs were sorted from 5040 L water surface and 504 g of dry sediment, respectively. Sorting and quantification data were later expressed as items/L (surface water) and items/g (sediment). A representative of MPs was then photographed using a Dyno-eye camera. A scanning electron microscope (SEM) (JEOL JSM-636 OLA) was used to observe morphological variations on the surface of the different MPs. A representative of the samples was selected, mounted on aluminum stubs, and coated with a thin layer of gold before it was observed under a SEM.

2.5. Chemical characterizations

The representative of each MPs for each ST and sample matrices was selected for polymer characterization (a total of 12 samples). Milli-Q

water was centrifuged at 4000 rpm for 30 min to enhance the separation of the MPs and water (Ibrahim et al., 2017). The supernatant was removed using a micropipette and the residue (containing MPs) was dried in a closed clean chamber before it was transferred on the diamond plate of Fourier transform infrared (FTIR) spectroscopy instrument (Perkin Elmer; Spectrum 65) for polymer identification. The analytical instrument (FTIR) was equipped with deuterated triglycine sulfate (DTGS) detector and operated in the spectra range between 450 and 4000 cm^{-1} of the attenuated total reflectance (ATR) mode at a rate of 45 scans per analysis. In this work, polymer identification was only made for the filament type of MPs, which had higher particle numbers than the other types. Fragment detection was not available because of the small size of samples and particles had been lost during handling. The detection size limit for ATR-FTIR is 200 μm . During the analysis, each MP particle was analyzed for 3 times to avoid misinterpretation. All spectra were interpreted based on the functional group and compared with the polymer library (RS0023 Perkin Elmer Raman Polymer Library). Additionally, peak assignment for the functional group was interpreted based on existing findings by Jung et al. (2018) and Cai et al. (2019).

Subsequently, one filament sample from the sediment and water samples was randomly chosen for further analysis by Pyr-GC/MS. This technique can identify polymer compounds and organic additives in plastic materials (Mai et al., 2018). In brief, the MPs in each sample were thermally decomposed into smaller fractions using a pyrolyzer (630 °C). The decomposed fractions were then separated by gas chromatography using the DB5 Ms. Ultra Inert column (Agilent JNW, USA) and final determination was performed using mass spectroscopy (MS) (Agilent Tech., USA). Pyrogram results were interpreted based on the high peak of the pyrolytic compounds and were compared with polymer standard references. Under these conditions, the pyrolytic compounds acted as an indicator for specific polymers in the tested sample. Compounds with a major retention time (in the GC Total Ion Chromatogram, TIC) were only selected if they had higher than an 80% match with the NIST library (NIST, v.14.L), according to the mass spectra. Conversely, pyrolytic products from the tested sample were

also validated using additional literature studies (Dekiff et al., 2014; Kusch, 2017).

2.6. Statistical analysis

The XLStat (ver. 2019, USA) and R statistical analysis version 4.0.4 (R Development Core Team, 2011) software were used to analyze and interpret the acquisition datasets. In the initial stage, the normality (Shapiro–Wilk) test was conducted ($p < 0.05$, two-tailed). From the analysis, the results showed that all data sets were not normally distributed. To study the spatial pattern (between station) and temporal pattern (between sampling period), the Kruskal – Wallis with Steel – Dwass – Critchlow – Fligner test was performed as the post hoc analysis. The Wilcoxon Signed Rank ($p < 0.05$, two-tailed) was computed in order to study the significant differences between two dependent variables. In this study, the Wilcoxon Rank was used to determine the significant differences between monsoonal season (southwest monsoon (SWM) and northeast monsoon (NEM)). Principal component analysis (PCA) using the eigenvalue decomposition (varimax rotation) method was performed to identify latent information generated from the spatiotemporal difference variations. The Kaiser criterion was used to differentiate between significant principal components. An eigenvalue > 1 was considered a key component of the definition. A nonparametric test of Spearman's rank order was conducted to identify the correlation between MP concentration in different samples and the physicochemical analysis of the water (pH, DO, temperature, and salinity). The correlation was significant if p -value < 0.05 and the strength of correlation was determined in three different classes (strong ($r = \geq 0.70$), moderate ($r = 0.30 \leq 0.69$), weak $r = \leq 0.29$). In addition, multiple linear regression was used to identify a precise model for determining the relationship between environmental factors and MPs in surface water and sediments.

3. Results

3.1. Distribution of microplastics

The results of the MP analysis in the sediment and seawater during a specific sampling time started from November 2016 until November 2017 for the six stations are shown in Fig. 2(a)–(d). Microplastics in

surface water ranged from 0.251 ± 0.139 items/L (ST1) to 0.540 ± 0.139 items/L (ST3). Individually, ST4 was found to have the lowest level of MPs with 0.042 items/L, and the highest level of MPs was found in ST3 with 1.375 items/L. Both results were sampled in November 2016. The total mean value for all six STs was 0.36 ± 0.250 items/L. From the total mean value for MPs in water, ST1, ST4, ST5, and ST6 were found to be comparable to one another. However, ST2 and ST3 were found to have 1.5 to 2.0 times higher levels compared with the other four stations. A Kruskal–Wallis with Steel–Dwass–Critchlow–Fligner test as pos hoc analysis was conducted to identify any significant differences between the spatial analyses. The MPs in sediments ranged from 0.750 ± 3.838 to 14.25 ± 4.343 items/g, with the lowest and highest abundance of MPs found at ST6 and ST2, respectively. Even so, there were still non-significant differences between stations ($K(5,40) = 1.67, p = 0.89$).

Compared to SWM, NEM has a significant influence on the Setiu Wetland. Figs. 2(b) and (d) show that the total MP abundance in Setiu Wetland with both periods have an influence to the distribution of the MPs, but with opposite consequences in surface waters and the sediment. In water, MPs showed higher abundance toward NEM and lower during the SWM. In contrast, MPs showed very high variability in sediments during the SWM, but this was lower during the NEM. Throughout November 2016 to November 2017, as many as 14.77 items/L and 245.33 items/g of MPs were collected in water surface and sediments across the stations, respectively. During this period, July 2017 was the only month that showed the lowest level of MPs, with 0.90 items/L in water; however, there were non-significant differences between temporal studies ($K(5,41) = 2.39, p = 0.11$). There was a significant difference between temporal study in studies in sediment where November 2016 recorded only 11.67 items/g in sediments ($K(5,41) = -1.16, p = 0.01$), which was contradictory to our expectations. To study the difference between SWM and NEM relative to MPs variation in sediment and surface water, the Wilcoxon Signed Rank was computed. From that, it can be seen that MPs in surface water have a vary significantly during NEM with $p = 0.014$. Conversely, sediment samples did not display any significant variations with $p = 0.587$.

Owing to the differentiation between MP type and color across spatio-temporal orientation, PCA can more effectively observe MP distribution. The rotated varimax PCAs of the two types of variables, i.e., color

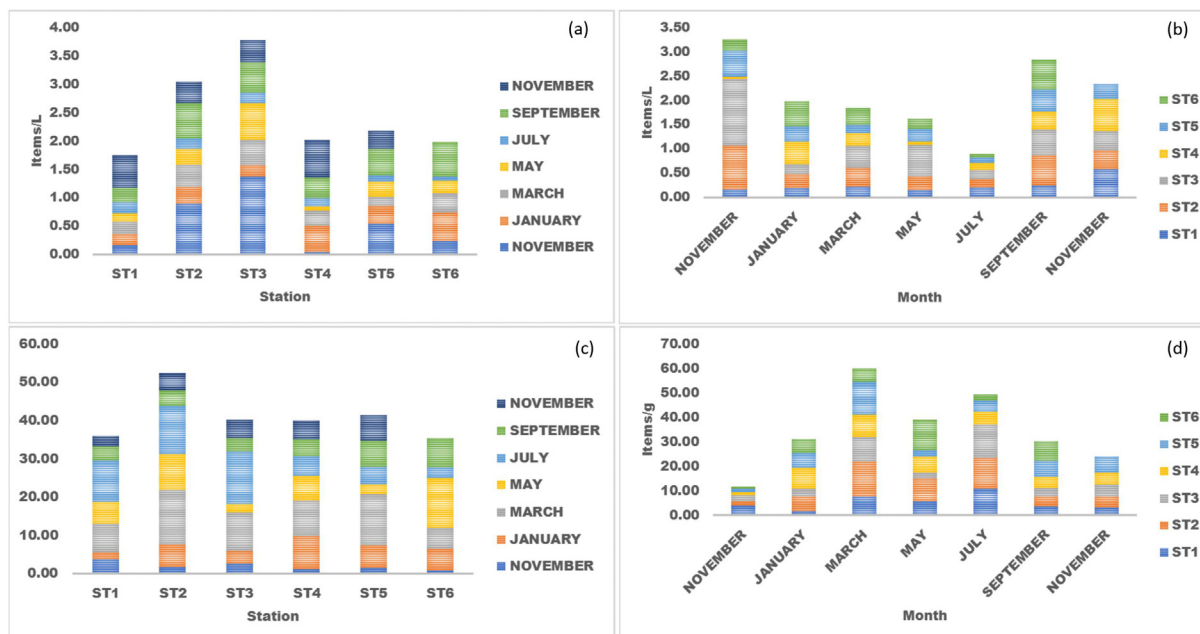


Fig. 2. The spatiotemporal abundance of MPs' distribution during a year-long study Click here to access/download;Figure;Fig. 2.jpg in Setiu Wetland; (a) (b): MPs in surface water, (c) (d): MPs in Sediment.

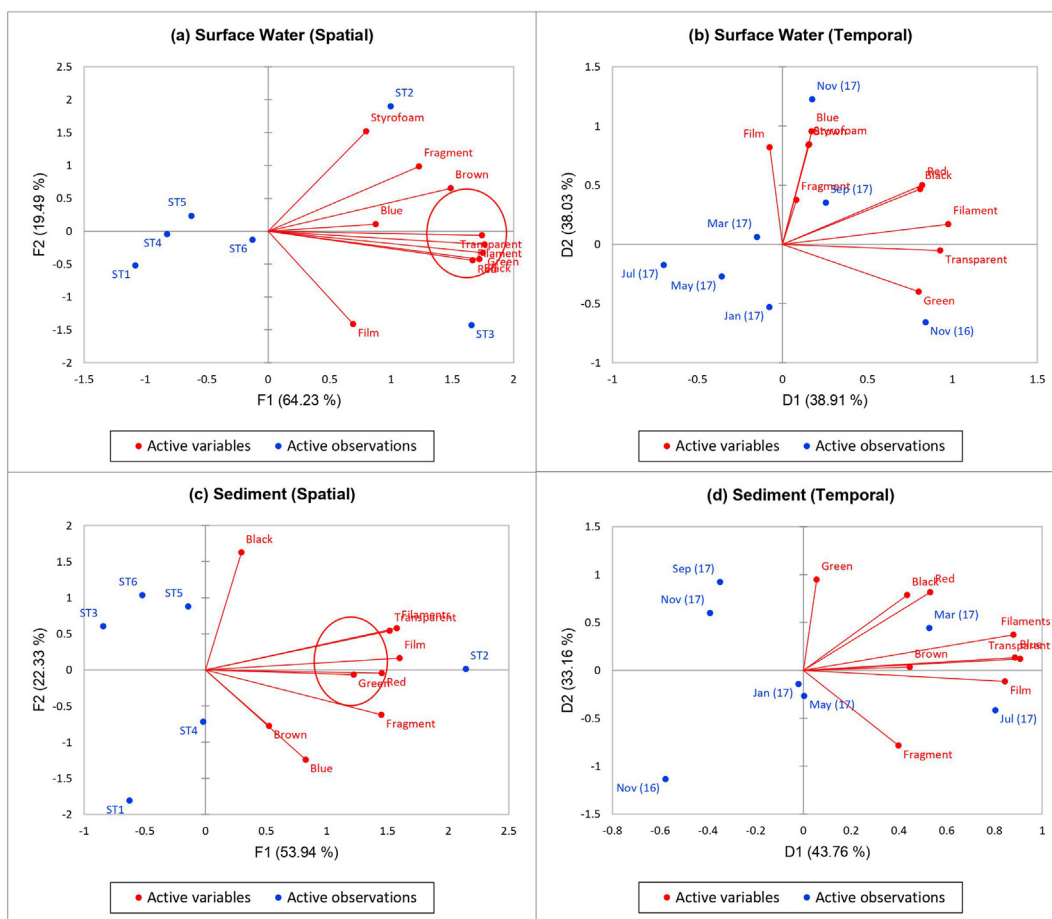


Fig. 3. Principal component analysis of MPs' characteristics in Setiu Wetland.

(transparent, brown, red, blue, green, and black) and type (filament, fragment, and film), describing the distribution of MP types in the water surface and sediment from the Setiu Wetland are shown in Supplementary 2. Fig. 3(a)–(d) show the PCA of six different colors and four types of MPs in water surface and sediments. In addition, the MPs characteristic are correlated with the samples collected during NEM, whereas MPs in sediment proved contradictly. For spatial analysis, Fig. 3(a) shows the contribution of the first component as dominated by transparent, red, green, and black colors and filament type (64.23%), and the second component is dominated by fragment and styrofoam types (19.49%). Meanwhile, Fig. 3(c) exemplifies the domination of transparent and red colors, and filament and film types in sediments for the first component (53.94%), and the second component contributed black and blue colors (22.33%). It can be seen that the transparent color and filament type were dominant types in both matrices (water surface and sediment). The temporal PCA analysis showed a lower contribution by the first and second components compared with the results for spatial analysis. In Fig. 3(b), the first component of water surface showed a strong contribution from transparent, filament, red, green, and black types (38.91%). Like water surface, the first component for PCA analysis (Fig. 3c) strongly correlates with transparent, blue, filament, and film types for a total of 43.76%. The images in the Fig. 4 illustrated the examples of shapes and colors of MPs found in this work, while the Scanning Electron Microscopy (SEM) images in Fig. 5 (a), (c) and (e) illustrated the morphology for the fragment, film and filament MPs found. In addition the microscopic image of respective surface (enlarged view) were shown in Fig. 5 (b), (d) and (f). The surface topography of analyzed MPs was found to be rough, eroded and cracked together with brittle fractures and irregular shape of the surface which signifies the weathering and mechanical fragmentations of MPs due to degradation processes.

3.2. The relationship between physicochemical analysis of water quality and MP distribution

Bimonthly in situ data (salinity, pH, temperature, and DO) from ST1 to ST6 from November 2016 to November 2017 were used to identify the major factors affecting the water quality in the tidally mixed estuarine system. In Supplementary 3, a total of 14 correlations are identified. Among these, only five correlations showed a moderate association between the measured parameters. Furthermore, nine correlations were analyzed as weak correlations. A consistent moderate correlation of $\alpha = 0.05$ (CI: 95%) was found for temperature/salinity ($r = 0.458$, $p = 0.003$), pH/DO ($r = 0.353$, $p = 0.022$), pH/MPs water ($r = -0.323$, $p = 0.037$), salinity/MPs sediment ($r = 0.367$, $p = 0.017$), and pH/MPs sediment ($r = -0.413$, $p = 0.007$). From four moderate correlations, the pH/MPs correlation was the only one indicated as inversely proportionate. In Supplementary 3, an illustration can be found of the heat map influence of the in-situ parameter toward the MPs in water and sediment during SWM and NEM. Based on the result, MPs in surface water were moderately affected by pH with $r = -0.38$ and $r = -0.41$, during NEM and SWM, respectively. Other than that, the MPs in sediment were only moderately affected by salinity with $r = 0.54$ only during NEM season. Subsequent multiple linear regressions (Table 1) demonstrated that a significant ($p < 0.05$) relationship existed between salinity and MP abundance in sediments ($p = 0.019$).

3.3. Chemical characterizations

A polymer was identified in both sample matrices. Attenuated total reflectance–Fourier transform infrared spectroscopy (ATR–FTIR) spectra interpreted this polymer as polypropylene (see Supplementary 4).

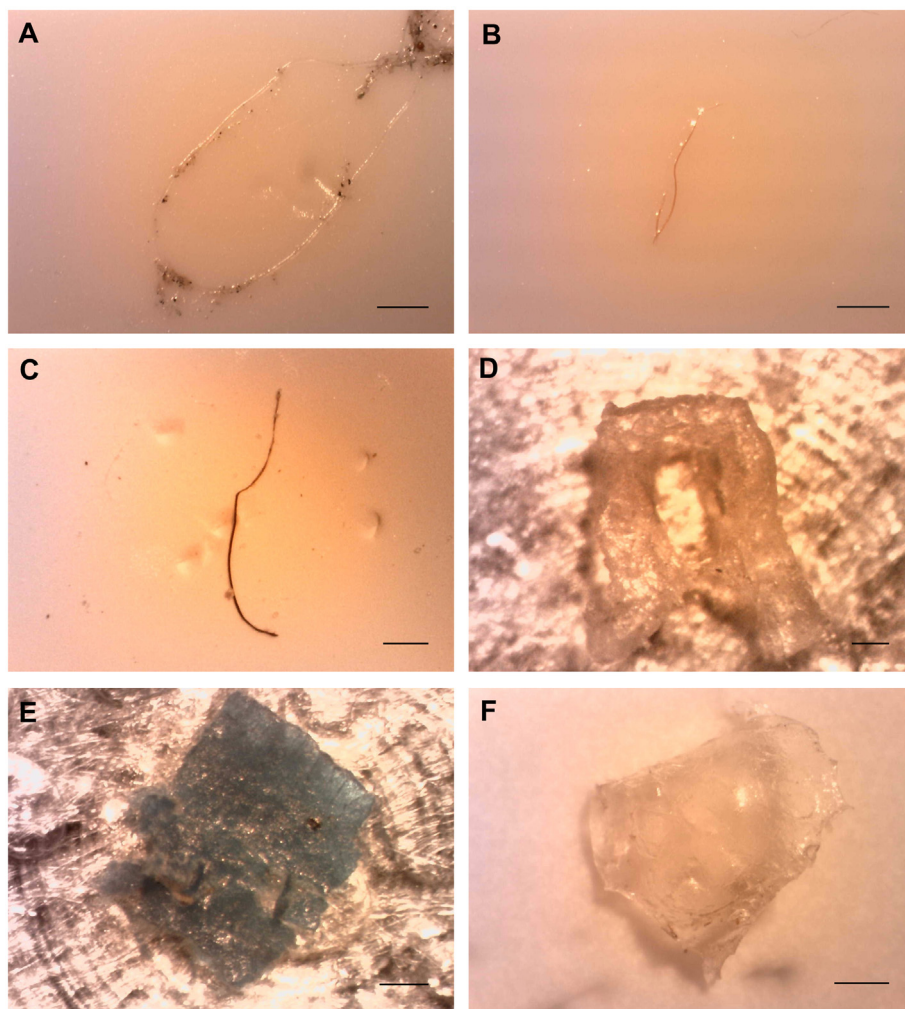


Fig. 4. Images of MPs with different shapes and colors. (A–C) filament, (D–E) fragment, and (F) film. Scale bars: 0.5 mm.

The peak at 2839 to 2955 cm^{-1} was identified as a C—H alkyl stretch. Meanwhile, the peak exhibited at 1458 and 1381 cm^{-1} was C—H bending of methylene (CH_2) and methyl (CH_3) groups, respectively. Pyrolysis–gas chromatography–mass spectrometry complemented and reconfirmed the results obtained from ATR–FTIR, and this is because both infrared spectra showed a similar interpretation of a polypropylene polymer linked to the functional groups. Table 2 shows the pyrolyzed products eluted in the range of $t_r = 5.99$ to 14.39 min retention time. The table shows that both samples included a similar pyrolytic cyclohexane derivative product.

4. Discussion

4.1. Microplastics spatial variability

It is difficult to compare MP abundance with other studies because of the different methodologies in sample collection and sample processing (Table 3). Different tools can also lead to different results, making it difficult to discover the actual concentration of MPs because of underestimation or overestimation. In the present study, the abundance of MPs in estuarine water was lower than in a study conducted in the estuarine area of Shanghai (27.84 ± 11.81 items/L; Zhang et al., 2019). However, the findings in this study indicate that the MP distribution of sediments is higher than in other mangrove areas such as Singapore (36.8 ± 23.6 items/kg) and Shanghai (121 ± 9 items/kg) (Mohamed Nor and

Obbard, 2014; Peng et al., 2017). Different anthropogenic activities will nevertheless result in the dominance of different types of MPs. As shown in the Table 3, different results are attributed to a different range of sources. Filaments were commonly isolated from different estuarine environments but originated from different sources. For example, laundering activities at the nearby Changjiang estuary contributed to the dominance of 93% fiber and 42% transparent color in the Shanghai mangrove area (Peng et al., 2017). Earlier, Browne et al. (2011) suggested that, this could be one of the main drivers of microfiber pollution worldwide. The findings of the current study support those results, where microplastic is believed to have originated from washing of clothes. However, the chemical characterization indicated MPs' disintegration from general aquaculture and fisheries materials. Meanwhile, discharge from the Dagu Sewage River included 66.9% fiber MPs, and 31.8% of red color was reported to have originated from wastewater treatment plants (Wu et al., 2019). According to Suratman et al. (2016), the Setiu Wetland is essentially a closed system. The area has been protected, but geographical conditions may be another factor for MP accumulation in the estuarine area. Furthermore, anthropogenic activities may lead to the high abundance of contamination contributed by these MP types (Ding et al., 2019).

Microplastic filaments are reported as the most abundant (up to 98.49% in the present study). Khalik et al. (2018), in their study on MPs in the South China Sea reported that MP abundance accounted for 0.69 items/L in marine water, whereby the filaments comprised

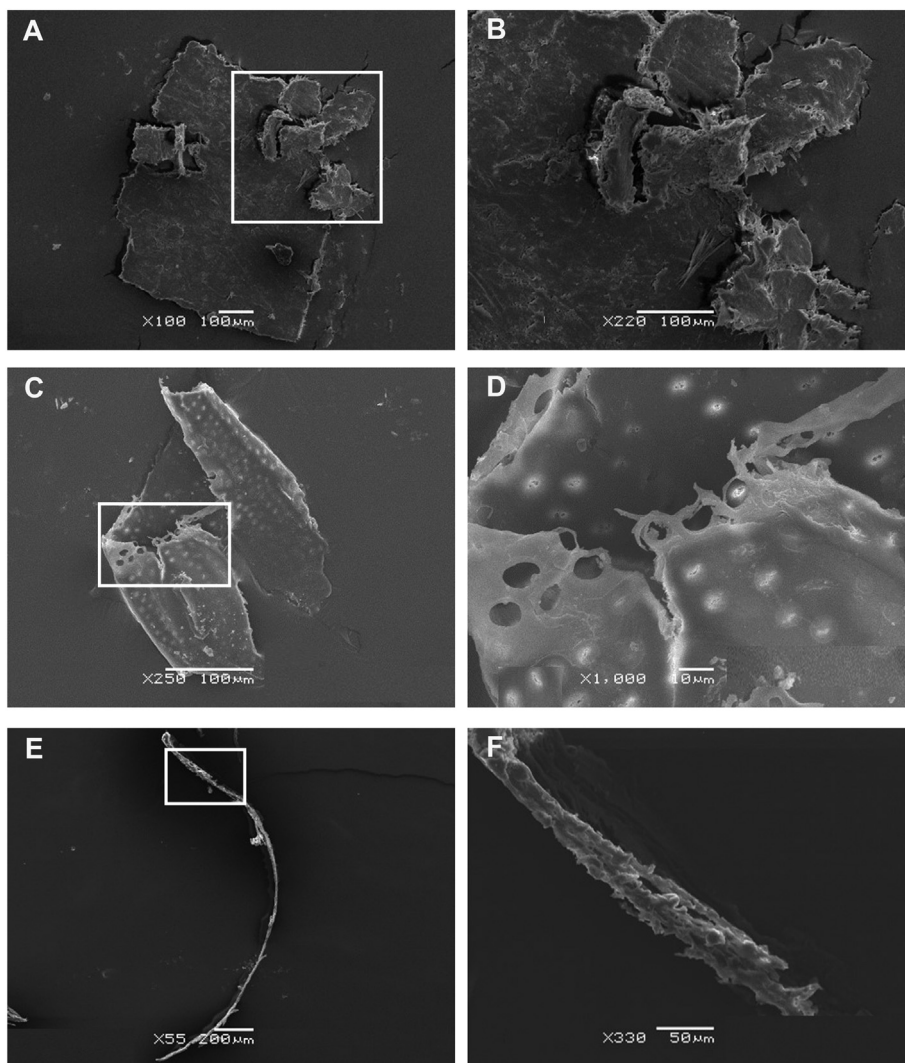


Fig. 5. The SEM images of weathered MPs: (A) fragment; (B) enlarged view of fragment A; (C) film; (D) enlarged view of film C; (E) filament; and (F) enlarged view of filament E.

more than 23% of total MPs. In addition, in a more recent study in the vicinity, microplastics were recorded for nine items/L, in which 70% of the total number of MPs were filaments (Amin et al., 2020). These studies indicate that subsequently, floating MPs may be transported to estuarine environments. These wetlands receive input streams from the Setiu and Ular rivers, as well as marine water that is channeled into the estuary from the South China Sea (Azmi et al., 2012). Accordingly, it should not be surprising that the MPs floating in the water samples

taken from the river discharge and seawater influx will eventually contaminate the study area. Surface water and sediments act as mobilization factors for floating and sinking MPs, respectively. Filaments have been observed settling deeper within sediments over time (Willis et al., 2017). Thus, the abundance of filaments may penetrate the sediment, where they may remain for an extended period. Consequently, MPs will persistently and continuously increase. Moreover, current findings showed that transparent MPs were dominant, but black MPs

Table 1
Results of the best model multiple regression analyses among MPs in surface water, sediment, and environmental factors.

	Source	Value	Standard error	t	Pr > t	Lower bound (95%)	Upper bound (95%)
Surface Water	Intercept	-0.692	0.687	-1.008	0.319	-2.081	0.696
	SALINITY	-0.006	0.004	-1.582	0.122	-0.014	0.002
	pH	0.000	0.000				
	TEMPERATURE	0.038	0.024	1.595	0.119	-0.010	0.087
	DO	0.000	0.000				
Sediment	Intercept	10.270	3.945	2.603	0.013	2.291	18.250
	SALINITY	0.111	0.045	2.453	0.019	0.019	0.202
	pH	-0.931	0.566	-1.647	0.108	-2.075	0.213
	TEMPERATURE	0.000	0.000				
	DO	0.000	0.000				

Values in bold are different from 0, with a significance level of alpha = 0.05.

Table 2

Overall pyrolytic products of Pyr–GC/MS in the filament type microplastic from water surface and sediment.

Sample	Retention time, t_r (min)	Pyrolytic products	m/z
Water surface	5.99	1,3,5-trimethylcyclohexane	126.23
	7.16	1-ethyl-3-methylcyclohexane	126.23
	7.23	1-ethyl-4-methylcyclohexane	126.23
	6.49	1,3,5-trimethylcyclohexane	126.23
	7.16	1-ethyl-3-methylcyclohexane (cis, trans)	126.23
	7.23	1-ethyl-4-methyl-, trans-cyclohexane	126.23
	7.55	trans-1-ethyl-4-methyl-cyclohexane	126.23
	9.03	1-methyl-3-propyl-cyclohexane	140.26
	10.55	decahydro-naphthalene	138.25
	11.37	cis-decahydro-naphthalene	138.25
	11.67	cis-anti-1-methyl-decalin	152.28
	12.04	1-ethylcyclohexene	110.20
	12.09	1-propylcyclohexene	124.22
	12.18	trans-1,3,3-trimethylbicyclo[3.1.0]hexane-1-carboxaldehyde	152.23
Sediment	12.61	cyclopentylcyclohexane	152.28
	14.05	tridecane	184.37
	14.39	2,2,4,4,6,8,8-heptamethylnonane	226.44
	5.99	1,3,5-trimethylcyclohexane	126.23
	7.16	1-ethyl-3-methylcyclohexane	126.23
	7.23	1-ethyl-4-methylcyclohexane	126.23
	6.49	1,3,5-trimethylcyclohexane	126.23
	7.16	1-ethyl-3-methylcyclohexane (cis, trans)	126.23
	7.23	1-ethyl-4-methyl-, trans-cyclohexane	126.23
	7.55	trans-1-ethyl-4-methyl-cyclohexane	126.23
	9.03	1-methyl-3-propyl-cyclohexane	140.26
	10.55	decahydro-naphthalene	138.25
	11.37	cis-decahydro-naphthalene	138.25
	11.67	cis-anti-1-methyl-decalin	152.28
12.04	1-ethylcyclohexene	110.20	
12.09	1-propylcyclohexene	124.22	
12.18	trans-1,3,3-trimethylbicyclo[3.1.0]hexane-1-carboxaldehyde	152.23	
12.61	cyclopentylcyclohexane	152.28	
14.05	tridecane	184.37	
14.39	2,2,4,4,6,8,8-heptamethylnonane	226.44	

were the most dominant in marine water (Khalik et al., 2018). This can be explained by considering that MPs may vary within different environments.

The presence of MPs in all STs was observed at all STs, in both surface water and sediment samples. The spatial distributions of MPs in surface water and sediments are listed in Supplementary 5. The biplot interaction of both principal components shows that ST2 and ST3 had significant MP abundance in the surface water, and the sediment at ST2 was the most affected (Fig. 3). Historically, the area at ST3 was headed to the old opening sea surrounded by mangroves, where local fishermen moored in and out of the wetland. This may be a direct consequence of the higher distribution in the surface water at both stations, where MPs became trapped and accumulated, similar to what is described in a report by Li et al. (2018), which showed that mangroves had trapped marine debris.

4.2. Microplastics temporal variability

In Malaysia, there are two main monsoonal seasons, i.e., the SWM and NEM. During the SWM (late May to early October), Malaysia faces drier and hotter conditions in which the wind direction is mostly south-west of Indonesia (Mahmud et al., 2018). The NEM (early November to late March) brings more extreme rainfall from the northeast of Indochina region. Between these periods, there is an inter-monsoon (IM1 and IM2) when the wind speed is lower than usual (Varikoden et al., 2011). Setiu is located in the eastern part of the Malaysian Peninsula and is directly adjacent to the South China Sea. Furthermore, small-scale aquaculture activities at nearby ST3 may have contributed to the increment in the abundance of MPs (Ibrahim et al., 2017). Contrarily,

MP abundance in sediments only dominated at ST2 compared to the other stations. It is known that a wider hydrological areas, with a higher volume of water, tend to accumulate MPs than smaller region (Su et al., 2018). Therefore, a smaller area, as represented by ST2, proved to have accumulated more MPs in sediments than other stations. Consequently, these stations may be exposed to severe environmental problems such as chemical pollution due to a high concentration of MPs (Xu et al., 2018).

The Setiu Wetland is influenced by Asia's tropical monsoon season, particularly the strong NEM, with heavy precipitation occurring from September to March every year (Suratman et al., 2016). As a total comparison, temporal patterns have a stronger effect, especially between monsoonal seasons for surface water in determining the transportation of MPs compared to spatial pattern. However, MP distribution in the surface water and sediment shows a strong variation based on sampling time, which can influence the distribution of MPs in sediments differently. The fifth sampling (July 2017) showed the lowest abundance of MPs on the water surface. The temporal distributions of MPs in the surface water and sediment are listed in Supplementary 2. The biplot interaction shows MPs' classification tendencies in surface water in November 2016, September 2017, and November 2017, where the wetlands received rainfall during the monsoon season (Fig. 3(b)). During this time, there was heavy rain, and subsequently, flooding occasionally occurred. Rainfall and floods transported debris from the land, increasing the abundance of MPs (Gündoğdu et al., 2018). The second biplot interaction shows that MP abundance in the sediment tended to become dominant during the third (March 2017) and fifth (July 2017) samplings, but it was negatively correlated in the first sampling (November 2016) (Fig. 3(c)). March and July are known to be the dry season in this area (east side of Peninsular Malaysia) when the south-west monsoon occurs on the west side of Peninsular Malaysia. A hot climate may accelerate the fragmentation of MPs. Consequently, the fragmentation process occurred and increased MPs' abundance (Andrady, 2015). Therefore, a longer time-series analysis is needed to assume accumulation and degradation of MPs in seawater and sediment. The results of this investigation imply that filament, film, and transparent types are the primary MP categories found in the water surface and sediment of the Setiu Wetland. Moreover, in our assumption, the characteristics of MP abundance analyzed in this study could have been highly correlated with the nearest local aquacultural activity, as discussed earlier.

4.3. Relationship between physicochemical analysis of water quality and MP distribution

The statistical analysis clearly showed that MPs in sediments had a relationship with the salinity value of the estuarine environment (Table 1). Thus, the origin of the MPs in the estuarine environment may therefore be clarified. In addition, each polymer has different density properties, where, for instance, a less-dense polymer will float in a denser medium (Hidalgo-Ruz et al., 2012), while marine water plays an important role in the transfer of MPs to the estuarine environment included in this study. Wind and water currents serve as driving forces for floating MPs in water. Consequently, the movement of floating MPs is not stable relative to nonmobile sediments. However, biofouling increases the driving force of MPs, which are continually deposited from the water surface and are persistent in sediments. For example, a light-weight polypropylene polymer was discovered in sediments in the current study. This indicates that water and sediments act as mobilizing forces and contribute to the sinking of MPs.

The pH value is an important indicator for monitoring the quality of water. Low pH values were recorded at ST2 and ST3, both of which are located nearby cage culture sites. Therefore, the degradation of organic waste such as fecal matter and food pellets can also result in acidic water columns and the distribution of MPs (Ibrahim et al., 2017). In addition, repeated loss and degradation from the site will result in the abundance of filaments (e.g., from fishnets and fishing line) ending up

Table 3

A summary of worldwide comparisons of MPs' distribution in estuarine areas in different environmental matrices.

No.	Location	Equipment	Type of sample	MPs (mean/range)	MPs (shape)	Source	Polymer	Reference
1	Coastal mangrove, Singapore	Quadrat (1.5 m × 1.5 m)	Sediment	36.8 ± 23.6 items/kg	Fiber Film Granule	Aquaculture & Tourism activities	PP, PE, Nylon, PVC	Mohamed Nor and Obbard, 2014
2	Gulf of Mexico	Quadrat (0.25 m × 0.25 m)	Sediment	5–117 items/m ²	Fiber Fragment, Film Foam	Marine water input	PP, PE, PS, PES, PA ES, PA	Wessel et al., 2016
3	Changjiang, China	Box corer	Sediment	121 ± 9 items/kg	Fiber Fragment Pellet	Laundry activities	Rayon, PE, acrylic, PET, Poly (ethylene,propylene,diene), PS	Peng et al., 2017
4	Derwent Estuary, Tasmania, Australia	Core	Sediment	571 items/kg	Fiber Sheet Fragment Microbead	Sewage & stormwater outfall drains	Not available	Willis et al., 2017
5	Changjiang, China	Stainless steel sieve (70 µm)	Water	230 ± 180 items/m ³	Fiber Fragment Film	Aquaculture & Tourism activities	PE, PP, PVC, PA, ABS, PS, PC, ASA, PUR, SAN	Xu et al., 2018
6	Yondingxinhe, China	Stainless steel sieve (48 µm)	Water	788.0 ± 464.2 items/m ³	Fiber Fragment Foam Pellet	Freshwater & marine water intrusion	PE, PP, PS, PVC, PET	Wu et al., 2019
	Haihe, China	Stainless steel sieve (48 µm)	Water	1485.7 ± 819.9 items/m ³				
		Quadrat (1 m × 1 m)	Sediment	216.1 ± 92.1 items/kg				
7	Pearl River, China	Stainless steel sieve (50 µm)	Water	8902 items/m ³	Film Granule Fiber	Wastewater discharge	PA, PP, PE, cellophane, VACs, PVC	Yan et al., 2019
8	Shanghai, China	Stainless steel material	Water	27,840 ± 11,810 particles/m ³	Fiber Granule Film Fragment	Commercial & tourism activities	PE, PP, PS, PC	Zhang et al., 2019
9	Jagir, Indonesia	Ekman dredge	Sediment	414 items/kg	Fiber Fragment Film Filament	Laundry activities & municipal waste discharge	PES, LDPE, PP	Firdaus et al., 2020
10	Setiu Wetland, Malaysia	Ponar grab	Sediment	0.750 ± 3.838–14.25 ± 4.343 items/g	Film Filament	Aquaculture, fisheries & other anthropogenic activities	PP	Present study
		Stainless steel bucket	Water	0.251 ± 0.139–0.540 ± 0.139 items/L	Film Foam	Freshwater & marine water intrusion		

in the sediments. Thus, both parameters turned out to be critical for describing the potential sources of MPs' distribution at Setiu Wetland. It is notable that, even if the pH was negatively correlated with the amount of MPs in the water surface and sediment, the accumulation of higher MPs at both stations is suggested to be due to water stagnation or less efflux during the sampling period, as well as both stations are far from the sea opening.

4.4. Microplastic analysis with emphasize on the plastic weathering and limitations of the study

During the sampling events, different MPs' shapes and colors were successfully identified (Fig. 4). Discoloration occurs when MPs were exposed to ultraviolet (UV) light for too long, subsequently accelerating pale and transparent colors (Karthik et al., 2018). Marine organisms may mistakenly ingest transparent MPs because of their broad distribution in the environment (Ibrahim et al., 2016). Thus, the abundance of transparent MPs in this study may cause many marine organisms to frequently mistaken MPs as a food source because of their high concentration and less visibility compared with colored MPs.

In addition, there is a possibility for the fragmentation of MPs due to thermo-oxidative (heat) and photo-oxidative (light) degradations, as clearly shown in SEM images in Fig. 5. The enlarged views in SEM images (Fig. 5b, d and f) show the cracked and roughness of the surface, thus proved the weathering and aging patterns of MPs found in this study, possibly caused by both thermo- and photo oxidative

degradation due to long exposure in the environment, thus in agreement with the previous report by Crawford and Quinn (2016). In addition, the irregular shape is evidence of the mechanical breakage of plastic to form secondary MPs, similarly reported by Wang et al. (2017). With a decrease in the size of MPs, the possibility of MPs' abundance in the surface water and sediment becomes higher. The sample collected from high oxidative weathering influenced the brittle structure of the sample, thereby indicating the weak resistance of MPs toward heat and UV light, which could also have been due to continuous exposure to the UV light (Tiwari et al., 2019). Contrary to optical inspection, SEM analysis can be regarded as a standard method for fast screening of MP particles but with visual and economical limitations. It is worthwhile to mention that while morphological observation by SEM is an excellent method for reconfirming the physical characteristics of MPs, a detail analysis with Energy Dispersive X-Ray spectroscopy (EDX/EDS) is suggested for further elemental analysis on the surface topography of the polymer. Previously, SEM was used in conjunction with EDS for screening of MPs in fish (Wang et al., 2017; Jonathan et al., 2021) and marine debris (Gniadek and Dabrowska, 2019). However, the shortcomings associated to this technique, for instance, cost and instrument availability are of concern.

The ATR-FTIR identified MPs as polypropylene polymer. It should be noted that because of the FTIR sample size limitation, only large MP particles (> 200 µm) could be characterized and identified by FTIR spectroscopy. However, its ability to characterize the associated polymer based on the characteristic and fingerprint regions makes it very useful

for obtaining chemical information about MPs (Jung et al., 2018). Interestingly, the spectrum peak shows the presence of a peak band at $\sim 1720\text{ cm}^{-1}$, distinguished as a carbonyl group ($\text{C}=\text{O}$) (Supplementary 4). Therefore, it is speculated that these MP particles have been oxidized when exposed to environmental conditions, where the attachment of the methyl group to the polymeric chain introduced a tertiary carbon (oxidation site) as shown at 1720 cm^{-1} (Crawford and Quinn, 2016). Zhu et al. (2018) stated that the polypropylene polymer was dominated by potential source materials related to fishery activities. Setiu Wetland is considered a natural protected area, with only small-scale brackish caged culture, farming and fishing activities (Azmi et al., 2012; Ibrahim et al., 2017). The fisheries tools (e.g. ropes, fishing lines, and nets) are possibly fragmented and dispersed in the aquatic environment, similar to the previously reported in the mangrove areas in Singapore and Shanghai (Mohamed Nor and Obbard, 2014; Peng et al., 2017). However, the limitation of the single ATR-FTIR model used (can only be used for a large number of analytes, i.e., filament) may discriminate against the identification of other types of polymers that may also have been present in this study.

Pyr-GC/MS is a thermal decomposition of materials where a molecule will be cleaved at a very high temperature in a pyrolyzer, thus produced a smaller components before they were separated in a GC column and detected by MS (Kusch, 2017). The pyrolytic products revealed the presence of cyclohexane derivatives in both samples, thus suggested as one of the significant products to identify the MPs polymer. This is somewhat similar to those previously reported by Dekiff et al. (2014). These derivatives act as an essential compound in polypropylene and other semisynthetic polymers. Previously, Kusch (2017) indicated that branched alkenes (C_6 and C_9) as major components for polypropylene polymer, and reflected the compounds listed in the Table 2. Furthermore, it is also found that tridecane ($\text{C}_{13}\text{H}_{28}$) and 2,2,4,4,6,8,8-heptamethyl-nonane are other fragmentation products of the polymer. Although, other fragments such as 2,4-dimethyl-1-heptene and 2,4-dimethyl-3-cyclohexene were not recorded in the pyrogram for the present study. The possible reasons include the differences in GC conditions/programs and pyrolyzer heating mechanisms used, and changes in the polymeric backbones due to external environmental factors. The MPs in the aquatic environment undergo environmental degradation, causing the molecular chain of polymers to change. This indicates that the degradation reaction of polypropylene will randomly occur with the breakdown of bonds between polymer molecules, thus forming a mixture of hydrocarbons (Tsuge et al., 2011).

It is also noteworthy that only two particles from FTIR analysis had been subjected to Pyr-GC/MS (each one from water and sediment samples), thus would undermine the identification and could not represent all analytes. Nevertheless, the Pyr-GC/MS technique used herein to identify polymers is also limited, e.g., selected standard references for polymer pyrolytic products are not readily available (Peters et al., 2018), and this instrument also not routinely accessible (i.e. costly). On the basis of the results, Pyr-GC/MS serves as a promising complementary analysis of chemical characterization to identify the polymer.

5. Conclusions

This study presented evidence of the widespread nature of MPs and their spatiotemporal distribution in Setiu Wetland Malaysian estuarine area for the first time. A high distribution of MPs in this area may be the result of floating MPs derived from marine water, water stagnation and in situ fragmentation from fisheries and aquaculture sites. In addition, cyclohexane and its derivatives, the pyrolytic products found associated to the thermal degradation of polypropylene, may leach out into the environment and endanger marine organisms. Therefore, further research is needed for a more comprehensive understanding of the chemistry of the polymers found in the area, and their associated impacts in the aquatic environment. The

results presented in this paper provide baseline information and good understanding of the distribution and occurrence of MPs in the Setiu Wetlands. This research can also be used as a reference for future studies in monitoring MPs' distribution in Malaysia mangrove areas and help to guide the policy maker in addressing their impact, thus support the implementation of Malaysia's Roadmap Toward Zero Single-Use Plastics 2018–2030: Toward a Sustainable Future and other regional environmental regulations.

Supplementary data to this article can be found online at <https://doi.org/10.1016/j.scitotenv.2021.147809>.

CRedit authorship contribution statement

S.R.H. carried out the sampling and laboratory works, including physical and chemical analysis, drafted the manuscript; S.T.A. performed the chemical analysis and interpretation; W.M.A.W.M.K and K.M.K.K.Y analyzed the data and performed the statistical analysis; Y.S.I. designed the study, carried out the sampling, drafted the manuscript and completed the manuscript.

Funding

This research was funded by a grant (FRGS 59457) under the Ministry of Higher Education (MOHE), Malaysia.

Declaration of competing interest

The authors declare that they have no known competing financial interests or personal relationships that could have appeared to influence the work reported in this paper.

Acknowledgments

The authors are very grateful to the Ministry of Higher Education (MOHE) for awarding research grant FRGS 59457 to Y.S. Ibrahim and financially support the research. The authors also thank UNESCO IOC-WESTPAC and other MRIG team members, Prof. Dr. Norhayati Tahir, Dr. Siti Aishah Abdullah, Che Mohd Zan Husin, Yuzwan Mohamad and Siti Syazwani Azmi for their guidelines and technical supports throughout the study. The authors are thankful to the Faculty of Science and Marine Environment, Institute of Oceanography and Environment (INOS) and Universiti Malaysia Terengganu for providing research facilities. The authors also wish to acknowledge all anonymous reviewers for their valuable comments.

References

- Alam, F.C., Sembiring, E., Muntalif, B.S., Suendo, V., 2019. Microplastic distribution in surface water and sediment river around slum and industrial area (case study: Ciwalengke River, Majalaya district, Indonesia). *Chemosphere* 224, 637–645. <https://doi.org/10.1016/j.chemosphere.2019.02.188>.
- Amin, M.R., Sohaimi, E.S., Tuan Anuar, S., Bachok, Z., 2020. Microplastic ingestion by zooplankton in Terengganu coastal waters, Southern South China Sea. *Mar. Pollut. Bull.* 150. <https://doi.org/10.1016/j.marpolbul.2019.110616>.
- Andrady, A.L., 2015. Persistence of plastic litter in the oceans. In: Bergmann, M., Gutow, L., Klages, M. (Eds.), *Marine Anthropogenic Litter*. Springer International Publishing, Cham, pp. 57–72. <https://doi.org/10.1007/978-3-319-16510-3>.
- Arthur, C., Baker, J., Bamford, H., 2009. *Proceedings of the International Research Workshop on the Occurrence, Effects, and Fate of Marine Debris*. NOAA Technical Memorandum NOS-OR&R-30. Available online at: <https://marinedebris.noaa.gov/file/2192/download?token=5dvqb-YY>.
- Azmi, W.A., Ghazi, R., Mohamed, N.Z., 2012. Importance of carpenter bee, *Xylocopa varipuncta* (Hymenoptera: Apidae) as pollination agent for mangrove community of Setiu Wetlands, Terengganu, Malaysia. *Sains Malaysiana* 41, 1057–1062.
- Barasarathi, J., Agamuthu, P., Emenike, C.U., Fauziah, S.H., 2014. Microplastic abundance in selected mangrove forest in Malaysia. *Proceeding of the ASEAN Conference on Science and Technology, Indonesia*, 2014, pp. 1–5.
- Besseling, E., Wegner, A., Foekema, E.M., Van Den Heuvel-Greve, M.J., Koelmans, A.A., 2013. Effects of microplastic on fitness and PCB bioaccumulation by the lugworm *Arenicola marina* (L.). *Environ. Sci. Technol.* 47, 593–600. <https://doi.org/10.1021/es302763x>.

- Browne, M.A., Crump, P., Niven, S.J., Teuten, E., Tonkin, A., Galloway, T., Thompson, R., 2011. Accumulation of microplastic on shorelines worldwide: sources and sinks. *Environ. Sci. Technol.* 45 (21), 9175–9179. <https://doi.org/10.1021/es201811s>.
- Cai, H., Du, F., Li, L., Li, B., Shi, H., 2019. A practical approach based on FT-IR spectroscopy for identification of semi-synthetic and natural celluloses in microplastic investigation. *Sci. Total Environ.* 669, 692–701. <https://doi.org/10.1016/j.scitotenv.2019.03.124>.
- Cole, M., Lindeque, P., Halsband, C., Galloway, T.S., 2011. Microplastics as contaminants in the marine environment: a review. *Mar. Pollut. Bull.* 62, 2588–2597. <https://doi.org/10.1016/j.marpolbul.2011.09.025>.
- Crawford, Christopher Blair, Quinn, B., 2016. *Microplastic Pollutants*. Elsevier, Amsterdam, p. 2017.
- Dekiff, J.H., Remy, D., Klasmeier, J., Fries, E., 2014. Occurrence and spatial distribution of microplastics in sediments from Norderney. *Environ. Pollut.* 186, 248–256. <https://doi.org/10.1016/j.envpol.2013.11.019>.
- Ding, L., Mao, R.F., Guo, X., Yang, X., Zhang, Q., Yang, C., 2019. Microplastics in surface waters and sediments of the Wei River in northwest of China. *Sci. Total Environ.* 667, 427–434. <https://doi.org/10.1016/j.scitotenv.2019.02.332>.
- Enders, K., Stedmon, C.A., Nielsen, T.G., 2015. Abundance, size and polymer composition of marine microplastics $\geq 10 \mu\text{m}$ in the Atlantic Ocean and their modelled vertical distribution. *Mar. Pollut. Bull.* 100, 70–81. <https://doi.org/10.1016/j.marpolbul.2015.09.027>.
- EO, S., Hong, S.H., Song, Y.K., Lee, J., Shim, W.J., 2018. Abundance, composition, and distribution of microplastics larger than 20 mm in sand beaches of South Korea. *Environ. Pollut.* 238, 894–902. <https://doi.org/10.1016/j.envpol.2018.03.096>.
- Farrell, P., Nelson, K., 2013. Trophic level transfer of microplastic: *Mytilus edulis* (L.) to *Carcinus maenas* (L.). *Environ. Pollut.* 177, 1–3. <https://doi.org/10.1016/j.envpol.2013.01.046>.
- Fauziah, S.H., Liyana, I.A., Agamuthu, P., 2015. Plastic debris in the coastal environment: the invincible threat? Abundance of buried plastic debris on Malaysian beaches. *Waste Manag. Res.* 33, 812–821. <https://doi.org/10.1177/0734242X15588587>.
- Firdaus, M., Trihadiningrum, Y., Lestari, P., 2020. Microplastic pollution in the sediment of Jagir Estuary, Surabaya City, Indonesia. *Mar. Pollut. Bull.* 150. <https://doi.org/10.1016/j.marpolbul.2019.110790>.
- Gniadek, M., Dabrowska, A., 2019. The marine nano- and microplastics characterisation by SEM-EDX: the potential of the method in comparison with various physical and chemical approaches. *Mar. Pollut. Bull.* 148, 210–216. <https://doi.org/10.1016/j.marpolbul.2019.07.067>.
- Gündoğdu, S., Çevik, C., Ayat, B., Aydoğan, B., Karaca, S., 2018. How microplastics quantities increase with flood events? An example from Mersin Bay NE Levantine coast of Turkey. *Environ. Pollut.* 239, 342–350. <https://doi.org/10.1016/j.envpol.2018.04.042>.
- Hidalgo-Ruz, V., Gutow, L., Thompson, R.C., Thiel, M., 2012. Microplastics in the marine environment: a review of the methods used for identification and quantification. *Environ. Sci. Technol.* 46, 3060–3075. <https://doi.org/10.1021/es2031505>.
- Ibrahim, Y.S., Azzura Azmi, A., Abdul Shukur, S., Tuan Anuar, S., Aishah Abdullah, S., 2016. Microplastics ingestion by *Scapharca cornea* at Setiu Wetland, Terengganu, Malaysia. *Middle-East J. Sci. Res.* 24, 2129–2136. <https://doi.org/10.5829/idosi.mejsr.2016.24.06.23654>.
- Ibrahim, Y.S., Rathnam, R., Anuar, S.T., Khalik, W.M.A.W.M., 2017. Isolation and characterization of microplastic abundance in *Lates calcarifer* from Setiu Wetlands, Malaysia. *Malaysian J. Anal. Sci.* 21, 1054–1064. <https://doi.org/10.17576/mjas-2017-2105-07>.
- Jaafar, N., Musa, S.M., Azfaralrifi, A., Mohamed, M., Yusoff, A.H., Lazim, A.M., 2020. Improving the efficiency of post-digestion method in extracting microplastics from gastrointestinal tract and gills of fish. *Chemosphere* 260, 127649. <https://doi.org/10.1016/j.chemosphere.2020.127649>.
- Jambeck, J.R., Geyer, R., Wilcox, C., Siegler, T.R., Perryman, M., Andrady, A., et al., 2015. Plastic waste inputs from land into the ocean. *Science* 347, 768–771. <https://doi.org/10.1126/science.1260352>.
- Jonathan, M.P., Sujitha, S.B., Rodriguez-Gonzalez, F., Villegas, L.E.S., Hernandez-Camacho, C.J., Sarkar, S.K., 2021. Evidences of microplastics in diverse fish species off the Western coast of Pacific Ocean, Mexico. *Ocean Coast. Manag.* 204, 105544. <https://doi.org/10.1016/j.ocecoaman.2021.105544>.
- Jung, M.R., Horgen, F.D., Orski, S.V., Rodriguez, V.C., Beers, K.L., Balazs, G.H., Jones, T.T., Work, T.M., Brignac, K.C., Royer, S.-J., Hyrenbach, K.D., Jensen, B.A., Lynch, J.M., 2018. Validation of ATR FT-IR to identify polymers of plastic marine debris, including those ingested by marine organisms. *Mar. Pollut. Bull.* 127, 704–716. <https://doi.org/10.1016/j.marpolbul.2017.12.061>.
- Kalnasa, M.L., Lantaca, S.M.O., Boter, L.C., Flores, G.J.T., Galarpe, V.R.K.R., 2019. Occurrence of surface sand microplastic and litter in Macajalar Bay, Philippines. *Mar. Pollut. Bull.* 149, 110521. <https://doi.org/10.1016/j.marpolbul.2019.110521>.
- Karbalaei, S., Golieskardi, A., Hamzah, H.B., Abdulwahid, S., Hanachi, P., Walker, T.R., et al., 2019. Abundance and characteristics of microplastics in commercial marine fish from Malaysia. *Mar. Pollut. Bull.* 148, 5–15. <https://doi.org/10.1016/j.marpolbul.2019.07.072>.
- Karthik, R., Robin, R.S., Purvaja, R., Ganguly, D., Anandavelu, I., Raghuraman, R., et al., 2018. Microplastics along the beaches of southeast coast of India. *Sci. Total Environ.* 645, 1388–1399. <https://doi.org/10.1016/j.scitotenv.2018.07.242>.
- Khalik, W.M.A.W.M., Ibrahim, Y.S., Tuan Anuar, S., Govindasamy, S., Baharuddin, N.F., 2018. Microplastics analysis in Malaysian marine waters: a field study of Kuala Nerus and Kuantan. *Mar. Pollut. Bull.* 135, 451–457. <https://doi.org/10.1016/j.marpolbul.2018.07.052>.
- Kusch, P., 2017. Application of pyrolysis-gas chromatography/mass spectrometry (Py-GC/MS). *Compr. Anal. Chem.* 75, 169–207. <https://doi.org/10.1016/bb.coac.2016.10.003>.
- Li, J., Zhang, H., Zhang, K., Yang, R., Li, R., Li, Y., 2018. Characterization, source, and retention of microplastic in sandy beaches and mangrove wetlands of the Qinzhou Bay, China. *Mar. Pollut. Bull.* 136, 401–406. <https://doi.org/10.1016/j.marpolbul.2018.09.025>.
- Ma, Z.F., Ibrahim, Y.S., Lee, Y.Y., 2020. Microplastic pollution and health relevance to the Malaysia's roadmap to zero single-use plastic 2018–2030. *Malays. J. Med. Sci.* 27 (3), 1–6. <https://doi.org/10.21315/mjms2020.27.3.1>.
- Maes, T., Van der Meulen, M.D., Devriese, L.L., Leslie, H.A., Huvet, A., Frère, L., Robbens, J., et al., 2017. Microplastics baseline surveys at the water surface and in sediments of the north-East Atlantic. *Front. Mar. Sci.* 4, 1–13. <https://doi.org/10.3389/fmars.2017.00135>.
- Mahmud, M.R., Hashim, M., Matsuyama, H., Numata, S., Hosaka, T., 2018. Spatial down-scaling of satellite precipitation data in humid tropics using a site-specific seasonal coefficient. *Water* 10, 409. <https://doi.org/10.3390/w10040409>.
- Mai, L., Bao, L.J., Shi, L., Wong, C.S., Zeng, E.Y., 2018. A review of methods for measuring microplastics in aquatic environments. *Environ. Sci. Pollut. Res.* 25, 11319–11332. <https://doi.org/10.1007/s11356-018-1692-0>.
- Masura, J., Baker, J., Foster, G., Arthur, C., 2015. In: Herring, C. (Ed.), *Laboratory Methods for the Analysis of Microplastics in the Marine Environment: Recommendations for Quantifying Synthetic Particles in Waters and Sediments*. NOAA Technical Memorandum.
- Ministry of Energy, Science, Technology, Environment & Climate Change (MESTECC), Malaysia, 2018. *Malaysia's Roadmap Towards Zero Single-use Plastics 2018–2030 Towards a Sustainable Future*.
- Mohamed Nor, N.H., Obbard, J.P., 2014. Microplastics in Singapore's coastal mangrove ecosystems. *Mar. Pollut. Bull.* 79, 278–283. <https://doi.org/10.1016/j.marpolbul.2013.11.025>.
- Ory, N.C., Gallardo, C., Lenz, M., Thiel, M., 2018. Capture, swallowing, and egestion of microplastics by a planktivorous juvenile fish. *Environ. Pollut.* 240, 566–573. <https://doi.org/10.1016/j.envpol.2018.04.093>.
- Peng, G., Zhu, B., Yang, D., Su, L., Shi, H., Li, D., 2017. Microplastics in sediments of the Changjiang Estuary, China. *Environ. Pollut.* 225, 283–290. <https://doi.org/10.1016/j.envpol.2016.12.064>.
- Peters, C.A., Hendrickson, E., Minor, E.C., Schreiner, K., Halbur, J., Bratton, S.P., 2018. Py-GC/MS analysis of microplastics extracted from the stomach content of benthivore fish from the Texas Gulf Coast. *Mar. Pollut. Bull.* 137, 91–95. <https://doi.org/10.1016/j.marpolbul.2018.09.049>.
- PlasticsEurope, 2018. *Plastics - The Fact 2018: An Analysis of European Plastics Production, Demand and Waste data*.
- Praveena, S.M., Shaifuddin, S.N.M., Akizuki, S., 2018. Exploration of microplastics from personal care and cosmetic products and its estimated emissions to marine environment: an evidence from Malaysia. *Mar. Pollut. Bull.* 136, 135–140. <https://doi.org/10.1016/j.marpolbul.2018.09.012>.
- R Development Core Team, 2011. R: A language and environment for statistical computing. R Foundation for Statistical Computing, Vienna <http://www.R-project.org>.
- Rochman, C.M., Browne, M.A., Underwood, A.J., van Franeker, J.A., Thompson, R.C., Amaral-Zerler, L.A., 2016. The ecological impacts of marine debris: unraveling the demonstrated evidence from what is perceived. *Ecology* 97, 302–304. <https://doi.org/10.1890/14-2070.1>.
- Sarijan, S., Azman, S., Said, M.I.M., Andu, Y., Zon, N.F., 2018. Microplastics in Sediment From Skudai and Tebrau river, Malaysia: A Preliminary Study. *MATEC Web Conf.*, p. 250. <https://doi.org/10.1051/mateconf/201825006012>.
- Su, L., Cai, H., Kolandhasamy, P., Wu, C., Rochman, C.M., Shi, H., 2018. Using the Asian clam as an indicator of microplastic pollution in freshwater ecosystems. *Environ. Pollut.* 234, 347–355. <https://doi.org/10.1016/j.envpol.2017.11.075>.
- Suratman, S., Hussein, A., Tahir, N.M., Latif, M.T., Mostapa, R., Weston, K., 2016. Seasonal and spatial variability of selected surface water quality parameters in Setiu Wetland, Terengganu, Malaysia. *Sains Malaysia* 45, 551–558.
- Tiwari, M., Rathod, T.D., Ajmal, P.Y., Bhargava, R.C., Sahu, S.K., 2019. Distribution and characterization of microplastics in beach sand from three different Indian coastal environments. *Mar. Pollut. Bull.* 140, 262–273. <https://doi.org/10.1016/j.marpolbul.2019.01.055>.
- Tsuge, S., Ohtani, H., Watanabe, C., 2011. *Pyrolysis-GC/MS Data Book of Synthetic Polymers. Pyrograms, Thermograms and MS of Pyrolyzates*. Elsevier, Amsterdam.
- Varikoden, H., Preethi, B., Samah, A.A., Babu, C.A., 2011. Seasonal variation of rainfall characteristics in different intensity classes over peninsular Malaysia. *J. Hydrol.* 404, 99–108. <https://doi.org/10.1016/j.jhydrol.2011.04.021>.
- Wang, Z.M., Wagner, J., Ghosal, S., Bedi, G., Wall, S., 2017. SEM/EDS and optical microscopy analyses of microplastics in ocean trawl and fish guts. *Sci. Total Environ.* 603–604, 616–626. <https://doi.org/10.1016/j.scitotenv.2017.06.047>.
- Wessel, C.C., Lockridge, G.R., Battiste, D., Cebrian, J., 2016. Abundance and characteristics of microplastics in beach sediments: insights into microplastic accumulation in northern Gulf of Mexico estuaries. *Mar. Pollut. Bull.* 109, 178–183. <https://doi.org/10.1016/j.marpolbul.2016.06.002>.
- Willis, K.A., Eriksen, R., Wilcox, C., Hardisty, B.D., 2017. Microplastic distribution at different sediment depths in an urban estuary. *Front. Mar. Sci.* 4, 1–8. <https://doi.org/10.3389/fmars.2017.00419>.
- Wu, N., Zhang, Y., Zhang, X., Zhao, Z., He, J., Li, W., et al., 2019. Occurrence and distribution of microplastics in the surface water and sediment of two typical estuaries in Bohai Bay, China. *Environ. Sci. Process Impacts* 21, 1143–1152. <https://doi.org/10.1039/c9em00148d>.

- Xu, P., Peng, G., Su, L., Gao, Y., Gao, L., Li, D., 2018. Microplastic risk assessment in surface waters: a case study in the Changjiang Estuary, China. *Mar. Pollut. Bull.* 133, 647–654. <https://doi.org/10.1016/j.marpolbul.2018.06.020>.
- Yan, M., Nie, H., Xu, K., He, Y., Hu, Y., Huang, Y., et al., 2019. Microplastic abundance, distribution and composition in the Pearl River along Guangzhou city and Pearl River estuary, China. *Chemosphere* 217, 879–886. <https://doi.org/10.1016/j.chemosphere.2018.11.093>.
- Zhang, J., Zhang, C., Deng, Y., Wang, R., Ma, E., Wang, J., et al., 2019. Microplastics in the surface water of small-scale estuaries in Shanghai. *Mar. Pollut. Bull.* 149, 110569. <https://doi.org/10.1016/j.marpolbul.2019.110569>.
- Zhu, L., Bai, H., Chen, B., Sun, X., Qu, K., Xia, B., 2018. Microplastic pollution in North Yellow Sea, China: observations on occurrence, distribution and identification. *Sci. Total Environ.* 636, 20–29. <https://doi.org/10.1016/j.scitotenv.2018.04.182>.

ARTICLES FOR FACULTY MEMBERS

MICROPLASTICS AND MARINE ENVIRONMENT

Title/Author	<p>Spatial and temporal variations of microplastic concentrations in Portland's freshwater ecosystems / Talbot, R., Granek, E., Chang, H., Wood, R., & Brander, S.</p>
Source	<p><i>Science of The Total Environment</i> Volume 833 (2022) 155143 Pages 1-14 https://doi.org/10.1016/J.SCITOTENV.2022.155143 (Database: ScienceDirect)</p>



Spatial and temporal variations of microplastic concentrations in Portland's freshwater ecosystems



Rebecca Talbot ^a, Elise Granek ^b, Heejun Chang ^{a,*}, Rosemary Wood ^b, Susanne Brander ^c

^a Department of Geography, Portland State University

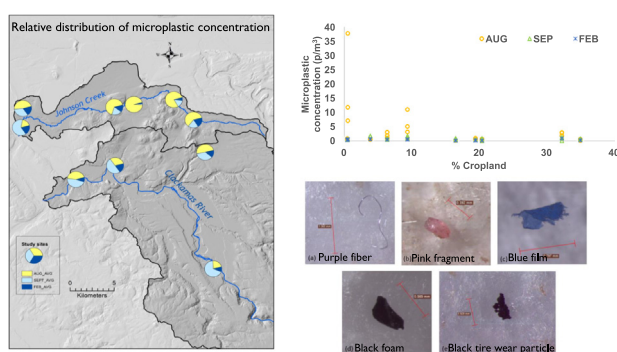
^b Department of Environmental Science and Management, Portland State University

^c Department of Fisheries, Wildlife, and Conservation Sciences; Coastal Oregon Marine Experiment Station, Oregon State University

HIGHLIGHTS

- Lower water velocity rates may have facilitated the accumulation of microplastics.
- Nearstream analyses explained more MP concentrations than watershed analyses.
- Larger size microplastics dominated in the high-flow event samples.
- Fragments were the dominant microplastic morphology observed.
- Polyethylene was the dominant polymer type, followed by polypropylene.

GRAPHICAL ABSTRACT



ARTICLE INFO

Editor: Thomas Kevin V

Keywords:

Microplastics
Freshwater pollution
Land use
Precipitation
Scale
GIS

ABSTRACT

While microplastics are a pollutant of growing concern in various environmental compartments, less is known regarding the sources and delivery pathways of microplastics in urban rivers. We investigated the relationship between microplastic concentrations and various spatiotemporal factors (e.g., land use, arterial road length, water velocity, precipitation) in two watersheds along an urban-rural gradient in the Portland metropolitan area. Samples were collected in August, September, and February and were analyzed for total microplastic count and type. Nonparametric statistics were used to evaluate potential relationships with the explanatory variables, derived at both the subwatershed and near stream scales. In August, microplastic concentrations were significantly higher than in February. August concentrations also negatively correlated with flow rate, suggesting that lower flow rates may have facilitated the accumulation of microplastics. Smaller size microplastic particles ($< 100 \mu\text{m}$) were found more in August than September and February, while larger size particles were more dominant in February than the other months. Microplastic concentrations were positively related to 24-h antecedent precipitation in February. Negative correlations existed between wet season microplastic concentrations and agricultural lands at the near stream level. The results indicate that near stream variables may more strongly influence the presence and abundance of microplastics in Portland's waterways than subwatershed-scale variables. Fragments were the most commonly observed microplastic morphology, with a dominance of gray particles and the polymer polyethylene. The findings of this study can inform management decisions regarding microplastic waste and identify hotspots of microplastic pollution that may benefit from remediation.

1. Introduction

Microplastics are an increasing concern in aquatic environments, capable of entering the food web and potentially endangering human health (Baldwin et al., 2020, Li et al., 2020). Microplastic research first gained

* Corresponding author.

E-mail address: changh@pdx.edu (H. Chang).

traction in the 1970s (Carpenter and Smith, 1972), with studies largely addressing marine environments over the next several decades. Freshwater microplastic pollution is a relatively new field of research, with articles published only within the last ten to fifteen years (Granek et al., 2020; Talbot and Chang, 2022). This research expansion has provided valuable insights into the microplastic cycle and the factors that influence their accumulation and distribution in freshwater bodies. River systems, in particular, are critical transportation pathways, carrying microplastics from inland regions to estuarine and marine environments (Jiang et al., 2019; Zhao et al., 2019). Thus, understanding their presence in freshwater environments can shed light on their abundance in marine waters, which may be greater than previously estimated due to recent evaluations of riverine microplastic flux (Hurley et al., 2018).

Developed and industrial regions have been closely linked with microplastic pollution, in part due to high rates of plastic production and increased littering (Huang et al., 2020; Ma et al., 2021; Mani et al., 2015; Townsend et al., 2019). Positive correlations have also been found between microplastic pollution and percent of impervious cover in watersheds, which greatly serves to enhance plastic transport to aquatic environments (Baldwin et al., 2016). In addition, wastewater treatment plants (WWTPs) are often situated in developed areas, and have been linked with increased microplastic concentrations downstream of effluent outfalls (Estahbanati and Fahrenfeld, 2016; Hoellein et al., 2017). Most treatment processes are not designed to remove tiny plastic particles, and may result in WWTPs serving as important delivery pathways of microplastics to freshwater environments (Mani et al., 2015; McCormick et al., 2016). Additionally, population density has been positively correlated with microplastic concentrations (Battulga et al., 2019; Huang et al., 2020; Kataoka et al., 2019; Ma et al., 2021; Mani et al., 2015; Valine et al., 2020; Yonkos et al., 2014).

Microplastic pollution may also be linked with agricultural regions (Kapp and Yeatman, 2018). Biosolids produced from WWTP processes are commonly used as a fertilizer for crops, yet their application on agricultural lands can result in the introduction of microplastics (particularly microfibrils) to these environments (Edo et al., 2020; Leslie et al., 2017). While agricultural soils may serve as a sink for many of these plastic particles (Feng et al., 2020), these soils and the plastics they contain may also be vulnerable to reentering surface water bodies during storms and subsequent runoff events (Kapp and Yeatman, 2018; Peller et al., 2019). Additionally, agricultural regions tend to include the heavy use of plastics (e.g., tarps), which can break down over time and potentially enter freshwater bodies (Campanale et al., 2020b; Feng et al., 2020; Grbić et al., 2020; Guerranti et al., 2017).

In addition to variations in spatial distribution, microplastic concentrations vary on a temporal basis as well (Talbot and Chang, 2022), in part due to precipitation and runoff (Cheung et al., 2019; Xia et al., 2020). For instance, many studies report increased microplastic concentrations during the wet season, as land-based microplastics may be introduced to waterways via storm runoff (Eo et al., 2019; Hurley et al., 2018). As such, precipitation may serve to flush microplastics into aquatic environments with subsequent increased microplastic concentrations reported (Hitchcock, 2020; Schmidt et al., 2018; Wong et al., 2020). However, negative relationships have also been observed between precipitation/discharge and microplastic abundance, with the former potentially causing decreased concentrations of the latter due to dilution effects (Barrows et al., 2018; Stanton et al., 2020). These findings indicate the need for additional research conducted on finer temporal scales. Flow rate has also been linked with microplastic concentrations, with gentler hydrodynamics potentially facilitating their accumulation (Kapp and Yeatman, 2018; Mani et al., 2015; Xiong et al., 2019; Watkins et al., 2019). Conversely, higher flow rates in the center of rivers have resulted in observations of decreased microplastic concentrations, with river banks serving as microplastic sinks (Tibbetts et al., 2018).

As research in the field of freshwater microplastics is still in the early stages, much is still unknown regarding their spatial and temporal distributions and links to potential sources. Many studies include a snapshot of

microplastic pollution (i.e., a single sampling session) in freshwater bodies (Di and Wang, 2018; Hoellein et al., 2017; Mao et al., 2020). Few studies have examined variations in microplastic concentrations as a function of seasonality, with even fewer addressing variations observed within the wet season. Differences likely exist between microplastic concentrations in the early versus the late wet season due to factors such as the flush effect and flow dependency (Watkins et al., 2019). Thus, our understanding of the drivers of microplastic abundance would greatly benefit from such a temporal comparison.

Additionally, there are few studies that address microplastic concentrations along a broad urban-rural gradient (Campbell et al., 2017; Campanale et al., 2020b; Lahens et al., 2018). Analyses of this type are particularly critical, as their examination could reveal potential sources and delivery pathways of microplastic pollution. Furthermore, while the presence of other pollutants and contaminants has been well-documented in rivers in the Portland area (Chang et al., 2019; Chen and Chang, 2019; Chen and Chang, 2014; Pratt and Chang, 2012), much remains unclear regarding the degree to which microplastics impact Portland's freshwater bodies (Valine et al., 2020).

This study aims to address these data and knowledge gaps by investigating microplastics in Portland watersheds with varying degrees of development, and by evaluating temporal variability in microplastic concentrations and attributes with different flow regimes. In particular, the objectives of this research are to (i) evaluate how watershed attributes such as land use, arterial road length, and slope influence microplastic concentrations, (ii) evaluate the influence of temporal variability on microplastic concentrations and attributes such as size and color, (iii) evaluate the influence of water velocity and precipitation on microplastic concentrations and loads, and (iv) determine the most common microplastic morphologies (e.g., fiber, fragment, etc.) to evaluate links with potential sources. It is hypothesized that larger size and higher concentrations and loads of microplastics will be found adjacent to developed and agricultural areas as well as in wet season samples, particularly early in the season due to flush effects.

2. Methods

2.1. Study area

Two Portland area watersheds served as the focal points for this study, including the Clackamas River watershed and the Johnson Creek watershed (Fig. 1). These watersheds were selected to assess potential microplastic distributions along an urban-rural gradient in the Portland metropolitan area. Both are comprised of a range of land cover characteristics, thus exposing their waterways to a multitude of anthropogenic activities. The upper reaches of Johnson Creek flow through a continuum of rural and agricultural lands, and the lower reaches are exposed to a much greater degree of development. The Clackamas River also spans an urban-rural gradient, with upper reaches adjacent to forested and mountainous regions and lower reaches located near agricultural lands and varying degrees of development. The Clackamas is a major tributary to the Willamette River and serves as a source of drinking water to 350,000 residents in the Portland metro area (Chen and Chang, 2019). The main soil type present in the study region is silt loam (Natural Resources Conservation Service, 2021).

Samples were collected from 10 study sites, with four located in the Clackamas River watershed and six in the Johnson Creek watershed (Table 1). The majority of sites were selected to coincide with USGS gaging stations, with the intent of using USGS flow data when riverine conditions prevented the collection of such data in situ. There are three exceptions to this, including one site located near the confluence of Rock Creek and the Clackamas River that was selected to further represent potential impacts of developed and residential regions on microplastic pollution. Additionally, one site is located on the North Fork of Deep Creek, a tributary to the Clackamas that is heavily influenced by agricultural activities. Lastly,

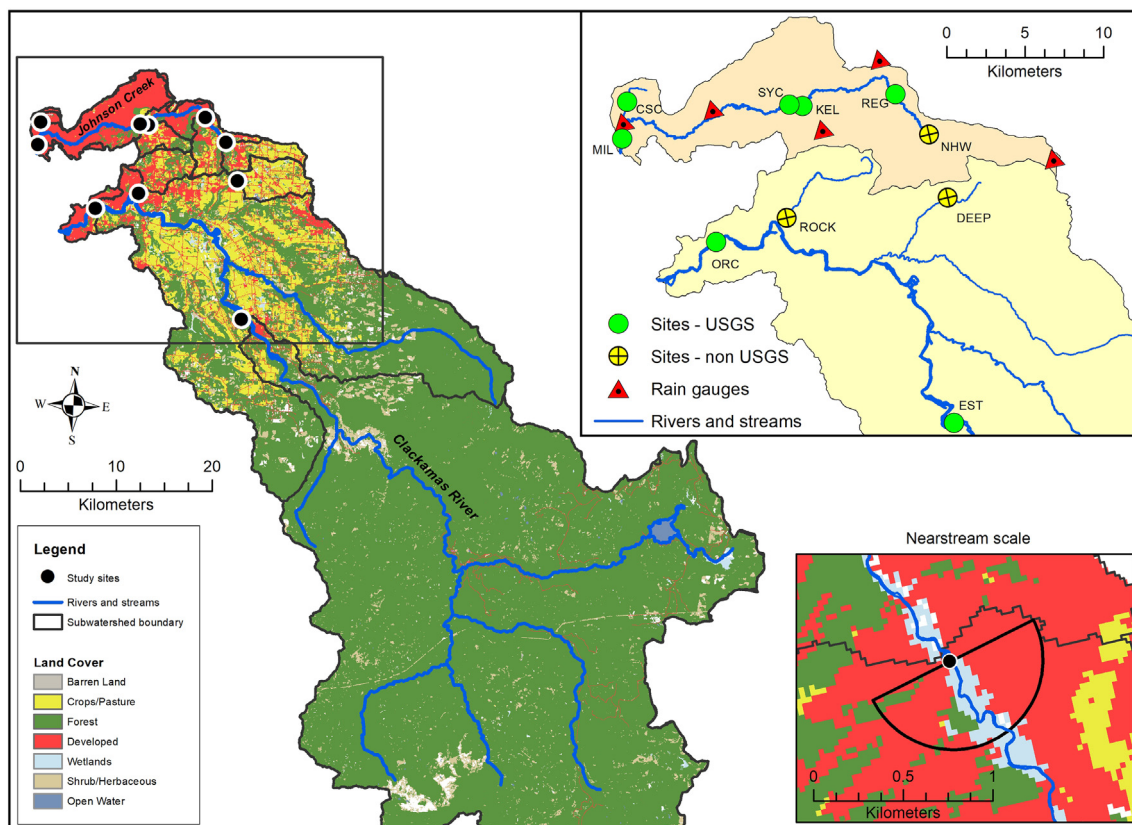


Fig. 1. Map of study area land cover, study sites and rain gauges, at the subwatershed and nearstream scales of analysis.

one site is located near the headwaters of Johnson Creek to further shed light on microplastic sources to the river.

2.2. Data and derivation of explanatory variables

Average flow velocity measurements over 60-second intervals were collected during each sampling session with a Marsh McBirney Flo-Mate flow meter. When river conditions prevented the safe collection of these data (namely the February sampling sessions for the Sycamore and Milwaukie sites), USGS data were downloaded from the National Water Information System (NWIS) database (USGS Water Data for the Nation, 2021) for

Table 1
Characteristics of stream monitoring sites used for analysis.

Monitoring sites	USGS gaging number	Drainage area (km ²)	Elevation (m)	Dominant land cover (%)
Johnson Creek				
Near headwaters* (NHW)	–		119	Agriculture (50%)
Regner Rd, Gresham (REG)	14,211,400	39.78	91.5	Developed (44%)
Kelley Creek (KEL)	14,211,499	12.15	74.7	Developed (47%)
Sycamore (SYC)	14,211,500	69.41	68.5	Developed (69%)
Milwaukie (MIL)	14,211,550	137.71	6.0	Developed (90%)
Crystal Springs Creek (CSC)	14,211,542	7.90	13.3	Developed (93%)
Clackamas River				
Estacada (EST)	14,210,000	1737.88	87.4	Forest (92%)
Deep Creek* (DEEP)	–		141.0	Agriculture (62%)
Rock Creek* (ROCK)	–		39.0	Developed (43%)
Near Oregon City (ORC)	14,211,010	2434.59	9.0	Forest (58%)

* Not a USGS monitoring site.

stream gauges corresponding with the microplastic sampling locations. In these instances, similar historical discharge/gauge measurements were identified and the corresponding velocity readings were included in the current study. For the Estacada site, 15-minute incremental precipitation data were obtained from the USGS gaging station located on site. Hourly precipitation data were obtained from the City of Portland HYDRA Rainfall Network for the remaining nine sites, and data from the gauges closest in proximity to the study sites were used (particularly if they were located upstream), and are thus estimates of precipitation at the sites (Bureau of Environmental Services, 2021).

Subwatersheds were delineated for each study site using ArcHydro Tools in ArcGIS 10.8.1 (ESRI, 2020), resulting in the creation of distinct, non-overlapping polygons (Mainali and Chang, 2018; Pratt and Chang, 2012). A land cover raster layer of Oregon was downloaded from the National Land Cover Dataset (NLCD) 2019 (Multi-Resolution Land Characteristics Consortium, 2021), and clipped to the subwatershed boundaries. Because the NLCD dataset includes a broad range of land cover categories, they were combined into a single category as appropriate (e.g., deciduous forest, evergreen forest, and mixed forest were combined into a single ‘forest’ category). Total percentage of each land cover category (agricultural, developed, forest, shrub, and barren) were then derived for each subwatershed by utilizing the zonal histogram tool in ArcGIS. Additionally, subwatershed area was derived for each site.

Nearstream buffer zones were also created in ArcGIS, in which a 500 m upstream buffer was derived for each study site. Mainali and Chang (2018) found that nearstream buffer zones (i.e., a 100 m circular upstream buffer and a 1 km riparian upstream buffer) more fully accounted for processes involved in water quality, with watershed-scale processes being less influential. As the current study included a single nearstream analysis, and as a 1 km upstream buffer would have resulted in overlapping buffer zones across several sites, 500 m was deemed an appropriate upstream buffer

(Fig. 1). Slope was derived in ArcGIS at both scales, in which the zonal statistics by table tool was used to calculate the average slope within each subwatershed and within each nearstream buffer zone (Table 2). In addition, total arterial road length in the nearstream buffer zones for each site was computed using the statistics function in ArcGIS.

2.3. Data collection

2.3.1. Preparatory work

Before collecting samples at the study sites, materials were prepared in the Applied Coastal Ecology (ACE) lab at Portland State University. Quart-sized glass mason jars were rinsed three times with filtered (0.7 μm) deionized (DI) water, with a layer of aluminum foil present underneath the cap to prevent contamination from the plastic ring present in the cap. Jars were then filled partway with filtered DI water, to be used for rinsing the contents of the cod-end into the sample mason jar. Mason jars were also labeled with appropriate sampling information, including the month, site, and subsample number.

2.3.2. Sample collection

Samples were collected via wading from the center of the stream, where possible. Sites for which this was not possible (namely sites directly along the Clackamas) required a different approach, which involved wading into the river and collecting samples at a standard depth of one meter. Otherwise, water depth at each sampling location was recorded using a meter stick. Where possible, stream width was also measured and recorded using a transect tape. Before beginning sample collection, the plankton net and cod-end were rinsed three times in the river water to prevent cross-contamination from previous sites.

Samples were captured by completely submerging an 80 μm mesh plankton tow net just below the water surface for 15-minute intervals (Valine et al., 2020) and holding it stationary. While excess water flowed directly through the net, microplastic particles and bits of organic debris (most commonly leaves, pine needles, and twigs) were captured in the cod-end that was attached to the tapered end of the plankton net (these larger pieces of organic debris were later rinsed thoroughly into the corresponding sample during processing and then discarded, see Appendix S1). Three replicates were collected per site to examine within-site microplastic variability, and given that within-site microplastic subsamples are not substantially different except for a few August samples (Table S1), these values were subsequently averaged (Campanale et al., 2020b; Valine et al., 2020). A control jar filled with DI water was placed next to the sampling site, and the lid was removed when each sampling session commenced and closed at the completion of sampling to capture airborne microplastics.

At the end of each sampling interval, the net was positioned upright and rinsed down thoroughly with river water to move microplastics down into the cod-end. The cod-end was tapped periodically as necessary to allow for excess water to escape, and the sample was poured into the appropriately labeled mason jar. The cod-end was then rinsed thoroughly with filtered DI water to collect any microplastics that may have been stuck to the sides, and poured into the mason jar. Once the lid was placed over the sample, the lid for the control jar was also replaced. The net and cod-end were then separated and thoroughly rinsed in the river before departing for the

next site. All samples were stored in refrigerators until the commencement of laboratory procedures.

Samples were collected during three sampling sessions to investigate the impacts of temporal variability on microplastic concentrations (Barrows et al., 2018). The first session took place on August 28–30, 2020 and represented microplastic abundances during the dry season and thus without the influence of antecedent precipitation. Only one session was conducted in the dry season, as microplastic concentrations are unlikely to vary significantly throughout summer baseflow conditions. The second sampling session took place on September 24–25, 2020, representing microplastic concentrations in the early wet season when land-based microplastics have been flushed into aquatic environments (Hitchcock, 2020; Kataoka et al., 2019). The last sampling session occurred in the middle of the wet season on February 2–4, 2021, when microplastic concentrations in rivers are potentially more flow-dependent and less impacted by flush effects (Kataoka et al., 2019; Yonkos et al., 2014).

Water volume for each subsampling was computed using the following equation:

$$\text{Volume} = A \times T \times V \text{ (m/s)}$$

Where: A = area of the net opening (m^2); T = sampling duration (s); V = average velocity of the water (m/s) (Campanale et al., 2020a).

Microplastic concentrations were computed by dividing the total count of each subsample by the water volume sampled, thus standardizing the data (de Carvalho et al., 2021). The microplastic concentrations of each subsample were then averaged at each site during each sampling session, resulting in a single microplastic concentration per site per season. In addition, daily microplastic loads were calculated by multiplying the average microplastic concentration at each site for each sample date by the corresponding daily average discharge (Park et al., 2020) and then multiplying by the total number of seconds in a day (86,400). It is important to note that these calculations were performed only at study sites for which USGS daily average discharge data were available (EST, ORC, REG, KEL, SYC, and MIL).

2.3.3. Sample processing

In preparation for microscope analyses, a series of laboratory procedures were conducted to isolate microplastics on filter papers (Whatman 1820-047 Glass Microfiber Binder Free Filter, 1.6 μm , 4.3 s/100 mL Flow Rate, Grade GF/A, 4.7 cm Diameter) (Valine et al., 2020). Samples were first put through an organic matter digestion step using a 10% potassium hydroxide solution (methods adapted from Baechler et al., 2020), then filtered through a 63 μm sieve, followed by density separation using a hypersaline solution. Lastly, they were vacuum filtered onto filter paper, each of which was stored in a petri dish in a covered cardboard box until microscope analysis with a Leica MZ6 dissecting microscope (12–120 \times magnification). Further details regarding laboratory procedures are given in Appendix S1.

For microscope analyses, stickers showing 12 numbered pie wedges were first affixed to the bottom of each petri dish to aid in both orientation and the tracking of relative locations of plastic particles. Filters were examined using a Leica MZ6 dissecting microscope, and methodologies outlined

Table 2
Variables used in analysis of microplastics in two Portland metro watersheds.

Variable type	Agency source	Data	Derived variable	Original data
Independent	MRLC	National land cover dataset 2019 (30 m)	Agriculture (%) Urban (%) Forest (%)	Pasture, cultivated crops, hay Low, medium, high intensity developed Deciduous, evergreen, mixed
Independent	Oregon Metro	Oregon 30 m DEM	Subwatershed and nearstream slope averages (deg)	Slope (deg)
Independent	Oregon Metro	Streets layer (m)	Total arterial road length in nearstream buffer zones	Arterial road length (m)
Independent	USGS	Streamflow (15–60 min intervals)	M/s at time of sampling	Discharge (cms)
Independent	HYDRA	Precipitation (60-min intervals)	24- and 72-h antecedent precip (mm)	Precipitation amount (mm)
Independent	USGS	Precipitation (15-min intervals)		
Dependent	This study	Microplastic concentration	Count per volume (particle/ m^3)	Total microplastic count and water volume sampled

in the Guide to Microplastic Identification (Marine & Environmental Research Institute, nd) were followed to aid in the distinction between microplastics and biotic material. For instance, particles showing cellular structure were excluded, along with fiber-like particles characterized by tapering. Additionally, particles that broke apart upon manipulation with a metal probe were also excluded. In these instances, the particle in question was assumed to be biological or non-plastic in nature.

Filter inspection began in the upper left section and continued in a straight line across the filter paper, with the aforementioned metal probe used to explore and prod particles to determine flexibility. Inspection of the row below commenced at the right side of the paper and continued to the left, and this horizontal pattern was repeated for each row of the filter paper. When a suspected microplastic was identified, information regarding type (fiber, fragment, film, foam, tire wear particle), color, maximum length, and magnification level were recorded on a datasheet. In addition, photographs were taken of each suspected microplastic and saved to a google drive for future reference and use. A control petri dish with a clean filter was placed next to the scope to assess contamination from airborne particles, and was evaluated for microplastics between each scoped study sample (Valine et al., 2020).

2.3.4. Quality control

Given the mesh size of the plankton tow net, the study focused on particles greater than 80 μm , but some particles between 63 and 80 μm were retained due to the use of a 63 μm sieve during processing; we include all microplastics >63 μm in our dataset. To minimize the risk of contamination, orange cotton jumpsuits were worn during sample collection, lab procedures, and microscope analyses. In addition, nitrile gloves were worn during all lab procedures and analyses. Any orange particles noted in samples were excluded from the final microplastic counts. Both field and laboratory controls were employed to evaluate background microplastic contamination in these environments (Brander et al., 2020). To address potential contamination during laboratory processing, lab controls comprised of 270 mL of filtered DI water underwent the same digestion procedures as field samples, with one control digested with each batch of field samples. Lab controls were also employed during density separation procedures to capture any airborne microplastics. To address contamination during sample collection, a field control jar with filtered DI water was present at each site for each sampling session, with the lid of the control open only during active sample collection.

2.3.5. Subsampling for analytical confirmation

A subset of particles was sent to the Ecotox and Environmental Stress Lab at Oregon State University for micro-Fourier transform infrared (μFTIR) spectroscopy analysis to identify specific polymers and validate total counts (Baechler et al., 2020; Wang et al., 2020). As part of the selection process, samples were first randomized, as were the 12 sections of each petri dish. To additionally ensure that particles were randomly selected, the authors agreed pre-microscopy to select the third observed microplastic within a specified section for μFTIR analysis. One hundred and one particles from field samples were selected by this randomized process, and an additional five were specifically selected to examine particles of interest. In addition, ten particles from controls were included for analysis.

It is important to note that tire wear particles are difficult to identify using μFTIR spectroscopy, and are more reliably confirmed through methods such as pyrolysis gas chromatography (Primpke et al., 2020; Werbowski et al., 2021). For this reason, the authors placed a cap on the total number of TWPs that were submitted for μFTIR analysis.

2.3.6. μFTIR analysis

Particles selected for μFTIR represented approximately 10% of the total suspected microplastics (Baechler et al., 2020; Harris et al., 2022). The proportion of particles analyzed was based on a combination of variability in particle morphologies found in our samples and funds available for analysis. We are confident that the particles analyzed are representative of the entire sample, and based our rationale for particle

subsampling and analysis on Brander et al. (2020) and Cowger et al. (2021). μFTIR methodologies were similar to those detailed by Harris et al., 2022. Briefly, under a laminar-flow hood, particles were picked from filters and stored between glass microscope slides. Each particle was confirmed under a Leica EZ4E to match with images from PSU. Samples were placed on a gold-plated slide and subsequently reflectance was measured using a Thermo Electron iN5 μFTIR (Thermo Fisher Scientific), followed by insertion of a germanium tip probe (ATIR) approximately 1–2 μm into the material's surface. A math match cut-off of 70 or greater was used for all samples, with all spectra being confirmed and smoothed via Open Specy (Cowger et al., 2021) and cross-checked with Omnic software per methods adapted from Baechler et al. (2020) and Harris et al., 2022 (Fig. S1).

2.3.7. Statistical analysis

Statistical analyses were conducted in R, version 1.4.1717 (R Core Team, 2021), using the corrplot (v0.90; Wei and Simko, 2021), the FSA (v0.9.1; Ogle et al., 2021), the lattice (Sarkar, 2008), the ggbiplot (v0.55; Vu, 2011), and the plyr (Wickham, 2011) packages. Because assumptions of normality and equal variance were not met, nonparametric statistics were used to assess potential relationships between explanatory variables and microplastic concentrations. To determine potential influences of temporal variability, a Kruskal-Wallis rank sum test was run to compare average microplastic size, concentrations, and morphologies across the three sampling sessions. To assess whether differences may exist between sites, the ten study sites were first divided into two groups based on land use. At the subwatershed scale, the Developed group was comprised of sites with subwatersheds characterized by greater than 40% developed land (CSC, MIL, SYC, ROCK, REG, and KEL), with the Mixed/Rural group comprised of the remainder (EST, ORC, DEEP, and NHW). At the nearstream scale, the Developed group was comprised of sites with nearstream regions characterized by greater than 60% developed land (DEEP, CSC, NHW, REG, SYC, and MIL), with the Mixed/Rural group comprised of the remainder (EST, ROCK, ORC, and KEL). These groups were then further subdivided based on sampling session, for a total of six groups. Kruskal-Wallis rank sum tests were then run to compare average microplastic concentrations based on these site categories as a function of sampling session, and to compare microplastic morphologies and size classes across the sampling sessions.

Spearman's rank correlation was used to compare average microplastic concentrations with spatial and temporal predictor variables. Spatial variables included subwatershed area, total arterial road length, land use, and slope (the latter two included both subwatershed and nearstream scales, see Table S2 for correlations between spatial explanatory variables). Temporal variables included average water velocity during each sampling session, 24-hour antecedent rainfall, and 72-hour antecedent rainfall.

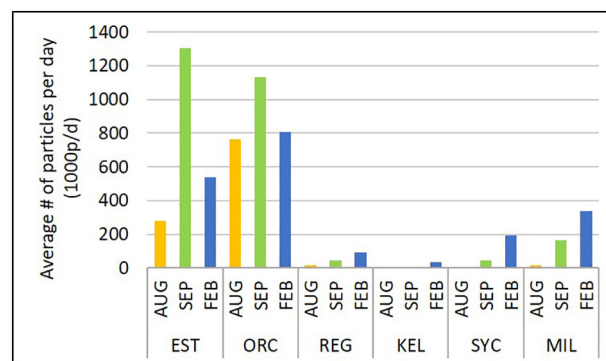


Fig. 2. Daily microplastic loads at six USGS gaging stations across the three sampling sessions.

3. Results

3.1. Characteristics of microplastics

Microplastics were found at all sites, with a total of 1009 particles observed across the 90 field samples. An additional 490 particles were found across the 30 field and 53 lab controls (Table S3A, Table S3B). Scope controls revealed minimal aerial deposition of microplastics, with a fiber typically noted every few field samples (Table S3C). Four microplastic morphologies were observed in field samples, including fragments ($n = 505$, 50.1%), fibers ($n = 173$, 17.1%), films ($n = 71$, 7%), and foams ($n = 23$, 2.3%) (Fig. 3). Additionally, 237 suspected tire wear particles (23.5%) were observed in field samples. Throughout the visual identification process, suspected TWPs displayed a unique set of characteristics that set them apart from other morphologies. More specifically, their appearance was generally bumpy/rough and rubbery in nature, typically cylindrical in shape, black in color, and quite pliable (Klasios et al., 2021; Parker et al., 2020).

Microplastics fell into one of nine color categories: gray ($n = 367$, 36.4%), black ($n = 313$, 31%), blue ($n = 174$, 17.2%), white/clear ($n = 66$, 6.5%), pink ($n = 39$, 3.9%), green ($n = 17$, 1.7%), red ($n = 17$, 1.7%), purple ($n = 10$, 1%), and yellow ($n = 6$, 0.6%) (Fig. 4). Microplastics were also divided into five size classes (Campanale et al., 2020b; Cheung et al., 2019; Huang et al., 2020): 63-100 μm ($n = 17$, 1.7%), 101-500 μm ($n = 402$, 39.8%), 501-1000 μm ($n = 318$, 31.5%), 1001-2000 μm ($n = 184$, 18.2%), and 2001-5000 μm ($n = 88$, 8.7%) (Fig. 5a). Thus, microplastics less than 0.5 mm in length comprised over 40% of the observed plastics, with nearly three-fourths of particles measuring less than 1 mm. μFTIR analyses of the 116 submitted particles identified a total of nine polymer types: polyethylene (PE), polypropylene (PP), polystyrene (PS), polyethylene terephthalate (PET), cellulose, cellophane, ethylene vinyl acetate, polyvinyl acrylonitrile, and styrene butadiene (likely tire particles). Dominant polymers in field samples included PE (30%), PP (27%), cellulose (17%), and PET (9%) (Fig. 6): See Fig. S1 for example spectra of PE, PP, PET, cellulose, and styrene butadiene and Fig. S2 for typical polymers.) For Fig. 6, it is important to note that the authors included very few TWPs in μFTIR analyses, due to the difficulty in identifying them via this method of spectroscopy. For this reason, TWPs appear to comprise a

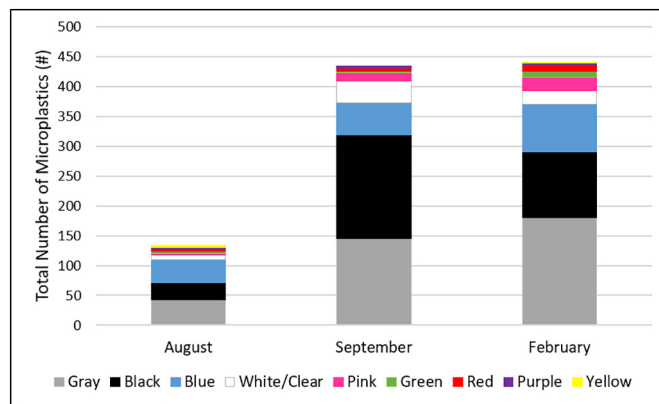


Fig. 4. Color composition of microplastics across three sampling sessions.

very small percentage of the observed polymers. Additionally, over half of the analyzed particles were fragments, with approximately one-quarter in the 101-500 μm size class. Every particle evaluated by μFTIR was either synthetic or anthropogenically impacted (modified by humans such as cellulose, wool clothing; per Harris et al., 2022).

3.2. Differences across sites and sampling sessions

While the highest microplastic abundances for each sampling session were observed at the MIL site (August: $n = 30$; September: $n = 207$; February: $n = 135$), the KEL site had the highest concentration for August (37.73 p/m^3), the MIL site had the highest concentration for September (1.76 p/m^3), and the NHW site had the highest concentration for February (0.89 p/m^3). Calculations of daily microplastic loads at six study sites showed the highest loads at the EST and ORC sites, particularly during the September sampling session (Fig. 2). The abundance of microplastics in the 101-500 μm size class differed significantly between August and September (Kruskal-Wallis, $H(2) = 9.2408$, $p < 0.05$), with these particles dominating in the September sampling session. In addition, the abundance of microplastics in the 2001-5000 μm size class differed significantly between September and

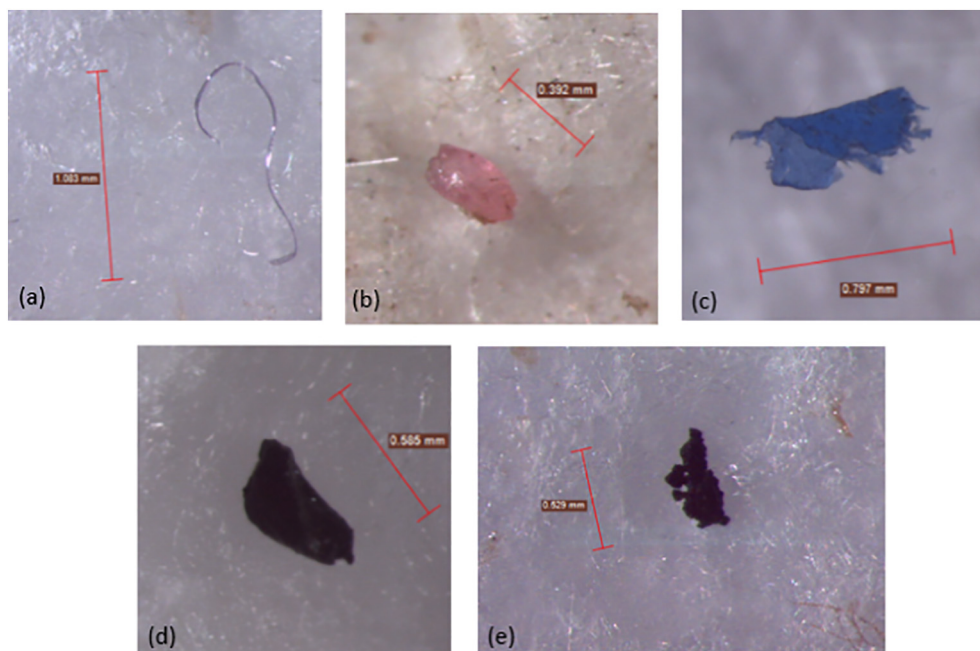


Fig. 3. Examples of microplastics found in Johnson Creek and the Clackamas River, Oregon USA: (a) purple fiber; (b) pink fragment; (c) blue film; (d) black foam; and (e) black tire wear particle.

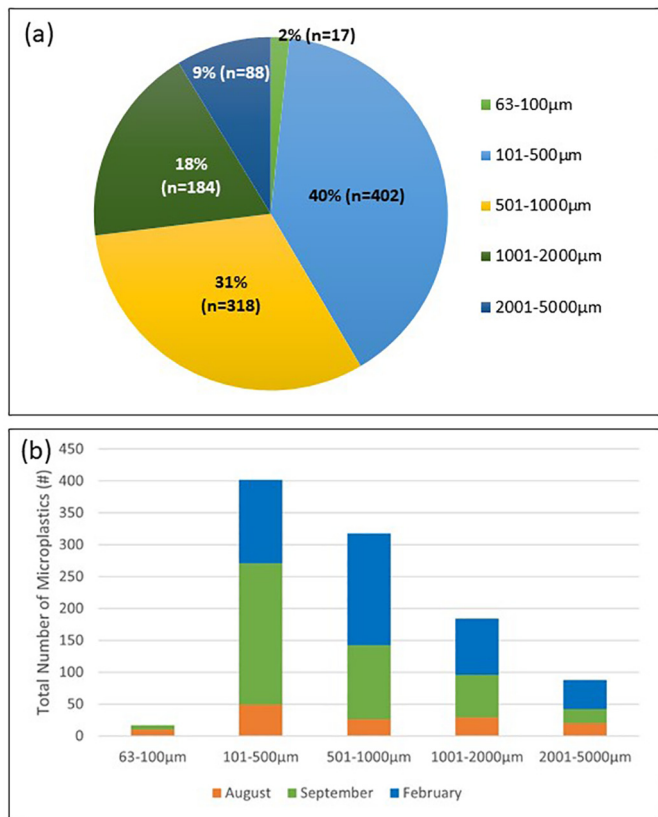


Fig. 5. (a) Size composition of microplastics; and (b) distribution of size classes across the three sampling sessions.

February (Kruskal-Wallis, $H(2) = 6.0872, p < 0.05$), with higher abundances observed in February (Fig. 5b). Differences were also found between the average microplastic concentrations observed during the three sampling sessions (Kruskal-Wallis, $H(2) = 6.1342, p < 0.05$). Results of a post-hoc Dunn test were inconclusive due to low statistical power, but an examination of boxplots indicated differences between August and February. More specifically, average microplastic concentrations were highest in August ($3.24 \pm$

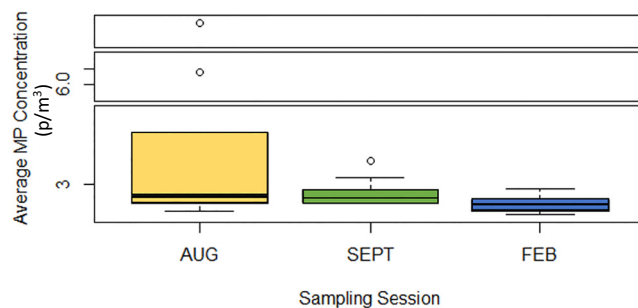


Fig. 7. Average microplastic concentrations in Johnson Creek and the Clackamas River, Oregon, USA during three sampling sessions in 2020 and 2021.

1.84 p/m^3) and lowest in February ($0.365 \pm 0.076 p/m^3$) (Fig. 7). Microplastic concentrations ranged from 0.19–18.86 p/m^3 in August, 0.43–1.69 p/m^3 in September, and 0.09–0.85 p/m^3 in February (Fig. 8).

At the subwatershed scale, no differences in average microplastic concentrations were observed between the Developed and Mixed/Rural groups (Kruskal-Wallis, $H(5) = 8.2333, p > 0.1$). A difference was observed at the nearstream scale (Kruskal-Wallis, $H(5) = 11.852, p < 0.05$), with a post-hoc test revealing a significant difference between the August sampling at Developed sites (higher concentrations) and the February sampling of Mixed/Rural sites (lower concentrations) (Dunn's test, $p < 0.05$). Thus, despite sampling across multiple land use types and sampling sessions, there only existed a difference between August and February, with no differences between the Developed and Mixed/Rural groups observed during any single sampling session.

Proportions of the microplastic morphologies appeared to vary across the sampling sites and sessions (Fig. 9). Of particular note is the relatively low proportion of fibers present at the EST and ORC sites in the dry season, which then became the dominant morphology for both sites in the mid-wet season. Conversely, three Johnson Creek sites (REG, KEL, and SYC) demonstrated the opposite trend, in which fibers were the dominant morphology in the dry season and then dropped to much lower proportions in the mid-wet season. Several morphologies showed statistically significant differences across sampling sessions, including fiber concentrations (Kruskal-Wallis, $H(2) = 8.0852, p < 0.05$), film concentrations (Kruskal-Wallis, $H(2) = 6.1258, p < 0.05$), and tire wear particle (TWP) concentrations (Kruskal-Wallis, $H(2) = 8.6157, p < 0.05$). A post-hoc Dunn test

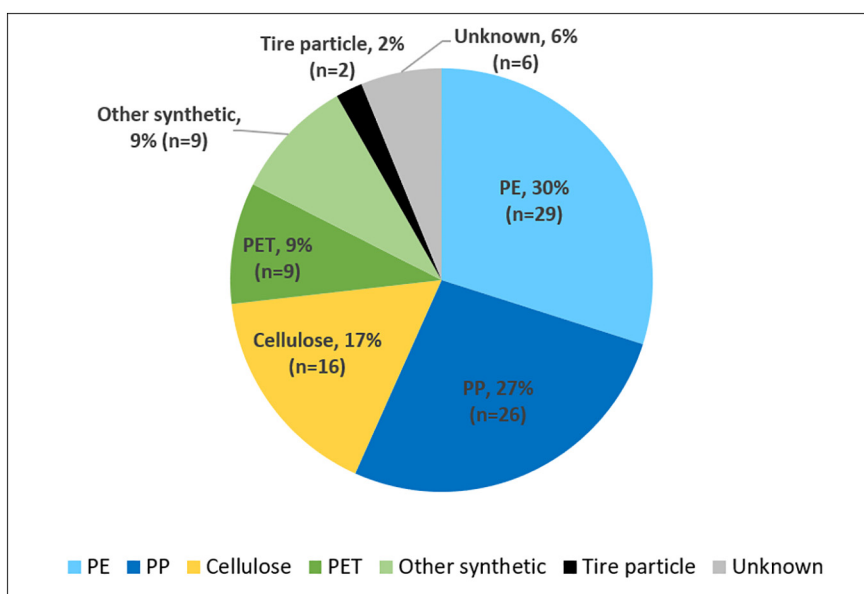
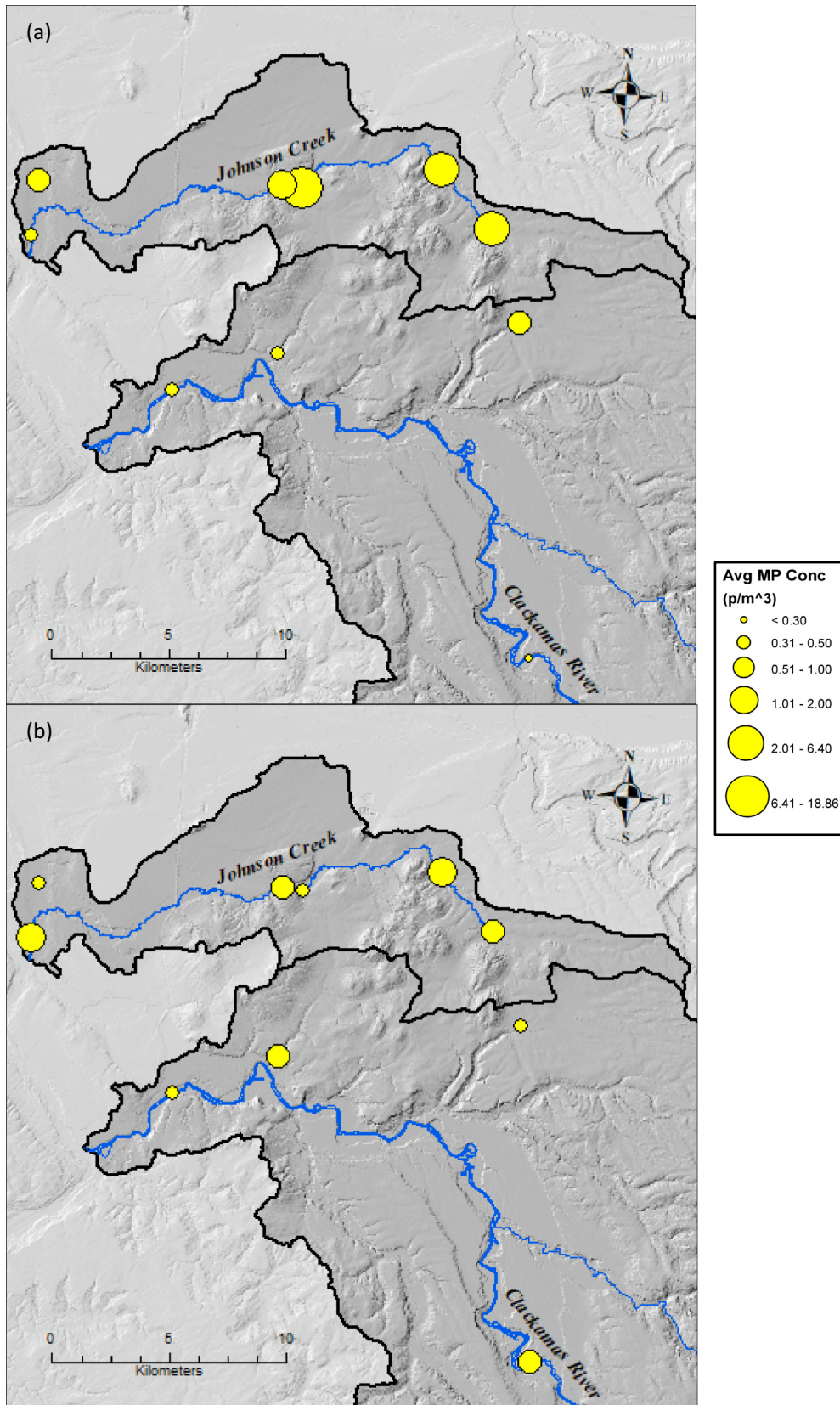


Fig. 6. Polymer composition of microplastics evaluated by μ FTIR spectroscopy. Note: only one PE particle was characterized as high-density PE, the rest were comprised of low-density PE.



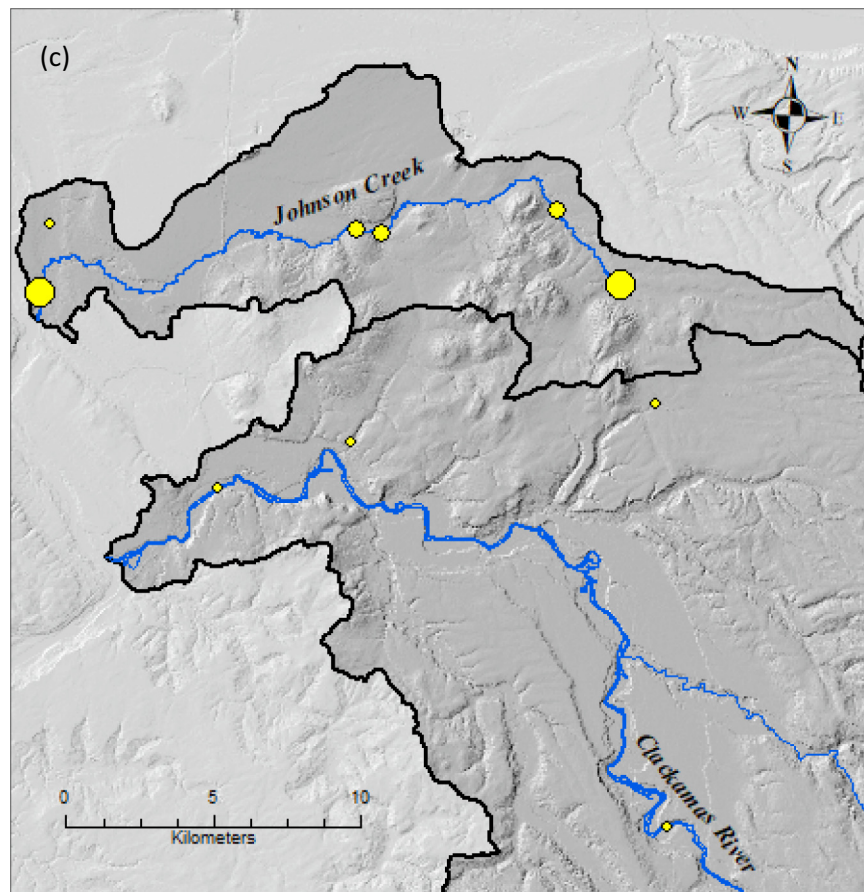


Fig. 8. Microplastic concentrations at each monitoring site in Johnson Creek and the Clackamas River, Oregon, USA during the sampling sessions of (a) August 2020 (b) September 2020 and (c) February 2021.

revealed that August TWP concentrations differed significantly from September concentrations ($p < 0.05$), with higher concentrations observed in September. August fiber and film concentrations differed from February concentrations ($p < 0.05$), with higher concentrations for both morphologies observed in August.

3.3. Correlations between microplastic concentrations and explanatory variables

Average microplastic concentrations for each of the three sampling sessions were correlated with several spatial and temporal variables (Tables 3 and 4, respectively). Only two correlations were significant with regard to temporal factors, with higher microplastic concentrations in August linked with lower average water velocities ($r = -0.854, p < 0.05$) and higher microplastic concentrations in February coinciding with increased rainfall in the 24 h preceding sample collection ($r = 0.638, p < 0.05$). At the spatial level, both September and February microplastic concentrations were lower in predominantly agricultural lands at the nearstream scale ($r = -0.721, p < 0.05$ and $r = -0.673, p < 0.05$, respectively). Sites with greater proportions of shrub land had lower microplastic concentrations in February at the subwatershed scale ($r = -0.721, p < 0.05$), and greater subwatershed area was linked with lower microplastic concentrations in August. ($r = -0.673, p < 0.05$).

4. Discussion

4.1. Microplastic characteristics

Fragments were the dominant morphology observed in this study, similar to findings from previous studies (Bertoldi et al., 2021; Mai et al., 2021; Tibbetts et al., 2018). Fibers have also been noted as a dominant

morphology (Belen Alfonso et al., 2020; Chen et al., 2020; Feng et al., 2020; Hu et al., 2020), though they were the second most common morphology at our study sites. The dominance of gray particles in the current study is unusual (with the bulk of gray particles analyzed by μ FTIR being PE, followed closely by PP), as the literature shows that dominant colors typically include blue (Barrows et al., 2018; Dris et al., 2018; Miller et al., 2017; Strady et al., 2020), clear/white (Baldwin et al., 2020; Di and Wang, 2018; Han et al., 2020; Huang et al., 2020), and black (Guerranti et al., 2017; Qin et al., 2020; Sang et al., 2021). Greater proportions of clear/white plastics in particular may result from processes such as photodegradation (Fan et al., 2019). We suspect that the dominance of gray particles in the current study is associated with particular industry sources (e.g., a warehousing and transportation company, an industrial refrigeration company).

The dominance of plastic particles under 1 mm in length is consistent with previous research (Bertoldi et al., 2021; Bujaczek et al., 2021; Sang et al., 2021; Wang et al., 2021). Indeed, an inverse relationship between microplastic size and concentration is a common finding in freshwater microplastic research (Battulga et al., 2019; Fan et al., 2019; Schmidt et al., 2018). Additionally, the abundance of microplastics in different size classes can vary across time. More specifically, a significantly greater abundance of particles in the largest size class (2001-5000 μ m) in February than in September is an interesting finding, and may indicate lower rates of degradation during the rainy season (Amrutha and Warriar, 2020). de Carvalho et al. (2021) reported a dominance in smaller size classes of microplastics during periods of low flows. Thus, the significantly greater abundance of small particles (101-500 μ m) in September as opposed to August in the current study is also interesting, as the August sampling session was conducted during low flow conditions.

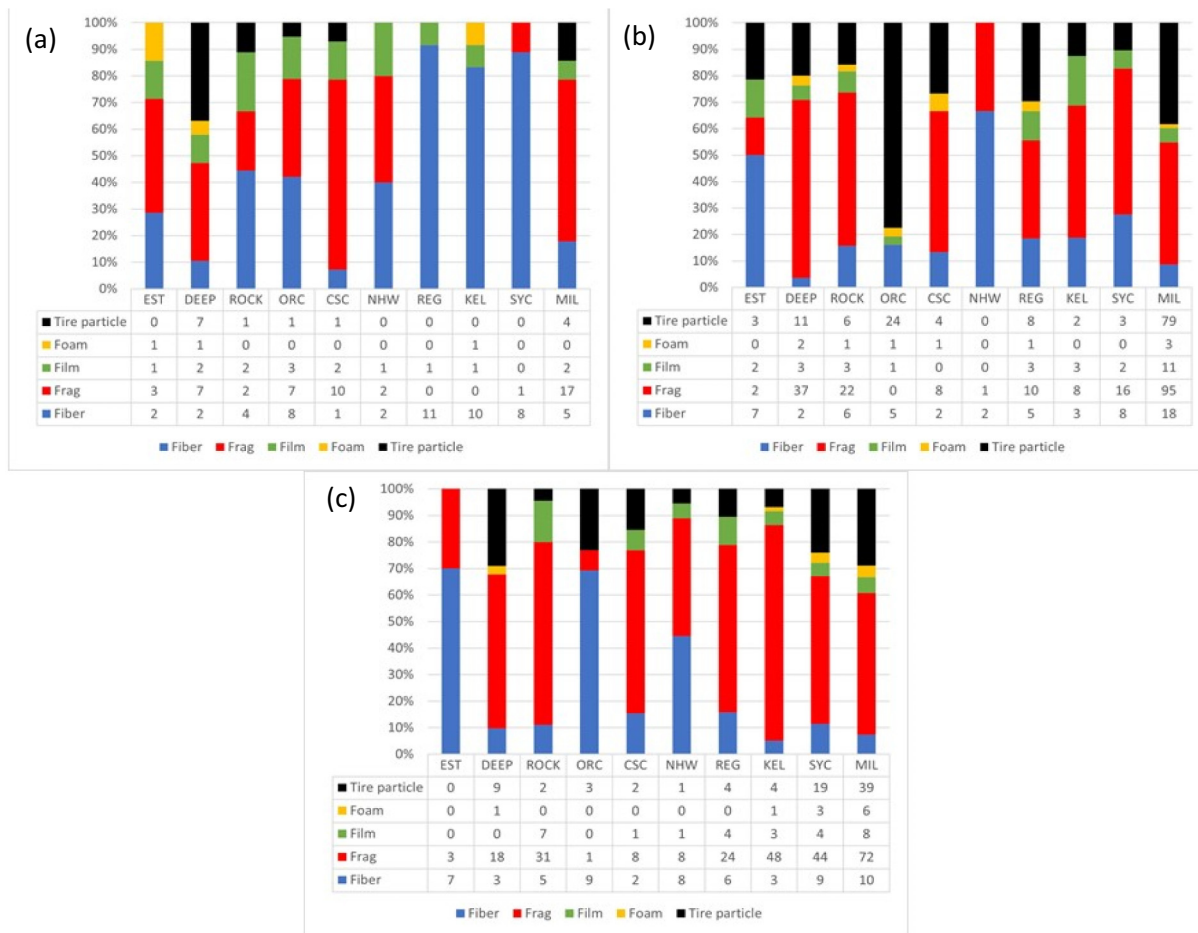


Fig. 9. Proportion of microplastic morphologies observed by site and by sampling session: (a) August 2020 (b) September 2020 and (c) February 2021.

Only one other study has evaluated microplastic concentrations in Oregon's freshwater bodies (Valine et al., 2020), including dry season sampling along the Willamette River (of which both Johnson Creek and the Clackamas River are tributaries) and adjacent to the Oregon Museum of Science and Industry (OMSI) in Portland. Valine et al. (2020) noted a dominance of fibers, reporting an average concentration of 3.19 fibers/m³ at the OMSI site. In comparison, dry season sampling in the current study showed two sites along Johnson Creek exceeding the average concentration reported at OMSI (KEL - 18.9 p/m³; REG - 6.4 p/m³), with the remaining eight sites showing average concentrations of less than 2.5 p/m³ during dry season sampling.

4.2. Temporal variability and hydrodynamic variables

Microplastics were identified at all sites throughout all sampling sessions, and an investigation of the literature shows similar findings of microplastic ubiquity (Ballent et al., 2016; Constant et al., 2020; Shruti

et al., 2019; Yin et al., 2020). Microplastic pollution varied temporally, with significantly higher concentrations observed during August (dry season) than during February (mid-wet season). It was expected that higher concentrations would be found during the early wet season than during the dry season due to first flush effects, yet the data did not support this hypothesis. While some studies find higher microplastic concentrations in the wet season (Eo et al., 2019; He et al., 2020), others have found that microplastics dominate in dry season samples (de Carvalho et al., 2021; Fan et al., 2021). This is potentially due to increased precipitation and runoff associated with the wet season resulting in dilution effects and lower observed microplastic concentrations (Fan et al., 2019; Stanton et al., 2020; Wu et al., 2020). While microplastic concentrations in the current study were negatively correlated with average flow rates in August (dry season), no correlations were observed between flow and concentrations in September and February (wet season).

There was little evidence that precipitation amount influenced microplastics at the study sites, similar to several previous studies showing

Table 3
Correlations between average microplastic concentrations and spatial factors.

		Area	Slope	Road density	Barren	Crops	Dev	Forest	Shrub
Aug	SWS	-0.673*	-0.321		-0.532	0.261	0.455	-0.358	-0.479
	Near		0.042	0.278	-0.337	-0.491	0.455	-0.274	-0.560
Sept	SWS	0.127	0.115		-0.625	-0.091	0.236	-0.127	-0.527
	Near		-0.212	0.127	0.078	-0.721*	0.297	-0.085	0.143
Feb	SWS	-0.430	-0.370		-0.607	0.152	0.564	-0.515	-0.721*
	Near		-0.285	0.491	-0.017	-0.673*	0.564	-0.432	-0.198

* Significant at the 0.05 level; SWS = Subwatershed scale.

Table 4
Correlations between average microplastic concentrations and temporal factors.

	Velocity (m/s)	24P (mm)	72P (mm)
August	-0.854*	-	-
September	-0.382	0.309	-0.486
February	-0.212	0.638*	-0.006

24P = 24-hour antecedent precipitation.

72P = 72-hour antecedent precipitation.

* Significant at the 0.05 level.

no relationship between the two (e.g., Constant et al., 2020; de Carvalho et al., 2021). There was a positive correlation between February microplastic concentrations and 24-hour antecedent precipitation, but the vast majority of precipitation values were estimates, with the closest HYDRA rain gauge at times located several miles away from a particular study site. As a result, data from a particular gauge were at times used for more than one site, a clear study limitation and potentially the reason for a difference between September and February.

In addition, localized rain events in September may have influenced the differences observed between early and mid-wet season antecedent precipitation and microplastic concentrations. These microstorms may have resulted in HYDRA rain gauges not reflecting accurate precipitation amounts at study sites in September. However, these gauges may have reflected more representative conditions in February due to widespread, less localized rain events. As such, precipitation may indeed be an important driver of microplastic concentrations in the study region, but the September sampling session may not have captured this effect. To ensure a clearer picture of potential relationships between precipitation and microplastics, obtaining precipitation data on a finer spatial scale with gauges located within very close proximity to study sites is ideal.

Our examination of microplastic loads at six of the study sites showed that the dry season sampling (August) consistently had the lowest microplastic loads. Conversely, the highest microplastic loads were present in the wet season, with two sites in the Clackamas River having the highest loads during the early wet season (September) and four in Johnson Creek having the highest loads during the mid-wet season (February). This dominance of wet season microplastic loads is consistent with previous research (e.g., Eo et al., 2019).

It is also important to note that the timing of data collection may be critical in evaluating the influence of precipitation. As previously noted, microplastic concentrations can vary drastically over very short periods of time as a function of hydroclimatic variables (Xia et al., 2020), even over the course of several hours (Cheung et al., 2019). Wet season sampling for the current study was conducted over a period of two or three days, due to the limited number of researchers involved in data collection. If multiple collection teams had been available to complete each wet season sampling event in a standardized amount of time and within a single day, this could have contributed to a clearer analysis regarding the impacts of precipitation on microplastic concentrations.

4.3. Watershed attributes

Few spatial variables were found to have significant relationships with microplastic concentrations, for either the subwatershed scale or the nearstream scale. Of important interest, however, were negative correlations between September and February microplastic concentrations and proportion of agricultural lands in the nearstream zones. This indicates that fewer microplastics were found in regions where the immediate upstream area was characterized by a greater degree of croplands, even during wet season periods when runoff is most likely to introduce plastic particles to freshwater bodies. The degradation of plastics used for agricultural purposes thus may not result in the flushing of substantial amounts of microplastics into nearby freshwater bodies; these microplastics may instead remain trapped in permeable agricultural soils (Feng et al., 2020).

Very few studies to date have evaluated microplastics in soils, and additional research is needed to shed further light on the microplastic cycle in both agricultural regions and other land use categories (Amrutha and Warriar, 2020; Feng et al., 2020).

Only one significant relationship was observed at the subwatershed scale, and included a negative correlation between February microplastic concentrations and proportion of shrub land. It is thus possible that nearstream analyses may shed more light when determining relationships between microplastic pollution and potential explanatory factors. Microplastics likely share delivery pathways with other contaminants and nutrients that threaten water quality (Mishell Donoso and Rios-Touma, 2020; Sarkar et al., 2019; Zhou et al., 2020), and as previously noted, recent water quality modeling research has highlighted the importance of nearstream as opposed to watershed-scale processes (Mainali and Chang, 2018). Similar sentiments were expressed by Barrows et al. (2018), whose analyses at the subwatershed scale spurred the belief that more localized analyses (e.g., on specific point sources) may be more useful in understanding the role of potential explanatory factors. A similar emphasis on specific sources of microplastics addressed at local scales was noted by Dikareva and Simon (2019).

While total microplastic counts were highest at the Milwaukie site, which is characterized by a high proportion of developed land cover, an unexpected finding was the lack of a correlation between microplastic concentrations and developed land, at either the subwatershed or nearstream scales. As previously mentioned, the two watersheds included in this study represent a range of land covers, yet it is possible that the selected sites may not represent the full urban-rural gradient, thus clouding potential relationships. For instance, many of the sites were located in mostly developed regions. Perhaps the incorporation of a greater number of study sites spanning a broader range of the gradient may reveal more specific results (Belen Alfonso et al., 2020; Dikareva and Simon, 2019), and this may also be the case with other watershed attributes such as slope. Additionally, as the net was submerged just under the surface of the water to ensure that water volume could be calculated, it is possible that some microplastics on the surface circumvented the net. Lastly, it is important to note that factors not evaluated by the current study (e.g., various microscale processes, sediment resuspension) may have exerted an influence on observed microplastic concentrations. Evaluating microplastic concentrations in sediment samples would have provided further insight regarding influential factors as well as a more comprehensive picture of the microplastic cycle at the monitoring sites.

4.4. Potential sources

Broad links can be made with regard to observed microplastic morphologies and potential sources. As previously mentioned, fragments were the dominant observed morphology, indicating that the breakdown of larger pieces of plastic and litter may be a critical source of microplastics in Portland's freshwater bodies. Fibers were also common, indicating that factors such as washing machine effluent (e.g., in residential regions surrounding the Regner and Kelley Creek sites) or recreational activities (e.g., at sites characterized by a high degree of water activity such as the Estacada and Near Oregon City sites) may play a role in microplastic pollution as well. Additionally, given that the September sampling session showed significantly higher tire wear particle concentrations than the August sampling session, it is likely that these particles accumulated on land during the dry period and were flushed into nearby waterways during the first wet season storm event. The influx of tire wear particles in the early wet season is particularly alarming, as recent research has highlighted the severe threat they pose to salmon (Tian et al., 2021).

The identification of specific polymer types can also shed light on potential sources of microplastic pollution. Polyethylene (PE) was the most commonly observed polymer, which is consistent with previous findings (Fan et al., 2019; Xiong et al., 2019). In particular, PE particles were composed of two sub-polymers with very different applications. Of the 116 particles assessed by μ FTIR spectroscopy,

low-density polyethylene (LDPE) particles were found at all but two of the study sites. These plastics are typically found in thin plastic bags, such as those used in grocery stores (Mishra et al., 2021). In contrast, only one high-density polyethylene (HDPE) particle was reported, and it was observed at the Milwaukie site. As HDPE particles are commonly used in construction activities and PVC pipes (Mishra et al., 2021), its presence at the more industrial Milwaukie site is unsurprising. Polypropylene (PP) was very common as well, and is often found in a variety of packaging materials as well as in synthetic clothing (Mishra et al., 2021). Of the samples that underwent μ FTIR analyses, PP particles were found at all but two of the sites, underscoring their ubiquity.

4.5. Conservative estimates of microplastics

The observed microplastic concentrations in this study are likely conservative, which may be due to several factors. For instance, the use of a hypersaline solution during density separation does not result in the flotation of 100% of plastic particles, as higher density plastics in particular often remain trapped with sediment (Mishra et al., 2021). Therefore, the vacuum filtration step may have missed microplastics that remained at the bottom of the sample jars (Di and Wang, 2018; Valine et al., 2020), thus resulting in a subset being isolated on the filter paper for microscope analysis. Similarly, the fact that sampling was conducted just below the surface of the water likely resulted in the underrepresentation of high-density particles such as TWPs, many of which may reside at lower depths in the water column or in benthic sediment (Wik and Dave, 2009).

Additionally, while microplastics in the smallest size class (63–80 μ m) were retained, this class is likely vastly underrepresented due to the use of an 80 μ m mesh net during sample collection. The current study also included the use of glass microfiber binder free filters, which are white in color. While the current study identified some white microplastic particles under the microscope, it is likely that others were missed due to the difficulty in identifying these particles against a white background. The inclusion of clear polycarbonate filters in future studies may facilitate the identification of white microplastics.

5. Conclusion

This study showed that microplastic concentrations in the Portland metropolitan area may be influenced by certain hydroclimatic variables and subwatershed characteristics. In the dry season, lower flow rates appeared to facilitate the accumulation of microplastics, with concentrations also potentially influenced by antecedent rainfall in the mid-wet season. Additionally, microplastic concentrations may be influenced more strongly by nearstream as opposed to subwatershed factors, particularly with regard to adjacent agricultural lands. Fragments were dominant in both watersheds, likely due to the breakdown of larger pieces of plastic. Gray particles were particularly common, and the 101–500 μ m size class of microplastics was the most highly represented. Higher concentrations of tire wear particles in the wet season suggest a flushing effect.

The findings of this study further our knowledge of riverine microplastic pollution in the Portland metro area and contribute to our understanding of potential sources of microplastics in freshwater environments. This information is beneficial to local officials and agencies in Portland, who are increasingly interested in knowing the potential sources and pathways of microplastics in their water bodies. Armed with such knowledge, they may be better equipped to enact policies that result in decreased concentrations of microplastics reaching aquatic environments. In addition, the findings of the research can identify hotspots of microplastic pollution that may benefit from remediation, and can potentially assist in projections of microplastic concentrations in other locations with similar characteristics, for which no microplastics data have yet been collected.

CRediT authorship contribution statement

Rebecca Talbot: Conceptualization, Data curation, Methodology, Laboratory analysis, Writing - original draft preparation.

Elise Grank: Conceptualization, Methodology, Supervision, Writing - Review & editing.

Heejun Chang: Conceptualization, Methodology, Supervision, Writing - Review & editing.

Rosemary Wood: Data curation, Methodology, Laboratory analysis.

Susanne Brander: Laboratory Analysis, Methodology, Writing - Review & editing.

Declaration of competing interest

The authors declare that they have no known competing financial interests or personal relationships that could have appeared to influence the work reported in this paper.

Acknowledgements

This research was supported by a Faculty Enhancement Grant at Portland State University and National Science Foundation (CBET 2115447 & SMB 1935028). Additional supports were provided by the City of Gresham, City of Portland, Clackamas River Water Providers, East Multnomah County Soil and Water District, and Sigma Xi. We acknowledge and thank Emily Pedersen in the Brander laboratory for conducting FTIR analyses on samples for this study. We appreciate three anonymous reviewers whose comments helped clarify many points of the article.

Appendix A. Supplementary data

Supplementary data to this article can be found online at <https://doi.org/10.1016/j.scitotenv.2022.155143>.

References

- Amrutha, K., Warriar, A.K., 2020. The first report on the source-to-sink characterization of microplastic pollution from a riverine environment in tropical India. *Sci. Total Environ.* 739, 140377.
- Baechler, B.R., Granek, E.F., Hunter, M.V., Conn, K.E., 2020. Microplastic concentrations in two Oregon bivalve species: spatial, temporal, and species variability. *Limnol. Oceanogr. Lett.* 5 (1), 54–65.
- Baldwin, A.K., Corsi, S.R., Mason, S.A., 2016. Plastic debris in 29 Great Lakes tributaries: relations to watershed attributes and hydrology. *Environ. Sci. Technol.* 50 (19), 10377–10385.
- Baldwin, A.K., Spanjer, A.R., Rosen, M.R., Thom, T., 2020. Microplastics in Lake Mead National Recreation Area, USA: occurrence and biological uptake. *PLoS One* 15 (5), e0228896 San Francisco.
- Ballent, A., Corcoran, P.L., Madden, O., Helm, P.A., Longstaffe, F.J., 2016. Sources and sinks of microplastics in Canadian Lake Ontario nearshore, tributary and beach sediments. *Mar. Pollut. Bull.* 110 (1), 383–395.
- Barrows, A.P.W., Christiansen, K.S., Bode, E.T., Hoellein, T.J., 2018. A watershed-scale, citizen science approach to quantifying microplastic concentration in a mixed land-use river. *Water Res.* 147, 382–392.
- Battulga, B., Kawahigashi, M., Oyuntsetseg, B., 2019. Distribution and composition of plastic debris along the river shore in the Selenga River basin in Mongolia. *Environ. Sci. Pollut. Res.* 26 (14), 14059–14072.
- Belen Alfonso, M., Scordo, F., Seitz, C., Mavo Manstretta, G.M., Carolina Ronda, A., Hugo Arias, A., Pablo Tomba, J., Ignacio Silva, L., Eduardo Perillo, G.M., Cintia Piccolo, M., 2020. First evidence of microplastics in nine lakes across Patagonia (South America). *Sci. Total Environ.* 733, 139385.
- Bertoldi, C., Lara, L.Z., Martins, F.C.G., Battisti, M.A., Hinrichs, R., Fernandes, A.N., 2021. First evidence of microplastic contamination in the freshwater of Lake Guaíba, Porto Alegre, Brazil. *Sci. Total Environ.* 759, 143503.
- Brander, S.M., Renick, V.C., Foley, M.M., Steele, C., Woo, M., Lusher, A., Carr, S., Helm, P., Box, C., Cherniak, S., Andrews, R.C., Rochman, C.M., 2020. Sampling and quality assurance and quality control: a guide for scientists investigating the occurrence of microplastics across matrices. *Appl. Spectrosc.* 74 (9), 1099–1125.
- Bujacek, T., Kolter, S., Locky, D., Ross, M.S., 2021. Characterization of microplastics and anthropogenic fibers in surface waters of the North Saskatchewan River, Alberta, Canada. *FACETS* 6, 26–43.

- Bureau of Environmental Services, City of Portlandcollab, 2021. City of Portland HYDRA Rainfall Network. <https://or.water.usgs.gov/non-usgs/bes/precip.html>. (Accessed 15 August 2021) UNSP 125486.
- Campanale, C., Savino, I., Pojar, I., Massarelli, C., Uricchio, V.F., 2020a. A practical overview of methodologies for sampling and analysis of microplastics in riverine environments. *Sustainability* 12 (17), 6755.
- Campanale, C., Stock, F., Massarelli, C., Kochleus, C., Bagnuolo, G., Reifferscheid, G., Uricchio, V.F., 2020b. Microplastics and their possible sources: the example of ofanto river in Southeast Italy. *Environ. Pollut.* 258, 113284.
- Campbell, S.H., Williamson, P.R., Hall, B.D., 2017. Microplastics in the gastrointestinal tracts of fish and the water from an urban prairie creek ed. D. Schindler. *FACETS* 2 (1), 395–409.
- Carpenter, E.J., Smith, K.L., 1972. Plastics on the Sargasso Sea surface. *Science* 175 (4027), 1240–1241.
- de Carvalho, A.R., Garcia, F., Riem-Galliano, L., Tudesque, L., Albignac, M., ter Halle, A., Cucherousset, J., 2021. Urbanization and hydrological conditions drive the spatial and temporal variability of microplastic pollution in the Garonne River. *Sci. Total Environ.* 769, 144479.
- Chang, H., Allen, D., Morse, J., Mainali, J., 2019. Sources of contaminated flood sediments in a rural-urban catchment: Johnson Creek, Oregon. *J. Flood Risk Manag.* 12 (4), e12496.
- Chen, H.J., Chang, H., 2014. Response of discharge, TSS, and E. coli to rainfall events in urban, suburban, and rural watersheds. *Environ Sci Process Impacts* 16 (10), 2313–2324.
- Chen, J., Chang, H., 2019. Dynamics of wet-season turbidity in relation to precipitation, discharge, and land cover in three urbanizing watersheds, Oregon. *River Res. Appl.* 35 (7), 892–904.
- Chen, H., Jia, Q., Zhao, X., Li, L., Nie, Y., Liu, H., Ye, J., 2020. The occurrence of microplastics in water bodies in urban agglomerations: impacts of drainage system overflow in wet weather, catchment land-uses, and environmental management practices. *Water Res.* 183, 116073.
- Cheung, P.K., Hung, P.L., Fok, L., 2019. River microplastic contamination and dynamics upon a rainfall event in Hong Kong, China. *Environ. Process.* 6 (1), 253–264.
- Constant, M., Ludwig, W., Kerherve, P., Sola, J., Charriere, B., Sanchez-Vidal, A., Canals, M., Heussner, S., 2020. Microplastic fluxes in a large and a small Mediterranean river catchments: the tet and the rhone, northwestern Mediterranean Sea. *Sci. Total Environ.* 716, 136984.
- Cowger, W., Steinmetz, Z., Gray, A., Munno, K., Lynch, J., Hapich, H., Primpke, S., De Frond, H., Rochman, C., Herodotou, O., 2021. Microplastic spectral classification needs an open source community: open specy to the rescue! *Anal. Chem.* 93 (21), 7543–7548.
- Di, M., Wang, J., 2018. Microplastics in surface waters and sediments of the three gorges reservoir, China. *Sci. Total Environ.* 616, 1620–1627.
- Dikareva, N., Simon, K.S., 2019. Microplastic pollution in streams spanning an urbanisation gradient. *Environ. Pollut.* 250, 292–299.
- Dris, R., Gasperi, J., Rocher, V., Tassin, B., 2018. Synthetic and non-synthetic anthropogenic fibers in a river under the impact of Paris megacity: sampling methodological aspects and flux estimations. *Sci. Total Environ.* 618, 157–164.
- Edo, C., González-Pleiter, M., Leganés, F., Fernández-Piñas, F., Rosal, R., 2020. Fate of microplastics in wastewater treatment plants and their environmental dispersion with effluent and sludge. *Environ. Pollut.* 259, 113837.
- Eo, S., Hong, S.H., Song, Y.K., Han, G.M., Shim, W.J., 2019. Spatiotemporal distribution and annual load of microplastics in the Nakdong River, South Korea. *Water Res.* 160, 228–237.
- Estabhanati, S., Fahrenfeld, N.L., 2016. Influence of wastewater treatment plant discharges on microplastic concentrations in surface water. *Chemosphere* 162, 277–284.
- ESRI, 2020. ArcGIS Desktop: Release 10.8.1. Environmental Systems Research Institute, Redlands, CA.
- Fan, Y., Zheng, K., Zhu, Z., Chen, G., Peng, X., 2019. Distribution, sedimentary record, and persistence of microplastics in the Pearl River catchment, China. *Environ. Pollut.* 251, 862–870.
- Fan, J., Zou, L., Zhao, G., 2021. Microplastic abundance, distribution, and composition in the surface water and sediments of the Yangtze River along Chongqing City, China. *J. Soils Sediments* 21 (4), 1840–1851.
- Feng, S., Lu, H., Tian, P., Xue, Y., Lu, J., Tang, M., Feng, W., 2020. Analysis of microplastics in a remote region of the tibetan plateau: implications for natural environmental response to human activities. *Sci. Total Environ.* 739, 140087.
- Granek, E.F., Brander, S.M., Holland, E.B., 2020. Microplastics in aquatic organisms: improving understanding and identifying research directions for the next decade. *Limnol. Oceanogr. Lett.* 5 (1), 1–4.
- Gričić, J., Helm, P., Athey, S., Rochman, C.M., 2020. Microplastics entering northwestern Lake Ontario are diverse and linked to urban sources. *Water Res.* 174, 115623.
- Guerranti, C., Cannas, S., Scopetani, C., Fastelli, P., Cincinelli, A., Renzi, M., 2017. Plastic litter in aquatic environments of Maremma Regional Park (Tyrrenian Sea, Italy): contribution by the ombrene river and levels in marine sediments. *Mar. Pollut. Bull.* 117 (1), 366–370.
- Han, M., Niu, X., Tang, M., Zhang, B.-T., Wang, G., Yue, W., Kong, X., Zhu, J., 2020. Distribution of microplastics in surface water of the lower Yellow River near estuary. *Sci. Total Environ.* 707, 135601.
- Harris, L.S.T., Beur, L.La, Olsen, A.Y., Smith, A., Eggers, L., Pedersen, E., Brocklin, J., Van, Brander, S.M., Larson, S., 2022. Temporal variability of microparticles under the Seattle Aquarium, Washington State: documenting the global covid-19 pandemic. *Environ. Toxicol. Chem.* 41 (4), 917–930. <https://doi.org/10.1002/etc.5190>.
- He, B., Goonetilleke, A., Ayoko, G.A., Rintoul, L., 2020. Abundance, distribution patterns, and identification of microplastics in Brisbane River sediments, Australia. *Sci. Total Environ.* 700, 134467.
- Hitchcock, J.N., 2020. Storm events as key moments of microplastic contamination in aquatic ecosystems. *Sci. Total Environ.* 734, 139436.
- Hoellein, T.J., McCormick, A.R., Hittie, J., London, M.G., Scott, J.W., Kelly, J.J., 2017. Longitudinal patterns of microplastic concentration and bacterial assemblages in surface and benthic habitats of an urban river. *Freshw. Sci.* 36 (3), 491–507.
- Hu, D., Zhang, Y., Shen, M., 2020. Investigation on microplastic pollution of dongting Lake and its affiliated rivers. *Mar. Pollut. Bull.* 160, 111555.
- Huang, Y., Tian, M., Jin, F., Chen, M., Liu, Z., He, S., Li, F., Yang, L., Fang, C., Mu, J., 2020. Coupled effects of urbanization level and dam on microplastics in surface waters in a coastal watershed of Southeast China. *Mar. Pollut. Bull.* 154, 111089.
- Hurley, R., Woodward, J., Rothwell, J.J., 2018. Microplastic contamination of river beds significantly reduced by catchment-wide flooding. *Nat. Geosci.* 11 (4), 251–257.
- Jiang, C., Yin, L., Li, Z., Wen, X., Luo, X., Hu, S., Yang, H., Long, Y., Deng, B., Huang, L., Liu, Y., 2019. Microplastic pollution in the rivers of the Tibet plateau. *Environ. Pollut.* 249, 91–98.
- Kapp, K.J., Yeatman, E., 2018. Microplastic hotspots in the Snake and lower Columbia rivers: a journey from the greater yellowstone ecosystem to the Pacific Ocean. *Environ. Pollut.* 241, 1082–1090.
- Kataoka, T., Nihei, Y., Kudou, K., Hinata, H., 2019. Assessment of the sources and inflow processes of microplastics in the river environments of Japan. *Environ. Pollut.* 244, 958–965.
- Klasios, N., De Frond, H., Miller, E., Sedlak, M., 2021. Microplastics and other anthropogenic particles are prevalent in mussels from San Francisco Bay, and show no correlation with PAHs. *Environ. Pollut.* 271, 116260.
- Lahens, L., Strady, E., Kieu-Le, T.-C., Dris, R., Boukerma, K., Rinnert, E., Gasperi, J., Tassin, B., 2018. Macroplastic and microplastic contamination assessment of a tropical river (Saigon River, Vietnam) transversed by a developing megacity. *Environ. Pollut.* 236, 661–671.
- Leslie, H.A., Brandsma, S.H., van Velzen, M.J.M., Vethaak, A.D., 2017. Microplastics en route: field measurements in the dutch river delta and Amsterdam canals, wastewater treatment plants, North Sea sediments and biota. *Environ. Int.* 101, 133–142.
- Li, C., Busquets, R., Campos, L.C., 2020. Assessment of microplastics in freshwater systems: a review. *Sci. Total Environ.* 707, 135578.
- Ma, M., Liu, S., Su, M., Wang, C., Ying, Z., Huo, M., Lin, Y., Yang, W., 2021. Spatial distribution and potential sources of microplastics in the Songhua river flowing through urban centers in northeast China. *Environ. Pollut.* 118384.
- Mai, Y., Peng, S., Lai, Z., Wang, X., 2021. Measurement, quantification, and potential risk of microplastics in the mainstream of the Pearl River (Xijiang River) and its estuary, southern China. *Environ. Sci. Pollut. Res.* 28 (38), 53127–53140.
- Mainali, J., Chang, H., 2018. Landscape and anthropogenic factors affecting spatial patterns of water quality trends in a large river basin, South Korea. *J. Hydrol.* 564, 26–40.
- Mani, T., Hauk, A., Walter, U., Burkhardt-Holm, P., 2015. Microplastics profile along the Rhine River. *Sci. Rep.* 5 (1), 1–7.
- Mao, R., Hu, Y., Zhang, S., Wu, R., Guo, X., 2020. Microplastics in the surface water of wuliangshai Lake, northern China. *Sci. Total Environ.* 723, 137820.
- McCormick, A.R., Hoellein, T.J., London, M.G., Hittie, J., Scott, J.W., Kelly, J.J., 2016. Microplastic in surface waters of urban rivers: concentration, sources, and associated bacterial assemblages. *Ecosphere* 7 (11), e01556.
- Miller, R.Z., Watts, A.J.R., Winslow, B.O., Galloway, T.S., Barrows, A.P.W., 2017. Mountains to the sea: river study of plastic and non-plastic microfiber pollution in the Northeast USA. *Mar. Pollut. Bull.* 124 (1), 245–251.
- Mishell Donoso, J., Rios-Touma, B., 2020. Microplastics in tropical andean rivers: a perspective from a highly populated equadorian basin without wastewater treatment. *Hydrobiol.* 6 (7), e04302.
- Mishra, Sujata, Swain, S., Sahoo, M., Mishra, Sunanda, Das, A.P., 2021. *Geomicrobiol. J.* <https://doi.org/10.1080/01490451.2021.1983670>.
- Multi-Resolution Land Characteristics Consortium, 2021. National Land Cover Dataset 2019 [11 August 2021].
- Natural Resources Conservation Service, 2021. United States Department of Agriculture Web Soil Survey [8 November 2021].
- Ogle, D.H., Doll, J.C., Wheeler, P., Dinno, A., 2021. FSA: Fisheries Stock Analysis. R package version 0.9.1. <https://github.com/droglen/FSA>.
- Park, T.-J., Lee, S.-H., Lee, M.-S., Lee, J.-K., Park, J.-H., Zoh, K.-D., 2020. Distributions of microplastics in surface water, fish, and sediment in the vicinity of a sewage treatment plant. *Water* 12 (12), 3333.
- Parker, B.W., Beckingham, B.A., Ingram, B.C., Ballenger, J.C., Weinstein, J.E., Sancho, G., 2020. Microplastic and tire wear particle occurrence in fishes from an urban estuary: Influence of feeding characteristics on exposure risk. *Mar. Pollut. Bull.* 160, 111539.
- Peller, J.R., Eberhardt, L., Clark, R., Nelson, C., Kostelnik, E., Iceman, C., 2019. Tracking the distribution of microfiber pollution in a southern Lake Michigan watershed through the analysis of water, sediment and air. *Environ Sci Process Impacts* 21 (9), 1549–1559.
- Pratt, B., Chang, H., 2012. Effects of land cover, topography, and built structure on seasonal water quality at multiple spatial scales. *J. Hazard. Mater.* 209–210, 48–58.
- Primpke, S., Christiansen, S.H., Cowger, W., De Frond, H., Deshpande, A., Fischer, M., Holland, E.B., Meyns, M., O'Donnell, B.A., Ossmann, B.E., Pittroff, M., Sarau, G., Scholz-Böttcher, B.M., Wiggan, K.J., 2020. Critical assessment of analytical methods for the harmonized and cost-efficient analysis of microplastics. *Appl. Spectrosc.* 74 (9), 1012–1047.
- Qin, Y., Wang, Z., Li, W., Chang, X., Yang, J., Yang, F., 2020. Microplastics in the sediment of Lake Ulansuhai of Yellow River Basin, China. *Water Environ. Res.* 92 (6), 829–839.
- R Core Team, 2021. R: A language and environment for statistical computing. R Foundation for Statistical Computing, Vienna, Austria. <https://www.R-project.org/>.
- Sang, W., Chen, Z., Mei, L., Hao, S., Zhan, C., bin Zhang, W., Li, M., Liu, J., 2021. The abundance and characteristics of microplastics in rainwater pipelines in Wuhan, China. *Sci. Total Environ.* 755, 142606.
- Sarkar, Deepayan, 2008. *Lattice: Multivariate Data Visualization With R*. Springer, New York 978-0-387-75968-5.
- Sarkar, D.J., Das Sarkar, S., Das, B.K., Manna, R.K., Behera, B.K., Samanta, S., 2019. Spatial distribution of meso and microplastics in the sediments of river ganga at eastern India. *Sci. Total Environ.* 694, 133712.
- Schmidt, L.K., Bochow, M., Imhof, H.K., Oswald, S.E., 2018. Multi-temporal surveys for microplastic particles enabled by a novel and fast application of SWIR imaging spectroscopy – study of an urban watercourse traversing the city of Berlin, Germany. *Environ. Pollut.* 239, 579–589.

- Shruti, V.C., Jonathan, M.P., Rodríguez-Espinoza, P.F., Rodríguez-González, F., 2019. Microplastics in freshwater sediments of Atoyac River basin, Puebla City, Mexico. *Sci. Total Environ.* 654, 154–163.
- Stanton, T., Johnson, M., Nathanail, P., MacNaughtan, W., Gomes, R.L., 2020. Freshwater microplastic concentrations vary through both space and time. *Environ. Pollut.* 263, 114481.
- Strady, E., Kieu-Le, T.-C., Gasperi, J., Tassin, B., 2020. Temporal dynamic of anthropogenic fibers in a tropical river-estuarine system. *Environ. Pollut.* 259, 113897.
- Talbot, R., Chang, H., 2022. Microplastics in freshwater: a global review of factors affecting spatial and temporal variations. *Environ. Pollut.* 292, 118393.
- Tian, Z., Zhao, H., Peter, K.T., Gonzalez, M., Wetzel, J., Wu, C., Hu, X., Prat, J., Mudrock, E., Hettlinger, R., Cortina, A.E., Biswas, R.G., Kock, F.V.C., Soong, R., Jenne, A., Du, B., Hou, F., He, H., Lundeen, R., Gilbreath, A., Sutton, R., Scholz, N.L., Davis, J.W., Dodd, M.C., Simpson, A., McIntyre, J.K., Kolodziej, E.P., 2021. A ubiquitous tire rubber-derived chemical induces acute mortality in coho salmon. *Science* 371 (6525), 185–189.
- Tibbetts, J., Krause, S., Lynch, I., Smith, G.H.S., 2018. Abundance, distribution, and drivers of microplastic contamination in Urban River environments. *Water* 10 (11), 1597.
- Townsend, K.R., Lu, H.-C., Sharley, D.J., Pettigrove, V., 2019. Associations between microplastic pollution and land use in urban wetland sediments. *Environ. Sci. Pollut. Res.* 26 (22), 22551–22561.
- USGS Water Data for the Nation, 2021. National Water Information System (NWIS).
- Valine, A.E., Peterson, A.E., Horn, D.A., Scully-Engelmeyer, K.M., Granek, E.F., 2020. Microplastic prevalence in 4 Oregon Rivers along a rural to urban gradient applying a cost-effective validation technique. *Environ. Toxicol. Chem.* 39 (8), 1590–1598.
- Vu, Vincent Q., 2011. ggbiplot: A ggplot2 based biplot. R package version 0.55. <http://github.com/vqv/ggbiplot>.
- Wang, G., Lu, J., Tong, Y., Liu, Z., Zhou, H., Xiayihazi, N., 2020. Occurrence and pollution characteristics of microplastics in surface water of the Manas River Basin, China. *Sci. Total Environ.* 710, 136099.
- Wang, G., Lu, J., Li, W., Ning, J., Zhou, L., Tong, Y., Liu, Z., Zhou, H., Xiayihazi, N., 2021. Seasonal variation and risk assessment of microplastics in surface water of the Manas River Basin, China. *Ecotoxicol. Environ. Saf.* 208, 111477.
- Watkins, L., Sullivan, P.J., Walter, M.T., 2019. A case study investigating temporal factors that influence microplastic concentration in streams under different treatment regimes. *Environ. Sci. Pollut. Res.* 26 (21), 21797–21807.
- Wei, T., Simko, V., 2021. R package 'corrplot': Visualization of a Correlation Matrix (Version 0.90). Available from <https://github.com/taiyun/corrplot>.
- Werbowski, L.M., Gilbreath, A.N., Munno, K., Zhu, X., Grbic, J., Wu, T., Sutton, R., Sedlak, M.D., Deshpande, A.D., Rochman, C.M., 2021. Urban stormwater runoff: a major pathway for anthropogenic particles, black rubbery fragments, and other types of microplastics to urban receiving waters. *ACS ES&T Water* 1 (6), 1420–1428.
- Wickham, H., 2011. The Split-apply-combine strategy for data analysis. *J. Stat. Softw.* 40 (1), 1–29. <http://www.jstatsoft.org/v40/i01/>.
- Wik, A., Dave, G., 2009. Occurrence and effects of tire wear particles in the environment – a critical review and an initial risk assessment. *Environ. Pollut.* 157, 1–11.
- Wong, G., Löwemark, L., 2020. Microplastic pollution of the Tamsui River and its tributaries in northern Taiwan: spatial heterogeneity and correlation with precipitation. *Environ. Pollut.* 260, 113935.
- Wu, P., Tang, Y., Dang, M., Wang, S., Jin, H., Liu, Y., Jing, H., Zheng, C., Yi, S., Cai, Z., 2020. Spatial-temporal distribution of microplastics in surface water and sediments of Maozhou River within Guangdong-Hong Kong-Macao Greater Bay Area. *Sci. Total Environ.* 717, 135187.
- Xia, W., Rao, Q., Deng, X., Chen, J., Xie, P., 2020. Rainfall is a significant environmental factor of microplastic pollution in inland waters. *Sci. Total Environ.* 732, 139065.
- Xiong, X., Wu, C., Elser, J.J., Mei, Z., Hao, Y., 2019. Occurrence and fate of microplastic debris in middle and lower reaches of the Yangtze River – from inland to the sea. *Sci. Total Environ.* 659, 66–73.
- Yin, L., Wen, X., Du, C., Jiang, J., Wu, L., Zhang, Y., Hu, Z., Hu, S., Feng, Z., Zhou, Z., Long, Y., Gu, Q., 2020. Comparison of the abundance of microplastics between rural and urban areas: a case study from East Dongting Lake. *Chemosphere* 244 UNSP 125486.
- Yonkos, L.T., Friedel, E.A., Perez-Reyes, A.C., Ghosal, S., Arthur, C.D., 2014. Microplastics in four estuarine rivers in the Chesapeake Bay, U.S.A. *Environ. Sci. Technol.* 48 (24), 14195–14202.
- Zhao, S., Wang, T., Zhu, L., Xu, P., Wang, X., Gao, L., Li, D., 2019. Analysis of suspended microplastics in the changjiang estuary: implications for riverine plastic load to the ocean. *Water Res.* 161, 560–569.
- Zhou, G., Wang, Q., Zhang, J., Li, Q., Wang, Y., Wang, M., Huang, X., 2020. Distribution and characteristics of microplastics in urban waters of seven cities in the Tuojiang River basin, China. *Environ. Res.* 189, 109893.

ABOUT UMT FACULTY

SDI

Selective Dissemination of Information (SDI) service is a current-awareness service offered by the PSNZ for UMT Faculty Members. The contents selection criteria include current publications (last 5 years), highly cited and most viewed/downloaded documents. The contents with pdf full text from subscribed databases are organized and compiled according to a monthly theme which is determined based on the topics of specified interest.

For more information or further assistance, kindly contact us at 09-6684185/4298 or email to psnz@umt.edu.my/sh_akmal@umt.edu.my

Thank you.

**Perpustakaan Sultanah Nur Zahirah
Universiti Malaysia Terengganu
21030 Kuala Nerus, Terengganu.**

Tel. : 09-6684185 (Main Counter)

Fax : 09-6684179

Email : psnz@umt.edu.my